

Technical Report

**TR-19-01**

September 2019



# Post-closure safety for a proposed repository concept for SFL

## Main report for the safety evaluation SE-SFL

SVENSK KÄRNBRÄNSLEHANTERING AB

SWEDISH NUCLEAR FUEL  
AND WASTE MANAGEMENT CO

Box 3091, SE-169 03 Solna  
Phone +46 8 459 84 00  
skb.se

SVENSK KÄRNBRÄNSLEHANTERING



ISSN 1404-0344

**SKB TR-19-01**

ID 1861959

September 2019

Updated 2020-02

# **Post-closure safety for a proposed repository concept for SFL**

## **Main report for the safety evaluation SE-SFL**

Svensk Kärnbränslehantering AB

*Keywords:* SFL, Long-lived low- and intermediate-level waste, Safety evaluation, Post-closure safety.

A pdf version of this document can be downloaded from [www.skb.se](http://www.skb.se).

© 2019 Svensk Kärnbränslehantering AB

## Update notice

The original report, dated September 2019, was found to contain factual errors which have been corrected in this updated version. The corrected factual errors are presented below.

### Updated 2020-02

Location	Original text	Corrected text
Page 155, Figure 7-13	Missing dotted lines. BHA: Cl-36 and Mo-93 BHK: C-14, Cl-36 and Ca-41	Figure updated with correct lines.
Page 164, Figure 8-5	Missing dotted line. Left graph, part of Ca-41	Figure updated with correct lines.
Page 171, Figure 8-11	Missing dotted lines. BHA and BHK: Cl-36	Figure updated with correct lines.
Page 183, Figure 8-20	Wrong colour on lines. BHA: Tc-99 BHK: Ni-59	Figure updated with correct colour.

# Preface

This report is the main report for the evaluation of post-closure safety for a proposed repository concept for the repository for long-lived waste (SFL) in Sweden. The report describes the applied methodology, initial state of the repository and its environs, a reference evolution as well as radionuclide transport and dose calculations. Furthermore, the outcome of the evaluation is discussed in view of the defined objectives.

Jenny Brandefelt has been the project leader for SE-SFL and is responsible for the safety evaluation. The main contributing authors for this report have been Jenny Brandefelt, Svante Hedström, Georg Lindgren (Kemakta Konsult AB), and Niko Marsic (SKB unless otherwise noted). Contributions in specific subject areas have been provided by Katrin Ahlford, Per-Anders Ekström (Kvot AB), Björn Herschend, Olle Hjerne, Ben Jaeschke (ÅF Pöyry AB), Ulrik Kautsky, Klas Källström, Anders Löfgren (Ecoanalytica Löfgren), Per Mårtensson, Jens-Ove Näslund, Ignasi Puigdomenech, Peter Saetre, Henrik von Schenck, Patrik Sellin, Patrik Vidstrand and Ola Wessely.

An initial review of this report was performed by Russel Alexander (Bedrock Geosciences GmbH, Switzerland), Jordi Bruno (Amphos<sup>21</sup> Consulting S.L., Spain), Michael Thorne (Mike Thorne and Associates Ltd., United Kingdom), and George William Lanyon (Fracture Systems Ltd., United Kingdom). Valuable support in the initial review process was also provided by Katrin Ahlford, Eva Andersson, Johan Andersson, Björn Gylling, Allan Hedin, Björn Herschend, Olle Hjerne, Ulrik Kautsky, Klas Källström, Nico Marsic, Diego Mas Ivars, Raymond Munier, Per Mårtensson, Jens-Ove Näslund, Magnus Odén, Ignasi Puigdomenech, Peter Saetre, Patrik Sellin and Jan-Olof Selroos. A formal review was subsequently carried out by Jordi Bruno and Michael Thorne.

Solna, September 2019

*Jenny Brandefelt*

Project leader SE-SFL



# Summary

The repository for long-lived waste (SFL) is planned to be constructed for disposal of the Swedish long-lived low- and intermediate-level radioactive waste. This document constitutes the main report for the first evaluation of post-closure safety for a proposed repository concept for SFL. According to this concept, SFL is designed as a deep geological repository with two waste vaults: BHA with a bentonite clay backfill for legacy waste, and BHK with a concrete backfill for reactor internal components. No site has yet been chosen for SFL, and only a first estimate of the initial inventory of radionuclides and other materials in SFL is available. The purpose of the safety evaluation for SFL (SE-SFL) is to provide input to the subsequent, consecutive steps in the development of SFL. More specifically, one objective is to evaluate conditions in the waste, barriers, and the repository environs under which the repository concept has the potential to fulfil the regulatory requirements for post-closure safety. Furthermore, the outcomes of SE-SFL can be used to prioritize areas in which the level of knowledge and adequacy of methods must be improved in order to perform a future full safety assessment for SFL.

The methodology used for SE-SFL follows the basic methodology established in the safety assessments SR-Site and SR-PSU, but is adapted in view of the objectives of SE-SFL. The evaluation focuses on a few sections of the Swedish radiation safety authority's (SSM) regulations on post-closure safety, the risk criterion and requirements on post-closure barrier robustness. The time scale of the evaluation is one million years. For SE-SFL a catalogue of features, events and processes (FEP) has been established as basis for the analysis. Furthermore, an initial state has been defined based on the proposed repository concept and example site data from SKB's site investigation programme at Laxemar, Oskarshamn municipality. Based on the initial state and assumed data a reference evolution is analysed to understand the overall evolution of the proposed repository concept. Three reference external conditions are defined to represent different climate conditions; present-day conditions, the influence of an increased greenhouse effect, and a simplified glacial cycle.

A set of evaluation cases is used to quantify the potential for the proposed repository concept to meet applicable criteria on the maximum annual effective dose to humans after closure. The set includes a simplified and stylized base case, and cases that evaluate alternative conditions in the waste vaults and the repository environment, uncertainties in bedrock properties, discharge area, and climate conditions. The results show that the intact barrier system of BHA and the slowly degrading concrete barrier system of BHK are very efficient for retaining radionuclides in the waste vaults given the conditions at the example site. The near-field barriers have the most important role for retention.

The evaluation shows that the repository concept for SFL has potential to fulfil regulatory requirements under suitable conditions, given that further efforts will need to be undertaken in a future full safety assessment to underpin a compliance discussion. In total the results of the radionuclide transport and dose calculations indicate that the conditions assumed in the base case yield doses that are too high to comply with the risk criterion. However, the full set of evaluation cases indicate conditions and further efforts that could improve the performance and analysis of the repository. These include obtaining suitable site conditions, such as low groundwater flow rates, and reduced uncertainties in the radionuclide inventory. Furthermore, technical developments and optimisation of the repository design and components can be used to improve repository performance. Generally, the results indicate that the barrier systems of BHA and BHK have the potential to withstand relevant FEPs. Further analysis and quantification of effects on doses are however necessary in future assessments to define the conditions under which the repository concept has the potential to fulfil the requirements on barrier system robustness. This is especially true for BHA.

Developments for future assessments should include an adaption of the safety analysis methodology and its implementation in a licensing context. Moreover, all relevant requirements need to be identified and addressed and the site selection and characterisation carried out. Research and development linked to the cautious or simplifying assumptions underlying the radionuclide transport and dose calculations can be used to improve a future safety analysis. Improvements can also arise from technical developments of components of the repository that take into account considerations of its interactions with its environs. Reduced uncertainties in the characterisation of the waste inventory and its chemical properties could potentially have a large impact on the results of the safety assessment.



# Sammanfattning

Slutförvaret för långlivat avfall (SFL) planeras att uppföras för slutförvaring av det svenska långlivade låg- och medelaktiva radioaktiva avfallet. Detta dokument utgör huvudrapporten för den första utvärderingen av säkerhet efter förslutning för ett föreslaget förvarskoncept för SFL. Enligt konceptet utformas SFL som ett geologiskt slutförvar med två bergssalar: BHA med bentonitåterfyllnad för historiskt avfall och BHK med betongåterfyllnad för interndelar från kärnkraftverken. Valet av plats för SFL har ännu inte skett och endast en första uppskattning av inventariet av radionuklider och andra material i SFL finns tillgänglig. Syftet med säkerhetsvärderingen för SFL (SE-SFL) är att tillhandahålla underlag för de efterföljande stegen i utvecklingen av SFL. En målsättning är att utvärdera under vilka förhållanden, i avfallet, barriärerna, och förvarets omgivning, den föreslagna förvarsutformningen har möjlighet att möta myndighetsföreskrifterna gällande strålsäkerhet efter förslutning. Vidare kan resultaten av SE-SFL användas för att prioritera de områden där kunskapsnivån eller metoder behöver förbättras för att kunna genomföra en framtida fullständig analys av säkerhet efter förslutning för SFL.

Metodiken som använts i SE-SFL följer den grundläggande metodiken som fastställts i säkerhetsanalyserna SR-Site och SR-PSU, men har anpassats givet målsättningen för SE-SFL. Utvärderingen fokuserar på två delar av SSM:s föreskrifter, riskkriteriet och krav på barriärernas tålighet. Tidsskalan för utvärderingen är en miljon år. Som utgångspunkt för analysen har en katalog över egenskaper, händelser och processer (FEP) etablerats för SE-SFL. Vidare har ett initialtillstånd definierats baserat på föreslaget förvarskoncept och data för en exempelplats från SKB:s platsundersökningsprogram i Laxemar i Oskarshamns kommun. Givet initialtillståndet och antagna data analyseras en referensutveckling i syfte att förstå den övergripande utvecklingen för det föreslagna förvarskonceptet. Tre varianter av externa referensförhållanden definieras för att representera olika klimatförhållanden; dagens förhållanden, påverkan av en ökad växthuseffekt, samt en förenklad glaciationscykel.

En uppsättning utvärderingsfall används för att kvantifiera möjligheten för det föreslagna förvarskonceptet att uppfylla tillämpliga kriterier för den maximala årliga effektiva stråldosen för människor efter förslutning. Uppsättningen inkluderar ett förenklat och stiliserat basfall, samt fall som utvärderar alternativa förhållanden i bergssalarna och i förvarets omgivning, osäkerheter i egenskaper i berggrunden, utsläppsområde, och klimatförhållanden. Resultaten visar att det intakta barriärsystemet i BHA och barriärsystemet i BHK, med långsamt degraderande betong, ger mycket effektiv retention av radionuklider i bergssalarna givet förhållandena på exempelplatsen. Barriärerna i närfältet spelar störst roll för retentionen.

Utvärderingen visar att förvarskonceptet för SFL har möjlighet att uppfylla myndighetsföreskrifterna under lämpliga förhållanden, givet att ytterligare ansträngningar måste göras i en framtida fullständig säkerhetsanalys för att underbygga en diskussion om uppfyllnaden. Som helhet indikerar resultaten av radionuklidtransport- och dosberäkningarna att de förhållanden som antas i basfallet ger för hög dos för att uppfylla riskkriteriet. Emellertid indikerar hela uppsättningen av utvärderingsfall förhållanden och ytterligare ansträngningar som kan förbättra prestandan och analysen av förvaret. Dessa inkluderar att få lämpliga platsförhållanden så som lågt grundvattenflöde, samt att minska osäkerheten i radionuklidinventariet. Dessutom kan teknisk utveckling och optimering av förvarsutformning och komponenter användas för att förbättra förvarets prestanda. Resultaten indikerar att barriärsystemen för BHA och BHK har möjlighet att motstå relevanta FEP. Ytterligare analys och kvantifiering av effekter på dosen är emellertid nödvändiga i framtida analyser för att definiera de förhållanden under vilka förvarskonceptet har möjlighet att uppfylla kraven på barriärsystemets tålighet. Detta gäller särskilt BHA.

Utvecklingen för framtida analyser bör omfatta en anpassning av säkerhetsanalysmetodiken och dess implementering till en tillståndsansökan. Dessutom måste alla relevanta krav identifieras och adresseras och valet och karakteriseringen av platsen för slutförvaret genomföras. Forskning och utveckling som kopplar till försiktiga eller förenklade antaganden som ligger till grund för radionuklidtransport- och dosberäkningarna kan användas för att förbättra en framtida säkerhetsanalys. Förbättringar kan också fås genom teknisk utveckling av komponenter i förvaret som tar hänsyn till dess interaktioner med dess omgivning. Minskade osäkerheter i karakteriseringen av avfallsinventariet och dess kemiska egenskaper kan potentiellt ha stor inverkan på resultaten av säkerhetsanalysen.



# Executive summary

## S1 Objectives

The repository for long-lived waste (SFL) is planned to be used for disposal of the Swedish long-lived low- and intermediate-level radioactive waste. This includes long-lived waste from the operation and decommissioning of the Swedish nuclear power plants, from early research in the Swedish nuclear programmes (legacy waste), from medicine, industry, and from research which includes the European Spallation Source (ESS) research facility.

This report constitutes the main report for the evaluation of post-closure safety for a proposed repository concept for SFL. The purpose of the SFL safety evaluation (SE-SFL) is to provide input to the subsequent, consecutive steps in the development of SFL. These consecutive steps include further development of the design of the engineered barriers and the site-selection process for SFL. More specifically, there are two main objectives for SE-SFL. The first is to evaluate conditions in the waste, barriers, and the repository environs under which the repository concept has the potential to fulfil the regulatory requirements for post-closure safety. The second is to provide SKB with a basis to prioritize areas in which the level of knowledge and adequacy of methods must be improved in order to perform a subsequent, full safety assessment for SFL.

## S2 Previous analyses, research and development

SFL is part of the Swedish system for management of radioactive waste and a first preliminary repository concept for SFL was presented in the context of cost calculations for radioactive waste management (Plan 93; SKB 1993). Because the purpose of Plan 93 was to give cost estimations, no safety related analyses were discussed. The first quantification related to safety was presented in a pre-study of final disposal of long-lived low- and intermediate-level waste. The objective was to make a first preliminary and simplified assessment of the near field as a barrier to radionuclide dispersion (Wiborgh 1995). In 1999, a preliminary safety assessment was presented that focussed on a quantitative analysis of the environmental impact for a reference scenario (SKB 1999a). The objective was to investigate the capacity of the facility to act as a barrier to the release of radionuclides and the importance of the repository location. The assessment was reviewed by the authorities (SKI/SSI 2001). One of the main comments was a lack of a clear account of the basis for the selection of the design and that no design alternatives had been considered.

Reflecting the comments from the authorities, possible solutions for management and disposal of the Swedish long-lived low- and intermediate-level waste were examined in the SFL concept study (Elfving et al. 2013). Among the considered alternatives a system was proposed as a basis for further assessment of post-closure safety, which is evaluated in the present safety evaluation for SFL.

The outcome of this evaluation is then to be used in further iterations of the safety analysis and development process that the SFL repository program follows. In accordance with the Nuclear Activities Act (SFS 1984:3), important research needs for the SFL programme that emerge as a result of SE-SFL will be reported in SKB's research, development and demonstration (RD&D) programme. An important aspect of this is to ensure that the industry has well-founded information to support long-term planning.

## S3 Prerequisites

### S3.1 Repository concept

The repository concept for SFL was proposed in the concept study of Elfving et al. (2013) based on an examination of a range of alternatives. According to this concept, SFL is designed as a deep geological repository with two different sections:

- One waste vault, designed with a concrete barrier, BHK, for metallic waste from the nuclear power plants.

- One waste vault, designed with a bentonite barrier, BHA, for the waste from Studsvik Nuclear AB, Cyclife Sweden AB and AB SVAFO.

A schematic illustration of SFL is displayed in Figure S-1. In SE-SFL, it is assumed that the waste vaults are located at 500 m depth. BHK is approximately 135 m long and BHA is approximately 170 m long. Both vaults have a cross sectional area of approximately  $20 \times 20 \text{ m}^2$  (see further details in Section 4.3).

In BHK, the barrier system is concrete based. The waste packages are placed in six separate concrete caissons and grouted. The vault is backfilled with concrete. The design of the waste vault along with the dimensions are briefly described in the following and a detailed account is given in Chapter 4.

BHA is designed for the disposal of waste packages with a low activity but less well-known material composition and radionuclide inventory. The waste vault comprises a concrete structure in which the waste is deposited and grouted. The structure is surrounded by a thick layer of bentonite with a high dry density and the top part of the vault is to be filled with bentonite pellets (Figure S-1). The bentonite functions as a low permeability medium enclosing the waste. The backfill material in BHA is assumed to have similar properties to the buffer material in the Spent Fuel Repository. The concrete structure provides radiation shielding during the operational phase.

To seal the waste vaults, tunnel sections adjacent to the vaults are filled with bentonite and are confined by mechanical plugs. Furthermore, the other tunnels at repository level are backfilled with crushed rock or a similar material. The access tunnels are backfilled with crushed rock and include a plug section made up of a hydraulically tight section of bentonite. The first 50 m of the access tunnels are backfilled with boulders and a concrete plug is cast to obstruct unintentional intrusion into the repository. The vertical shaft connecting different levels of the access tunnel and the repository is sealed at the connections to the tunnels to restrict the flow of water.

### S3.2 Inventory

About one third of the volume of the waste allocated to SFL originates from the Swedish nuclear power plants (NPPs). The long-lived low- and intermediate-level wastes from the NPPs that are allocated to BHK typically consist of neutron-activated components from inside or close to (0.5–1.0 m) the reactor core. The different components disposed in BHK are described in the Section 4.2.6.

The waste allocated to BHA originates from Studsvik Nuclear AB (SNAB), Cyclife Sweden AB and AB SVAFO, and comprises previous and future waste from research carried out at the Studsvik site as well as waste from decommissioning. Furthermore, the waste collected from other producers of radioactive materials in Sweden, such as those involved in medicine, industry and research, is included in the presented quantities.

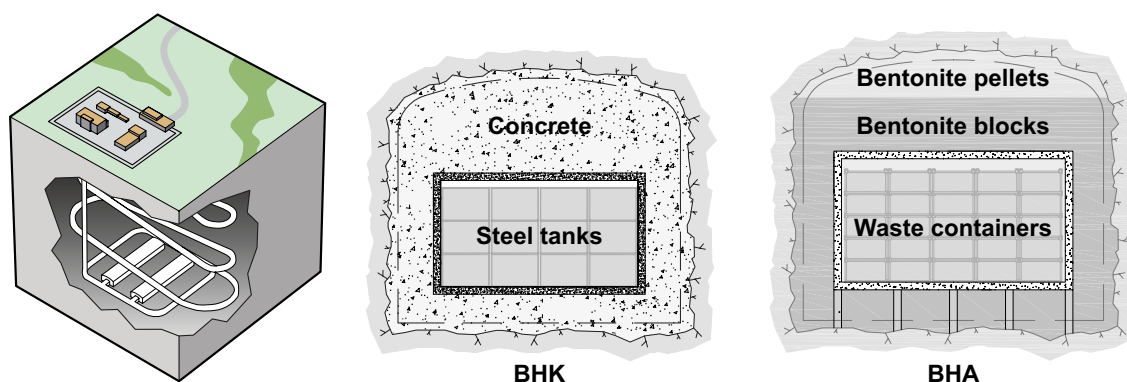


**Figure S-1.** Preliminary facility layout and the proposed repository concept for SFL (left), with one waste vault for metallic waste from the nuclear power plants (BHK, centre) and one waste vault for waste from Studsvik Nuclear AB, Cyclife Sweden AB and AB SVAFO (BHA, right).

The total radionuclide inventory in BHK at closure is estimated to be about  $2 \times 10^{17}$  Bq. This corresponds to 98 % of the total radioactivity in SFL at closure. The inventory at repository closure is dominated by the relatively short-lived radionuclides Ni-63 and Co-60 and one thousand years after closure only about 1 % of the initial radioactivity remains.

The radionuclide inventory of the legacy waste is highly uncertain. The total radionuclide inventory in the legacy waste is estimated to be about  $4 \times 10^{15}$  Bq at repository closure. The inventory is based on relatively sparse data from gamma spectroscopy and sampled surface contamination in combination with a correlation procedure. The radionuclide inventory data also include activity calculated from the reported actinide content (i.e. Th-232, U-235, U-238 and Pu-239). The estimated inventory at repository closure is dominated by the very long-lived radionuclides Tc-99 and Cl-36 and one million years after closure the radioactivity of the waste is about 2 % of the initial radioactivity. Details of the inventories and the different information sources that have been used to gather information on the waste disposed of in SFL as well as the calculation models used are given in Section 4.2.6 (BHK) and Section 4.2.7 (BHA).

The radioactive waste from the operation of the ESS is planned to be disposed of in SFL. The most active waste from ESS will be components that have been directly irradiated. Some of the components will be exchanged at regular intervals during the operational period, thus giving rise to operational waste, whereas others will not be disposed of until the decommissioning phase. Since the plans for the construction and operation of ESS are not yet finalised, only limited information is available concerning the amount and composition of the likely waste arising. Due to these uncertainties, the ESS waste volume and amount of material are not considered in SE-SFL. Instead, the ESS radionuclides that are not found in the BHK and BHA inventories, including decay chains, are included in a dedicated evaluation case to assess which of the two vaults is most suitable (Section 7.2).

### S3.3 Example site and data

No site has yet been selected for SFL and therefore data from SKB's site investigation programmes for the Spent Fuel Repository and for the extension of the repository for short-lived radioactive waste (SFR) have been utilized in SE-SFL. In order to have a realistic and consistent description of a site for geological disposal of radioactive waste, data from the Laxemar site in Oskarshamn municipality, for which a detailed and coherent dataset exists, are used. The example location for the SFL repository was selected based on an initial hydrogeological analysis for SE-SFL of the bedrock volume that was earlier found suitable for a potential Spent Fuel Repository within the Laxemar site (Section 1.2).

The repository design is based on the SFL concept study and repository components and geometries are detailed in Section 4.3. Material properties are to a large extent based on the properties of corresponding materials that are used in the Spent Fuel Repository and SFR. Information on climate and climate-related conditions, such as shoreline displacement, that is assumed within SE-SFL is described based on SKB's earlier safety assessments for Laxemar and Forsmark and updated information from the general literature as detailed in Sections 4.4, 6.2.1, 6.3.1 and 6.4.1. Data for the surface and bedrock systems are connected to the example site and data from Laxemar and Forsmark are used as described in previous paragraph (Sections 4.5 and 4.6).

## S4 Methodology – safety evaluation

The present analysis is denoted *safety evaluation* to reflect its status as a preliminary analysis that is intended to evaluate the proposed repository concept (Section S3.1). One intention with using the term *safety evaluation* has been to make it clear that SE-SFL does not aim at fulfilling the requirements in full, as stipulated for a *safety analysis* defined in the regulations. This gives the freedom to adapt the methodology to the needs of the current stage in the programme in contrast to strictly follow the objectives of the regulations.

The methodology used for SE-SFL follows the basic methodology established in the safety assessments SR-Site and SR-PSU. The methodology was however adapted for the purpose of addressing the general objectives of SE-SFL (Section S1). To meet the first objective, the influence of the conditions in the repository and its environs need to be evaluated based on the conditions at an example site and a design

based on the concept study. To meet the second objective, the resulting information can then be used as input to the site selection process and future safety analysis iterations that further develop the requirements on the geosphere and the technical barriers. This is in line with the iterative safety assessment process that all SKB's repository programmes follow. The iterative approach is standard internationally (NEA 2012) and planned and documented in SKB's RD&D programme (SKB 2019).

There is a degree of generalisation in the evaluation since no site has been selected and SE-SFL is the first evaluation of post-closure safety for the proposed repository concept. Therefore, some changes are introduced to the basic methodology and it is not applied as rigorously as in a safety analysis for a license application or a safety report for an operating facility (Section 2.1). The outline of the methodology in ten steps is shown in Figure S-2.

The evaluation focuses on a few sections of the Swedish radiation safety authority's (SSM) regulations on post-closure safety as detailed in Section 2.2. Based on the objectives of SE-SFL these are the risk criterion and requirements on post-closure barrier robustness. The timescale of the evaluation is chosen to be one million years.

The management of uncertainties is central to a safety analysis and is therefore given considerable focus in SE-SFL. In line with the general advice to SSM's regulations on disposal of nuclear waste, aspects of scenario uncertainty, system uncertainty, model uncertainty, parameter uncertainty, and spatial variation in parameters used to describe the bedrock are addressed. Efforts have been undertaken in SE-SFL to demonstrate an understanding of the repository evolution and to ensure the applicability of models, parameter values and other assumptions used for the description and quantification of repository performance. Within the modelling studies for the reference evolution and for the radionuclide transport, the applicability of the models and assumptions is discussed.

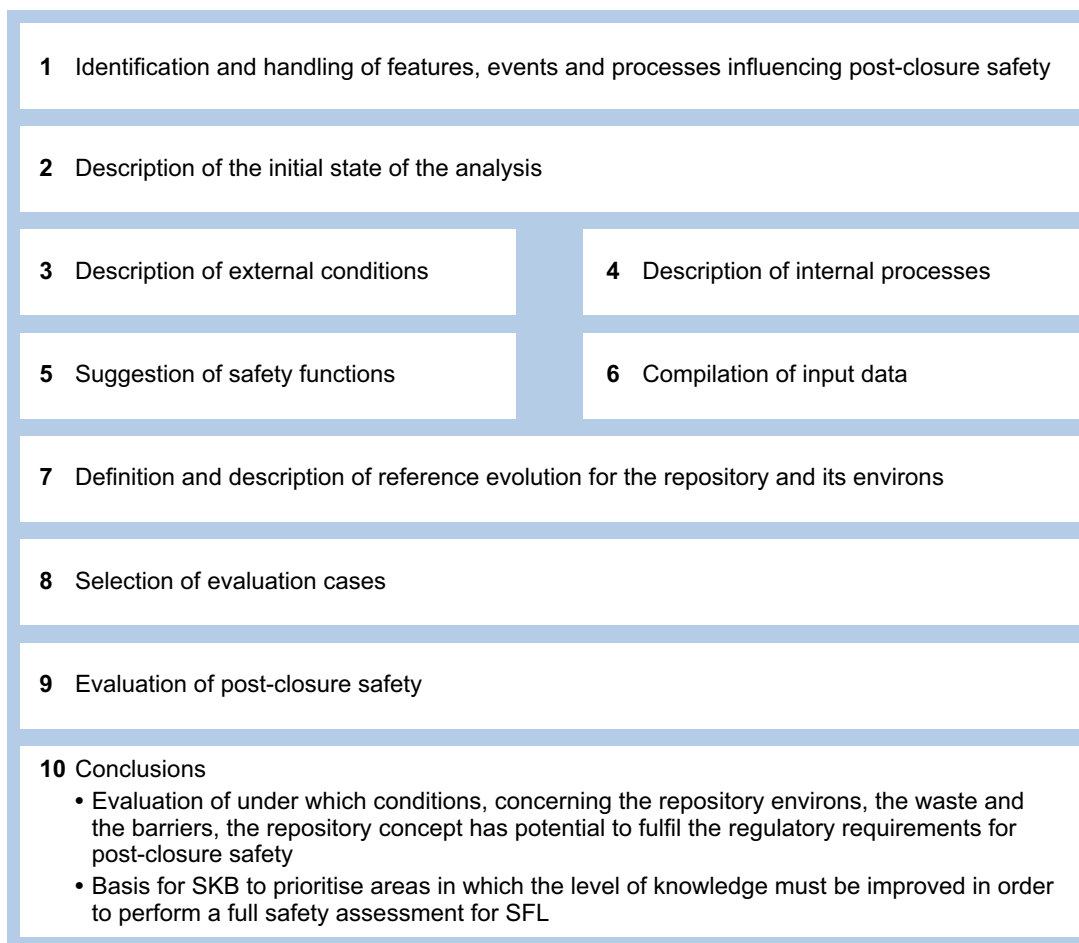


**Figure S-2.** Overview of the methodology applied for the evaluation of post-closure safety for the proposed repository concept for SFL.

SE-SFL has been conducted in accordance with SKB's quality management system. A quality plan for SE-SFL was established that points to the most relevant parts of SKB's quality management system and discusses the project-specific implementation of it. Modelling work in SE-SFL is documented following the requirements in SKB's quality management system. The goal has been to ensure, in a verifiable manner, that the applied input data are appropriately chosen for the computational tools and their underlying models. For the biosphere, a quality assurance process has been implemented based on the experience from SR-PSU (Section 2.7). The QA process is to make sure that information on the usage, sources, review, storage, and involved persons and their roles is documented and accessible.

## **S5 FEP analysis and documentation**

The first step in the safety evaluation involves identifying all features, events and processes (FEPs) that may influence post-closure safety and deciding which of these need to be included (see Chapter 3). This is done by screening potentially important FEPs that influence post-closure safety. Experience gained from previous safety assessments for the Spent Fuel Repository and for SFR, and international databases of relevant FEPs that affect post-closure safety are utilised (Section 3.2.1) for establishing the SE-SFL FEP catalogue. In particular, the SR-PSU FEP catalogue has been used as a basis with changes introduced to capture the differences between the SFR and SFL repositories. The objective of the FEP processing in SE-SFL is two-fold; to make sure that all factors that may influence post-closure safety are identified, and to document the handling of each FEP in the SE-SFL FEP catalogue. In this sense the SE-SFL FEP catalogue constitutes a "look-up-table" with a brief description of the handling of each FEP and references to relevant reports that detail the handling further. Further, FEPs are labelled either "considered" or "not considered". Considered FEPs have been taken into account in the reference evolution (Chapter 6), whereas non-considered FEPs have not been taken into account in SE-SFL.

## **S6 Initial state and compilation of data**

The initial state is defined as the expected state of the repository and its environs at closure, under the assumption that the repository is designed and constructed in accordance with the proposed repository concept and placed at the example location at approximately 500 m depth in the position in Laxemar assumed for SE-SFL (Chapter 4). Further, material properties for the repository components are taken from previous safety assessments. For instance, it is assumed that the BHA backfill is constructed with bentonite that is similar to that planned for the buffer in the Spent Fuel Repository, and the BHK backfill is constructed with concrete similar to the construction concrete employed in the existing SFR repository. In SE-SFL, the repository is assumed to be closed in 2075 AD.

All data used in the quantification of repository evolution and in radionuclide transport and dose calculations are selected using a structured process (Section 2.7). The selection of data is determined by the conditions that exist over the period of relevance.

## **S7 Safety functions**

Safety functions are utilised in SKB's safety analysis methodology to qualitatively define what roles a repository component has for post-closure safety and can generally be used for several purposes as detailed in Section 5.1. In SE-SFL, the main objective is to introduce a set of safety functions that can be used in the further development of the safety analysis and the design of the concept.

The idea behind the proposed concept for SFL is to use a system of engineered and natural barriers to reduce the mobility and transport of radionuclides. The system includes the waste form, packaging and surrounding grout, barriers, and closure components. In addition to the engineered barriers, the rock surrounding the repository as a natural barrier can also be attributed safety functions. The safety functions for SE-SFL are defined based on the safety principle for the proposed repository concept for SFL, *retardation* (Elfving et al. 2013). The nature of the safety functions is deduced from the requirements that the internal processes and external conditions put on repository performance.

The waste form, packaging and surrounding grout are handled as a single entity when it comes to safety functions in SE-SFL. For the waste domains of BHA and BHK, the safety function is *good retention*, as determined by pH, redox potential, concentration of complexing agents in BHA, available sorption surface area, and the corrosion rate in BHK. For the bentonite barrier of BHA and the concrete barrier in BHK the safety functions defined are *low flow in the waste vault* and *good retention*. For the closure components and the natural bedrock barrier the safety functions are *low flow*.

## S8 Reference evolution

The purpose of defining and analysing a reference evolution is to understand the overall evolution of the proposed repository concept at a relevant example location under representative external conditions that may influence post-closure safety. To this end, identified FEPs that can affect the post-closure performance of the system are considered. The understanding of the overall evolution serves as a basis for the evaluation of post-closure safety of the repository.

Three variants of reference external conditions are chosen for the evaluation. The *base variant* is a hypothetical condition in which external (climatic) conditions are assumed identical to those at the present-day during the complete analysis period of 1 million years. Thus, the initial state climatic conditions, defined in Chapter 4, are assumed in this variant. In addition, two variants, representing time-varying external conditions, are defined based on existing knowledge on past and future climate evolution (Section 2.5.3). In the second variant, a future climate affected by anthropogenic actions is described, which is denoted the *increased greenhouse effect climate variant*. The third variant is denoted the *simplified glacial cycle climate variant*. This variant is based on the overall climate development in the reconstruction of the last glacial cycle at a Swedish Baltic coastal site, with periods of temperate climate, periglacial conditions with permafrost, ice-sheet development and variations in shore-level (Figure S-3).

The starting point for the reference evolution is assumed to be the initial state defined in Chapter 4. For simplicity no analyses of the evolution during construction and operation of the repository are performed in SE-SFL, nevertheless the defined initial state is judged to be applicable. The evolution of the repository and its environs, given the external reference conditions in each of the reference evolution variants, has been analysed as described for the one-million-year analysis period in Chapter 6. The conditions and evolution of the repository (the deposited wastes, waste packaging, engineered barriers and other repository structures) and its environs (the bedrock surrounding the repository and the surface systems in the repository area) are described.

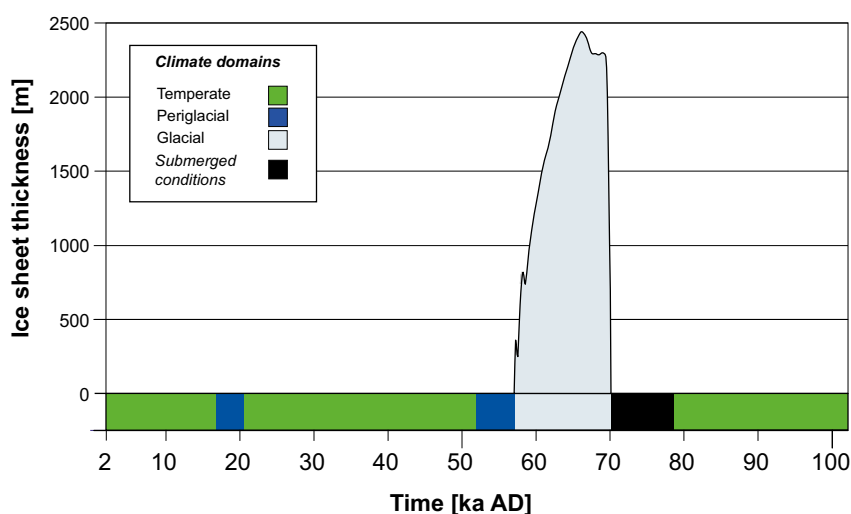


**Figure S-3.** Evolution of climate and climate-related conditions 100 000 years into the future for the simplified glacial cycle climate case for Laxemar, shown as a succession of climate domains and submerged periods (top panel). The submerged period following deglaciation shows the duration of water-covered conditions for the area which receives most of the discharge from the repository. The evolution from 2000 AD to 102 000 AD is repeated every 100 000 years until one million years after repository closure to represent the effects of repeated Late Quaternary glacial–interglacial cycles.

## S9 Evaluation of post-closure safety

### S9.1 Selection of evaluation cases and modelling methodology

To quantify the potential for the proposed repository concept to meet applicable criteria on the maximum annual effective dose to humans after closure, a set of evaluation cases is defined in SE-SFL (Section 2.5.8).

The performance of the repository design at the example location is first described and evaluated, based on the analysis of the results of the radionuclide transport and dose calculations for a base case, i.e. the *present-day evaluation case*. This evaluation case is defined for the base variant of the reference evolution (Section 6.2) and its implementation is described in Section 7.4. The base case is simplified and stylized for ease of interpretation and straightforward comparison with the other evaluation cases with alternative assumptions or temporal evolutions. The base case assumes constant, present-day climatic and other external conditions throughout the full assessment period. Realistic, and in some respects simplified, assumptions are made with respect to internal conditions, based on the current knowledge on the properties of the waste and available barrier materials as analysed in the reference evolution. The choice of simplified, rather than conservative, assumptions is motivated by the probing nature of SE-SFL. It is further assumed, as in all evaluation cases in SE-SFL, that the repository is constructed according to the proposed design concept. Importantly, since SE-SFL is not part of a licensing application, the base case is not intended to establish a main scenario as defined by the regulatory guidelines.

One important aspect that has been the objective of SE-SFL is to analyse under which conditions the repository concept has the potential to fulfil the regulatory criteria. Based on this objective a set of evaluation cases has been defined and analysed in SE-SFL that evaluate the sensitivity of the resulting activity release and dose in the base case to specific assumptions made for conditions in the repository and its environs, (Section 8.2). These cases are chosen to illustrate conditions in the repository and the repository environs that are likely to improve the repository performance in comparison with the base case. For instance, cases with *lower groundwater flow rate* than at the example location and *alternative concrete backfill* are included. Moreover, cases that evaluate the sensitivity of assessment endpoints to selected uncertainties in the geosphere and biosphere are included. The uncertainty relating to the future climate evolution is handled within separate cases, which are based on the *increased greenhouse effect* and *simplified glacial cycle* variants of the reference evolution. Finally, a case relating to exposure pathways including a drilled well is analysed. The potential to fulfil the regulatory criteria is evaluated against the dose corresponding to SSM's risk criterion and the requirements on post-closure barrier robustness.

The SE-SFL radionuclide transport modelling methodology is based on the experiences from SKB's previous safety assessments SR-Site and in particular SR-PSU, but includes some simplifications given the objectives of SE-SFL. Radionuclide transport and dose modelling is performed with a set of mathematical models representing different parts of the repository and its environs. The model chain starts with the near-field model that describes the release, transport and retention of radionuclides in the waste domain and the surrounding engineered barriers. Moreover, the activity release at the waste vault–bedrock interface is calculated. The geosphere model describes the subsequent transport and retention of radionuclides through the bedrock towards the surface. Finally, the biosphere model consists of sub-models describing transport and accumulation in the surface ecosystems, natural and cultivated, and determines the resulting doses to humans. The modelling approach, including radionuclides included in the analysis and the models utilized in SE-SFL to calculate radionuclide transport and dose are described in Sections 7.1–7.3.

### S9.2 Function of the repository design at the example location

The function of the repository design at the example location is described based on an analysis of the results of the radionuclide transport and dose calculations for the base case. The safety principle for the proposed repository concept, *retardation*, is achieved by upholding the safety functions *good retention* and *low flow* in the waste vaults and the bedrock for an adequate period of time (Chapter 5). Effective retardation ensures that annual near-field releases are only small fractions of the total activity inventory at repository closure. Additionally, releases and resulting doses are further decreased by retention and radioactive decay, which is most effective for radionuclides with short half-lives relative to their retention time in the near field (or geosphere).

The intact barrier system of BHA is very efficient for retaining radionuclides in the inventory given the postulated groundwater flow rates, as the analysis of the base case shows (Section 7.5). The initial activity of C-14, Mo-93, and Ni-59 is substantially reduced within the near-field (see Figure S-4). In addition, for the very long-lived radionuclides Tc-99 and Cl-36, a substantial part of the inventory decays in the near-field. Retention is linked to diffusion-controlled transport within and out of the bentonite, as well as sorption onto cement in the waste and onto bentonite in the backfill. The maximum annual doses are limited due to the considerable transport resistance offered by the bentonite.

The barrier system of BHK is also efficient for retaining radionuclides in the inventory, as the analysis of the base case shows (Section 7.5). In general, the mechanisms contributing to the retention are the slow release of induced activity from the metal through corrosion, the rate of which is reduced due to the alkaline conditions in the concrete, sorption onto cement of many of the radionuclides in the inventory and slow advective transport through the concrete barrier. The maximum annual doses are limited due to the slow release relating to steel corrosion and considerable transport resistance offered by the concrete backfill.

Similar fractions of the initial inventory of C-14 decay in the near-fields of BHA and BHK (93 % and 98 % respectively, Figure S-4). However, the effect is achieved by different mechanisms, with retardation in bentonite backfill and limited diffusive transport into bedrock fractures being the main factor in BHA and slow release by corrosion in BHK. Retention is even more efficient for Mo-93 with more than 99 % decay in the near-field. This is because Mo-93 has a low but non-zero sorption for cement and a half-life that is somewhat shorter than that of C-14. Of the radionuclides that contribute significantly to the near-field release and eventual dose, decay of retained activity is least important for the long-lived and low-sorbing Cl-36; only about 40 % of the initial inventory in either waste vault decays in the near-field. However, retention in the near-field is still important since it leads to distribution of the release in time, which reduces the annual release to a small fraction of the inventory. For Tc-99, with a half-life similar to that of Cl-36 (211 ka as compared to 301 ka for Cl-36), retention in the BHA and BHK near-fields is stronger than for Cl-36 due to sorption. Tc-99 retention in the backfill is significantly stronger in BHK than in BHA, since sorption of Tc-99 in BHA is assumed to be strongly reduced (by a factor of 10 000) due to formation of non-sorbing complexes with cellulose-degradation products.

The geosphere and biosphere also contribute to retention, but their roles are generally not as important as the near-field retention of radionuclides in BHA and BHK (Figure S-4).

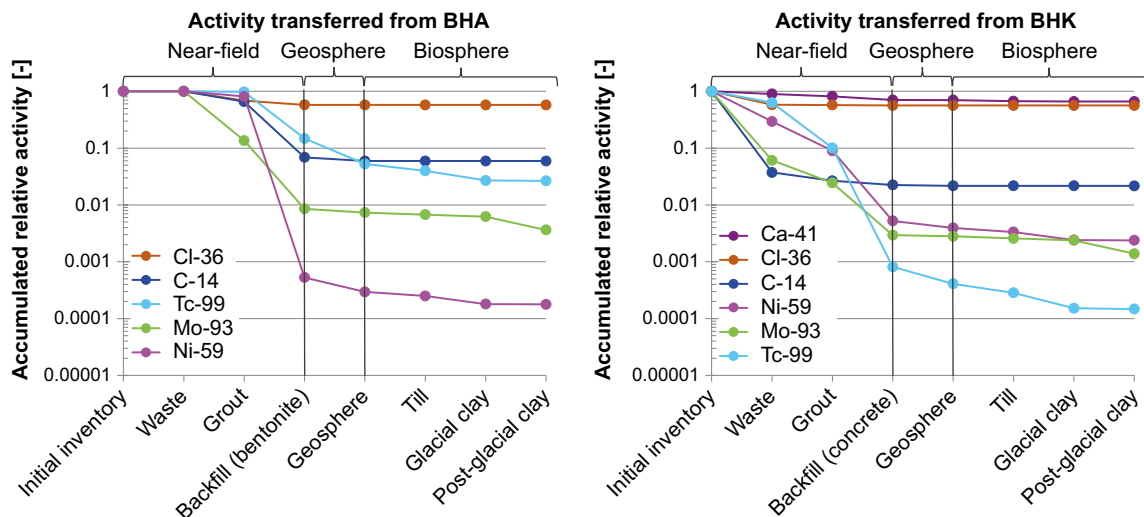


**Figure S-4.** Relative activity transferred along the pathway from the initial inventory in BHA (left panel) and BHK (right panel) to the biosphere, accumulated over the entire analysis period of one million years in the base case. A selection of relevant radionuclides that contribute significantly to the dose from BHA or BHK are shown.

In total the results of the radionuclide transport and dose calculations indicate that the conditions assumed in the base case yield doses that are too high to comply with the risk criterion for the BHA and BHK inventories underlying SE-SFL (Figure S-5). Further efforts are thus needed to improve the performance and analysis of the repository, which is discussed in Section S10 and Chapters 9 and 10.

The dose calculations show that the exposure pathways associated with the land use practice draining and cultivation of a mire in the discharge area, which is assumed in the base case, causes the highest doses. This is primarily because radionuclides can accumulate in peat over a long period of time prior to exposure, and because the dose-contributing radionuclides predominantly yield dose through ingestion of food.

## S10 Discussion and conclusions

The evaluation shows that the repository concept for SFL has potential to fulfil regulatory requirements under suitable conditions, given that further efforts will need to be undertaken in a future full safety assessment to underpin a compliance discussion. In total the results of the radionuclide transport and dose calculations indicate that the conditions assumed in the base case yield doses that are too high to comply with the risk criterion for the BHA and BHK inventories underlying SE-SFL. However, the full set of evaluation cases indicate conditions and further efforts that could improve the performance and analysis of the repository, as briefly described in the following and discussed in more detail in Chapters 9 and 10. The conclusions with respect to the two main objectives for SE-SFL as stated in Section S1 are presented in the following.

### S10.1 Conditions under which the repository concept has the potential to fulfil the regulatory criteria

One important aspect that has been the objective of SE-SFL is to analyse under which conditions the repository concept has the potential to fulfil the regulatory criteria. The evaluation focuses on the risk criterion and the potential of the barrier system to withstand relevant FEPs. Based on this objective a set of evaluation cases has been defined and analysed in SE-SFL. The set includes the effects of conditions in the waste vaults, conditions in the repository environments, uncertainties in bedrock properties, discharge area and a drilled well, as well as climate conditions.

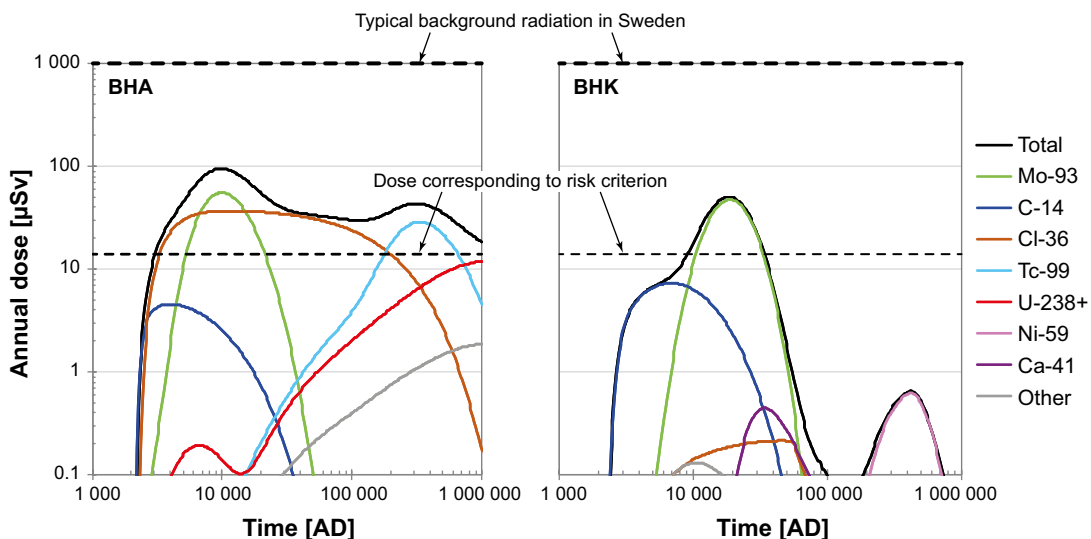


**Figure S-5.** Annual doses from BHA (left panel) and BHK (right panel) in the present-day evaluation case. The total dose (black line) is shown together with the contributions from individual radionuclides (coloured lines). Dashed black lines show the dose corresponding to the regulatory risk limit (14  $\mu\text{Sv}$ ), and a typical dose due to background radiation in Sweden (1000  $\mu\text{Sv}$ ). Figure corresponds to Figure 5-18 in the Radionuclide transport report.

### **Risk criterion**

Based on the results of these evaluation cases, the following can be concluded regarding the conditions under which the analysed repository concept for BHA has the potential to fulfil the regulatory criteria on risk:

- With an inventory for the dominating radionuclides Mo-93, Cl-36, C-14 that can be shown to be more than a factor 10 lower than the estimate used in SE-SFL, and not substantially higher for other radionuclides, the repository concept would have the potential to meet the risk criterion given the assumptions made in the base case.
- At times after 100 000 years after repository closure, Tc-99 becomes dominating. As for the other dose-dominating radionuclides, a 10 times lower inventory would imply that the dose corresponding to the regulatory risk limit would not be exceeded. An even more pronounced effect can be achieved if the cautious assumption of high concentrations of complexing agents in the waste domain persisting for the entire analysis period can be relaxed. A further consideration is that according to SSM's general advice, a strict comparison with the risk limit is not meaningful after 100 000 years after closure. Besides using supplementary indicators of the protective capability of the repository, the underlying causes of a risk exceeding the criteria after 100 000 years after closure should be reported together with possible measures to improve the protective capability of the repository.
- With 100 times lower groundwater flow rates than assumed in the base case (i.e. with a typical advective travel time in the bedrock of  $10^4$  years) the resulting doses become significantly lower than the dose corresponding to the risk criterion given the other assumptions in the base case. In contrast, a factor 10 lower groundwater flow rate (i.e. with a typical advective travel time in the bedrock of  $10^3$  years) implies dose results exceeding the dose corresponding to the risk criterion. Lower flows can be achieved by selecting a site with lower flows than at the example site or possibly by increasing the depth of the repository.
- Initially submerged conditions, with initially 100 times lower groundwater flow rates than assumed in the base case that limit the near-field releases, are advantageous for the protective capability of the repository for as long as they persist. But since the BHA inventory, as shown in the base case, potentially can sustain releases for hundreds of thousands of years that yield doses comparable to the dose criterion, submerged conditions would have to persist for a time span of similar length to ensure conditions that have the potential to fulfil the risk criterion.
- The expected evolution of the bentonite barrier needs to be analysed in a full assessment to demonstrate that it will uphold its safety functions for relevant time scales. Moreover, the detailed design of the waste domain and bentonite barrier should be optimised in order to improve repository performance.

For BHK the following can be concluded regarding the conditions under which the repository concept has potential to fulfil the regulatory criteria on risk:

- Less pessimistic assumptions regarding the steel corrosion rate than in the base case improves the potential for the repository to meet regulatory requirements. The potential for reduced releases and doses from BHK associated with the uncertainty in corrosion rate needs to be evaluated in relation to the assumptions about, and uncertainty in, the initial distribution of the radionuclide inventory between the instant release and thicker metal fractions. If smaller instant release fractions can be substantiated, the effect of less pessimistic corrosion rates increases.
- An optimized concrete backfill material that has low hydraulic conductivity, porosity, and diffusivity improves the potential for the repository to meet regulatory requirements. The properties of the concrete developed for the extension of SFR potentially yields a sufficiently good near-field performance. Improved concrete properties should also improve the ability of the concrete to withstand degradation due to cement leaching. The effect on gas transport thereby needs to be considered.
- With 10 times lower groundwater flow rates than assumed in the base case (i.e. with a total flow through BHK of  $10^{-1}$  m<sup>3</sup>/a), the doses resulting from BHK become significantly lower than the dose corresponding to the risk criterion, given the other assumptions in the base case.

- Initially submerged conditions, with initially 100 times lower groundwater flow rates than assumed in the base case and thus with a total flow through BHK of  $10^{-2}$  m<sup>3</sup>/a, are advantageous and yield low doses for as long as they persist. It would require a submerged period of about 50 000 years, with low releases associated with the low groundwater flows, for the dose-contributing radionuclides to decay sufficiently to result in doses that do not exceed the dose criterion given the estimated BHK inventory and other underlying assumptions.
- The detailed design of the waste domain and concrete barrier, for example its geometry and material parameters, should be optimised in order to improve repository performance.

The external conditions related to different climate sequences as analysed in the *increased greenhouse effect* and *simplified glacial cycle* evaluation cases result in doses that are similar to, or lower than, the base case. The *alternative regional climate* evaluation case furthermore shows that there is no large difference between the biosphere responses to releases in different locations along the coast of Sweden that represent alternative regional climates.

The analysis of biosphere transport in the base case assumes that the releases will occur in a specific biosphere object at the example site. The conditions simulated will therefore not necessarily represent the actual discharges at a future selected site. However, the calculations are judged to capture the main features of transport, accumulation and exposure for a suite of possible future conditions. The results of the *alternative discharge area* evaluation show that the resulting doses can vary within several orders of magnitude depending on the biosphere object properties, and that the base case yields among the highest doses. Moreover, the radionuclide-specific dose response to object properties may differ between radionuclides. In consequence, the conditions under which the repository concept has the potential to meet the risk criterion are linked to the properties of the biosphere objects at the selected site. Potential uncertainties regarding into which biosphere objects releases occur are therefore important to consider in future site-specific analyses.

### **Potential to withstand relevant FEPs**

For BHA the most relevant FEPs that influence the temporal evolution of the barrier system are processes that act on the bentonite barrier and these are discussed in the reference evolution (Section 6.2.9). The following emerges from the analyses in SE-SFL:

- Preliminary analysis of the montmorillonite transformation process, described in the reference evolution, indicates that it needs to be considered further, for instance in relation to the design of the bentonite backfill. Furthermore, the process needs to be assessed in terms of its influence on the safety functions of the bentonite, i.e. *low flow in the waste vault* and *good retention*. The aim should be to adequately conceptualise the process in the radionuclide transport calculations, in order to quantify the effect of the transformation process on the resulting dose in future assessments of SFL.
- The bentonite colloid release from the backfill in BHA due to chemical erosion, which requires groundwater with low ionic strength, is discussed in the reference evolution (Sections 6.2.9 and 6.2.7). The process has, however, not been quantified for the conditions at the example site. The results of the geochemical characterisation and modelling of the example site under the assumption of present-day climate indicate that the conditions at repository depth are expected to inhibit colloid release at least for tens of thousands of years (Section 6.2.7). For glacial conditions, however, the results indicate that dilute waters may penetrate to repository depth at the example site (SKB 2010f). The geochemical conditions are site specific and further study is needed in a future assessment for a selected site to assess if the process may lead to erosion and if so whether the amount of bentonite erosion from the BHA backfill is large enough to have implications for the safety functions of the bentonite barrier. It can thereby be noted that the thickness of the bentonite backfill is a design consideration that is linked to this process.
- The mechanical evolution of the bentonite backfill, in particular during the process of bentonite resaturation, is discussed in the reference evolution (Section 6.2.9). The discussion indicates that effects of the resaturation process on the conditions in the waste domain and resulting near-field releases should be analysed in more detail to be able to underpin the discussion on barrier system robustness.

- It can be noted that the bedrock as a natural barrier is part of the barrier system to which the requirement on the ability to withstand relevant FEPs applies. Site characteristics that are favourable for upholding barrier integrity and limiting radionuclide transport will contribute to the potential to meet the regulatory requirement on the ability to withstand relevant detrimental FEPs. The evaluation is thus bound to the site characteristics and a full assessment needs to be carried out when a site has been selected for SFL.

In conclusion, a quantitative analysis of the effect of the evolution of the conditions in the BHA waste vault and associated safety functions is needed in order to define the conditions under which the repository concept has the potential to fulfil the requirements on barrier system robustness. Moreover, it can be noted that the analysis of montmorillonite transformations, colloid release and other processes analysed in the reference evolution can give input to the optimisation of the bentonite barrier properties and geometry when defining the detailed reference design for SFL.

For BHK the most relevant FEPs that influence the evolution of the safety functions over time are processes that act on the concrete barrier. Concrete degradation in BHK leads to alteration of the pH, porosity, hydraulic conductivity and effective diffusivity, and is mainly driven by groundwater interactions.

The main conclusions from the analyses in SE-SFL in relation to the potential to withstand relevant FEPs are the following for BHK:

- The main process that is expected to drive the degradation of the concrete barriers is calcium leaching, which leads to a gradual loss of portlandite and CSH-gel. The degradation rate is very low, primarily due to the low water flow rate in the concrete backfill. The initial porosity and transport properties of the concrete have a stronger impact on the degradation than the concrete composition.
- The low degradation rate in relation to the half-lives of the radionuclides that dominate the initial inventory leads to the conclusion that the barrier is able to withstand these FEPs, granted a sufficiently low initial porosity and favourable transport properties of the concrete (see the *alternative concrete backfill in BHK evaluation case*; Section 8.3.3) or favourable transport properties due to low flow in the repository surroundings (see the *lower groundwater flow evaluation case*; Section 8.4.1).
- Chemically induced changes in the performance of the concrete barrier could potentially degrade the mechanical performance of the barrier, both in terms of stiffness and strength. Further, the concrete backfill of BHK may also be affected by mechanical stress from the rock adjacent to the repository (Sections 6.2.10, 6.4.10). Simulations indicate that limited mechanical damage may occur internally in the concrete backfill, at the corners of the waste domain. The effect of this degradation is not explicitly considered in the radionuclide transport calculations. However, the calculations account for the damage due to leaching, which is likely to have a similar effect on radionuclide releases and doses. An exception is the case that considers glaciation-induced stresses. In that case, mechanical damage can be substantial, extending over large regions of the concrete backfill (Section 6.4.4). However, since glaciation is likely to occur only well after tens of thousands of years (Section 6.4.1), when Mo-93 and C-14 have substantially decayed, it is likely that any mechanical effects on the concrete barrier will not have substantial adverse impacts on radionuclide releases and doses.
- The effects of potential earthquakes have not been taken into account in SE-SFL. These need to be analysed in a future assessment to evaluate their effect on the potential of the BHK repository concept to fulfil the requirement on its ability to withstand relevant FEPs.

## S10.2 Needs for future efforts

One central objective of SE-SFL is to provide SKB with a basis to prioritize areas in which the level of knowledge and adequacy of methods must be improved in order to perform a full safety assessment for SFL. The following areas have been distinguished for which efforts have been identified that can contribute to establishing a full safety analysis that can serve as part of a license application:

- The safety analysis methodology and its implementation should be considered, given that the methodology in SE-SFL has been adapted to the purposes of the evaluation and has not strived to fulfil all regulatory requirements related to methodology. For instance, given the reference design and potential site chosen for a full safety assessment, it should be reconsidered if the different

climate evolutions together adequately illustrate the most important and reasonably foreseeable sequences of future climate states. If not, modified or additional climate evolutions will need to be defined. The climate sequences do not necessarily need to be more detailed, but the aim should be to identify and cover the climate states that affect the protective capability and environmental consequences of the repository. Furthermore, the safety functions should be adjusted to the chosen reference design and selected site. The role of the safety functions in the scenario selection in a future safety assessment may also have implications for their definition. A comprehensive set of scenarios need to be defined and assessed with respect to resulting risk.

- Identification and definition of all requirements, and efforts to underpin compliance discussions for requirements not addressed in SE-SFL. In a future safety assessment for SFL that is to underpin a license application, all relevant regulatory requirements need to be addressed. Among other things, this implies that not only the effects on humans need to be assessed, but also that the effects on non-human biota need to be considered. A further requirement that needs to be addressed in future analyses is the effects of single deficiencies in a barrier. Furthermore, regulatory compliance needs to be shown for the requirements on the application of best available technique and optimisation, which may imply a need for supporting assessments.
- Research and development linked to the cautious or simplifying assumptions underlying the radionuclide and dose calculations in SE-SFL. SE-SFL builds on a thorough understanding of the FEPs affecting the repository near-field and its environs. Various simplifications have, however, been introduced of which some are cautious. This includes the availability of radionuclides from the source term, handling of complexing agents, and geosphere retention properties. Further research and development, relating to some of the cautious simplifying assumptions, may contribute to a more realistic representation of the future evolution of the repository and its environs in the scenarios and thus a better basis for the assessment of post-closure safety for SFL.
- Technical developments that are related to the components of the repository and its interactions with its environs, waste characterisation, as well as effective methods to assess post-closure safety for SFL. In a future full safety assessment for SE-SFL, the design of the facility will need to be refined to establish a reference design that, in principle, could be implemented for a future facility at a selected site. Technical developments might be advantageous to optimize the reference design, e.g. regarding geometry and material properties in order to improve the repository robustness and to further reduce releases and doses. In connection to this, increased functionality in the ground-water flow and radionuclide transport modelling chain might be advantageous to guide choices on BAT and optimization. A fundamental aspect is the characterisation of the waste inventory and its chemical properties. Reduced uncertainties could potentially have a large impact on the results of the safety assessment.



# Contents

<b>1</b>	<b>Introduction</b>	27
1.1	Background	27
1.2	The SE-SFL safety evaluation	29
1.3	The SE-SFL report hierarchy	30
1.4	The role of this report in SE-SFL	32
1.5	Structure of this report	32
<b>2</b>	<b>Methodology</b>	33
2.1	Introduction	33
2.2	Handling of regulatory requirements in SE-SFL	34
2.3	Post-closure safety	35
2.3.1	Safety principles and safety functions for the proposed repository concept	35
2.3.2	Time period covered by the evaluation	36
2.4	System boundary	37
2.5	SE-SFL methodology	37
2.5.1	Processing of features, events and processes influencing post-closure safety	37
2.5.2	Description of the initial state	38
2.5.3	Description of external conditions	39
2.5.4	Description of internal processes	40
2.5.5	Suggestion of safety functions	41
2.5.6	Compilation of input data	41
2.5.7	Description of reference evolution	41
2.5.8	Selection of evaluation cases	42
2.5.9	Evaluation of post-closure safety	42
2.5.10	Conclusions	43
2.6	Overall uncertainty management	43
2.7	Documentation and quality assurance	44
<b>3</b>	<b>Processing of features, events and processes influencing post-closure safety</b>	47
3.1	Introduction	47
3.2	SE-SFL FEP processing procedure	48
3.2.1	FEP sources	48
3.2.2	Classification of the SE-SFL FEPs	50
3.3	FEP audit	52
3.3.1	Audit against the SR-PSU FEP catalogue	52
3.3.2	Audit against the list of NEA PFEPs considered irrelevant in SR-PSU	52
3.4	FEP processing	53
3.4.1	Processing results for the NEA PFEPs	53
3.4.2	Processing results for the SE-SFL FEP catalogue	54
3.5	The SE-SFL FEP catalogue	60
<b>4</b>	<b>Initial state of the repository and its environs</b>	61
4.1	Introduction	61
4.2	Waste	61
4.2.1	Origin and waste types	61
4.2.2	Waste acceptance criteria and waste type descriptions	63
4.2.3	Waste packaging for BHK	63
4.2.4	Waste packaging for BHA	64
4.2.5	Waste and waste packaging material quantities and volumes	65
4.2.6	Radionuclide inventory in BHK	67
4.2.7	Radionuclide inventory in BHA	68

4.3	Repository	69
4.3.1	Waste vault for reactor internals, BHK	69
4.3.2	Waste vault for legacy waste, BHA	70
4.3.3	Closure components	72
4.4	Climate	74
4.4.1	Temperature and precipitation	74
4.4.2	Shoreline displacement	74
4.5	Surface systems	74
4.5.1	Topography and regolith	75
4.5.2	Near-surface hydrogeology, water chemistry and limnic ecosystems	75
4.5.3	Marine ecosystems	76
4.5.4	Terrestrial ecosystems	77
4.6	Bedrock system	78
4.6.1	Local geological setting	79
4.6.2	Rock composition and division into rock domains	80
4.6.3	Deformation zones and fracture domains	81
4.6.4	Bedrock temperature and thermal conditions	81
4.6.5	Rock mechanical conditions	81
4.6.6	Bedrock hydraulic properties	82
4.6.7	Geochemistry	83
<b>5</b>	<b>Safety functions</b>	<b>85</b>
5.1	Role of safety functions in safety analyses	85
5.2	Safety functions in SE-SFL	86
<b>6</b>	<b>Reference evolution of the repository and its environs</b>	<b>89</b>
6.1	Introduction	89
6.2	Base variant of the reference evolution	89
6.2.1	External conditions	89
6.2.2	Development of surface systems	90
6.2.3	Thermal evolution	92
6.2.4	Mechanical evolution	92
6.2.5	Regional hydrogeological conditions	92
6.2.6	Repository hydrological evolution	96
6.2.7	Geochemical evolution	100
6.2.8	Evolution of the waste	103
6.2.9	Evolution of engineered barriers in BHA	108
6.2.10	Evolution of engineered barriers in BHK	112
6.2.11	Evolution of plugs and other closure components	115
6.3	Increased greenhouse effect variant of the reference evolution	115
6.3.1	Evolution of external conditions	116
6.3.2	Development of surface systems	117
6.3.3	Thermal evolution	117
6.3.4	Mechanical evolution	117
6.3.5	Regional hydrogeological evolution	117
6.3.6	Repository hydrological evolution	118
6.3.7	Geochemical evolution	118
6.3.8	Evolution of the waste	118
6.3.9	Evolution of engineered barriers in BHA	118
6.3.10	Evolution of engineered barriers in BHK	118
6.3.11	Evolution of plugs and other closure components	118
6.4	Simplified glacial cycle variant of the reference evolution	119
6.4.1	Evolution of external conditions	119
6.4.2	Development of surface systems	119
6.4.3	Thermal evolution	121
6.4.4	Mechanical evolution	121
6.4.5	Regional hydrogeological evolution	122
6.4.6	Repository hydrological evolution	123
6.4.7	Geochemical evolution	123

6.4.8	Evolution of the waste	125
6.4.9	Evolution of engineered barriers in BHA	125
6.4.10	Evolution of engineered barriers in BHK	125
6.4.11	Evolution of plugs and other closure components	126
<b>7</b>	<b>Evaluation of post-closure safety for the repository design at the example location</b>	<b>127</b>
7.1	Introduction	127
7.2	Radionuclides included in the analysis	127
7.3	Modelling approach	129
7.3.1	Model chain and data flow	129
7.3.2	Near-field	130
7.3.3	Geosphere	134
7.3.4	Biosphere	138
7.4	Present-day evaluation case	141
7.4.1	Rationale	141
7.4.2	Handling in the near-field	142
7.4.3	Handling in the geosphere	147
7.4.4	Handling in the biosphere	149
7.4.5	Simplifications in comparison to the reference evolution	150
7.5	Function of the repository design at the example location	152
7.5.1	Retention in the near-field model	152
7.5.2	Retention in the geosphere model	154
7.5.3	Retention in the biosphere model and annual doses	155
<b>8</b>	<b>Potential of the repository concept to meet applicable criteria</b>	<b>159</b>
8.1	Introduction	159
8.2	Selection of evaluation cases	159
8.3	Conditions in the waste vaults	161
8.3.1	No effect of complexing agents in BHA	161
8.3.2	Lower steel corrosion rate in BHK	163
8.3.3	Alternative concrete backfill in BHK	164
8.3.4	Placement of ESS-specific radionuclides	165
8.4	Conditions in the repository environs	166
8.4.1	Lower groundwater flow	166
8.4.2	Initially submerged conditions	169
8.4.3	Alternative geosphere retention properties	170
8.4.4	Alternative regional climate	172
8.5	Uncertainties in bedrock properties, discharge area and effect of drilled well	173
8.5.1	Alternative realisations of stochastic bedrock fractures	173
8.5.2	Alternative discharge area	174
8.5.3	Drilled well	177
8.6	Climate conditions	179
8.6.1	Increased greenhouse effect	179
8.6.2	Simplified glacial cycle	180
<b>9</b>	<b>Discussion</b>	<b>185</b>
9.1	Basic considerations for the safety evaluation	185
9.2	Evaluation under what conditions the repository concept has potential to fulfil regulatory requirements	187
9.2.1	BHA	188
9.2.2	BHK	191
9.2.3	Repository environs	193
9.3	Development in SE-SFL	194
9.3.1	Repository near-field	194
9.3.2	Bedrock system	196
9.3.3	Surface ecosystems	197
9.3.4	Integration and presentation of results	198

9.4	Areas of further efforts for a forthcoming safety assessment	199
9.4.1	Safety analysis methodology and its implementation	199
9.4.2	Handling of regulatory requirements	200
9.4.3	Siting process and site characterisation	201
9.4.4	Research and development	202
9.4.5	Technical developments	204
<b>10</b>	<b>Conclusions</b>	<b>205</b>
10.1	Conditions under which the repository concept has potential to meet regulatory criteria	205
10.1.1	BHA	206
10.1.2	BHK	206
10.1.3	Repository environs	207
10.2	Suggested future efforts	208
	<b>References</b>	<b>211</b>
<b>Appendix 1</b>	<b>Piping and erosion calculations</b>	<b>221</b>

# 1 Introduction

This report constitutes the main report for the evaluation of post-closure safety for a proposed repository concept for the repository for long-lived waste (SFL) in Sweden. The purpose of the SFL safety evaluation (SE-SFL) is to provide input to the subsequent, consecutive steps in the development of SFL. This chapter gives the background to the project and an overview of the safety evaluation. Moreover, the role of this report is described in the context of the evaluation.

## 1.1 Background

The Swedish power industry has been generating electricity by means of nuclear power for more than 40 years. The Swedish system for managing and disposal of the waste from operation of the reactors has been developed over that period. When finalised, this system will comprise three repositories: the repository for short-lived radioactive waste (SFR), the repository for long-lived waste (SFL), and the Spent Fuel Repository.

The system for managing radioactive waste is schematically depicted in Figure 1-1. SKB currently operates SFR at Forsmark in Östhammar municipality to dispose of low- and intermediate-level waste produced during operation of the various nuclear power plants, as well as to dispose waste generated during applications of radioisotopes in medicine, industry, and research. Further, SFR is planned to be extended to permit the disposal of waste from decommissioning of nuclear facilities in Sweden. The spent nuclear fuel is presently stored in the interim storage facility for spent nuclear fuel (Clab) in Oskarshamn municipality. Clab is planned to be complemented by the Encapsulation Plant, together forming Clink. SKB has also applied to construct, possess and operate the Spent Fuel Repository at Forsmark in Östhammar municipality. The current Swedish radioactive waste management system also includes a ship and different types of casks for transport of spent nuclear fuel and other radioactive waste.

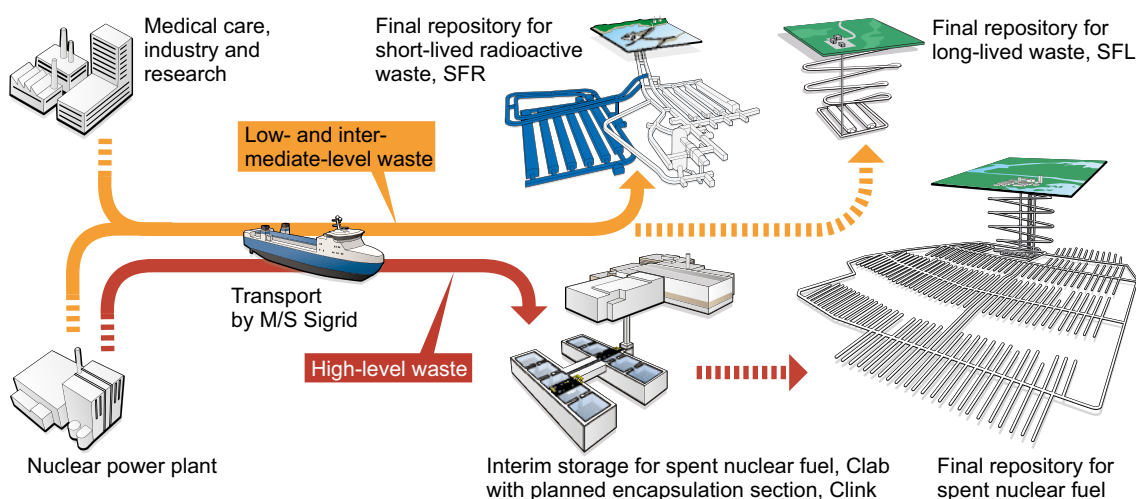


**Figure 1-1.** The Swedish system for radioactive-waste management. Dashed arrows indicate future waste streams to facilities planned for construction.

SFL will be used for disposal of the Swedish long-lived low- and intermediate-level waste. This comprises long-lived waste from the operation and decommissioning of the Swedish nuclear power plants, from early research in the Swedish nuclear programmes (legacy waste), from medicine, industry, and from research which includes the European Spallation Source (ESS) research facility. The long-lived low- and intermediate-level waste from the nuclear power plants consists of neutron-activated components and control rods and constitutes about one third of the waste planned for SFL. The rest originates mainly from the Studsvik site, where Studsvik Nuclear AB and Cyclife Sweden AB both produce and manage radioactive waste from medicine, industry and research. The legacy waste to be disposed of in SFL is currently managed by the company AB SVAFO.

A first preliminary repository concept for SFL was presented in the context of cost calculations for radioactive waste management (Plan 93; SKB 1993). Since the purpose of Plan 93 was to give cost estimates, no safety related analyses were discussed. The first quantification related to safety was presented in a pre-study of final disposal of long-lived low and intermediate level waste. The objective was to make a first preliminary and simplified assessment of the near-field as a barrier to radionuclide dispersion (Wiborgh 1995). In 1999, a preliminary safety assessment was presented that focussed on a quantitative analysis of the environmental impact for a reference scenario (SKB 1999a). The objective was to investigate the capacity of the facility to act as a barrier to the release of radionuclides and the importance of the repository location. The assessment was reviewed by the authorities (SKI/SSI 2001). One of the main comments was a lack of a clear account of the basis for the selection of the design and that no design alternatives had been considered.

Reflecting the comments from the authorities, possible solutions for management and disposal of the Swedish long-lived low- and intermediate-level waste were examined in the SFL concept study (Elfving et al. 2013). After a first screening, four waste vault concepts were evaluated with respect to two evaluation factors; feasibility of making a post-closure safety assessment and robustness of the barrier safety functions (Evins 2013). Based on the evaluation, a system was proposed as a basis for further assessment of post-closure safety. According to this system, SFL is designed as a deep geological repository with two different sections:

- One waste vault, designed with a concrete barrier, BHK, for metallic waste from the nuclear power plants.
- One waste vault, designed with a bentonite barrier, BHA, for the waste from Studsvik Nuclear AB, Cyclife Sweden AB and AB SVAFO.

A schematic illustration of the proposed facility layout and waste vault concepts for SFL is displayed in Figure 1-2. BHK is approximately 135 m long and BHA is approximately 170 m long. Both vaults have a cross sectional area of approximately  $20 \times 20 \text{ m}^2$  (see further details in Section 4.3). In SE-SFL it is assumed that the waste vaults are located at 500 m below the surface and that this depth is sufficient to avoid adverse effects of permafrost during future glacial cycles.

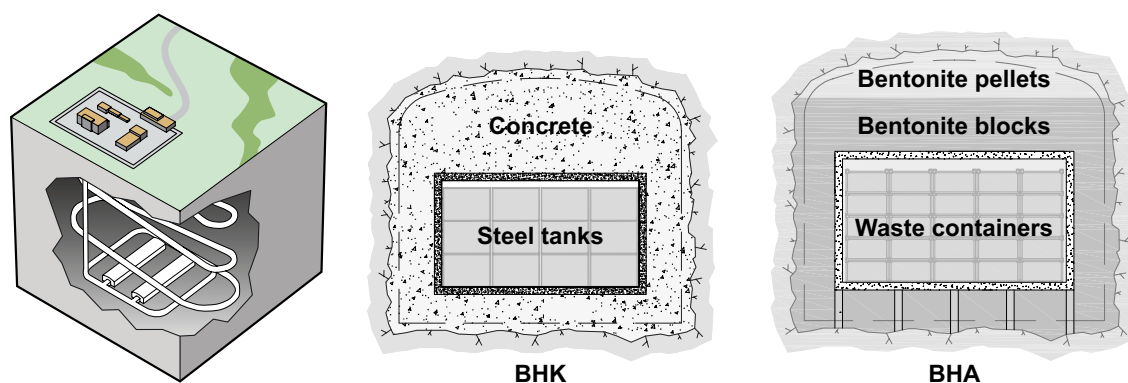


**Figure 1-2.** Preliminary facility layout and the proposed repository concept for SFL (left), with one waste vault for metallic waste from the nuclear power plants (BHK, centre) and one waste vault for waste from Studsvik Nuclear AB, Cyclife Sweden AB and AB SVAFO (BHA, right).

## 1.2 The SE-SFL safety evaluation

The purpose of SE-SFL is to provide input to the subsequent, consecutive steps in the development of SFL. These consecutive steps include further development of the design of the engineered barriers and the site-selection process for SFL. More specifically, there are two main objectives for SE-SFL. The first is to evaluate conditions in the waste, the barriers, and the repository environs under which the repository concept has the potential to fulfil the regulatory requirements for post-closure safety. The second is to provide SKB with a basis for prioritizing areas in which the level of knowledge and adequacy of methods must be improved in order to perform a full safety assessment for SFL. This is in line with the iterative safety analysis process that the SFL and other repository program follow, in which the results from post-closure safety analyses and related activities (e.g. information from a site selection process and development of numerical methods) are used to successively inform and improve the analysis. In accordance with the Nuclear Activities Act (SFS 1984:3), important research needs for the SFL programme that emerge as a result of SE-SFL will be reported in the research development and demonstration (RD&D) programme. An important aspect of this is to ensure that the industry has well founded information to support long-term planning of the nuclear waste management.

The safety analysis methodology as applied in SE-SFL is a first evaluation of post-closure safety for the repository concept proposed by Elfving et al. (2013) and is not part of a license application. As such, the methodology has been adapted to suit the needs of SE-SFL and thus differs from the methodology established by SKB for the most recent safety assessments for the extended SFR (SR-PSU; SKB 2015a) and for the Spent Fuel repository (SR-Site; SKB 2011a). This also implies that the regulatory requirements on the methodology have not been applied rigorously, which would be needed for a safety analysis that is part of a license application. The evaluation is intentionally simplified as compared with SR-Site and SR-PSU, and more focus is given to aspects connected to the further development of the repository concept and related analyses. This is also reflected in using the term safety evaluation in contrast to safety assessment. The differences between SE-SFL and a full safety assessment are described in more detail in Section 2.1. The adaptation of the methodology for the purposes of SE-SFL is described in Section 2.5.

To the extent applicable, SE-SFL builds on knowledge from SR-PSU and SR-Site. There are commonalities regarding the waste, engineered barriers, bedrock, surface ecosystems and external conditions relevant to post-closure safety. For instance, SE-SFL and SR-Site both address timescales of one million years (see Section 2.3). A further similarity is the proposed depth of 300–500 m. There are similarities between SFR and SFL regarding the waste and waste packaging and the proposed engineered barriers.

In SE-SFL, a first evaluation of a suitable repository design for disposal of the ESS waste is carried out. Since the information regarding the ESS inventory is not yet as well defined as for the other waste streams, the protective capability of the different waste vaults in relation to this waste is analysed separately.

No site has yet been selected for SFL and therefore data from SKB's site investigation programmes for the Spent Fuel Repository and for the extension of SFR have been utilized in SE-SFL. In order to have a realistic and consistent description of a site for geological disposal of radioactive waste, data from the Laxemar site in Oskarshamn municipality (see Figure 1-3), for which a detailed and coherent dataset exists, are used. Based on an initial hydrogeological analysis for SE-SFL, the example location for the SFL repository was selected to be a part of the rock volume that was earlier found suitable for a potential Spent Fuel Repository within the Laxemar site (SKB 2011b).

SE-SFL is further developed in comparison to the previous assessments, which were mentioned in Section 1.1. Important improvements are an updated inventory and more elaborate account of internal and external processes. Moreover, the biosphere was, in the preliminary assessment, handled in a simplified manner, whereas it is handled in a more realistic way in SE-SFL. The availability of data from the Spent Fuel Repository site investigations also allows for more detailed representations of the geosphere. In general, SKB's experiences with safety analysis work have led to many developments since the late 1990s.

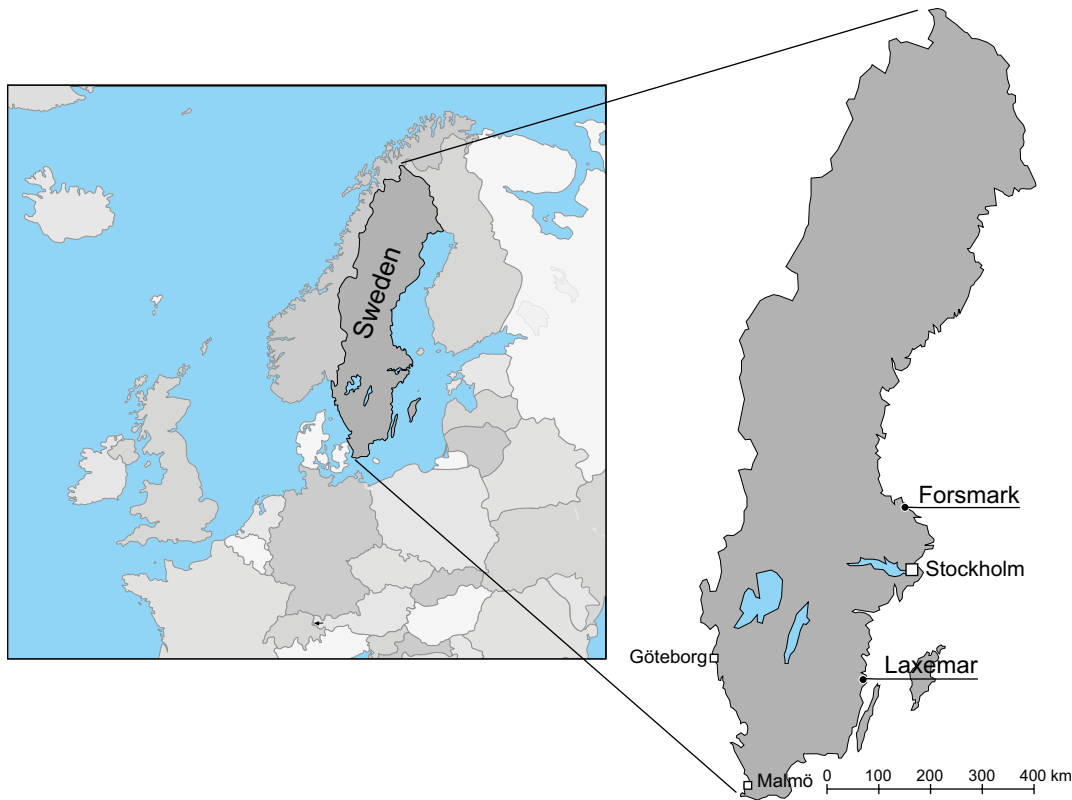


**Figure 1-3.** Map showing the location of Laxemar and Forsmark. Data from the site investigations in Laxemar, along with the data from the SR-Site and SR-PSU assessments from Forsmark, are used in SE-SFL to obtain a coherent dataset of common conditions in Swedish crystalline bedrock and surface ecosystems.

### 1.3 The SE-SFL report hierarchy

The **Main report** and main references in SE-SFL are listed in Table 1-1, also including the abbreviations by which they are identified in the text (abbreviated names in bold text). It can be noted that there are no dedicated process reports for SE-SFL. The SFR and SFL waste and repository concepts have many similarities, for instance the use of similar barrier materials and thus similar process interactions with the surrounding bedrock environment (Section 2.5.4). Therefore, the descriptions of internal processes for the waste (SKB 2014a) and the barriers (SKB 2014b) in SR-PSU are used in SE-SFL. For the bedrock system, the descriptions of internal processes for the geosphere in SR-Site (SKB 2010a) and SR-PSU (SKB 2014c) are used. There are also additional references, which include documents compiled within SE-SFL, for instance input data reports for the radionuclide transport and dose calculations (Shahkarami 2019, Grolander and Jaeschke 2019). In addition, SE-SFL also relies on references to documents that have been compiled outside of the project, either by SKB or other similar organisations, or are available in the scientific literature. In Figure 1-4, the hierarchy of the **Main report**, main references and additional references within SE-SFL is shown.

**Table 1-1. Main references in SE-SFL and the abbreviations by which they are identified in the text, where they are bolded.**

Abbreviation used when referenced in this report	Text in reference list
Main report	<b>Main report, 2019.</b> Post-closure safety for a proposed repository concept for SFL. Main report for the safety evaluation SE-SFL. SKB TR-19-01, Svensk Kärnbränslehantering AB.
Biosphere synthesis	<b>Biosphere synthesis, 2019.</b> Biosphere synthesis for the safety evaluation SE-SFL. SKB TR-19-05, Svensk Kärnbränslehantering AB.
Climate report	<b>Climate report, 2019.</b> Climate and climate-related issues for the safety evaluation SE-SFL. SKB TR-19-04, Svensk Kärnbränslehantering AB.
FEP report	<b>FEP report, 2019.</b> Features, events and processes for the safety evaluation SE-SFL. SKB TR-19-02, Svensk Kärnbränslehantering AB.
Initial state report	<b>Initial state report, 2019.</b> Initial state for the repository for the safety evaluation SE-SFL. SKB TR-19-03, Svensk Kärnbränslehantering AB.
Radionuclide transport report	<b>Radionuclide transport report, 2019.</b> Radionuclide transport and dose calculations for the safety evaluation SE-SFL. SKB TR-19-06, Svensk Kärnbränslehantering AB.

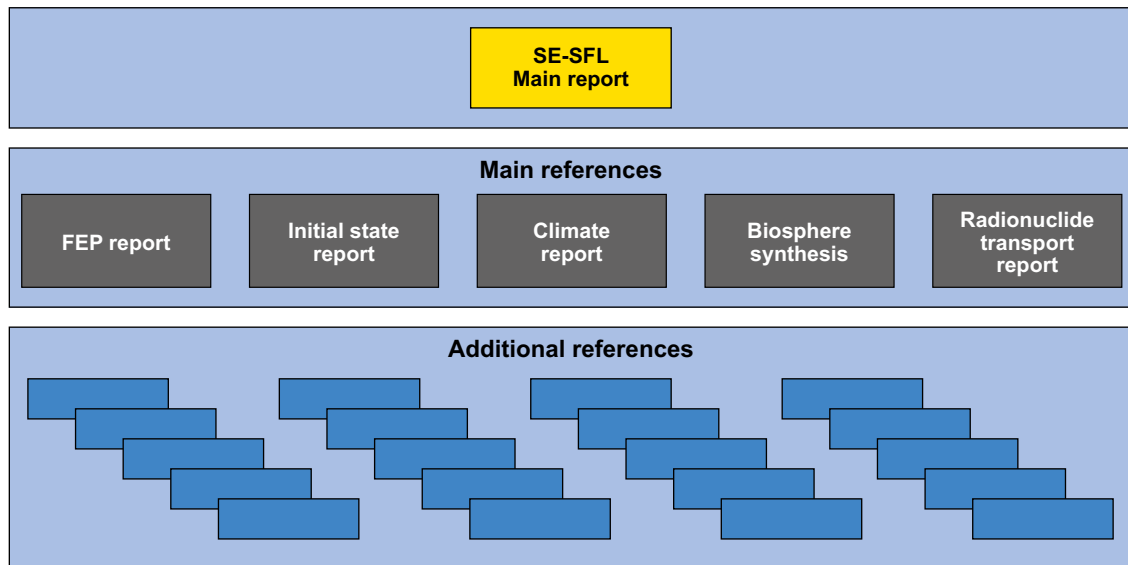


**Figure 1-4.** The hierarchy of the Main report, main references and additional references in the safety evaluation of post-closure safety SE-SFL. The additional references either support the Main report or one or more of the main references.

## 1.4 The role of this report in SE-SFL

In this main report of SE-SFL, the evaluation of post-closure safety for the proposed repository concept for SFL is presented. In some parts of the report, information is mainly drawn and summarised from the main references. However, the report also includes parts that were developed within the project and are presented for the first time in this report. Specifically this includes the chapters relating to the methodology, the safety functions, the reference evolution, and the discussion of the implications of the results in view of the objectives of SE-SFL.

## 1.5 Structure of this report

**Chapter 1 – Introduction.** This chapter describes the background and gives a brief overview of the post-closure safety evaluation SE-SFL.

**Chapter 2 – Methodology.** The chapter provides a description of the relation of the objectives of SE-SFL to the regulatory requirements and the methodology used for the safety evaluation. The chapter also discusses aspects such as post-closure safety principles, time scales, the iterative safety analysis process, uncertainty management, and quality assurance.

**Chapter 3 – Features, events and processes (FEP) influencing post-closure safety.** The chapter describes the methodology for the systematic screening of relevant FEPs to be addressed in the evaluation. The chapter also describes the handling of internal processes and external conditions.

**Chapter 4 – Initial state of the repository and its environs.** The chapter describes the initial state, defined as the expected state of the repository and its environs at the time of repository closure. The chapter includes descriptions of the deposited wastes, waste packaging, engineered barriers and other repository structures. It furthermore presents information on the repository environs, i.e. the bedrock surrounding the repository and the surface systems in the repository area, as well as the climate at the example location.

**Chapter 5 – Safety functions.** The chapter describes the general role of safety functions in safety analyses. Furthermore, the use and definition of safety functions in SE-SFL for the two vaults, closure components, and natural barriers is presented.

**Chapter 6 – Reference evolution of the repository and its environs.** In this chapter, a reference evolution of the repository and its environs is defined and analysed. It includes three variants: the *base variant*, where bedrock system, surface system and external conditions are assumed to remain identical to the present-day situation during the complete analysis period, the *simplified glacial cycle variant* and the *increased greenhouse effect variant*.

**Chapter 7 – Evaluation of post-closure safety for the reference evolution.** In this chapter, the results of the evaluation cases related to the reference evolution are presented. It also gives brief descriptions of the radionuclide transport and dose models used, as well as the important assumptions made in the evaluation cases.

**Chapter 8 – Evaluation of post-closure safety – sensitivity to conditions in the repository and to site-specific conditions.** In this chapter, the sensitivity of the results of the radionuclide transport and dose calculations to conditions in the repository and site-specific conditions is discussed.

**Chapter 9 – Discussion.** In this chapter, the results of the safety evaluation are discussed in relation to the objectives of SE-SFL. The discussion is based on the information provided in the preceding chapters.

**Chapter 10 – Conclusions.** In this chapter the conclusions of SE-SFL are presented in the context of the objectives of the safety evaluation.

## 2 Methodology

### 2.1 Introduction

This chapter outlines the methodology applied in the evaluation of post-closure safety for the proposed repository concept for SFL (SE-SFL). SKB has established a methodology for post-closure safety assessments that has been used within the programmes for the Spent Fuel Repository and the repository for short-lived radioactive waste (SFR), which includes the extension of the facility. In the last two safety assessments, SR-Site and SR-PSU, the same basic methodology has been used, but some adjustments have been made to suit the needs of the different facility programmes (SKB 2011a, 2015a). The methodologies of these analyses were based on the SR-Can analysis (SKB 2006a). SKB's methodology development has been influenced and inspired by several safety assessment studies in e.g. Switzerland (Nagra 2002), Finland (Vieno and Nordman 1999), Belgium (ONDRAF/NIRAS 2001), Japan (JNC 2000), the U.S. (McNeish 2002), Canada (Gierszewski et al. 2004) and France (Andra 2005) and by international cooperation in the area organised by the OECD Nuclear Energy Agency (NEA 1997a, 1999a, 2001, 2004a, b, 2009, 2012).

The methodology used for SE-SFL follows the basic methodology established in the safety assessments SR-Site and SR-PSU. The methodology was however adapted for the purpose of meeting the general objectives of SE-SFL. The first objective of SE-SFL is to evaluate conditions under which the repository concept has the potential to fulfil the regulatory requirements for post-closure safety. Thus, the influence of the conditions in the repository and its environs need to be evaluated based on the conditions at an example site and a design based on the concept study. To meet the second objective of SE-SFL, the resulting information can then be used as input to the site selection process and future safety analysis iterations that further develop the requirements on the geosphere and the technical barriers. This is in line with the iterative safety assessment process that all SKB's repository programmes follow. The iterative approach is standard internationally (NEA 2012) and planned and documented in SKB's RD&D programme (SKB 2019).

SE-SFL is the first evaluation of post-closure safety for the proposed repository concept for the SFL repository for which no site has been selected. This means that some changes have to be introduced to the basic methodology previously utilised and that the methodology is not applied as rigorously as in a safety analysis for a license application or a safety report for an operating facility. In this context, however, it should be kept in mind that SR-Site and SR-PSU were preceded by several earlier analyses for these facilities (SKB 1999b, 2006a, 2008a, Andersson et al. 1998) and the methods developed were sufficiently mature to support license applications according to the Swedish Act of Nuclear Activities (SFS 1984:3).

The present analysis is denoted *safety evaluation* to reflect its status as a preliminary analysis that is intended to evaluate the concept proposed by Elfving et al. (2013). In principle, however, the term *safety analysis* or *safety assessment* (which according to IAEA's safety glossary often are used interchangeably (IAEA 2018)) could have been used. There are similar types of analyses that do not support license applications that are so described, for instance SKB's SR-Can analysis (SKB 2006a), the Belgian implementer ONDRAF/NIRAS's SAFIR analysis (ONDRAF/NIRAS 2001), or a Canadian safety assessment (Gierszewski et al. 2004). But it is also noted that the French implementer Andra uses the term *safety evaluation* for its Dossier Argile 2005 analysis (Andra 2005). Andra's analysis aims to assess the feasibility of a spent nuclear fuel repository from a safety viewpoint within the context of a considered clay laboratory site. The term *safety analysis* is well defined in the Swedish regulations and one intention with using the term *safety evaluation* has been to make it clear that SE-SFL does not aim at fulfilling the requirements stipulated in the regulations in full. This gives the freedom to adapt the methodology to the needs of the current stage in the programme in contrast to strictly following the objectives of the regulations.

To assess the conditions under which the repository concept has the potential to be radiologically safe, the dose consequences over the relevant assessment period have to be determined. This can be done following SKB's safety analysis methodology as applied in SR-Site and SR-PSU. However, since the repository concept for SFL is not mature, it is not considered meaningful to make an analysis that covers all technical details in full depth. Instead, as much information as possible is drawn from SKB's previous safety analyses, and, specifically, SR-PSU, since there are a number of commonalities regarding the repository concepts. These simplifications must be considered when assessing the potential for the repository to be radiologically safe over time.

The methodology adopted for SE-SFL is detailed in the following sections of this chapter and some of the main differences from the methodology used for SR-Site and SR-PSU are touched upon. This chapter has the following structure:

- The relation between the objectives of SE-SFL and regulatory requirements is discussed in Section 2.2.
- The approach to post-closure safety and its evaluation is explained in Section 2.3, including safety functions, the timescale of the safety evaluation, the iterative safety analysis process, and RD&D.
- The system and system boundaries are described in Section 2.4.
- The steps of the SE-SFL safety evaluation methodology are described in Section 2.5.
- The overall handling of uncertainties in SE-SFL is addressed in Section 2.6.
- The approach to documentation and quality assurance for SE-SFL is described in Section 2.7.

## 2.2 Handling of regulatory requirements in SE-SFL

One of the main objectives of SE-SFL is to evaluate under what conditions the repository concept has the potential to fulfil regulatory requirements. Since there is no intention in SE-SFL to evaluate regulatory compliance in full, it is important to consider which regulatory requirements the evaluation focuses on. SSM has issued two regulations that relate to the disposal of nuclear waste. SSMFS 2008:21 (SSM 2008a) concerns safety and SSMFS 2008:37 (SSM 2008b) the protection of human health and the environment. Both regulations and the associated general guidance include methodological aspects. Given that the starting point for the methodology of SE-SFL is taken from safety analyses underlying license applications, it is based on the regulatory methodology requirements. However, the adjustments made for SE-SFL imply that the requirements are not strictly followed.

A central requirement in SSMFS 2008:37 in view of the post-closure repository protective capability is Section 5 that states that *a repository for spent nuclear fuel or nuclear waste shall be designed so that the annual risk of harmful effects after closure does not exceed  $10^{-6}$  for a representative individual in the group exposed to the greatest risk. [...]*.

The risk should according to the general advice to the regulations be calculated based on a scenario analysis that fulfils certain requirements. The scenarios shall according to SSMFS 2008:21 include a main scenario that takes into account the most probable changes in the repository and its environment. Further, SSM recommends that the complete set of scenarios should together illustrate the most important courses of development of the repository, its surroundings and the biosphere. Such a comprehensive analysis has not been the aim of SE-SFL. Not all potential aspects of future climate evolution are analysed and the focus is to a large degree on important aspects related to siting and barrier properties. In order to distinguish the analysis performed within SE-SFL from scenarios in the sense of the regulations, evaluation cases are defined in SE-SFL. Among these there is a base case that is used for comparisons with other evaluation cases that analyse various aspects of the repository and the repository environs. The base case is intentionally simplified and does not necessarily represent the most probable changes in the repository and its environment (Section 2.5.8).

In SKB's methodology as applied in SR-Site and SR-PSU, the selection of scenarios was based on the safety functions that were defined for the given repository. In SE-SFL, safety functions are suggested but they will need to be refined to be in line with a future reference design. Therefore, the selection of the evaluation cases has not been coupled to the safety functions.

A central requirement in SSMFS 2008:21 is Section 5 that relates to barrier robustness which states that *the barrier system shall be able to withstand such features, events and processes that can affect the post-closure performance of the barriers.*

A prerequisite for evaluating if the repository barrier system can withstand such features, events and processes (FEPs) that can affect the post-closure performance is a comprehensive FEP analysis that identifies the FEP that can affect the post-closure performance of the barriers. In SE-SFL a FEP analysis is carried out and the evolution of the repository and its environs described based on the identified FEPs. The evaluation of under what conditions the repository concept has the potential to fulfil the requirements of barrier system robustness is then discussed based on the analysed evolution of the barrier system. Some FEPs have, however, not been further considered in SE-SFL and therefore there are limitations that will need to be considered in future safety analysis work as discussed in Chapter 9.

The sections in the regulations that are related to the operational phase of the facility (SSMFS 2008:21, Sections 4, 8, and second paragraph of Section 11) are not relevant before the facility is in operation and need not be considered in SE-SFL. Sections defining the applicability of the regulations, definitions and general considerations (SSMFS 2008:21, Section 1, SSMFS 2008:37, Sections 1–3) are important but do not directly relate to the objectives of SE-SFL. The sections that relate to basic design principles (SSMFS 2008:21, Sections 2–3), methodology (SSMFS 2008:21, Sections 9–11, SSMFS 2008:37, Section 4 second paragraph, Section 5 second paragraph, Sections 9–12), or reporting (SSMFS 2008:21, Section 8 and 11 second paragraph, SSMFS 2008:37, Section 8) are either trivial to show compliance with, not directly coupled to the performance of the repository, or of less interest in the present stage of the development of the repository concept for SFL. Therefore, these requirements are not discussed further.

The simplifications introduced in SE-SFL in comparison to a full safety analysis imply that requirements on use of best available technique and optimisation (SSMFS 2008:21, Section 6 and SSMFS 2008:37, Section 4) have not been addressed. Also, the requirement that necessary safety is maintained despite a single deficiency in a barrier (SSMFS 2008:21, Section 7) has not been evaluated. As discussed in Section 9.4.2 such analyses need to be introduced in future safety analysis work.

In SE-SFL focus is given to requirements related to human health, and the protection of the environment is not analysed (SSMFS 2008:37, Sections 6–7). This prioritisation is based on the experience from SR-Site and SR-PSU that indicates that compliance with human health requirements generally requires a higher level of repository performance than compliance with environmental protection requirements. In a future safety analysis, relevant aspects of the protection of the environment will be included as discussed in Section 9.4.2.

Additional aspects on how the post-closure safety is evaluated in SE-SFL are discussed in Section 2.5.9.

## **2.3 Post-closure safety**

### **2.3.1 Safety principles and safety functions for the proposed repository concept**

The safety principle<sup>1</sup> chosen for SFL is *retardation* (Elfving et al. 2013). The idea behind the concept for SFL is thus to use a system of engineered and natural barriers to achieve and enhance retardation of radionuclides. Elfving et al. (2013) describe the design principles of the barriers for post-closure safety in the proposed repository concept. The key elements of each repository vault with respect to post-closure safety are defined and how the different elements and their interactions are supposed to contribute to the safety principle.

---

<sup>1</sup> It can be noted that the term safety principle is not uniquely defined. In SE-SFL, the term is used in the same way as in SR-PSU, i.e. to denote the basic idea underlying the repository concept (SKB 2015a). The term has, however, also been used in SR-Site to denote a starting point underlying the development of the KBS-3 concept including, for instance, the choice to use natural materials that are long-term stable in the repository environment (SKB 2011a). The term safety principle is also used in IAEA's Safety Fundamental SF-1 to denote the ten safety principles that are associated with the fundamental safety objective to protect people and the environment from harmful effects of ionizing radiation (IAEA 2018).

Safety functions that the system ideally maintains over time are defined in SE-SFL to make clear what roles a repository component has for post-closure safety. The safety functions are defined based on the safety principles and the knowledge of the initial state, internal processes, and external processes. To these safety functions, quantifiable safety function indicators are coupled that can be used to evaluate the state of the safety functions as the system evolves with time. The selection of the safety functions is described in detail in Chapter 5.

In SKB's general methodology, safety function indicators are also used to identify scenarios. From the most important scenarios, design basis cases can then be defined and, together with the safety functions, requirements on the barrier system can be identified. Since no scenario analysis is carried out in SE-SFL, this role of the safety functions is not pursued.

### **2.3.2 Time period covered by the evaluation**

A timescale for the safety evaluation needs to be established since this provides a general limit on the scope of the assessment and cut-off times for e.g. radionuclide transport calculations. The issue is addressed in applicable regulations as cited below.

#### ***Regulatory requirements and guidance***

The regulatory requirements pertaining to post-closure safety for a repository for long-lived nuclear waste in Sweden are given in SSM regulations SSMFS 2008:21 and SSMFS 2008:37. SSMFS 2008:21 states that "a safety analysis shall comprise the required duration of the barrier functions, though a minimum of ten thousand years".

The general advice to SSMFS 2008:37 states that "for a repository for spent nuclear fuel or other long-lived nuclear waste the risk analysis should at least include approximately one hundred thousand years or the period for a glaciation cycle to illustrate reasonably predictable external strains on the repository. The risk analysis should thereafter be extended in time as long as it provides important information about the possibility of improving the protective capability of the repository, although at the longest for a period of up to one million years".

The general advice to SSMFS 2008:37 also states that, for the first 100 000 years, quantitative risk analysis should be carried out using supplementary indicators of the repository's protective capability, such as barrier functions, radionuclide fluxes and concentrations in the environment, to strengthen the confidence in the calculated risks.

For the time beyond approximately one hundred thousand years, the general advice states that: "A strict quantitative comparison of calculated risk in relation to the criterion for individual risk in the regulations is not meaningful. The assessment of the protective capability of the repository should instead be based on reasoning on the calculated risk together with several supplementary indicators of the protective capability of the repository such as barrier functions, radionuclide fluxes and concentrations in the environment."

#### ***Timescale covered by the safety evaluation***

SFL is designed for the safe disposal of long-lived nuclear waste from operational and decommissioning nuclear power plants and other nuclear facilities. In accordance with the regulations and general advice cited above, the timescale for the SE-SFL post-closure safety evaluation is one million years. The radiotoxicity of the radionuclide inventory evaluated in SE-SFL stemming from the reactor internals decreases to less than 0.01 percent due to decay during that period (Figure 2-1). The radiotoxicity of the legacy waste decreases to a couple of percent of its initial value at closure during the one-million-year analysis period. For comparison, it can be noted that the total radiotoxicity at closure is about 10 times the corresponding value for the extended SFR and less than the corresponding value for a single copper canister in the Spent Fuel Repository.

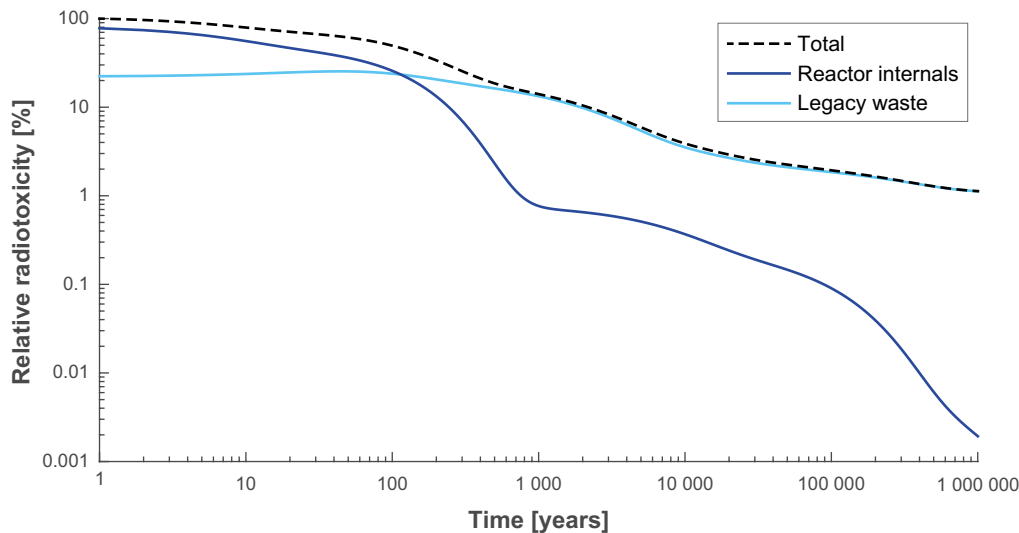


**Figure 2-1.** Time dependency of the radiotoxicity of the radionuclide inventory evaluated in SE-SFL. The black line shows the total inventory, the blue line the inventory of the legacy waste (BHA), and the red line the inventory for the reactor internals (BHK).

## 2.4 System boundary

The repository and its environs comprise the disposed radioactive waste, the engineered barriers surrounding the waste packages, the geosphere and the biosphere in the proximity of the repository.

In general, a strict boundary definition is neither possible nor necessary, and the same boundaries will not necessarily be relevant to all parts of the safety evaluation. The biosphere studied in the site investigations, i.e. an area of the order of 100-300 km<sup>2</sup> above the repository, is regarded as part of the system that is represented within the analysis. The analysis of the biosphere extends downward to the bedrock surface. The corresponding portion of the geosphere down to a depth of about 1 000 m is regarded as part of the analysed system.

Future human behaviour on a local scale is included in the system, but not issues related to the characteristics and behaviour of future society at large.

Depending on the context of the analysis, these definitions may be modified. For example, the local groundwater model has a smaller projected surface area than 100 km<sup>2</sup>, whereas e.g. larger areas than 300 km<sup>2</sup> and greater depths than 1 000 m may be required for regional groundwater modelling.

## 2.5 SE-SFL methodology

The safety evaluation SE-SFL consists of 10 main steps that are partly carried out concurrently and partly consecutively. A graphical illustration of the steps in the SE-SFL methodology is shown in Figure 2-2.

### 2.5.1 Processing of features, events and processes influencing post-closure safety

This is the first step in the safety evaluation and involves identifying all factors that may influence post-closure safety and deciding which of these need to be included. This is carried out by screening potentially important FEPs that influence post-closure safety. Experience gained from previous safety assessments for the Spent Fuel Repository and for the SFR, and international databases of relevant FEPs that affect post-closure safety are utilised (Section 3.2.1). SKB's FEP database was originally developed for a repository for spent nuclear fuel, and subsequently extended to include SFR. In SE-SFL, this database has been further extended to include SFL.

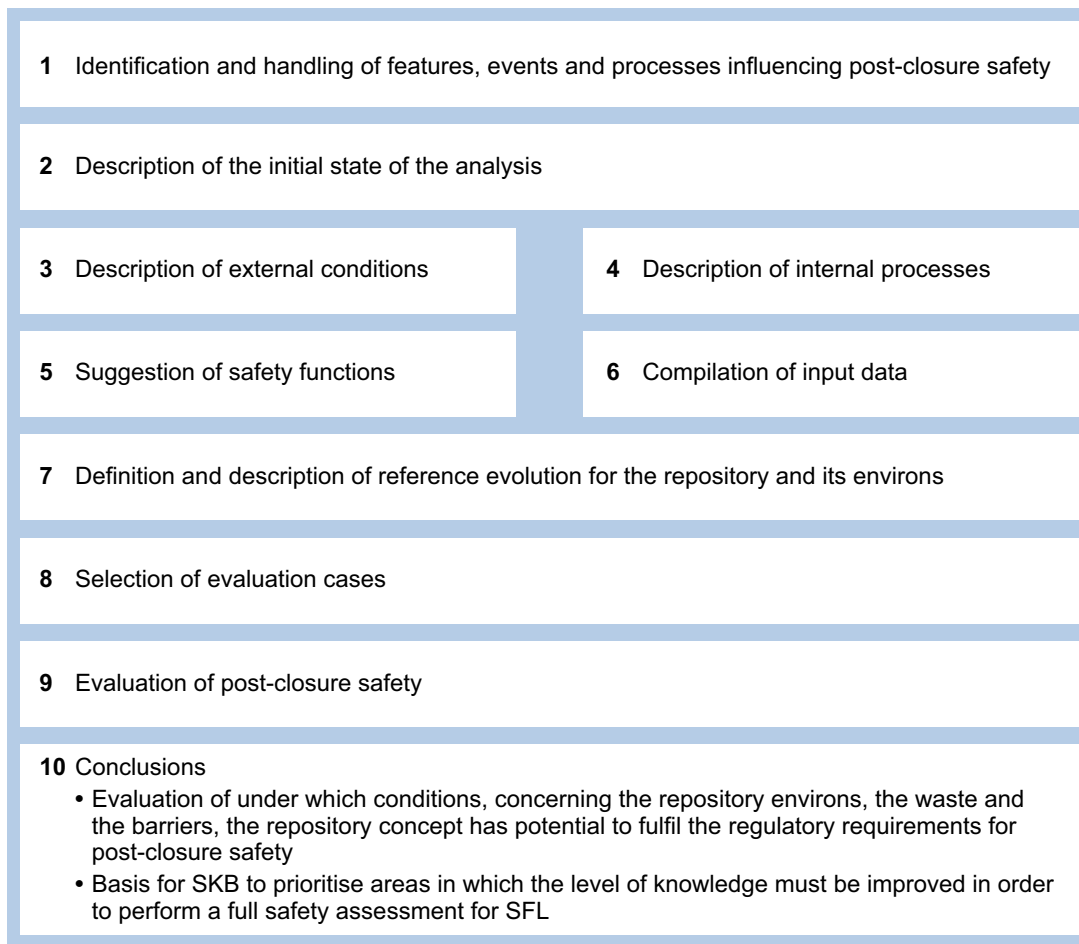


*Figure 2-2. Overview of the methodology applied for the evaluation of post-closure safety for the proposed repository concept for SFL.*

Most of the FEPs in the database are classified as i) initial state FEPs, ii) internal processes or iii) external FEPs. The remaining FEPs are either related to the assessment methodology in general or have been categorized as irrelevant to SFL. Based on the results of the FEP processing, a specific SFL FEP catalogue, required to contain all FEPs needed to be considered in SE-SFL, has been compiled. A simplified approach to FEP processing as compared with the work performed in SR-PSU and SR-Site has been used in SE-SFL. For instance, the FEP catalogue is based on the SR-PSU FEP catalogue with relevant changes made to capture the differences between the SFR and SFL repositories. The main reason for selecting the SR-PSU FEP catalogue as a base for the SE-SFL FEP catalogue is the similarities in the waste, waste packaging and technical barriers proposed. The similarities between SFL and the Spent Fuel Repository are not as extensive and mainly limited to similar repository depth and containing long-lived radioactive waste. A more rigorous FEP analysis will be performed in a future full safety assessment for SFL.

This step of identifying FEPs that influence post-closure safety is further described in Chapter 3 and in the **FEP report**.

## 2.5.2 Description of the initial state

The initial state for the analysis is defined as the expected state of the repository and its environs at closure of the repository. To obtain a detailed, realistic and coherent dataset for the evaluation of the proposed repository concept, data from SKB's site investigation programme for the Spent Fuel Repository in Laxemar are used as an example to represent the initial state of the repository environs (Section 1.2). Thus, the initial state of the repository environs is assumed to be similar to present-day conditions, as described in the site descriptive model (SDM) for Laxemar (SKB 2009) and the

**Biosphere synthesis.** The proposed repository is assumed to be located at approximately 500 m depth at the example location within the site investigation area in Laxemar. Further, material properties for the repository components are taken from previous safety assessments. For instance, it is assumed that the BHA backfill is constructed with bentonite that is similar to that planned for the buffer in the Spent Fuel Repository and the BHK backfill is constructed with concrete similar to the construction concrete employed in the existing SFR repository. The repository is assumed to be closed in 2075 AD and, under these assumptions, the initial state of the repository is defined based on current estimates of the properties of the waste and the repository components at repository closure (see **Initial state report**). A summary of the initial state of the repository and its environs is given in Chapter 4.

SE-SFL provides SKB with a basis to assess under what conditions the proposed repository concept has the potential to meet applicable criteria. To this end, some of the assumptions of the initial state are considered in defining the evaluation cases, see further Section 2.5.8.

The FEP processing performed in step 1 identified several relevant FEPs related to deviations from the initial state. These FEPs are not considered in the present analysis but will be handled in future safety analyses as discussed in Section 3.4.2.

### **2.5.3 Description of external conditions**

A key point in the handling of external conditions in SKB's post-closure safety analyses is the establishment of reference external conditions for the subsequent analysis. External conditions can be described as: climate and climate-related issues, large-scale geological processes and effects, and future human actions. A central part of the description of external conditions is the formulation of a well-founded future evolution of the climate and climate-related processes.

#### ***Strategy for defining reference external conditions***

The methodology for handling the future evolution of climate and climate-related issues in SKB's post-closure safety assessments for radioactive waste repositories involves:

- Identifying and describing a range within which future climatic conditions and climate-related processes may vary at the repository site. Within these limits, characteristic climate-related conditions of importance for repository safety can be identified. The conceivable climate-related conditions can be represented as climate-driven process domains (Boulton et al. 2001), where such a domain is defined as "a climatically determined environment in which a set of characteristic processes of importance for repository safety appear". In the following parts of this report these climate-driven process domains are referred to as climate domains.
- Identifying and describing several future potential climate evolutions, here called climate cases, based on information from climate modelling, natural palaeo-climate archives and process understanding. The climate cases shall together cover the wide range of possible future climate developments on the timescale of the safety assessment at hand.

The set of climate cases for a specific safety assessment is chosen to represent conditions covering the range of possible future climate development at the repository site that may influence post-closure safety for the specific repository. Thus, the set of climate cases included in a particular safety assessment is dependent both on the geographic location of the repository site and characteristics of the repository concept and waste type analysed, see Näslund et al. (2013).

The strategy for the selection and description of climate cases in SE-SFL is the same as in SR-Site (SKB 2010b) and SR-PSU (SKB 2014d). However, for SE-SFL, the chosen future climate developments are intentionally simplified and limited in number compared with those that would be adopted in a full safety assessment (e.g. SR-site).

#### ***Selection of reference external conditions***

Three variants of reference external conditions are chosen for the evaluation. The base variant is, for simplicity, a hypothetical condition in which external (climatic) conditions are assumed identical to those at the present-day during the complete analysis period of 1 million years. Thus, the initial state

climatic conditions, defined in Chapter 4, are assumed in this variant. In addition, two climate cases, representing time-varying external conditions, are defined in SE-SFL. These are identified and defined based on the following existing knowledge:

- Characteristic climate-related conditions of importance for repository safety at a Swedish Baltic coastal site can be represented by the temperate, periglacial and glacial climate domains described in Section 2.1 of the **Climate report**.
- The reconstruction of the last glacial-interglacial cycle, utilised in previous safety assessments, e.g. in SR-Site (SKB 2010b, 2011a), provides a relevant example of a reasonable succession of climate domains during a glacial-interglacial cycle.
- It is highly likely that the current interglacial, the Holocene, will be significantly longer than previous interglacials. It may last for 50 000, 100 000 years, or even longer, because of limited future variations in insolation and as a consequence of human emissions of atmospheric greenhouse gases such as CO<sub>2</sub> (see e.g. Berger and Loutre (2002), Ganopolski et al. (2016), SKB (2014d, Section 3.3.5)).

As SE-SFL addresses a timescale of up to one million years, the range of future climatic conditions and climate-related processes is similar to that described for SR-Site (SKB 2011a). A reference glacial cycle for the coming 120 ka was described in SR-Site, which repeated the conditions reconstructed for the last glacial cycle. Five additional climate cases described alternative future developments at Forsmark. The overall climate development in the reconstruction of the last glacial cycle at a Swedish Baltic coastal site, with periods of temperate climate, periglacial conditions with permafrost, ice-sheet development and variations in shore-level, is described in the SE-SFL *simplified glacial cycle climate case* (see Section 4.3 in the **Climate report**), whereas a future climate affected by anthropogenic actions is described in the *increased greenhouse effect climate case* (see Section 4.2 in the **Climate report**). The climate cases considered in SE-SFL are listed in Table 2-1.

**Table 2-1. Selected reference external conditions for the SE-SFL.**

Variant name	Description
<i>Base variant</i>	Present-day external conditions throughout the evaluation period.
<i>Increased greenhouse effect</i>	Initial period of 50 000 years with an initially warmer and wetter climate than at present, followed by present-day temperature conditions.
<i>Simplified glacial cycle</i>	Early permafrost development, ice-sheet overriding, and subsequent submerged conditions.

In SE-SFL, the repository is assumed to be located at a depth to which permafrost and freezing conditions will not penetrate during future periods of cold climate, see Section 2.2.4 of the **Climate report**.

This step in the methodology is mainly documented in the **Climate report** and supports the description and analyses of the reference evolution of the repository and its environs as described in step 7 (Section 2.5.7).

### **Other external conditions**

Large-scale geological processes and effects are described in step 1 of the methodology (see Section 3.4.2).

Future human actions of relevance at a coastal site in Sweden are also identified in step 1 (see Section 3.4.2). Detailed analyses of the potential effects of future human actions on post-closure safety for SFL will be performed in a future full safety assessment.

## **2.5.4 Description of internal processes**

The identification and handling of processes judged to be relevant for post-closure safety is a key element in SKB's post-closure safety analyses. Relevant processes are identified in the processing of FEPs (step 1). In SE-SFL the descriptions of processes for the waste (SKB 2014a) and the barriers (SKB 2014b) in SR-PSU are used. This is judged to be adequate since there are similarities between the SFR and SFL repository concepts. For instance, BHK contains induced activity in metal components that are

surrounded by cement grout, which is similar to the situation with the segmented steel reactor vessels in SFR that also contain induced activity and that are planned to be grouted with cement. In the silo of SFR the concrete is surrounded by bentonite clay, which is similar to the BHA concept with the waste domain being surrounded by bentonite backfill. Given the same combination of materials the interactions between the repository components are controlled by the same processes, even if the detailed conditions in the two repositories will differ to some degree. A difference between the vaults in SFR and SE-SFL is that the waste vaults in SFR, for instance 2BMA, are backfilled by highly transmissive material, whereas BHK and BHA are backfilled by material with low transmissivity.

For the bedrock system, the descriptions of processes for the geosphere in SR-Site (SKB 2010a) and SR-PSU (SKB 2014c) are used. This is judged to be adequate since the repository depth of the Spent Fuel Repository is similar to that evaluated in SE-SFL. Descriptions of processes for the surface systems are given in the **Biosphere synthesis**.

The handling of the internal processes identified in the FEP processing is described in the SE-SFL FEP database (see Section 3.4.2).

### 2.5.5 Suggestion of safety functions

In SE-SFL, safety functions connected to the different parts of the barrier system are suggested based on the safety principle *retardation* (Section 2.3.1) and the knowledge of the initial state (step 2), internal processes (step 4), and external processes (step 1 and 3).

The selection of safety functions is described in Chapter 5. Since the repository design, barrier system, and the site for SFL have not been decided, the selection and definitions of the safety functions might need to be evaluated in subsequent safety analyses as already discussed in Section 2.3.3. Moreover, the FEP handling is simplified in SE-SFL and a deepened future FEP analysis might show that additional processes should be considered in the selection of the safety functions. Further, the SE-SFL assumption that permafrost does not reach repository depth will need to be evaluated in future safety analyses for SFL, when a site is selected.

### 2.5.6 Compilation of input data

In this step, all data to be used in the quantification of repository evolution and in radionuclide transport and dose calculations are selected using a structured process.

The selection of data is determined by the conditions that exist over the period of relevance. In this evaluation, the input data to the radionuclide transport calculations for the repository and bedrock system are described in Shahkarami (2019) and the input data to the radionuclide transport and dose calculations for surface systems are described in Grolander and Jaeschke (2019).

### 2.5.7 Description of reference evolution

A reference evolution of the repository and its environs is defined and analysed, starting from the initial state (defined in step 2, Section 2.5.2) and following the reference external conditions defined in step 3 (Section 2.5.3). The reference evolution constitutes three variants. The *base variant* is a hypothetical condition where external (climatic) conditions are assumed identical to the present-day situation during the complete analysis period of 1 million years. Further, the overall climate development in the reconstruction of the last glacial cycle, with periods of temperate climate, periglacial conditions with permafrost, ice-sheet development and variations in shore-level, is described in the *simplified glacial cycle variant*, and a future climate affected by anthropogenic action is described in the *increased greenhouse effect variant* of the reference evolution.

The purpose of defining and analysing the reference evolution is to understand the overall evolution of the proposed repository concept at a relevant example location under representative external conditions that may influence post-closure safety. To this end, identified FEPs that can affect the post-closure performance of the system are considered. The associated development of the safety functions is touched upon, but not discussed in depth due to the preliminary nature of the safety functions and the simplified analysis. The understanding of the overall evolution and safety functions serves as a basis for the selection and analysis of evaluation cases that follows in step 8.

### 2.5.8 Selection of evaluation cases

To assess the potential for the proposed repository concept to meet applicable criteria on the maximum annual dose for humans after its closure, a set of evaluation cases is defined in SE-SFL. In the evaluation cases the maximum annual effective dose for humans after closure (Section 2.2) is calculated. As described in Section 2.2 the term evaluation case is chosen instead of scenario, since a broader approach is applied in the selection of the cases than proposed in SSM's recommendations for scenario selection. In SSM's guidance to the regulation SSMFS 2008:21, no scenarios for design alternatives or different siting alternatives are included, since the regulations apply to a licensed facility at a given location and with a certain design. In SE-SFL, cases with alternative designs or aspects of siting are central for the evaluation and further development of the repository concept and site selection process. It is noted that these evaluation cases are not directly related to the scenario categories (main scenario, less probable scenarios and residual scenarios) that the SSM guidance define.

A base case is defined (Section 7.4). It is simplified and stylized for ease of interpretation and straightforward comparison with the other evaluation cases with alternative assumptions or temporal evolutions. The base case assumes constant, present-day climatic and other external conditions throughout the full assessment period. Realistic, and in some respects simplified, assumptions are made with respect to internal conditions, based on the current knowledge on the properties of the waste and available barrier materials as analysed in the reference evolution (Chapter 6.2). The choice of simplified, rather than conservative, assumptions is motivated by the probing nature of SE-SFL. It is further assumed, as in all evaluation cases in SE-SFL, that the repository is constructed according to the proposed design concept. Importantly, since SE-SFL is not part of a licensing application, the base case is not intended to establish a main scenario as defined by the regulatory guidelines (SSMFS 2008:21, Section 2.2). It can, however, be noted that the assumed base case addresses the regulatory requirement that the assessment of the repository's protective capability shall include a case based on the assumption that the biospheric conditions prevailing at the time when an application for a license to construct the repository is submitted will not change (SSMFS 2008:37, Section 10).

Further, a set of evaluation cases that evaluate the sensitivity of the resulting activity release and dose to specific assumptions made regarding conditions in the repository and the repository environs are included in the analysis. These cases are chosen to illustrate conditions in the repository and the repository environs which are likely to improve the repository performance in comparison to the base case. For instance, cases with *lower groundwater flow rate* than at the example location and *alternative concrete backfill* are included. Moreover, cases that evaluate the sensitivity of assessment endpoints to selected uncertainties in the geosphere and biosphere are included. The uncertainty relating to the future climate evolution is handled within separate cases, which are based on the *increased greenhouse effect* and *simplified glacial cycle* variants of the reference evolution. Finally, a case relating to the exposure pathway including a drilled well is analysed. The set of evaluation cases included in SE-SFL is described in Section 8.2.

It is not possible to deduce any meaningful probability for the occurrence of the evaluation cases. Thus, a risk summation is not meaningful. Instead the post-closure safety is evaluated as described in Section 2.5.9.

### 2.5.9 Evaluation of post-closure safety

Mathematical models are used to calculate radionuclide releases from the repository, transport from the repository to the surface system, uptake and transfer in the biosphere, and the resultant annual doses to humans. The calculations are based on an approximate representation of the main physical, chemical and biological processes controlling the release and fate of radionuclides at SFL. The calculations are performed for the full set of evaluation cases that have been defined (Section 8.2).

In SE-SFL, the term annual dose is defined as the mean annual effective dose over a lifetime for an individual living in the area with the highest concentration of radionuclides. Furthermore, adults are considered to provide a sufficiently good approximation of the average exposure during a lifetime. This is in line with the ICRP recommendations for long-lived solid waste (ICRP 2000, 2006). To estimate annual exposure during the lifetime of an individual, projected doses have been averaged over a period of 50 years, which is the integration period used by ICRP in the derivation of dose coefficients for adults. The dose coefficients used in the dose calculations take into account retention of radionuclides in the human body and exposure from radioactive progeny, as well as the different radiation

sensitivities of various tissues and organs. Doses calculated using these coefficients are committed effective doses, which are appropriate for calculating the probability of harmful effects of ionizing radiation using the dose to risk factors given in the Swedish regulation (SSMFS 2008:37).

The models utilized in SE-SFL are briefly described in Section 7.1 and the results of the radionuclide transport and dose calculations are summarized in Chapters 7 and 8. Details of the assumptions that have been made and the results obtained are provided in Chapters 5–7 in the **Radionuclide transport report**.

The conditions under which the repository concept has the potential to meet applicable criteria is evaluated with respect to SSM's risk criterion as outlined in Section 2.2. That is, a set of evaluation cases is defined that allows evaluation of which aspects and conditions are favourable for repository performance. In a full safety assessment, the main scenario should result in an annual dose that is below the dose (14  $\mu$ Sv) corresponding to the risk criterion, whereas less probable scenarios with higher dose consequences can be acceptable if their contribution to risk, e.g. by a low probability of occurrence, is small enough that the summed risk does not exceed SSM's criterion. A full scenario analysis is therefore needed to be able to link the calculated doses to a risk value together with adequate representation of data and model uncertainty within the cases. Such an analysis has not been carried out in SE-SFL; the dose criterion per year is used instead as a reference value for evaluating the protective capability of the repository vaults. Evaluation cases that result in annual doses higher than the dose criterion indicate that the conditions and assumptions in the calculations represent a situation for which the repository does not perform well enough to meet the risk criterion. In contrast, evaluation cases that result in annual doses considerably lower than the dose criterion indicate that the assumed conditions are favourable for meeting the risk criterion.

The discussion of the potential of the SFL repository concept to meet criteria on repository robustness is based on the reference evolution and specifically the temporal evolution of the barrier system components together with the results of the evaluation cases. The simplifications in the reference evolution thereby need to be considered. It is important to recognise, however, that a preliminary repository design is the basis for the evaluation. Moreover, uncertainties may have been introduced since the evolution of the barrier system is analysed partly at a high level of technical detail and partly at a more general level utilizing the information from SR-Site and SR-PSU.

### 2.5.10 Conclusions

The assessment of the post-closure safety of SFL is based on an integrated evaluation of both quantitative and qualitative results. The conclusions indicate the potential of the repository to fulfil the regulatory requirements. Moreover, the conclusions indicate under what conditions, concerning the repository environs, the disposed waste, and the barriers, the proposed repository concept has the potential to meet these criteria. Areas that require further investigation or improved input data for a future full safety analysis are discussed and prioritised based on the outcome of SE-SFL together with the earlier suggestions from the SFL-concept study (Grahm et al. 2013, Evins 2013).

The results of the safety evaluation depend on the initial state of the system and on the understanding of internal and external processes. Therefore, the discussion of confidence in the results also considers the assumptions and simplifications introduced in the initial state description and the FEP processing.

## 2.6 Overall uncertainty management

The management of uncertainties is central to a safety analysis and is therefore given considerable focus in SE-SFL. In the general advice to SSM's regulations on disposal of nuclear waste, uncertainties are categorised into scenario uncertainty, system uncertainty, model uncertainty, parameter uncertainty, and spatial variation in parameters used to describe the bedrock. The overall handling of these uncertainties in SE-SFL is briefly described below.

Scenario uncertainty relates to external and internal conditions in terms of type, degree of expression and time sequence, whereas system uncertainty relates to the completeness of the set of features, events and processes (FEPs) included in the analysis. The external and internal FEPs that may influence the post-closure repository evolution are treated in the first step in the methodology applied in SE-SFL

(Chapter 3). The FEP processing builds on the experiences from SR-PSU and SR-Site (SKB 2011a, 2015a), that made use of international work on the matter (e.g. NEA 2006). The methodology strives to obtain a comprehensive treatment of all relevant FEPs. As detailed in Section 3.4.2, some FEPs are not considered in SE-SFL. These are FEPs considered irrelevant for post-closure safety for the proposed repository concept, or FEPs that may be relevant to post-closure safety but have not been considered in SE-SFL. FEPs in the latter category have not been considered due to the nature of SE-SFL not being a full safety assessment. This implies that the basis for handling scenario and system uncertainty can be refined. However, scenario uncertainty is still addressed in relation to several important FEPs that are treated in the analysis. For instance, external climate forcing is treated by introducing three different climate variants. In addition, different alternative internal conditions are discussed for several aspects of the disposal system. Thus, the modelling of the hydrochemical evolution in the bedrock that is part of the reference evolution is carried out for three different assumptions regarding controlling processes (Section 6.2.7). Finally, different possible processes relating to concrete and bentonite evolution are discussed in the reference evolution (Sections 6.2.9 and 6.2.10).

Uncertainty in the calculation models used in the analysis is treated to various degrees in the numerous models used. For instance, the hydrogeological modelling relies on a stochastic approach to handle the uncertainty in the geometry of the flowing fracture network (Joyce et al. 2019). In general, efforts have been made to underpin the trustworthiness of the models, for example by validation or benchmarking exercises. In a future safety analysis, the documentation of the handling of models will need to be more wide-ranging. For instance, a dedicated model summary report would give details on the quality assurance methods applied to the models used in these analyses.

Parameter uncertainty, including the spatial variation of parameters in the geosphere, has to a large extent been handled. The site descriptive model for the Laxemar site includes a comprehensive treatment of parameter uncertainty. In some cases, the data have been sampled, for instance in relation to the stochastic hydrogeological fracture network modelling, whereas in other contexts data have been handled deterministically. When it comes to engineered barrier properties, evaluation cases have been used in SE-SFL to analyse the effects of their variability. The effect on resulting doses of parameters that are affected by the site has also been analysed to some degree, for instance in relation to groundwater flow magnitudes, geosphere retention parameters, or biosphere characteristics. Separate input data reports for the radionuclide transport and dose calculations discuss the uncertainty in the input data (Shahkarami 2019, Grolander and Jaeschke 2019).

All in all, efforts have been undertaken in SE-SFL to demonstrate an understanding of the repository evolution and to ensure the applicability of models, parameter values and other assumptions used for the description and quantification of repository performance. In Chapter 6 and the underlying modelling studies the understanding of the repository evolution is presented. Within the modelling studies for the reference evolution and for the radionuclide transport, the applicability of the models and assumptions is discussed in varying degrees of detail. Given the nature of SE-SFL, there remains a need for a more elaborate analysis and documentation of uncertainties. However, the efforts undertaken in SE-SFL are substantial and should therefore increase the credibility of the results.

## 2.7 Documentation and quality assurance

SE-SFL has been conducted in accordance with SKB's quality management system. A quality plan for SE-SFL was established that points to the most relevant parts of SKB's quality management system and discusses the project specific implementation of it<sup>2</sup>. The plan also defines which categories of tasks are to be carried out and who is responsible for them. The quality plan is a part of, and included as a supplement to, the project plan, which is the steering document that defines the project. Information on decisions and changes to the project that have been approved by the project sponsor is documented in the project decision document.

---

<sup>2</sup>Brandefelt J, 2015. Kvalitetsplan SFL Säkerhetsvärdering. SKBdoc 1479123 ver 1.0, Svensk Kärnbränslehantering AB. (In Swedish.) Internal document.

The quality of the end products, i.e. reports, is secured by a factual expert review followed by a quality control. For SE-SFL, this implies that each report is subject to a factual review by at least two expert reviewers. The factual review focusses on the adequacy of the results, technical professionalism, and objective content. The quality control is to ensure that the report meets high standards in relation to objective reasoning and editorial quality. The reviews are documented in accordance with the requirements in SKB's quality management system.

The quality requirements are based on SKB's quality management system. No efforts have, however, been made in SE-SFL to extend the requirements to ensure that all applicable regulatory requirements are met that need to be fulfilled in a safety analysis that would underlie a license application. This will be part of future safety analyses for SFL.

Modelling work in SE-SFL is documented following the requirements in SKB's quality management system. The data selected for the analysis of the near-field and geosphere is presented in Shahkarami (2019). The goal has been to ensure, in a verifiable manner, that the applied input data are appropriately chosen for the computational tools and their underlying models. For the biosphere, a quality assurance process has been implemented based on the experience from SR-PSU (**Biosphere synthesis**). The QA process is to make sure that information on the usage, sources, review, storage, and involved persons and their roles is documented and accessible.



## 3 Processing of features, events and processes influencing post-closure safety

### 3.1 Introduction

This chapter describes the processing of FEPs influencing post-closure safety for the proposed repository concept at the example location evaluated in SE-SFL. The processing of FEPs is one of the main steps in the safety evaluation methodology, described in Chapter 2.

Processing of FEPs involves

- Identification of all factors that may influence post-closure safety for the proposed repository concept at the example location evaluated in SE-SFL, by screening of potentially important FEPs that are contained in international databases and SKB's previous safety assessments.
- For each FEP identified it is decided if it needs to be included in the analysis.
- Documentation of the handling of each identified FEP in the SE-SFL FEP catalogue.

The SR-PSU FEP Database was used as a basis for the identification of all factors that may influence post-closure safety for the proposed repository concept at the example location for SE-SFL. The main reason for this choice is the similarities in the waste, waste packaging and technical barriers proposed. Further, the SR-PSU FEP Database, including the FEP catalogue and the collection of NEA Project-specific FEPs (PFEPs) that were judged irrelevant for PSU, constitutes a complete set of currently known factors that can influence post-closure safety for a geological repository for radioactive waste. The procedures and sources used to identify relevant features, events and processes are described in Section 3.2.1.

Decisions during the FEP audit and processing stages regarding the treatment of FEPs were made by several groups of SKB experts in the different FEP categories and system components, guided by the corresponding decisions made in SR-PSU and SR-Site. Procedures, rules and criteria used in the SE-SFL FEP audit work are described in Section 3.3.

The objective of the FEP processing in SE-SFL is two-fold; to make sure that all factors that may influence post-closure safety are identified, and, to document the handling of each FEP in the SE-SFL FEP catalogue. In this sense the SE-SFL FEP catalogue constitutes a "look-up-table" with a brief description of the handling of each FEP and references to relevant reports that detail the handling further. Further, FEPs are labelled either "considered" or "not considered", according to how they are handled in the safety evaluation. Considered FEPs have been taken into account in the reference evolution (Chapter 6), whereas non-considered FEPs have not been taken into account in SE-SFL. Some of the not-considered FEPs will be or may be considered in future safety assessments for SFL, indicating that the FEP was left out of the SE-SFL analysis due to the more limited scope of the safety evaluation compared with a full safety assessment, or that relevant data needed to handle the process adequately were missing. The classification of the SE-SFL FEPs is described in Section 3.4.2.

The different steps and results from the FEP processing work are further described in the following sections, whereas full documentation of the work is provided in the **FEP report**.

### 3.2 SE-SFL FEP processing procedure

The SE-SFL FEP processing procedures are similar, but simplified, to the procedures established in SR-PSU (SKB 2014e). The procedure comprises the following steps:

1. Selection of FEP sources.
2. Creation of a SE-SFL preliminary FEP catalogue.
3. FEP audit.
4. FEP processing.
5. Establishment of the SE-SFL FEP catalogue.
6. Establishment of the SE-SFL FEP Database.

The procedure is also schematically illustrated in Figure 3-1 and summarised in the following sections.

#### 3.2.1 FEP sources

The SKB FEP Database is used as a tool for documentation of the outcome of the different steps in the FEP processing procedure. Thus, the FEP Database in itself is regarded as a quality assurance instrument. The overall structure of the SKB FEP Database is shown in Figure 3-2. In each of the SR-Site and SR-PSU FEP Databases, the complete list of PFEPs included in the NEA FEP Database version 2.1 (NEA 2006) is included. Each NEA PFEP belongs to one of the categories relevant or irrelevant to the

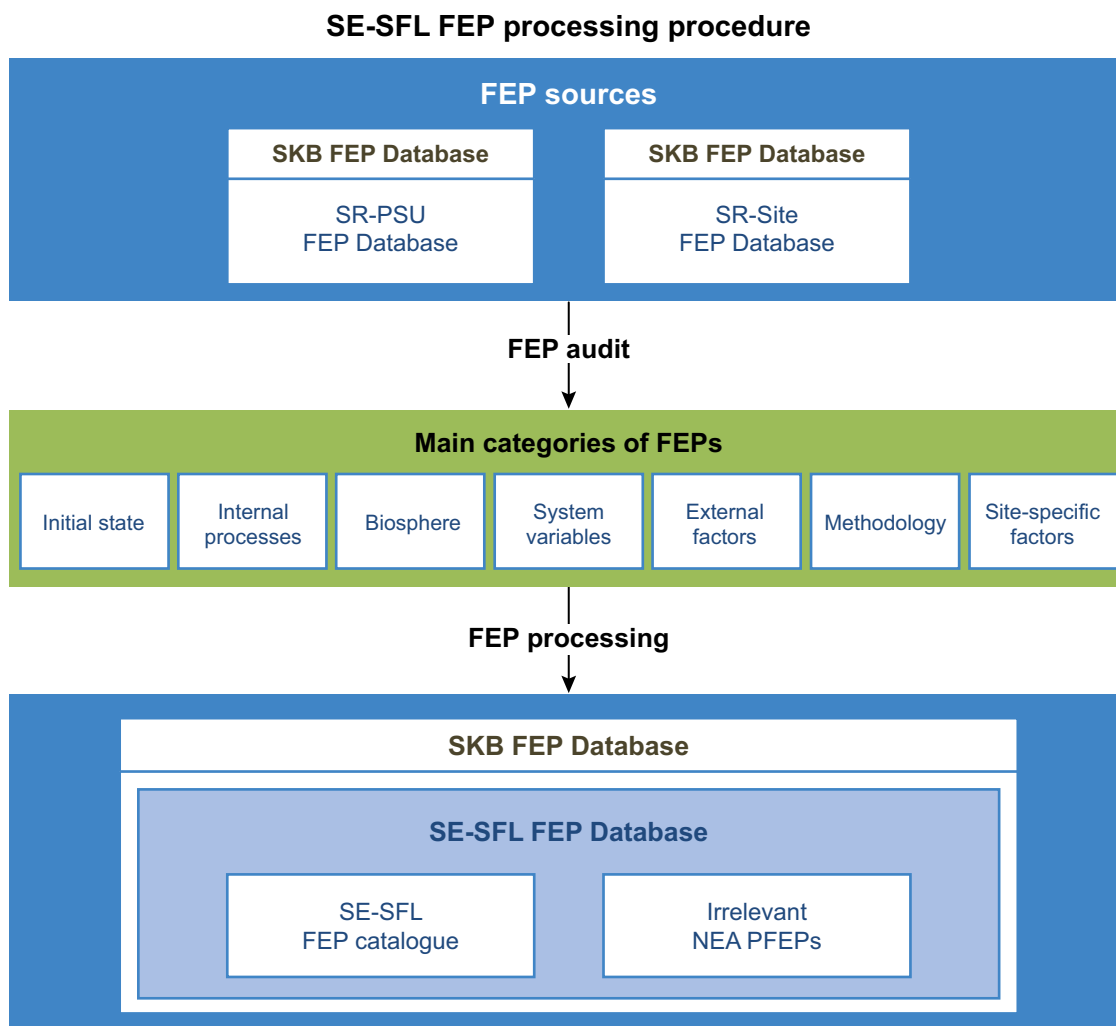


**Figure 3-1.** Schematic illustration of the SE-SFL FEP processing procedure that starts with the SKB FEP databases which include the complete list of NEA PFEPs and results in the SE-SFL FEP catalogue and a list of irrelevant NEA PFEPs.

specific safety assessment. The NEA PFEPs considered to be relevant to the specific safety assessment are mapped to FEPs defined and included in the FEP Database for that specific assessment. The NEA PFEPs considered to be irrelevant to the specific assessment, are included in a list of assessment-specific irrelevant NEA PFEPs. Thus, each of these databases constitutes a complete set of currently known factors that can influence post-closure safety for a geological repository for radioactive waste. The dashed line separating the SR-Can and SR-Site FEP catalogues in Figure 3-2 is indicating that the SR-Site FEP catalogue constitutes a development of the SR-Can version. Similarly, the SR-PSU FEP catalogue used the SR-Site version as input together with the SFR 1 Interaction Matrices.

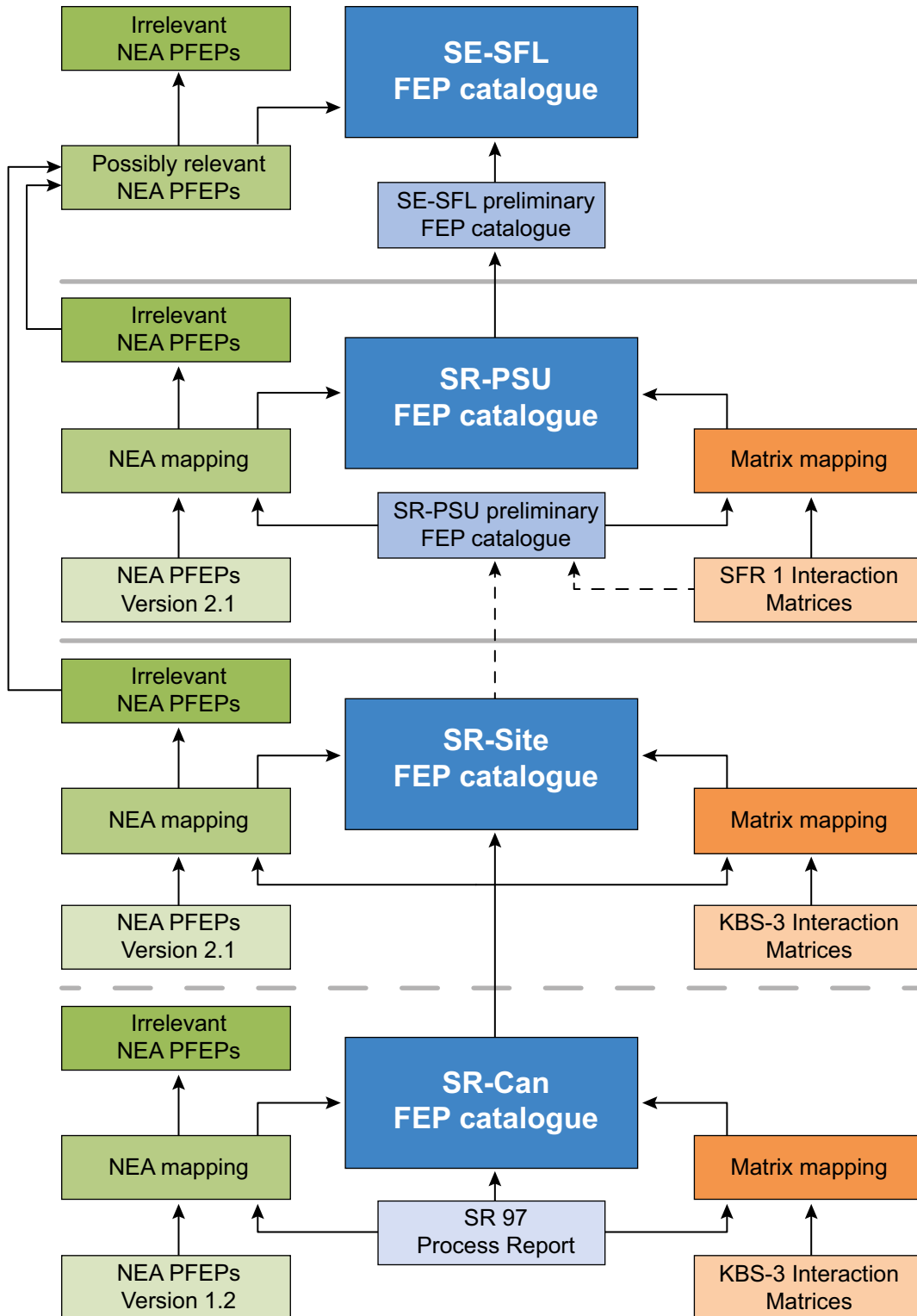


Figure 3-2. Overall structure of the SKB FEP Database.

As illustrated in Figure 3-3, there is an overlap between the PFEPs screened out in SR-Site and SR-PSU, but there are also PFEPs that were uniquely screened out in each of the two safety assessments.

As described in Section 3.1, the SR-PSU FEP Database was used as a basis for the identification of relevant features, events and processes influencing post-closure safety for the proposed repository concept at the example location for SE-SFL. Since both the SR-Site and SR-PSU FEP Databases were informed by the NEA FEP Database, the NEA FEP Database has not been screened in SE-SFL. The set of NEA PFEPs judged irrelevant in SR-PSU were also compared with the corresponding set of NEA PFEPs judged irrelevant in SR-Site. This is to make sure that all FEPs that are relevant for the proposed repository concept for SFL at the example location are included in SE-SFL.

### 3.2.2 Classification of the SE-SFL FEPs

FEPs are classified using the same main categories as were used in the FEP processing for SR-PSU (SKB 2014e) and SR-Site (SKB 2010c). Consequently, the SE-SFL FEPs are divided into the following seven main categories; *initial state*, *internal processes*, *system variables*, *biosphere*, *external factors*, *methodology* and *site-specific factors*. The categories are listed in Table 3-1.

The system analysed in SE-SFL, i.e. the repository and its environs, comprises the disposed radioactive waste and packaging, the engineered barriers surrounding the waste packages, the geosphere and the biosphere in the proximity of the repository. For the *internal processes* and *system variables* main categories in the FEP database, the system is divided into the following system components; *waste form*, *concrete and steel packaging*, *BHK barriers*, *BHA barriers*, *plugs and other closure components*, *geosphere* and *biosphere*.

The main category *biosphere* comprises the subcategories; *biosphere processes*, *biosphere subsystem components* and *biosphere variables*. To illustrate the nature of the *biosphere processes* they are subdivided into six subcategories; *biological processes*, *processes related to human behaviour*, *chemical, mechanical and physical processes*, *transport processes*, *radiological and thermal processes* and *landscape development processes*.

The main category *external factors* comprises the subcategories; *climatic processes and effects*, *large-scale geological processes and effects*, *future human actions* and *other*.

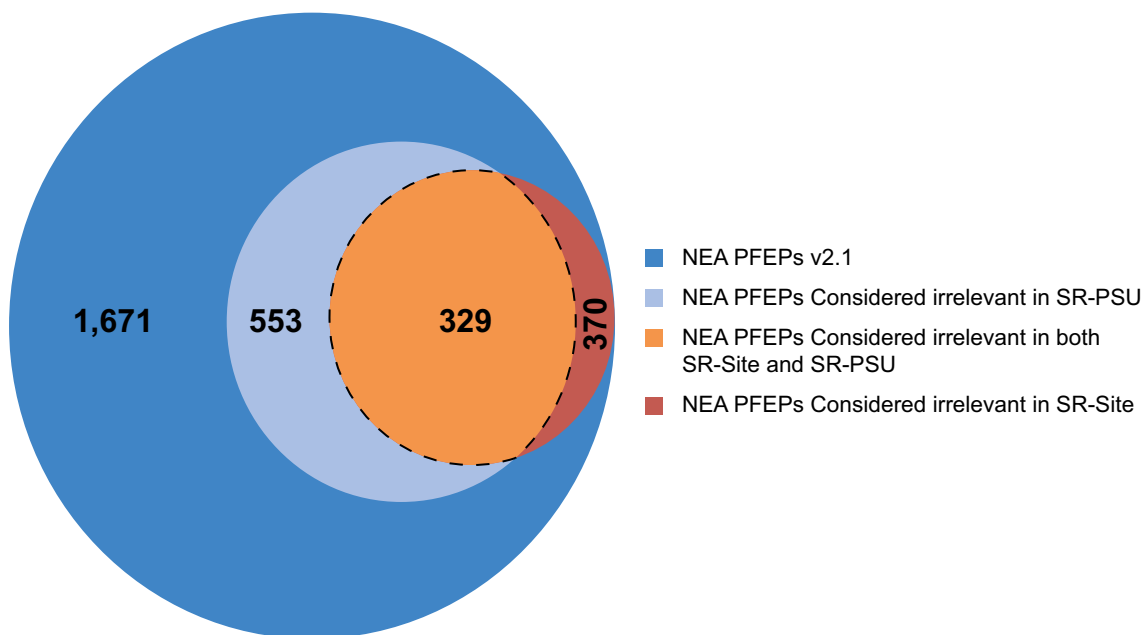


**Figure 3-3.** Illustration of the relation between the subsets of the 1671 NEA PFEPs that are considered irrelevant in SR-PSU (553 PFEPs) and SR-Site (370 PFEPs).

**Table 3-1. Classification of FEPs in the final SE-SFL FEP catalogue.**

<b>Main category</b>
<i>System component or Subcategory</i>
<b>Initial state</b>
<b>Internal processes</b>
<i>Waste form</i>
<i>Concrete and steel packaging</i>
<i>Plugs and other closure components</i>
<i>Geosphere</i>
<i>BHA barriers</i>
<i>BHK barriers</i>
<b>System variables</b>
<i>Waste form</i>
<i>Concrete and steel packaging</i>
<i>Plugs and other closure components</i>
<i>Geosphere</i>
<i>BHA barriers</i>
<i>BHK barriers</i>
<b>Biosphere</b>
<i>Biosphere processes</i>
<i>Biosphere subsystem components</i>
<i>Biosphere variables</i>
<b>External factors</b>
<i>Climatic processes and effects</i>
<i>Large-scale geological processes</i>
<i>Future human actions</i>
<i>Other</i>
<b>Methodology</b>
Site-specific factors

It should be noted that these definitions were set up primarily to facilitate the auditing procedure and the development of the SE-SFL part of the SKB FEP Database. Therefore, all these definitions are not necessarily relevant in subsequent treatments of FEPs in the safety evaluation, e.g. through modelling.

The first five system components listed above all constitute different parts of the repository. A detailed description of each of these is given in Chapter 4 in the present report and in the **Initial state report**. The last two system components listed above, representing the bedrock surrounding the repository and the surface environment in the repository area, are defined as:

*Geosphere.* This system component comprises the bedrock surrounding the repository. It also includes grout injected into fractures in the bedrock during construction of the repository to prevent water inflow to tunnels and other repository cavities. Upwards, the geosphere is bounded by the geosphere–biosphere interface, defined as the top of the weathered bedrock.

*Biosphere.* This system component comprises the near-surface properties and processes, both abiotic and biotic, as well as humans and human behaviour.

As described in Section 2.4, the biosphere studied in the site investigations, i.e. an area of the order of 100-300 km<sup>2</sup> above the repository, is regarded as part of the system that is represented within the analysis. The analysis of the biosphere extends downward to the bedrock surface. The corresponding portion of the geosphere down to a depth of about 1 000 m is regarded as part of the analysed system.

### 3.3 FEP audit

The purpose of the FEP audit is to ensure that all relevant factors influencing post-closure safety for the proposed repository concept at the example location for SE-SFL are identified. As described in Section 3.2.1, the SR-PSU FEP Database was used as a basis for this work. The following sections describe the procedures, rules and criteria used in the SE-SFL FEP audit work.

#### 3.3.1 Audit against the SR-PSU FEP catalogue

As a first audit step, a SE-SFL preliminary FEP catalogue was created based on the contents of the SR-PSU FEP catalogue. This means that all FEPs in the SR-PSU FEP catalogue were considered for inclusion in the SE-SFL FEP catalogue.

During the second audit step, several FEP audit meetings were arranged where both generalists and experts on the different FEP main categories and system components were engaged in discussions. The list of FEPs in the SE-SFL preliminary FEP catalogue was screened for relevance with respect to the proposed concept for SFL. Typically, each meeting was dedicated to one of the main categories or system components. During the screening process, the list of FEPs was changed accordingly to meet the requirements of SE-SFL.

Whereas the system components *waste form, concrete and steel packaging, plugs and other closure components* and *geosphere* are present in both SFR and SFL, the remaining system components dealing with the barriers are not. In SFR, system components representing the barriers in the Silo, BMA, BLA, BRT and BTF, respectively, are used. For SE-SFL, system components for the barriers in BHA and BHK are used. Due to the similarities in barrier properties and function between two of the system components in SR-PSU and the two vaults in SE-SFL it was decided to re-use these FEPs with some minor modifications. Therefore, the FEPs for the system component *silo barriers* in the SR-PSU FEP catalogue were copied and renamed to corresponding FEPs for *BHA barriers* in the SE-SFL preliminary FEP catalogue. The same procedure was performed for the SR-PSU FEPs for the system component *BMA barriers*, which were copied and renamed to corresponding FEPs for *BHK barriers* in the SE-SFL preliminary FEP catalogue. This procedure included FEPs in the main categories *internal processes* and *system variables*. All other FEPs from the SR-PSU FEP catalogue that were kept in the SE-SFL preliminary FEP catalogue retained their names and numbering in order to keep the structure of the two FEP catalogues as consistent as possible.

In the second audit step, the FEPs within the main categories *internal processes* and *system variables* corresponding to the BLA, BRT and BTF barriers were removed from the SE-SFL preliminary FEP catalogue. However, before removing any FEPs, it was ensured that all relevant *internal processes* as well as *system variables* defined in the SR-PSU FEP catalogue for the removed system components were represented in the SE-SFL preliminary FEP catalogue, for the system components BHA and BHK respectively.

The resulting SE-SFL preliminary FEP catalogue consists of 280 FEPs. The SE-SFL preliminary FEP catalogue was then distributed to relevant experts according to their areas of expertise for further processing, aiming at establishing the final product, the SE-SFL FEP catalogue, as described in Section 3.4

#### 3.3.2 Audit against the list of NEA PFEPs considered irrelevant in SR-PSU

Following the initial screening process of FEPs in the SE-SFL preliminary FEP catalogue, the work continued in the third and final audit step to make sure that all FEPs that are relevant for the proposed repository concept for SFL at the example location are included in SE-SFL. As described in Section 3.2.1, the SR-PSU database constitutes a complete set of currently known factors that can influence post-closure safety for a geological repository for radioactive waste. Thus, to complete the audit step, the set of NEA PFEPs judged to be irrelevant in SR-PSU were reviewed.

The screening process was conducted in a series of consecutive steps where the PFEPs were determined either to be relevant or irrelevant to the SE-SFL safety evaluation. In each step, the number of possibly relevant PFEPs left for a final more in-depth analysis was reduced. Several experts participated in the discussions and decision making in the screening process of NEA PFEPs. The relevance

of each NEA PFEP for the system analysed in SE-SFL was considered based on the same relevance criteria as used in the SR-PSU (SKB 2014e) and SR-Site (SKB 2010c) FEP processing, but adapted to the system analysed in SE-SFL.

The PFEPs were screened out if one of the following relevance criteria was fulfilled:

- *Inadequately defined or too general.*
- *Irrelevant for long-term safety, safety assessment or the current safety evaluation.*
- *Considered irrelevant in both SR-Site and SR-PSU* (however, as an additional precaution, the PFEPs were checked again to verify that the screening process in SR-Site was still valid for SE-SFL).
- *Irrelevant for the actual geographical, geological setting or site-selection issues* (some of the PFEPs could be screened out using criteria related to the site-selection process, e.g., areas with a potential for oil, gas or thermal heat production are excluded from being selected as locations for SFL. The potential for future human activities that may lead to disturbed performance conditions for SFL will also be a factor in the site-selection process for SFL).
- *Irrelevant for the actual repository design* (most of these PFEPs were screened out because they are defined for a different repository design including the use of copper canisters with or without a buffer surrounding).
- *Irrelevant for the actual waste form, waste package or waste packaging design* (many PFEPs are defined for waste forms not planned for SFL, e.g. spent nuclear fuel, other high-level waste or vitrified waste).

Since the naming of the NEA PFEPs in some instances can be misleading, the screening was based on the NEA PFEP description, rather than the PFEP name. Any associations outside the primary meaning of the PFEP that arose from consideration of the PFEP description were also documented.

It should be emphasised that certain aspects given in a NEA PFEP description could be relevant for the system analysed in SE-SFL, even though the PFEP mainly relates to a system differing from the SFL system. Such examples are PFEPs related to e.g. bentonite barriers, corrosion and criticality in a spent fuel repository concept, which are all features and processes also relevant to the system analysed in SE-SFL.

It should also be noted that the general strategy in the screening of PFEP relevance was to judge PFEPs as relevant rather than to screen them out at an early stage, unless it was obvious that they are irrelevant. By using this approach, the final decision regarding the relevance of a PFEP and reasons for the decision as to whether it should be included was left to the various experts involved in the further processing of the audit results.

Finally, after the FEP audit was completed, a total of 52 PFEPs possibly relevant for SE-SFL remained. These NEA PFEPs were sent to further FEP processing as described in Section 3.4.

## **3.4 FEP processing**

The FEP list produced during the FEP audit process was further processed by the involved experts in accordance with their different areas of expertise. During this work, the description and handling of each FEP within each of the categories was updated to correspond to the work performed in SE-SFL.

### **3.4.1 Processing results for the NEA PFEPs**

The possibly relevant NEA PFEPs remaining after the third and final audit step were discussed together with the involved experts from different disciplines. The FEPs were then distributed to the experts for further processing and a final screening for relevance to SE-SFL. Depending on the outcome of the processing, the NEA PFEP was treated as follows:

- If the PFEP was considered irrelevant to SE-SFL and screened out during this stage of the FEP processing, this was commented accordingly in the documentation using the wording “*Considered irrelevant in SE-SFL*”, followed by a reason as to why the FEP was considered irrelevant.

If the FEP was considered relevant to SE-SFL, the FEP was treated in one of the two following ways:

- If the PFEP was already covered by existing FEPs in the SE-SFL FEP catalogue, this was commented on accordingly in the documentation using the wording “*Included in the SE-SFL FEP catalogue*” and the SE-SFL FEPs of relevance were referenced by their FEP ID and FEP name.
- If the PFEP was not covered by any existing FEP in SE-SFL FEP catalogue, this was commented on accordingly in the documentation using the wording “*New FEP added to the SE-SFL FEP catalogue*” and the new SE-SFL FEP was referenced by the FEP ID and FEP name. The new FEP was then added to the SE-SFL FEP catalogue together with the required FEP record information, provided by the expert; FEP id, FEP name, description and handling.

A total of 52 PFEPs possibly relevant for SE-SFL were remaining after the FEP audit. It was concluded that 11 of these were irrelevant and 41 were relevant for SE-SFL. However, 32 of the relevant PFEPs were already covered by one or more existing FEPs in the SE-SFL preliminary FEP catalogue. The other 9 PFEPs all concerned the criticality process. This may occur if a sufficient mass and appropriate density of fissile material can accumulate in one place. It also requires the presence of a suitable amount and type of moderator material. Criticality, if it were to occur, would affect the radionuclide inventory and the thermal output and, in extreme cases, might damage the integrity of the engineered barriers and the bedrock. It is not likely that criticality will occur in SFL, but the potential for it to happen still needs to be analysed and the amount of fissile material that can be disposed of without any risk of initiating criticality determined.

Consequently, a new FEP (FEP ID: *WM23* and FEP name: *Criticality*) was added to the SE-SFL preliminary FEP catalogue in the main category *internal processes* and system component *waste form*. This is the only FEP added to the SE-SFL preliminary FEP catalogue as a result of the audit against the NEA PFEPs. This also concluded the work on establishing the final product, the SE-SFL FEP catalogue, which consists of 281 FEPs. The catalogue was then further processed with respect to the information regarding the description and handling of each FEP. This work is described in detail in Section 3.4.2.

A complete list of all NEA PFEPs that were considered in the SE-SFL FEP analysis is provided in the **FEP report** (Table A2-1 in Appendix 2).

### 3.4.2 Processing results for the SE-SFL FEP catalogue

The SE-SFL FEP catalogue was treated in a similar way to the list of NEA PFEPs in the FEP processing. Based on the results from the FEP audit, subsets of the SE-SFL FEP catalogue were filtered out and distributed to relevant experts. The description and handling of each FEP included in the SE-SFL FEP catalogue was updated, or, if necessary, completely re-written, by the experts according to the conditions in the SFL repository and treatment in SE-SFL. Many FEPs are handled in the same manner as in SR-PSU but, for others, the handling is simplified in SE-SFL.

In the SE-SFL FEP catalogue, all FEPs are labelled according to how they are handled in the safety evaluation. The labelling is documented using a separate field (*Handling status in SE-SFL*) in the FEP record where one of the labels *Considered* or *Not considered* is stored for each FEP. The definitions of FEP handling status in SE-SFL, used during the labelling process are described below.

FEPs labelled “*Considered in SE-SFL*” fall into one of the following categories:

- FEP taken into account in the reference evolution that are judged to be of negligible importance for the radionuclide transport and dose calculations.
- FEP taken into account in the reference evolution and included in the radionuclide transport and dose calculations.

FEPs labelled “*Not considered in SE-SFL*” fall into one of the following categories:

- FEP considered irrelevant for post-closure safety for the proposed repository concept.
- FEP may be relevant to post-closure safety, but has not been considered in SE-SFL.

The handling status is mainly used for sorting FEPs in the SE-SFL FEP catalogue and to clearly show how the FEP is handled in the analysis. A more detailed description of the handling is found in a separate field (*Handling*) in the FEP record.

There are several FEPs which for different reasons are *Not considered in SE-SFL*. In many cases, it is stated that the not-considered FEP will be or may be considered in future safety assessments for SFL, indicating that the FEP was left out of the SE-SFL analysis due to the more limited scope of the safety evaluation compared with a full safety assessment, or that relevant data needed to handle the process adequately were missing. In a few cases, where a FEP is clearly irrelevant for SE-SFL, it was still decided to keep it in the SE-SFL FEP catalogue for the sake of completeness relative to SR-PSU and for future reference to show that the process was not overlooked in the analysis.

Finally, the compiled results from the FEP processing of the SE-SFL FEP catalogue were included in the SE-SFL FEP catalogue in the SE-SFL FEP Database, within the SKB FEP Database. In the following sections, the FEP processing is described for each of the main categories in the SE-SFL FEP catalogue.

### **Initial state**

This category of FEPs is related either to the expected *initial state* of the system components within acceptable variations/tolerances, or to deviations from the expected *initial state* outside those tolerances. These FEPs are not system specific but are related to more general considerations and deviations from the *initial state* that follow from undetected mishaps, sabotage, failure to close the repository, etc. There are five *initial state* FEPs in the SE-SFL FEP catalogue:

- *ISGen01 – Major mishaps/accidents/sabotage*, is related to severe perturbations like fire, explosions, sabotage and severe flooding. The reasons for excluding this FEP are (i) the probabilities for such events are low and (ii) if they occur, they shall be reported to SSM, their consequences assessed and correcting or mitigating actions made accordingly.
- *ISGen02 – Effects of phased operation*. This may be considered in future safety assessments for SFL if phased operation is relevant.
- *ISGen03 – Incomplete closure*, concerns the effects of an abandoned, not completely sealed repository or open monitoring boreholes. This will be considered in future safety assessments for SFL.
- *ISGen04 – Monitoring activities*, is related to effects detrimental to safety after repository closure caused by monitoring activities. This FEP was excluded from further analysis because this type of monitoring will not be accepted.
- *ISGen05 – Design deviations – Mishaps*, concerns undetected design deviations and mishaps during manufacturing, transportation, deposition and repository operations etc. This will be considered in future safety assessments for SFL.

Thus, the five *initial state* FEPs are labelled *Not considered in SE-SFL*.

The initial state of the repository and its environs for SE-SFL, defined in step 2 of the methodology (Section 2.5.2), is summarised in Chapter 4. FEPs in the main category *internal processes*, related to the expected initial state of the repository and its environs are associated with the appropriate *system variables* and system components and included in the description of the initial state for the system component in question. The evolution of the waste, waste packaging, engineered barriers as well as of the conditions of the repository environs as a result of operation and construction of the facility are taken into account in defining the initial state.

### **Internal processes**

There are 127 FEPs belonging to the main category *internal processes*. These are subdivided into the SFL system components *waste form, concrete and steel packaging, BHA barriers, BHK barriers, plugs and other closure components*, and the *geosphere*. Each FEP in this category describes a process relevant to one or several of the system components defined for the SE-SFL safety evaluation, excluding the *biosphere*. The *biosphere* FEPs are handled as a separate category in the FEP catalogue, see below. The various system components are also characterised by several *system variables*, see below. Within a system component, each process is influenced by one or several of the *system variables* describing the state of the component, and the process, in turn, influences one or several of the *system variables*.

Since the SFR and SFL waste packaging, technical barriers and other repository components have many similarities, the descriptions of *internal processes* for the *waste form* (SKB 2014a) and the *barriers* (SKB 2014b) in SR-PSU are used also in SE-SFL. For the bedrock system, the descriptions of *internal processes* for the *geosphere* in SR-Site (SKB 2010a) and SR-PSU (SKB 2014c) were used.

The results from the FEP processing for the main category *internal processes* are described separately for each system component in the following subsections.

**Waste form.** There are 23 FEPs included for the system component *waste form* in the SE-SFL FEP catalogue. These are the same FEPs as defined in SR-PSU, with the addition of *WM23* that concerns criticality. One of the FEPs is labelled *Not considered in SE-SFL*:

- *WM13 – Colloid formation and transport.*

This FEP will be considered in future safety assessments for SFL.

**Concrete and steel packaging.** There are 16 FEPs included for the system component *concrete and steel packaging* in the SE-SFL FEP catalogue. These are the same FEPs as defined in SR-PSU. Five of the FEPs are labelled *Not considered in SE-SFL*:

- *Pa03 – Water uptake and transport during unsaturated conditions.*
- *Pa04 – Water transport under saturated conditions.*
- *Pa05 – Fracturing/deformation.*
- *Pa06 – Advective transport of dissolved species.*
- *Pa07 – Diffusive transport of dissolved species.*

For all these FEPs it is assumed the respective process is not affected by the presence of the packaging.

**BHA barriers.** There are 26 FEPs included for the system component *BHA barriers* in the SE-SFL FEP catalogue. These are the same FEPs as defined for the *silo barriers* in SR-PSU. Two of the FEPs are labelled *Not considered in SE-SFL*.

- *BHABa07 – Mechanical processes.* No mechanical analysis has been performed within SE-SFL.
- *BHABa19 – Montmorillonite colloid release.* Process neglected.

Both FEPs will be considered in future safety assessments for SFL.

**BHK barriers.** There are 19 FEPs included for the system component *BHK barriers* in the SE-SFL FEP catalogue. These are the same FEPs as defined for the *BMA barriers* in SR-PSU. All *BHK barrier* FEPs are labelled *Considered in SE-SFL*.

**Plugs and other closure components.** There are 21 FEPs included for the system component *plugs and other closure components* in the SE-SFL FEP catalogue. These are the same FEPs as defined in SR-PSU. Three of the FEPs are labelled *Not considered in SE-SFL*.

- *Pg06 – Piping/erosion.* The process is neglected in SE-SFL.
- *Pg15 – Montmorillonite transformation.* The process is neglected in SE-SFL.
- *Pg16 – Montmorillonite colloid release.* The process is neglected in SE-SFL.

All these FEPs will be considered in future safety assessments for SFL, when a more detailed description of the repository design and the conditions in the repository environs becomes available.

**Geosphere.** There are 22 FEPs included for the system component *geosphere* in the SE-SFL FEP catalogue. These are the same FEPs as defined in SR-PSU. Five of the FEPs are labelled *Not considered in SE-SFL*.

- *Ge05 – Deformation of intact rock.*
- *Ge06 – Displacements along existing fractures.*
- *Ge07 – Fracturing.*
- *Ge09 – Erosion and sedimentation in fractures.*
- *Ge21 – Earth currents.* Earth currents are not accounted for in SE-SFL.

All these FEPs will be considered in future safety assessments for SFL.

## System variables

There are 50 FEPs belonging to the main category *system variables*. In the same way as for *internal processes*, these FEPs are subdivided into the SFL system components *waste form, concrete and steel packaging, BHA barriers, BHK barriers, plugs and other closure components*, and the *geosphere*. Within a system component, each process is influenced by one or several of the *system variables* describing the state of the component, and the process, in turn, influences one or several of the *system variables*. The FEPs are used to characterise the system components, both in terms of the initial state of these variables and their states during repository evolution. The *biosphere* FEPs are excluded from the main category *system variables* in the same way as they are from the *internal processes*. Instead, the *biosphere* FEPs are handled as a separate main category in the FEP catalogue with their own processes and variables, see below.

Since the SFR and SFL waste and repository concepts have many similarities, the *system variables* given for the *waste form* and *packaging* (SKB 2014a) and the engineered *barriers* (SKB 2014b) in SR-PSU are used also in SE-SFL and the initial state of these system components is described in the SE-SFL **Initial state report**. For the bedrock system, the *system variables* of *internal processes* for the *geosphere* in SR-Site (SKB 2010a) and SR-PSU (SKB 2014c) are used. A description of the initial state of the *geosphere* and *biosphere* is provided in Chapter 4 in the present report. Each *system variable* in these reports is also associated with a FEP record in the SE-SFL FEP catalogue.

The following *system variables* are defined for all system components:

- Gas variables.
- Geometry.
- Hydrological variables.
- Material composition.
- Mechanical stresses.
- Temperature.
- Water composition

For the *waste form*, two additional FEPs are defined for the radionuclide inventory and radiation intensity. For the *geosphere*, the number of system variable FEPs is larger with slightly different and more detailed definitions, but they essentially cover the same topics.

For all *system variable* FEPs defined for the system components *waste form, concrete and steel packaging, BHK barriers, BHA barriers* and *plugs and other closure components*, the FEP description and handling are identical to SR-PSU. These FEPs are all included in the description of the reference evolution in Chapter 6 in the present report.

For the *system variable* FEPs defined for the *geosphere*, the handling is missing in SR-PSU so a comparison between these and the SE-SFL FEPs is not possible. However, all but one of the *system variable* FEPs are considered in SE-SFL and are included in the description of repository evolution. Thus, one *system variable* FEP is labelled *Not considered in SE-SFL*;

- *VarGe07 – Rock stresses*, as a function of time and space. A 3D stress field based on a geological history model is needed to assess the spatial and temporal stress variability and its consequences in terms of fracture and deformation zone reactivation as well as potential for fracture generation and propagation under subsequent external loads. Since this aspect is strongly site-dependent and no site has been selected for SFL, this analysis has been omitted at this stage but will be considered in future safety assessments for SFL.

## Biosphere

The *biosphere* FEPs describe a subsystem, a variable or a process relevant to one or several of the subsystems. There are 68 *biosphere* FEPs in the SE-SFL FEP catalogue, identified as 12 *biosphere subsystem components* (divided into 10 *physical components* and 2 *boundary components*), 6 *biosphere variables* (features), and 50 *biosphere processes*. These are treated separately in the FEP catalogue in the same way as was done for SR-PSU, i.e. they are not included in the main categories *internal processes* or *system variables*. The biosphere system components and variables are given in the **Biosphere synthesis**.

A major effort was directed to the formulation of the *biosphere* FEPs in the safety assessment SR-PSU (SKB 2013a, 2014e, 2015d), building on work done for SR-Site (SKB 2010d) and previous safety assessment for SFR. This work also served as a basis for the analysis of biosphere FEPs in SE-SFL. SKB (2014e) contains general descriptions of the processes considered to be of importance for the safety assessment. In addition, it contains definitions of subsystems of the biosphere and variables needed to describe the evolution of the biosphere in relation to those aspects that are of importance for radionuclide accumulation and transport. For each *biosphere process*, *biosphere subsystem component* and *biosphere variable* defined in SKB (2013a), a *biosphere* FEP has been included in the SE-SFL FEP catalogue.

To illustrate the nature of *biosphere processes*, they have been grouped into six subcategories (*biological processes*, *processes related to human behaviour*, *chemical, mechanical and physical processes*, *transport processes*, *radiological and thermal processes* and *landscape development processes*). In the **Biosphere synthesis**, these process categories are defined, and key processes are briefly described, pointing out mainly the changes compared with SR-PSU. In addition, features of the physical components are also briefly described.

Not all identified *biosphere processes* are expected to be quantitatively important for transport and accumulation of radionuclides from a repository in the bedrock at the assessment site. Of the 50 identified *biosphere processes*, 46 were considered relevant and sufficient to consider for a safety assessment of the repository. All processes, considered as well as those not considered, have a record in the SE-SFL FEP catalogue. The identification of relevant FEPs and model development has been going on in parallel at SKB for the last 20 years and thus knowledge of important FEPs has been considered in the development and improvements of the radionuclide model for the biosphere. However, to incorporate all 46 relevant FEPs into the radionuclide transport model would result in a very complex model. Instead, many of the FEPs are included in supporting modelling used to derive parameter values for the radionuclide model. A mapping of identified *biosphere* FEPs to the different modelling activities has been performed showing that all the relevant FEPs are included in one or more modelling activities. All SE-SFL *biosphere* FEPs are identical to those in SR-PSU, except for three (*Bio09*, *Bio11* and *Bio20*, see descriptions below) which were reconsidered after review. Two of the FEPs (*Bio11* and *Bio20*) that were not considered in SR-PSU were *Considered in SE-SFL*:

- *Bio11 – Movement induced by organisms*, which was included since filter feeders can dominate the benthic biomass in the model area and cannot generally be ruled out in marine areas.
- *Bio20 – Change of pressure*, which affects the water level in the enclosed bays and thus also the water circulation.

One FEP (*Bio09*) that was *considered* in SR-PSU was *Not considered in SE-SFL*. The four *biosphere process* FEPs that are labelled *Not considered in SE-SFL* are:

- *Bio09 – Intrusion* (of organism), which is not relevant at several 100 m depth for organisms other than humans and thus is excluded from the FEP list of the biosphere. For humans this FEP is handled in *future human actions*.
- *Bio23 – Loading*, is the exertion of force caused by the weight of material on the underlying bedrock. This process was excluded since it is not important to consider for a repository located where the regolith is thin. Ice load affects the geosphere directly.
- *Bio44 – Irradiation* (by ionising radiation), is the process whereby an object is exposed to radiation and absorbs energy. This process was excluded since the expected radionuclide levels at the surface are too low to affect regolith and water in regolith by irradiation.
- *Bio46 – Radiolysis*, is the disintegration of molecules caused by radiation. This process was excluded since the expected radionuclide levels are too low to affect regolith and water in regolith by irradiation.

### **External factors**

This category comprises FEPs that act outside the boundary of the system analysed in SE-SFL. There are 27 *external factor* FEPs in the SE-SFL FEP catalogue, divided into the subcategories *climatic processes and effects*, *large-scale geological processes and effects*, *future human actions* and *other*, see sections below. The results from the FEP processing for the main category *external processes* are described separately for each subcategory in the following subsections.

**Climatic processes and effects.** The handling of climate and climate-related issues is documented in the **Climate report**. There are seven *climatic processes and effects* FEPs included in the SE-SFL FEP catalogue. These are the same FEPs as were defined for SR-PSU. These climate FEPs are fewer than those defined for SR-Site since, during the FEP work in SR-PSU, it was found appropriate to combine some of the climate FEPs defined in SR-Site and thus reduce the number of FEPs in the SR-PSU FEP catalogue. All *climatic processes and effects* FEPs are labelled *Considered in SE-SFL*. For some of the FEPs, e.g. surface denudation, a full safety assessment for SFL will include more aspects of the FEP.

**Large-scale geological processes and effects.** These issues are covered by two FEPs in the SE-SFL FEP catalogue. These FEPs are the same as those defined for SR-PSU and SR-Site and the descriptions provided in SR-PSU (SKB 2014c) and in the SR-Site geosphere process report (SKB 2010a) apply also for SE-SFL. Both FEPs are labelled *Not considered in SE-SFL*:

- *LSGe01 – Mechanical evolution of the Shield* concerns the geological history of the Baltic Shield and its consequences for the current mechanical conditions of the Baltic Shield.
- *LSGe02 – Earthquakes.* The layout of the repository and its geographic location, i.e. the local properties of the geosphere, will to a very large degree steer the outcome of a safety assessment. As both the layout and siting are still at a conceptual stage, there is no defensible rationale for engaging in any advanced seismic hazard analyses. In particular, the spatio-temporal variability of the magnitude-frequency relations needs to be addressed over a glacial cycle. This is a major undertaking that did not fit into the scope of this assessment.

**Future human actions (FHA).** There are 17 *future human actions* FEPs defined in the SE-SFL FEP catalogue. These are the same as were used in SR-PSU and reported in SKB (2014g). No further analysis was performed for these FEPs and all FEPs are labelled *Not considered in SE-SFL* but they are still defined as FEPs in the SE-SFL FEP catalogue. Detailed analysis of the potential effects of future human actions on post-closure safety for SFL will be performed in future full safety assessments. The justification for excluding these FEPs from further analysis is documented in the respective FEP records. For most FEPs, it is stated that it either may, or will, be considered in future safety assessments for SFL. For two of the FEPs, it is considered unlikely for the event to have any effect on the repository:

- *FHA14 – Landfill*, is related to the construction of a dump or landfill. It is considered unlikely that releases at a landfill would have an impact at the repository depth.
- *FHA15 – Bombing or blasting, explosions and crashes*, is related to deliberate or accidental explosions and crashes near the repository. Due to the large depth of SFL, explosions and crashes are considered highly unlikely to have any effect on the repository.

**Other.** As in the SR-PSU FEP catalogue, there is only one SE-SFL FEP included in the subcategory *other* and it deals with meteorite impact. This FEP is labelled *Considered in SE-SFL* but is not handled in SE-SFL. The motivation for this is that there is very little likelihood that a meteorite big enough to damage the repository will impact the Earth. The probability that the impact will occur on the repository site is very low. Moreover, such an impact would cause great damage to the local and regional biosphere, humans included. These direct effects of a meteorite impact are judged to be far more serious than any possible radiological consequences.

## **Methodology**

The *methodology* FEPs address issues relevant to the basic assumptions for the assessment and to the methodology used in it. There are two *methodology* FEPs included in the SE-SFL FEP catalogue. These are the same as in the SR-PSU and SR-Site FEP catalogues, with some differences in the handling. Both *methodology* FEPs are labelled *Considered in SE-SFL*. The *methodology* applied in the safety evaluation SE-SFL is described in Chapter 2 in the present report.

## **Site-specific factors**

The *site-specific factor* FEPs represent issues that are specifically relevant to the selected site. The FEPs included in the SR-PSU FEP catalogue (SKB 2014e) are specific for the Forsmark site, where the SFR repository is placed, with proximity to the nuclear power plant at Forsmark and the power

cable to Finland, Fenno-Skan. Since SE-SFL is based on data from the Laxemar site, the description of the corresponding FEPs used for Laxemar in SR-Can (SKB 2006b) were used instead with minor modifications. Depending on what site is selected for the SFL repository, these FEPs will be updated with relevant site-specific information in a future full safety assessment for SFL. It could be argued that it is not meaningful to define site-specific factors at this stage since no site has been selected yet. However, for the sake of comprehensiveness, these two FEPs were, as in SR-PSU (SKB 2014e) and SR-Site (SKB 2010c), also propagated to the SE-SFL FEP catalogue and both are labelled *Not considered in SE-SFL*:

- *SiteFact02 – Construction of nearby rock facilities.* This will be considered in future safety assessments for SFL.
- *SiteFact03 – Nearby nuclear power plant.* This will be considered in future safety assessments for SFL, provided that the repository is located close to a nuclear power plant.

### 3.5 The SE-SFL FEP catalogue

Based on the FEP processing described above, a SE-SFL FEP catalogue was established. The resulting FEP catalogue contains all FEPs defined for the SE-SFL safety evaluation. The SE-SFL FEP catalogue is included in the SKB FEP Database together with documentation of the FEP processing results which is included as separate tables in the SE-SFL FEP Database. The SKB FEP Database also encompasses the SR-PSU FEP Database, as well as the SR-Site, SR-Can and SR 97 FEP Databases (see Section 3.2.3 and Figure 3-2). A digital version of the SKB FEP Database (i.e. a FileMaker™ runtime version) is available for download from the SKB web page together with instructions on how to navigate the database.

Table 3-1 summarises the classification of FEPs in the final SE-SFL FEP catalogue. In total, the SE-SFL FEP catalogue comprises **281 FEP records**, of which 234 are labelled *Considered in SE-SFL* and 47 are labelled *Not considered in SE-SFL*. The FEPs in the latter category are briefly discussed in Section 3.4.2.

In the SE-SFL FEP catalogue, each FEP is represented by a FEP record specifying the FEP id, FEP name, main category, system component and/or subcategory, handling status, description, handling, reference and revision. A complete listing of the SE-SFL FEP catalogue is provided in the **FEP report** (Table A1-1 in Appendix 1). For practical reasons, only the FEP ID, FEP name, main category, system component or subcategory and a short note on handling, are shown in the table. The full descriptions and handling can be very extensive for some FEPs, which makes the inclusion of these fields impractical. The complete information for each FEP is, however, present in the SE-SFL FEP catalogue.

In parallel with the development of the SE-SFL FEP catalogue, a major update of the layout and functionality in the SKB FEP Database was conducted. The work focused on the SE-SFL version of the SKB FEP Database, whereas the other versions, SR-PSU, SR-Site and SR-Can, were left unchanged. It is however planned to update the layouts in all other versions of the SKB FEP Database in the future so that the visual appearance, as well as the user experience, is made consistent throughout the database.

## 4 Initial state of the repository and its environs

### 4.1 Introduction

This chapter describes the initial state of the repository and its environs for SE-SFL. The definition of the initial state is one of the main steps in the safety evaluation methodology, described in Chapter 2.

The initial state is defined as the expected state of the repository and its environs at closure, under the assumption that the repository is designed and constructed in accordance with the proposed repository concept and placed at the example location at approximately 500 m depth in the position in Laxemar assumed for SE-SFL (Section 1.2). At closure the closure components are installed including backfilling and plugging of the vaults, tunnel system, shaft and boreholes. Further, material properties for the repository components are taken from previous safety assessments. For instance, it is assumed that the BHA backfill is constructed with bentonite that is similar to that planned for the buffer in the Spent Fuel Repository, and the BHK backfill is constructed with concrete similar to the construction concrete employed in the existing SFR repository. The repository is assumed to be closed in 2075 AD.

The description of the initial state is divided into two major parts: the first part describes the waste and the repository with the waste vaults, tunnel system and closure components (Sections 4.2 and 4.3) and the second part describes the environs (Sections 4.4–4.6). The description of the environs at closure comprises information about the climate, surface system, and bedrock system. The information and the assumptions that serve as a basis for the initial state of the waste and the repository are compiled in the **Initial state report**, including general descriptions together with initial state values of variables applied to evaluate the post-closure safety of the repository. The initial state of the climate is described in detail in the **Climate report** and the initial state of the surface system is described in the **Biosphere synthesis**. The geosphere properties are compiled in the present chapter based on the site descriptive modelling of the example site at Laxemar (SKB 2009).

SE-SFL provides SKB with a basis to assess under what conditions the proposed repository concept has the potential to meet applicable criteria. To this end, some of the assumptions made concerning the initial state are evaluated in the evaluation cases, see further Section 2.5.8.

Deviations from the initial state may occur, through undetected mishaps, sabotage, failure to close the repository, etc. As described in Section 3.1, the consequences of such events will be analysed in a full safety assessment for SFL, but are not analysed in SE-SFL.

It is important that the analysis of post-closure safety is based on well-founded assumptions and therefore methods for testing and inspecting the materials and methods used during construction of SFL will be developed and defined during the detailed design phase of the repository. The control programme is to ensure that the repository will reach its desired initial state and retain the required post-closure properties. The aim is furthermore to confirm that the system components with a function for post-closure safety will comply with the requirements.

### 4.2 Waste

In this section, the waste and waste packaging are described based on the information contained in the **Initial state report**.

#### 4.2.1 Origin and waste types

A large portion of the waste allocated to SFL originates from the Swedish nuclear power plants (NPPs). The long-lived low- and intermediate-level wastes from the NPPs that are to be disposed of in BHK typically consist of neutron-activated components from inside or close to (0.5–1.0 m) the reactor core. For most of these components, only a limited part is close enough to the core to accumulate a significant level of induced activity.

The different components planned for disposal in BHK are described in the **Initial state report** and include:

- Core shroud (BWR).
- Core grid (BWR).
- Core shroud head (BWR).
- Control rod guide tubes and control rods (BWR).
- Detectors, guide tubes, boron plates and fuel assembly components (BWR).
- Miscellaneous scrap metal (BWR).
- PWR components and reactor pressure vessels (including that from the Ågesta reactor).
- Secondary waste (in the form of swarf, filters, abrasives and decommissioned segmentation equipment).

For the parts further away from the reactor core, the major source of activity is surface contamination. These parts can therefore be separated from those with significant levels of induced activity, cleaned and deposited in SFR. This procedure has been taken into account when estimating the amount of waste for disposal in SFL. However, since details on how to separate the long-lived from short-lived waste have not yet been specified, the total activity calculated for each component has been attributed to the parts that will be deposited in SFL.

The waste that is to be disposed of in BHA originates from Studsvik Nuclear AB (SNAB) and Cyclife Sweden AB and comprises previous and future waste from research carried out at the Studsvik site as well as waste from decommissioning. The waste consists mainly of ion-exchange resins, precipitation sludge, exchanged components from the research reactor at Studsvik, tools, instruments, consumables laboratory ware, ashes, glove boxes and radiation sources<sup>3</sup>. Furthermore, the waste collected from other producers of radioactive materials in Sweden, such as those involved in medicine, industry and research, is included in the presented quantities (**Initial state report**, Section 3.8.2).

Low- and intermediate-level radioactive waste is currently stored at the Studsvik site. Some decommissioning waste that has been close to the core in the R2 research reactor at Studsvik, such as control rods and other core components is classified as long-lived and allocated to SFL. Similarly, systems containing more than  $10^{10}$  Bq C-14 are allocated to SFL (SKB 2015b).

The waste from AB SVAFO company comprises legacy waste from the early operations at the Studsvik site as well as from Swedish military research. Another fraction of the waste from AB SVAFO originates from the operation and decommissioning of the Swedish research reactor R1, a research reactor at the Royal Institute of Technology and the R2 and R2.0 research reactors at the Studsvik site. Also, the decommissioning waste from the remaining facilities at the Studsvik site is included in the presented waste quantities.

Decommissioning waste from the Ågesta reactor is also handled by AB SVAFO and will be deposited in SFL. The legacy waste from AB SVAFO is already conditioned, but information about the radionuclide and other materials content is limited.

The radioactive waste from the operation of the ESS is planned to be deposited in SFL. Since the plans for the construction and operation of ESS are not yet finalised, only limited information is available concerning the amount and composition of the likely waste arising (Persson 2015). The waste volume and amount of material from ESS are not considered in the safety evaluation of SFL. The most active waste from ESS will be components that have been directly irradiated. Some of the components will be exchanged at regular intervals during the operational period, thus giving rise to operational waste, whereas others will not be disposed of until the decommissioning phase (**Initial state report**, Section 3.1).

---

<sup>3</sup> Herschend B, 2015. Long-lived waste from AB SVAFO and Studsvik Nuclear AB. SKBdoc 1431282 ver 1.0, Svensk Kärnbränslehantering AB. Internal document.

#### 4.2.2 Waste acceptance criteria and waste type descriptions

There are no waste acceptance criteria (WAC) to date for the waste to be deposited in SFL. Therefore, the waste that is being produced and is assigned to SFL is not allowed to be finally conditioned i.e. it must be retrievable in order to make sure that the future WAC can be fulfilled.

Waste type descriptions are a part of SKB's system to facilitate the administrative handling of waste. The waste is divided into waste types and, since the late 1980s, waste type descriptions have been used to document the waste to be deposited in SFR. The waste type descriptions include an overview of the origin of the waste and the handling sequence, detailed descriptions of properties and characteristics of the waste, including the material codes, type of packaging and treatment methods etc. This includes a description of production data, results from investigations and calculations as well as control methods used. Description of the controls on packaging, waste form and waste package are also given. Waste type descriptions will also be determined for each waste type to be disposed in SFL.

#### 4.2.3 Waste packaging for BHK

Today, large steel tanks are used for storage of the core components from maintenance of the NPPs. It is planned to also use these tanks for final disposal of the waste in BHK, given the assumption that they can comply with the WAC that will be developed for the waste packages. These tanks will need to be handled by the SFL handling and transport systems.

The outer dimensions of the steel tanks are  $3.3 \times 1.3 \times 2.3$  m (length  $\times$  width  $\times$  height) giving a total volume of about  $10 \text{ m}^3$ . There are tanks available with wall thicknesses of 50, 100, 150 or 200 mm. The waste is loaded in a cassette which is placed in the steel tank, see Figure 4-1. Both the cassettes and the steel tanks are made of carbon steel. The cassette is designed for loading of 12 tonnes of waste. However, experience from the nuclear power plants in Oskarshamn and Forsmark indicates that most of the tanks contain only about 3 tonnes, with a maximum of 6–7 tonnes. In order to improve the packing density, additional segmentation of the waste would be required. Further details are provided in the **Initial state report**.

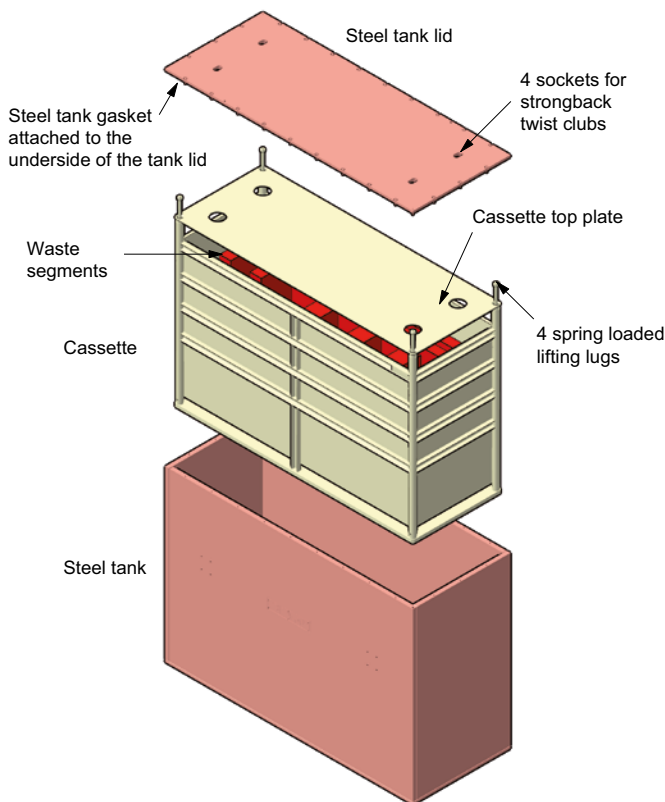


**Figure 4-1.** Schematic illustration of the steel tank for neutron-activated components.

Moulds of dimension  $1.2 \times 1.2 \times 1.2$  m are used for storage of secondary waste from Forsmark and Oskarshamn. The secondary waste includes filters, abrasives and decommissioned segmentation equipment. The volume estimates for the secondary waste have been based on these dimensions (Herschend 2014).

The biological shields from the Ringhals PWRs are accounted for in the SFL-inventory. However, the volume is included without packaging since it is unrealistic to assume that the entire biological shield will be segmented and disposed of in steel tanks (Herschend 2014). Since the details of the handling of the biological shield have not been decided yet, the assumption in SE-SFL is that it is accounted for without packaging. However, it may show that the best way forward is to use packaging for parts of the material, and it could also be studied if parts of the material could possibly be disposed of in SFR.

#### 4.2.4 Waste packaging for BHA

Most of the legacy waste currently stored at the Studsvik site is stored in 200 L drums containing a mixture of waste and concrete. To provide for safe storage and handling, these drums have recently been placed in new 280 L drums. Solidified sludge is stored in steel drums containing the mixers used in the solidification process. Ashes, general waste and scrap metal are stored in steel drums with inner 100 L steel drums surrounded by concrete. Some of the waste at the Studsvik site is also stored in steel and/or concrete moulds. Further details are provided in the **Initial state report**.

The current plan is to dispose of the waste to BHA according to the packaging descriptions below, which comprises overpacks for standard moulds (Figure 4-2a), standard 200 L drums (Figure 4-2b) and 280 L protection drums (Figure 4-2c).

The waste packaging consists of a welded framework of square tubes, the sides of which are made of corrugated steel panels designed to withstand the forces from grouting of the inner waste packages. The design of the waste packaging is similar for all waste types, with adaptations to the height of the waste packaging and, for the 280-litre protection drums, the inner dimensions. The 200-litre drums are first placed on trays to facilitate handling. There are four drums on each tray. The bottom plate of the waste packaging is equipped with stiffeners arranged like a cross inside the waste packaging. They also act as guides when placing the moulds or trays with drums in the waste packaging. The waste packaging is assumed to be filled with grout to the top. No steel lid will be used. The grout surface will be leveled with the top of the steel frame. Reinforcement bars will be placed on top of the waste to prevent cracking of the top-most layer of the grout. It should be noted that before grouting the waste, the lids of the 280-litre protection drums will be removed in order to fill the void between the 280-litre protection drums and the 200-litre drums containing the waste with grout. Further details are provided in the **Initial state report**.

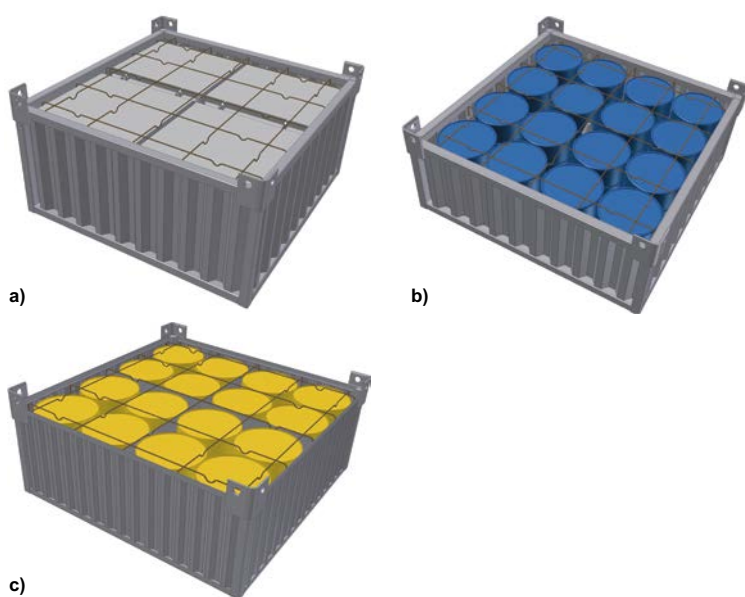


**Figure 4-2.** 3D-view of waste packages loaded with a) standard moulds, b) standard 200 L drums, and c) 280 L protection drums. Reinforcement bars that will stabilise the future grout on top of the moulds are also shown.

#### 4.2.5 Waste and waste packaging material quantities and volumes

Waste quantities, volumes and the number of waste packages for the waste vaults are presented in Table 4-1. These are also described in more detail in the **Initial state report**. It is assumed that the PWR reactor pressure vessels are to be segmented and packed into the steel tanks prior to disposal. The material inventory, the surface area of metals in the waste, the waste packaging materials, and the contents of complexing agents are described in the following subsections.

**Table 4-1. Total weights, volumes and voidage of waste and waste packaging in BHK and BHA (data from Section 3.6 in the Initial state report).**

	BHK	BHA
Weight waste (tonnes)	4 619	2 716
Weight packaging and grout (tonnes)	17 700	11 900
Waste volume <sup>a</sup> (m <sup>3</sup> )	-	4 140
Disposal volume <sup>b</sup>	6 774	10 742
Void in waste (m <sup>3</sup> )	1 200	1 300
Initial state pore volume (m <sup>3</sup> )	3 100	5 000
Number of waste packages	606 <sup>c</sup>	1 325

<sup>a</sup> Inner waste package volume for the BHA waste.

<sup>b</sup> Volume the waste packages will occupy in the concrete cassettes.

<sup>c</sup> Steel tanks. In addition, 115 m<sup>3</sup> secondary wastes and 659 m<sup>3</sup> of the PWR biological shields are expected to be deposited in BHK, according to Herschend (2014, Table 5-3, 5-4 and 5-5).

#### Material inventory

The material inventory has been calculated from the reported and calculated waste amounts and specifications of construction materials for each component. Material specifications have been taken from the radionuclide inventory calculations for the decommissioning studies (Griffiths et al. 2008, Lindow 2012, Anunti et al. 2013, Larsson et al. 2013, Hansson et al. 2013) and are summarised in Herschend (2014). The material quantities that will be deposited in BHA<sup>4</sup> are based on information and assumptions available from SNAB and AB SVAFO. Figure 4-3 shows the material quantities that are planned for disposal in BHK and BHA.

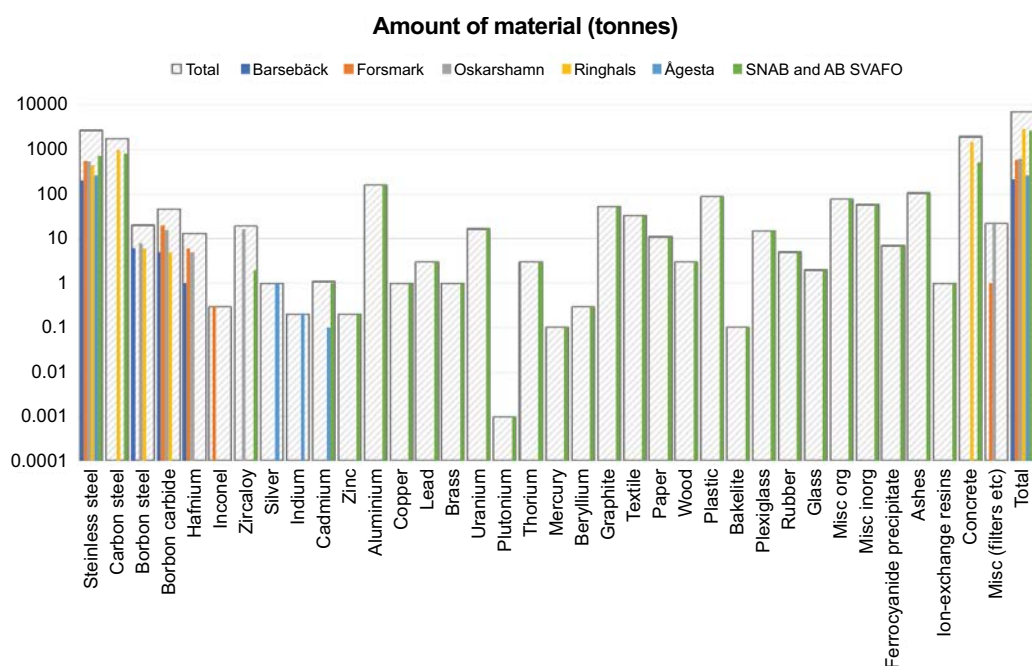


**Figure 4-3. Estimated material quantities in the waste (data from Table 3-21 in the Initial state report).**

<sup>4</sup> Herschend B, 2015. Long-lived waste from AB SVAFO and Studsvik Nuclear AB. SKBdoc 1431282 ver 1.0, Svensk Kärnbränslehantering AB. Internal document.

### Surface area

The total surface area of the different metals in the waste has been calculated for BHK (Herschend 2014) and for BHA<sup>5</sup> and is summarised in Table 4-2.

**Table 4-2. Surface area (m<sup>2</sup>) of different metals (data from Table 3-22 in the Initial state report).**

Material	BHK	BHA
Stainless steel	67 960	38 429
Carbon steel	1 313	40 763
Boron steel	7 472	-
Hafnium	946	-
Inconel	18	-
Zircaloy	1 797	146
Silver	7	-
Indium	1	-
Cadmium	0.4	44
Zinc	-	13
Aluminium	-	25 158
Copper	-	33
Lead	-	102
Brass	-	25

### Waste packaging material

In addition to the waste characteristics, the waste packages are of importance for the initial state of the repository. The waste packages contribute to the total amount of steel and concrete in the repository, contributing to a low redox potential, high hydraulic resistance and pH control. The calculated void inside each waste package is also of importance when assessing concentrations of e.g. radionuclides and organic complexing agents. Table 4-3 shows the materials in the waste packaging for BHK (Herschend 2014) and BHA<sup>6</sup> respectively. Information on the weight of the packaging and grout is given in Table 4-1.

**Table 4-3. Material in waste packaging and the grout between the inner and outer waste packaging (data from Table 3-25 in the Initial state report).**

	BHK	BHA
Carbon steel (tonnes)	12 285	2 882
Carbon steel (m <sup>2</sup> )	53 679	85 857 <sup>a</sup> (200 991) <sup>b</sup>
Concrete and grout (tonnes)	5 415	8 649

<sup>a</sup> Surface area of the outer packaging.

<sup>b</sup> Surface area of the drums and moulds placed within the outer waste packaging for SFL, see Section 3.4.

### Organic complexing agents and cellulose degradation products

In BHK, the waste exclusively consists of metallic parts. Hence, no organic material that might form metal-organic complexes will be present in this waste vault. In BHA, the waste could possibly contain ethylenediaminetetraacetic acid (EDTA), Nitrilotriacetic acid (NTA), citric acid, gluconate, tributyl phosphate (TBP) and cellulose (it is estimated that about 47 tonnes of cellulose will be present).

<sup>5</sup> Herschend B, 2015. Long-lived waste from AB SVAFO and Studsvik Nuclear AB. SKBdoc 1431282 ver 1.0, Svensk Kärnbränslehantering AB. Internal document.

The amounts of complexing agents allowed for disposal will be regulated by the means of waste acceptance criteria (WAC). Microbes might utilise some of the material deposited in SFL as energy sources, cellulose in particular is a favourable energy source for microbes, but other sources could occur within the waste form. The microbial population initially present in the waste form depends on the origin of that waste form.

Of the total acids released in the degradation of cellulose, 3-deoxy-2-C-hydroxymethyl- D-erythro-pentonic acid ( $\alpha$ -ISA) and 3-deoxy- 2-C-hydroxymethyl-D-threo-pentonic acid ( $\beta$ -ISA) are the most abundant. ISA show strong complexing properties with divalent, trivalent and tetravalent cations resulting in soluble organometallic complexes that exhibit different retardation behaviour compared with the unbound cations (e.g. Van Loon and Glaus 1998).

#### 4.2.6 Radionuclide inventory in BHK

Of the total radioactivity in SFL 98 % is found in the waste types to be disposed in BHK. The radionuclide inventory in the reactor internals is summarised in Figure 4-4. A discussion of the uncertainties of the radionuclide inventory is given in Herschend (2014, Section 6.3). Details of the inventories and the different information sources that have been used to gather information on the waste to be deposited in SFL as well as the calculation models used are given in the **Initial state report**.

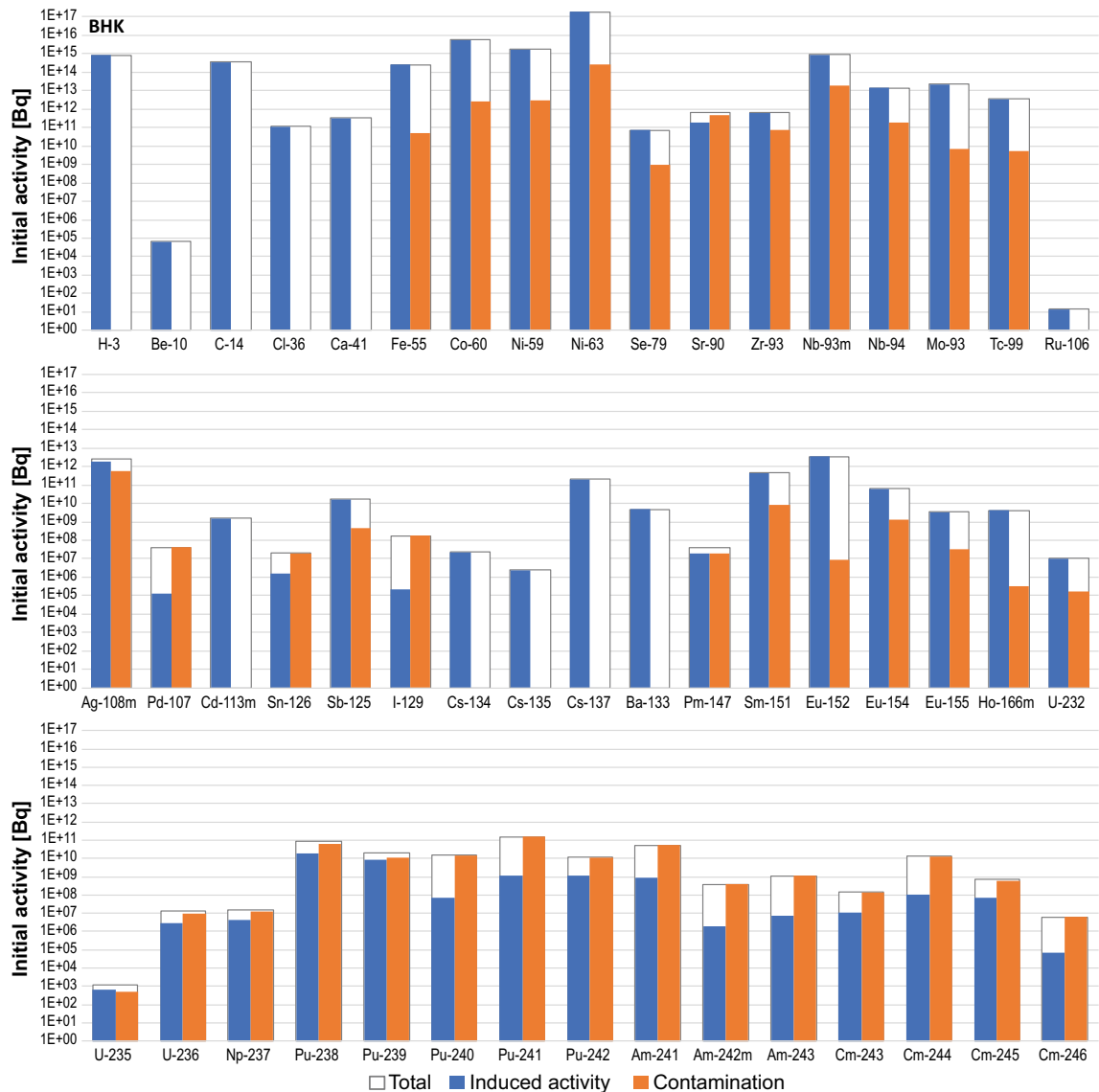


Figure 4-4. Estimated radionuclide inventory in BHK at the end of 2075. Data from Table 3-26 in the Initial state report.

### 4.2.7 Radionuclide inventory in BHA

Only 2 % of the radioactivity in SFL is found in the waste planned for disposal in BHA. The waste includes legacy waste plus existing and forecast operational wastes, which are briefly described in the following subsections.

#### Legacy waste

The radionuclide inventory of the legacy waste is highly uncertain. The inventory is based on relatively sparse data from gamma spectroscopy and sampled surface contamination in combination with a correlation procedure.

The total radionuclide inventory in the legacy waste is summarised in Figure 4-5 at the reference date 2075-12-31. The radionuclide inventory data also includes activity calculated from the reported actinide content (i.e. Th-232, U-235, U-238 and Pu-239). The decay products of Th-232 have not been taken into account.

#### Existing operational waste

The operational waste is generally better characterised than the legacy waste and its radionuclide inventory is also given in Figure 4-5, at the reference date 2075-12-31.

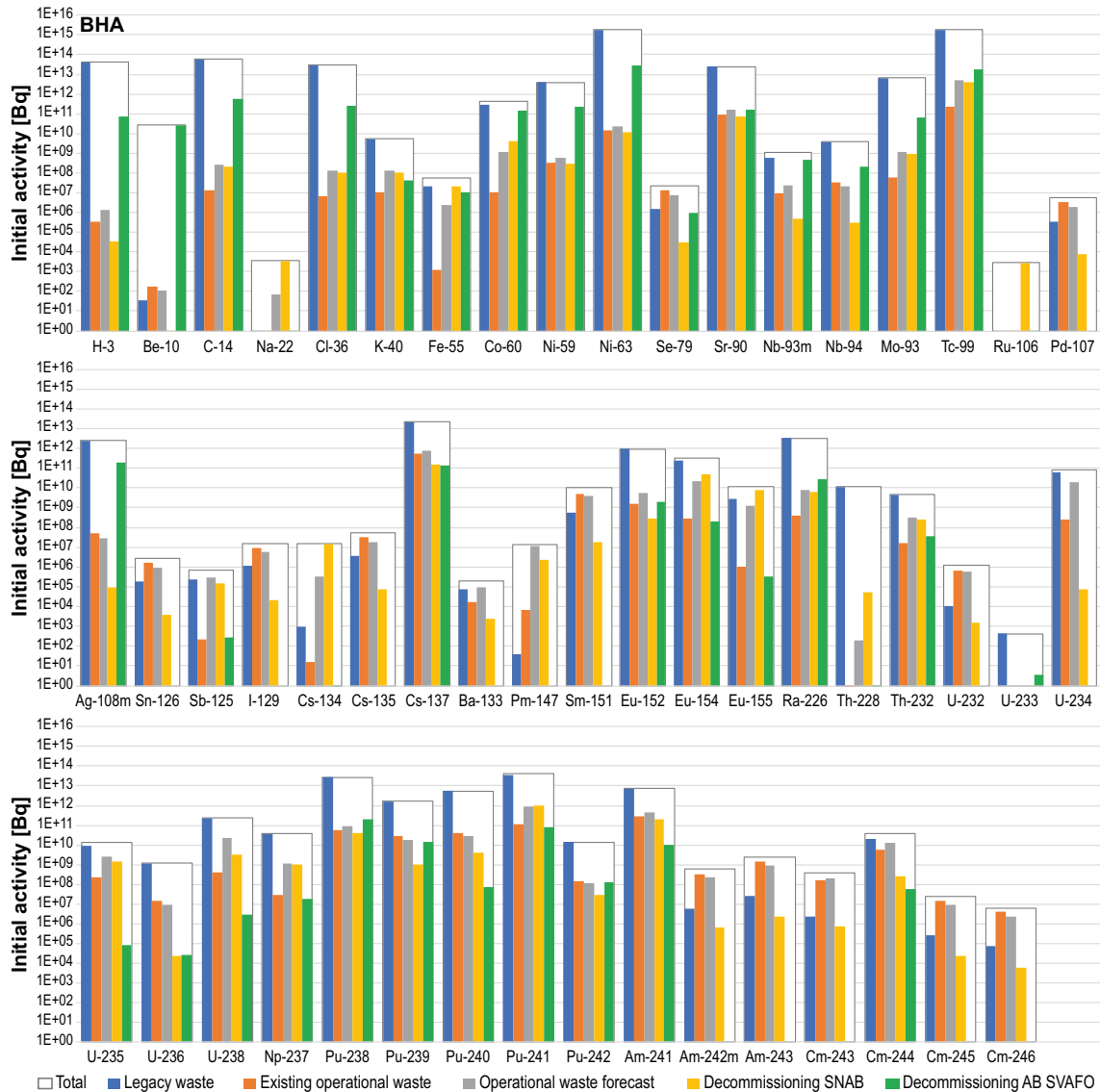


Figure 4-5. Estimated radionuclide inventory in BHA on 2075-12-31 (data from Table 3-27 in the Initial state report).

### Operational waste forecast

A forecast on operational waste from SNAB has been reported for each facility at the Studsvik site. The inventory also includes 400 drums of the S.09 type from AB SVAFO. These drums were previously intended for disposal in SFR but have been excluded from the SFR inventory and are therefore included here. The waste is assumed to be produced at a constant rate until 2045.

No additional estimates of activity in the forecast operational waste have been reported by the producers. Hence, the radionuclide inventory is based on the average radionuclide inventory of corresponding waste types in the existing operational or legacy waste. Radioactive decay is calculated from a fixed reference time (2030-01-01) and the inventory is presented in Figure 4-5 at the reference date 2075-12-31.

### Decommissioning waste from SNAB and AB SVAFO

For the decommissioning waste from R2 and R2.0, data from the recent decommissioning plan for the R2 facility have been used to estimate the radionuclide inventory. For all other decommissioning waste, the radionuclide inventory is based on source terms for corresponding waste types in the existing waste. The inventory from decommissioning waste is presented in Figure 4-5 at the reference date 2075-12-31.

## 4.3 Repository

### 4.3.1 Waste vault for reactor internals, BHK

In BHK, a concrete-based barrier system will be used. The system will comprise six separate caissons, into which the waste packages will be placed. There is grout between and inside the waste packages and the vault will be backfilled with concrete. The design of the waste vault along with the dimensions are described in the following based on the concept study of Elfving et al. (2013).

The waste vault will have a width of approximately 20.6 m and a height of approximately 19.6 m. An illustration of the cross section of the vault is shown in Figure 4-6. The length of the vault is approximately 134 m and six concrete caissons are planned based on the expected waste volume. The caissons provide radiation shielding during the operational phase. Each caisson has lateral dimensions of 15 m × 16 m and a height of 8.4 m. The thickness of the caisson walls, floor and lid is 0.5 m.

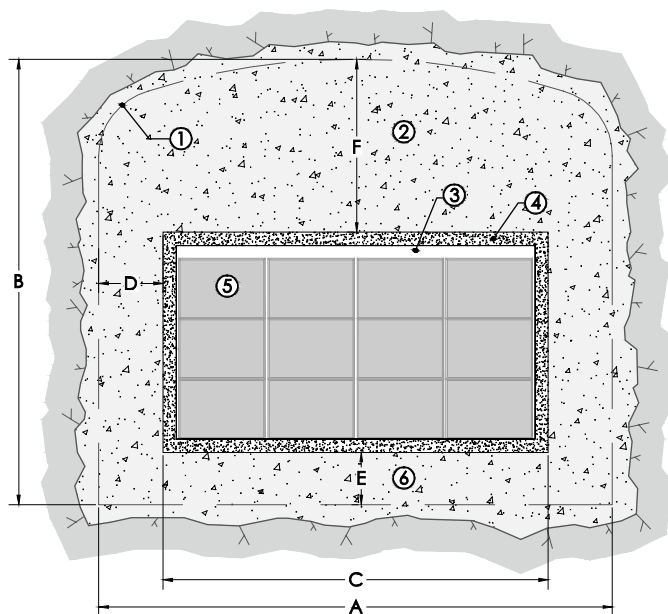


**Figure 4-6.** Schematic cross-sectional layout of BHK from Elfving et al. (2013). Legend: 1) Theoretical tunnel contour. 2) Concrete backfill. 3) Grout. 4) Concrete structure (0.5 m). 5) Steel tanks. 6) Concrete. Approximate dimensions: A = 20.6 m, B = 19.6 m, C = 15 m, D = 2.8 m, E = 2.4 m, F = 8.8 m.

When the waste packages have been placed in the caisson, the space between the waste packages will be filled with grout in order to stabilise the stack of waste packages and to reduce voidage. In addition, the grout will stabilise the waste packages and improve strength by reducing deformation caused by the external forces on the walls, floor and lid during backfill and re-saturation of the repository. The grout also contributes to the high alkalinity in the vault and thus also the passivation of steel components in the waste packages, which thereby reduces the corrosion rate.

### ***Main components of the engineered barrier system***

The main components of the engineered barrier system are made up of a reinforced concrete structure in which the steel tanks containing the waste are placed before they are grouted. At closure, the space between the concrete structure and the bedrock is backfilled with concrete. The dimensions of the vault and concrete structure are shown in Figure 4-6.

### ***Safety functions of the engineered barrier system***

The primary safety function of this repository section is retardation (Section 5.2). This is achieved by limiting the flow of groundwater through the waste and further by limiting the diffusive transport of substances to and from the waste. The concrete in the barrier – in both structures and backfill – will provide an alkaline environment in the repository section, which will create a passivating layer on the surface of the steel components and reduce the corrosion rate of steel. The low corrosion rate results in a low gas production rate, which is considered beneficial for permitting gas transport within the barriers without negative effects on them. Concrete has a high sorption coefficient for many radionuclides (except for the anions formed by e.g. chlorine and molybdenum). The values of the variables that are used to describe the initial state of the barriers in BHK are given in the **Initial state report** (Section 7.3).

## **4.3.2 Waste vault for legacy waste, BHA**

BHA is designed for the disposal of waste packages with a low activity but less well-known material composition and radionuclide inventory. The waste vault comprises a concrete structure in which the waste is deposited, and which is surrounded by a thick layer of bentonite with a high dry density. It will function as a low permeability medium enclosing the waste.

The safety principle of this repository section is retardation (Section 5.2). The barriers limit the flow of groundwater through the waste and thus make diffusion the predominant transport process for radionuclides.

### ***Main components of the engineered barrier system***

The waste vault will have a width of approximately 20.6 m and a height of approximately 18.4 m. An illustration of the cross section of the vault is shown in Figure 4-7. The length of the vault is approximately 170 m. A concrete structure with lateral dimensions of approximately 16 m × 140 m and a height of 8.4 m is planned based on the expected waste volume. The thickness of the walls, floor and lids is 0.5 m. The structure provides radiation shielding during the operational phase.

When the waste packages have been placed in the vault, the space between the waste packages will be filled with grout in order to stabilise the stack of waste packages and to reduce the void space. In addition, the grout will stabilise the waste packages and improve the strength of the structure by reducing the deformations caused by the external forces on the walls, floor and lid during backfill and re-saturation of the repository. The grout also contributes to the high alkalinity in the waste domain and thus also the passivation of steel components in the waste packages, which thereby reduces the corrosion rate. The concrete walls, lid, grout, the floor and the bentonite constitute chemical barriers that enhance sorption of radionuclides in the vault. The thick bentonite layer constitutes the main barrier that primarily reduces the flow of water through the repository but also increases the sorption capacity of the vault. The concrete and bentonite will interact chemically, which is considered in the reference evolution.

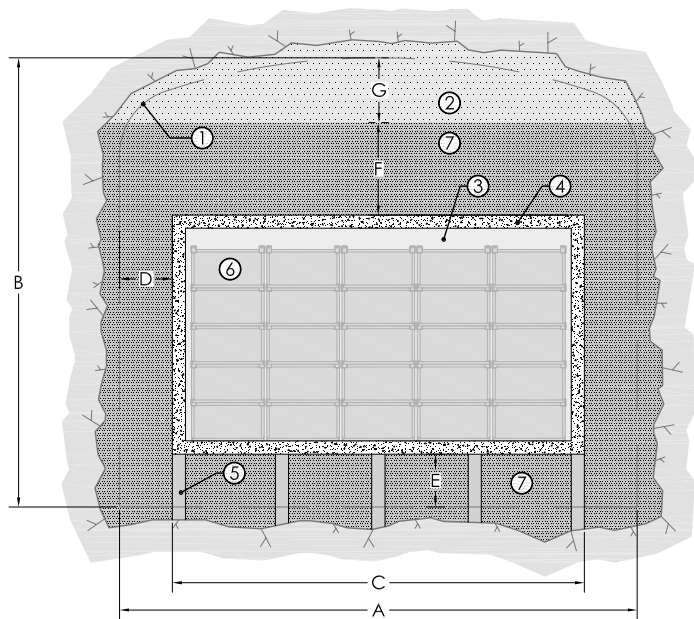


**Figure 4-7.** Schematic cross-sectional layout of BHA from Elfving et al. (2013). Legend: 1) Theoretical tunnel contour. 2) Bentonite pellets. 3) Grout. 4) Concrete structure (0.5 m). 5) Granite pillars. 6) Waste packages. 7) Bentonite blocks. Approximate dimensions: A = 20.6 m, B = 18.5 m, C = 16 m, D = 2.3 m, E = 2.4 m, F = 4 m, G = 3.7 m.

Bentonite blocks will be placed beneath the base slab as well as on the sides and on top of the concrete structure. The top part of the vault is to be filled with bentonite pellets. No bentonite will be placed in the vault until the time of closure. The total volume filled with bentonite blocks and pellets is about 51 000 m<sup>3</sup> with different parts of the volume specified in Table 4-4.

The backfill material in BHA is assumed to have similar properties to the buffer material in the Spent Fuel Repository. For MX-80 material, this would mean a target dry density of about 1 570 kg m<sup>-3</sup> or a saturated density of 2 000 kg m<sup>-3</sup>, which implies a hydraulic conductivity of  $1 \times 10^{-13}$  m/s (SKB 2010e, Posiva SKB 2017, Chapter 5). If another bentonite is used, the dry density would be adjusted to achieve approximately the same swelling pressure and hydraulic conductivity. The effective diffusivity of non-charged and hydrolysable elements (cations except cesium) in the bentonite is assumed to be  $1.2 \times 10^{-10}$  m<sup>2</sup>/s, whereas it is  $1.0 \times 10^{-11}$  m<sup>2</sup>/s for anions and  $3.0 \times 10^{-10}$  m<sup>2</sup>/s for cesium ions (Ochs and Talerico 2004, p 90).

**Table 4-4. Dimensions, volumes and assumed porosity available for water resaturation in bentonite and the waste domain in BHA. Void volumes are used for the calculation of the extent of piping/erosion. It should be noted that the porosities in the table represent the value available for resaturation during the operational phase, not the total porosity.**

Component	Dimensions (L × W × H m)	Volume (m <sup>3</sup> )	Assumed porosity (%) available for inflowing water	Void (m <sup>3</sup> )
Pellets ceiling <sup>1</sup>	170 × 20.6 × 3.7	12 957.4	48	6 220
Bentonite blocks <sup>1,2</sup>	170 × 20.6 × 14.8	33 013.6	2	660
Side filling (2x) <sup>1</sup>	170 × 0.5 × 18.5	3 145	48	1 510
Bottom filling <sup>1</sup>	170 × 20.6 × 0.5	1 751	48	840
Front/rear filling <sup>1</sup>	0.5 × 20.6 × 18.5	381.1	48	183
Caissons and waste <sup>1,3</sup>	140 × 16 × 8.4	18 816	9	1 750

<sup>1</sup> The assumed porosity available for inflowing water is taken from Åkesson et al. (2010).

<sup>2</sup> The dimensions of the bentonite blocks include the caissons and the waste, which are subtracted to obtain the volume.

<sup>3</sup> The void for the waste domain is calculated based on the assumption of a porosity of 31 % and a degree of saturation of 70 % (Input data report, Section 2.5.1, Höglund 2014).

### **Safety functions of the engineered barrier system**

The low permeability of the bentonite allows only an insignificant advective flow, which makes diffusion the dominant transport mechanism for radionuclides through the bentonite. Late installation ensures good control of the condition of the bentonite at closure of the repository. The clay has beneficial mechanical properties; it can be deformed without cracking and exhibits self-healing properties. Bentonite is a natural material, and its long-term properties have been well characterised in earlier research. Bentonite clay can effectively filter colloids. This is an advantage for this category of waste, since it contains more actinides than the metallic waste. Actinides, together with mixed organic material, could form various types of actinide-carrying colloids.

### **4.3.3 Closure components**

In a geological repository, the bedrock surrounding the vaults is part of the barrier system that will prevent the radioactive substances from harming human health or the environment. The tunnels that provide access to the waste vaults may impair the barrier function of the bedrock through the creation of open flow paths in the bedrock. These flow paths must be closed by installing closure components, i.e. plugs and seals. The backfills in the vaults are considered barriers and not part of the closure components. The main purposes of the closure components are:

- Reducing the water transport in the tunnels.
- Reducing the water flow from the tunnels to the waste vaults.
- Supporting the rock and thereby preventing a collapse of the tunnel roof and walls.
- Preventing unauthorised human access to the radioactive waste.

In this section, the closure components and the probable methods used to close SFL at some point in the future are briefly outlined. At this stage, it is assumed that the design of the components and method for installation will not differ significantly between the different repository sections.

The sealing sections of SFL are schematically illustrated in Figure 4-8. The suggested design in this report constitutes solutions that are technically feasible. However, it is foreseen that the design of closure components for each of the individual section can be further developed and optimised before closure of SFL.

In BHK, the space between the caissons and the bedrock will be filled with concrete in order to further limit the water flow through the waste and contribute to high alkalinity and sorption sites for the radionuclides. In BHA, the space between the concrete structure holding the waste and the bedrock will be filled with bentonite in order to further limit the water flow through the waste and contribute to sorption sites for the radionuclides. Being part of the barrier system the concrete backfill in BHK and the bentonite backfill in BHA are described in depth in previous Sections 4.3.1 and 4.3.2.

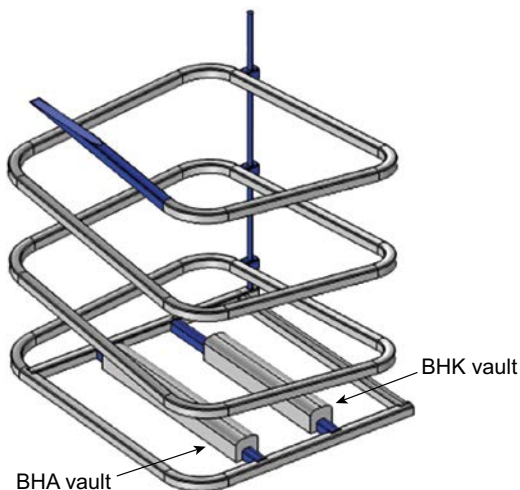


**Figure 4-8.** Sealing sections (blue) installed at closure in the tunnel sections connecting the vaults and access tunnels, the vertical shaft and in the access ramp.

To seal the waste vaults, tunnel sections adjacent to the vaults will be filled with bentonite and confined by mechanical plugs. The bentonite acts as hydraulic seal to reduce the axial flow of groundwater through the waste vault. The properties of the bentonite are in SE-SFL assumed to be the same as for the bentonite in the barrier in BHA. This solution is in accordance with previous investigations and concepts developed by SKB for the Spent Fuel Repository (Luterkort et al. 2012).

The tunnels at repository level in connection with the sealed sections of the waste vaults are planned to be backfilled with crushed rock or a similar material. The hydraulic conductivity in the crushed rock is assumed to be  $10^{-5}$  m/s, the porosity 0.3, and the effective diffusivity  $6.0 \times 10^{-10}$  m<sup>2</sup>/s (SKB 2001).

The access tunnel is also planned to be backfilled with crushed rock. In addition, a plug section will be installed, made up of a hydraulically tight section of bentonite to further reduce the groundwater flow through the tunnel, surrounded by concrete plugs as mechanical support. Figure 4-9 illustrates an example of such a technically feasible plug.

The first 50 m of the access tunnels are planned to be backfilled with boulders and a concrete plug will be cast to obstruct unintentional intrusion into the repository. Finally, the ground surface will be restored to match the surroundings.

The vertical shaft connecting different levels of the access tunnel and the repository is planned to be sealed at the connections to the tunnels to restrict the flow of water. The suggested solution comprises a hydraulically tight section with bentonite surrounded by upper and lower concrete plugs for mechanical support. The properties of the bentonite are assumed to be the same as for the bentonite barrier in BHA.

In the present study, investigation boreholes are not considered in the modelling of the hydrogeology or radionuclide transport. After the site investigation program for SFL, it will be necessary to consider the presence of boreholes and to have a plan for sealing them.

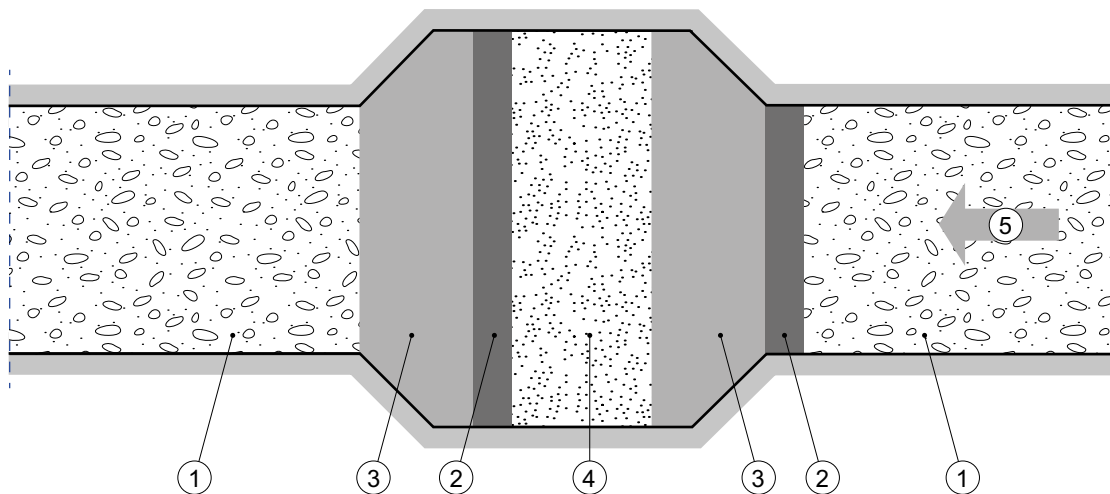


**Figure 4-9.** Schematic design of a sealing plug (Luterkort et al. 2014). Legend: 1) Backfill of crushed rock or similar. 2) Retaining concrete walls. 3) Cast concrete. 4) Bentonite. 5) Backfill direction (from the waste vault and out). 6) Backfill material.

## 4.4 Climate

### 4.4.1 Temperature and precipitation

A main assumption in the SE-SFL safety evaluation for the bedrock and surface systems is that the initial state conditions at repository closure at 2075 AD are present-day conditions. For consistency, the same assumption is made for the climate. The initial state with regard to air temperature and precipitation in Laxemar is therefore based on the present-day climate as described by the 30-year average for the normal period 1961–1990. During this period, the mean annual air temperature in the Laxemar area was +6.4 °C, and the annual precipitation was 553 mm (**Climate report**, Table 3-1). The site-average annual specific discharge is estimated to be on the order of 160–170 mm, and the precipitation demonstrates a near-coastal gradient, with less precipitation at the coast compared with areas further inland.

As a result of an increasing greenhouse effect, the annual mean temperature and precipitation in Laxemar are expected to increase up until the time of repository closure at 2075 AD (see **Climate report**, Section 4.2). In the most recent assessment by the Intergovernmental Panel on Climate Change (IPCC), the increase in air annual average temperature and precipitation for the Laxemar region is estimated to be ~3–4 °C and ~20–30 % respectively by 2100 AD, as compared with the present day (**Climate report**, Section 4.2). Part of this increase would occur up until the time of repository closure. The effect of an increased greenhouse effect is described in the SE-SFL *increased greenhouse effect climate case* (**Climate report**, Section 4.2). This climate case is based on the IPCC intermediate emissions scenario RCP4.5, in which radiative forcing is stabilised shortly after 2100 AD, assuming a future with relatively ambitious reductions in carbon emissions. However, as mentioned above, a main assumption in SE-SFL is that the initial state conditions for the geosphere, surface and climate, at 2075 AD, are present-day conditions. Therefore, the *increased greenhouse effect climate case* describes present-day climate conditions up until 2075 AD, after which the temperature and precipitation increases. Consequently, care must be taken when comparing the highly simplified climate development in the SE-SFL *increased greenhouse effect climate case* to the development of air temperature and precipitation in the IPCC RCP4.5 scenario (see **Climate report**), since they increasingly differ up until 2075 AD. However, given the overall approach of using highly simplified climate developments in the SE-SFL evaluation, the distinction is regarded as insignificant.

### 4.4.2 Shoreline displacement

Changes in shoreline position in the Laxemar area are determined by the contributions of eustasy (i.e. changes in sea level due to e.g. changes in the volume and spatial distribution of sea water in the world's oceans) and isostasy. (i.e. vertical movement of the Earth's crust, which in Laxemar is dominated by rebound following the last glaciation). The present vertical shoreline displacement at Laxemar is ~1 mm a<sup>-1</sup> (see **Climate report**, Appendix B). In a climate dominated by global warming, the eustatic contribution to shoreline displacement is expected to increase during the coming centuries to millennia, so that shoreline displacement will slow down or even change direction to transgression (see **Climate report** and SKB 2014d). However, in line with the notion that the initial conditions at repository closure should reflect present-day conditions, it is assumed that the shoreline position and shoreline displacement at 2075 AD is the same as today. Present-day conditions in the hydrogeological and hydrogeochemical calculations of Joyce et al. (2019) are represented by the situation at 2000 AD, noting that the land uplift from 2000 AD to the present is less than 2 cm.

## 4.5 Surface systems

The initial state of the surface systems in the repository environs is assumed to be similar to present-day conditions, as described by the site descriptive model (SDM) for Laxemar (SKB 2009) and the **Biosphere synthesis**.

#### 4.5.1 Topography and regolith

The Laxemar-Simpevarp area is characterised by a mildly uneven topography at a relatively low altitude, but with marked both short and longer valleys/topographical depressions (Figure 4-10, left panel). The south-western and central parts of the Laxemar-Simpevarp area are characterised by hummocky moraine and so lower topographic relief. The most elevated areas are located at c. 50 metres above the current sea level. The whole area is located below the highest coastline associated with the latest glaciation, and the area has emerged from the Baltic Sea during the last 11 000 years. During the deglaciation at c. 12 000 BC, the area was situated 50–100 m below sea level and the first parts of the Laxemar-Simpevarp area emerged from the sea around 9400 BC (**Climate report**, Section 3.2). The still ongoing uplift of ca 1 mm per year does not influence the Laxemar-Simpevarp site *per se*, but will influence today's landscape closer to the shoreline of the Baltic Sea (Figure 4-10, right panel). Sea bottoms are being continuously transformed to new terrestrial areas or freshwater lakes, and lakes and wetlands will successively be covered by peat.

The predominantly thin regolith is mainly located in the valleys, whereas the higher-altitude areas are dominated by exposed bedrock or thin layers of till and peat. Glacial till is the most common Quaternary deposit and covers half of the terrestrial part of the Laxemar-Simpevarp area. Sandy-gravelly till overlies the bedrock in the whole area, also in most areas with exposed/shallow bedrock (which may have a regolith depth of up to c. 0.5 m). The exceptions are some of the exposed/shallow bedrock areas, in which organic soil and a thin vegetation layer directly overlies the bedrock.

#### 4.5.2 Near-surface hydrogeology, water chemistry and limnic ecosystems

SKB has performed comprehensive investigations of surface and near-surface hydrogeology, including monitoring of surface-water levels in lakes and bays of the Baltic Sea, stream discharges, groundwater levels in regolith, and “winter parameters” such as snow depth and ice freeze/breakup.

The Laxemar-Simpevarp area as defined in the SDM contains 26 catchments, 5 lakes and several streams. Only one of the lakes, Lake Frisksjön (0.13 km<sup>2</sup>), is situated within the Laxemar area that is considered in the local biosphere model. Wetlands in total cover c 3 % of the catchment areas of the lakes (Brunberg et al. 2004). Most of the streams are, to a great extent, influenced by human activities such as land improvement, drainage operations, and altering of channels by various technical encroachments. There is flow throughout the year in the streams Laxemarån, Kåreviksån downstream from Lake Frisksjön and Kärriksån. The other monitored small streams are dry during parts of the year. Except for some minor wetlands, the surface waters (lakes, streams and wetlands) are associated with low-altitude areas. These surface waters are mainly underlain by glacial and post-glacial sediments. Specifically, the general bottom-up stratigraphy of regolith below surface waters is till and glacial clay, overlain by postglacial sediments (sand/gravel, gyttja clay/clay gyttja, overlain by fen peat and bog peat in the wetlands).



**Figure 4-10.** Left panel: Typical valley with steep sides. The valleys are partly filled with gyttja and peat (valley of River Laxemarån, South eastern Laxemar). Right panel: An inlet with gyttja deposition in progress in the eastern part of the Laxemar-Simpevarp area (North eastern part of the island of Äspö, view to the west).

Groundwater levels in the regolith are shallow; the average depth to the groundwater table is less than 1 m for 50 % of the time. Generally, the depth to the groundwater table is greater in higher-elevation areas than in lower-elevation areas, but this variation is much smaller than the variation in absolute groundwater levels in the area. Accordingly, there is a close correlation between the ground-surface topography and groundwater levels in the regolith, which in turn implies that topography has a strong influence on near-surface patterns of groundwater recharge and discharge.

Hydrochemical and regolith data are presented in Tröjbom and Söderbäck (2006) and Tröjbom et al. (2008). The hydrochemistry of elevated areas is influenced by atmospheric deposition and weathering processes driven by free H<sup>+</sup> ions generated by degradation of biogenic carbon. In areas of lower elevation, close to the coast, the hydrochemistry is governed by meteoric recharge and flushing of remnants of marine waters. The hydrochemistry of near-coastal groundwater samples indicates additional discharge of deeper groundwaters.

The freshwater systems in the Laxemar-Simpevarp area are generally classified as mesotrophic brown-water (dystrophic) types. Most waters are markedly coloured due to the high content of humic substances and show high levels of dissolved organic carbon. Streams and lakes are also relatively rich in nitrogen and phosphorus. Fresh surface waters and shallow groundwaters in the area are neutral to slightly acid, and concentrations of most major ions are normal from a Swedish perspective (Tröjbom and Söderbäck 2006).

Light penetration is poor, and the depth of the photic zone is generally limited as a consequence of the dark water colour. As a result, macrophyte coverage is restricted and the biota is dominated by heterotrophic organisms, particularly bacteria. Perch is the dominant fish species in lakes in the area, in numbers as well as in biomass. Five fish species have been noted in Laxemarån; ide (Sw: id), roach (Sw: mört), burbot (Sw: lake), pike (Sw: gädda) and ruffe (Sw: gers), and there are indications that the streams are an important spawning site for both ide and roach (Andersson 2010). Most lakes in the area are affected by human activities. The naming of some wetlands and minor fields indicates that several previous lakes have disappeared during the last few centuries due to human activities, probably with the intention of increasing productive farmland. There are also indications that the water level of several of the remaining lakes has been lowered by human activities.

### 4.5.3 Marine ecosystems

The Laxemar-Simpevarp area is situated on the coast of the Baltic Proper. The marine area in Laxemar-Simpevarp is separated from the open sea in the east by the island of Öland, forming a funnel-like strait with its wide end to the north and the narrow end southwards. The sea bottom along the Laxemar-Simpevarp coast slopes gradually in the offshore direction. The maximum depth recorded in the regional area is c. 45 m.

The sea floor in the area can be divided into three marine sub-areas with more or less distinct characteristics regarding ecosystem structuring factors, such as wave exposure, light penetration and substrate type. These sub-areas are; secluded bays (e.g. Borholmsfjärden and Granholmsfjärden), shallow exposed archipelago in the southeast, and deep, exposed areas at the coast and the open sea in the eastern parts of the regional area.

The coastal water in the Laxemar-Simpevarp area has an average light penetration depth (Secchi depth) of 5.5 m, which is low compared with the value at the national monitoring station located further out in the Baltic Proper (8.7 m). However, the light penetration varies within the area, and the sheltered inner bays have Secchi depths of only 2–3 m.

Large parts of the coastal area are shallow enough for light to reach the bottoms. Accordingly, the marine primary producers in the regional model area are dominated by benthic primary producers.

On soft bottoms situated within the photic zone, green algae, stonewort (*Chara sp.*) and yellowgreen algae (*Vaucheria sp.*) dominate. On hard substrates, i.e. till or bedrock, bladderwrack (Sw: blåstång) dominates in the shallow areas, whereas red algae dominate in the deeper areas. Three species domi-

nate the benthic fauna, the blue mussel (Sw: blåmussla), Baltic mussel (Sw: Östersjömussla) and a small amphipod (Sw: vitmärla). Perch (Sw: abborre), roach (Sw: mört) and white bream (Sw: björkna) have consistently dominated the catches in the monitoring of warm-water species in the area (Aquilonius 2010), representative for the inner bays in the area. In the more offshore areas, the marine cold-water species herring (Sw: strömming) dominates the fish community. In the open sea, the zooplankton community is dominated by meso-zooplankton, especially copepods. However, in the summer a more diverse zooplankton community with cladocerans, rotifers and larvae of some benthic macroinvertebrates occurs.

#### 4.5.4 Terrestrial ecosystems

The location of the investigated area close to the sea makes the seashore a prominent feature in the east along with conifer forests and some agricultural land. The terrestrial vegetation is strongly influenced by the characteristics of the regolith and by human land use. Below follows a brief description of three major vegetation types within the investigation area (see Löfgren 2010, cf. Chapter 4 therein for more details).

Forests cover approximately 73 % of the land area of the main catchments in the Laxemar-Simpevarp regional model area as defined in the SDM. The forests are dominated by Scots pine (Sw: tall) and Norway spruce (Sw: gran). Scots pine dominates on bedrock or in areas with a shallow soil layer, whereas Norway spruce becomes more abundant in areas with a deeper soil cover in combination with mesic-moist conditions. Deciduous tree species, mainly pedunculate oak (Sw: ek), but also hazel (Sw: hassel), rowan (Sw: rönn), Swedish whitebeam (Sw: oxel) and Norway maple (Sw: lönn), are more common near the coast, making the mixed forest the second most common forest type.

The predominant humus form in the Scots pine and Norway spruce forests is moder-humus, i.e. the intermediate form between mor and mull extremes. In these forests, the soil type regosol dominates, but podzols become more common where there is a deeper soil cover. The mull-like humus form becomes more dominant with increasing occurrence of deciduous trees (Lundin et al. 2005) and in this type of forest, the soil types regosol and umbrisol are found. The Laxemar-Simpevarp area has a long history of forestry, currently indicated by a fairly high percentage of younger and older clear-cuts in different successional stages in the landscape. Birch (Sw: björk) is the dominant species in many of the earlier successional stages until it is replaced by young Norway spruce or Scots pine, depending on soil type and/or management.

Wetlands cover only 1 % of the area in the main catchments. The wetlands consist of both coniferous/deciduous forest swamps and open mires. Although not so numerous, bogs are also present inland, and are continuously created due to the shoreline displacement and the mineral and nutrient leaching processes. In the northern part of the area, where bedrock outcrops are common, small peat-accumulating nutrient-poor wetlands are found in the depressions. Other important, but less common wetland types are the freshwater shores (wet meadows or marshes) and riparian wetlands along streams. The latter are flooded at least once a year and affected by overbank sedimentation. Such areas may be of importance for the retention of various substances that otherwise are transported by the water directly to the sea.

The agricultural land covers 8.5 % of the land area of the main catchments and is mainly located along the valleys. The agricultural land consists of arable land and grasslands. It provides food for humans, either directly as crop production or as production of fodder for animals.

The fauna is more difficult to associate to specific habitats than the vegetation, but for some species or functional groups an attempt has been made to distribute their consumption in the landscape, either by using their habitat preferences or their feeding preferences, or both. Density and biomass estimates for all mammals, birds, amphibians and reptiles are presented in Section 4-2 in Löfgren (2010), together with calculations of their production, consumption, egestion and respiration. The calculations are based on the field metabolic rate for each species.

## 4.6 Bedrock system

The initial state of the bedrock system in the repository environs is assumed to be similar to present-day conditions, as described by the site descriptive model (SDM) for Laxemar (SKB 2009).

Most of the bedrock in Sweden belongs to the Fennoscandian Shield and is typically crystalline rocks with a granitoid composition, formed during mid-crustal level metamorphism of the crust or by intrusions of igneous rocks at depth (Figure 4-11).

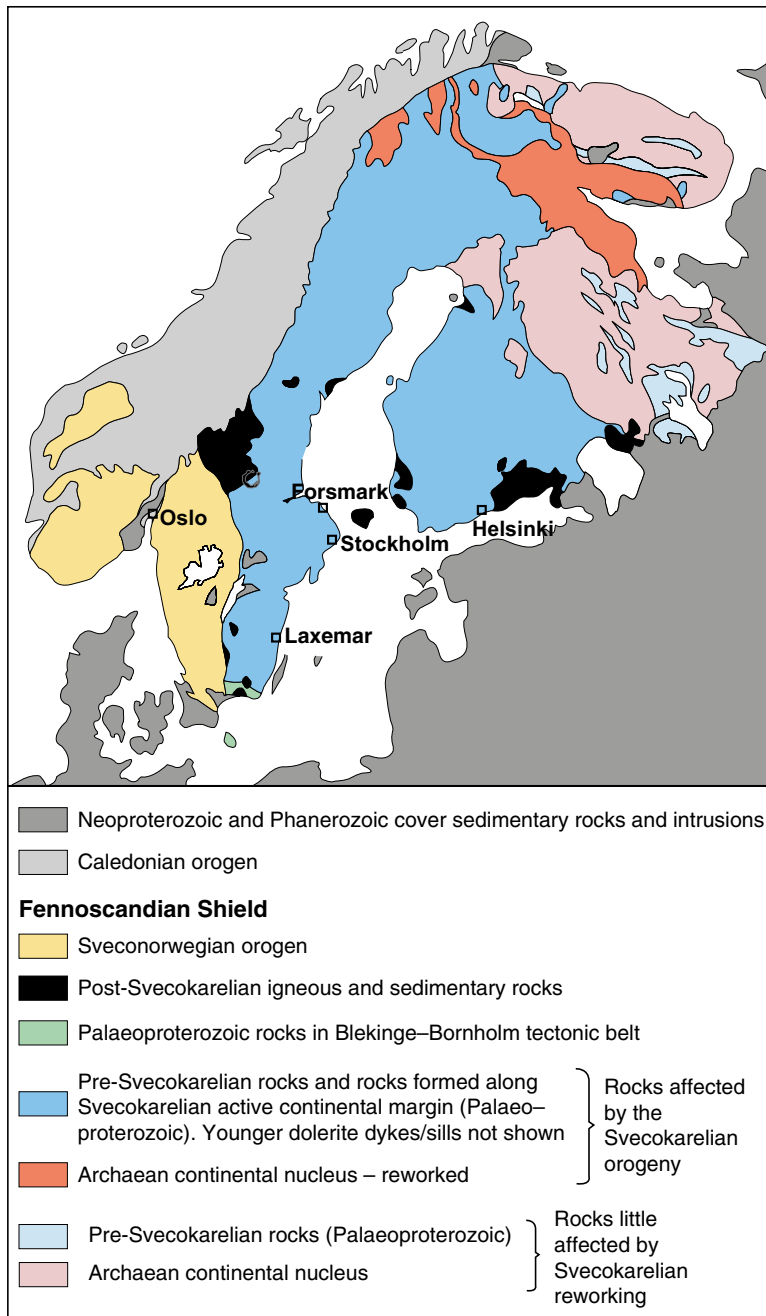


**Figure 4-11.** Map showing the major tectonic units in the northern part of Europe at the current level of erosion (modified after Koistinen et al. 2001).

In order to evaluate post-closure safety for the proposed repository concept, relevant data from locations with crystalline Swedish bedrock are necessary. For the Laxemar and Forsmark sites comprehensive data that are suitable for the needs of a safety evaluation are documented in the site descriptive models for the Spent Fuel Repository (SKB 2008b, 2009) and for the planned extension of SFR in Forsmark (SKB 2013b).

As described in Section 1.2, Laxemar is chosen as an example site for SE-SFL. In order to put the different sites into perspective Winberg (2010) has compared hydraulic test data from the site investigations in Forsmark and Laxemar with equivalent data from investigations of reference areas at earlier stages. The data expressed as hydraulic conductivities assessed from injection tests on a measurement scale of 20–25 m are displayed in Figure 4-12. In comparison, relatively high conductivity regions (associated with fractures and fracture zones) are much more frequent at Laxemar compared with Forsmark as well as compared with many of the older study sites.

The initial state of the bedrock and groundwater in SE-SFL is based on a combination of data and models from the SDM for the site investigation for the Spent Fuel Repository (SKB 2009) and new modelling performed within the SE-SFL project. The assumptions made for the initial state in SE-SFL are described in the following subsections.

#### 4.6.1 Local geological setting

Laxemar consists of crystalline bedrock that belongs to the Fennoscandian Shield formed along the Svecokarelian active continental margin (Figure 4-11, Söderbäck 2008, Wahlgren et al. 2008). The bedrock at the site is dominated by well-preserved ca. 1.8 Ga intrusive rocks varying between dioritic and granitic compositions.

Tectonic lenses, in which the bedrock is less affected by ductile deformation, are enclosed in-between ductile high-strain belts, primary north-east trending shear zones. The investigated bedrock structure chosen for SE-SFL is located in the north-western part of such a tectonic lens.

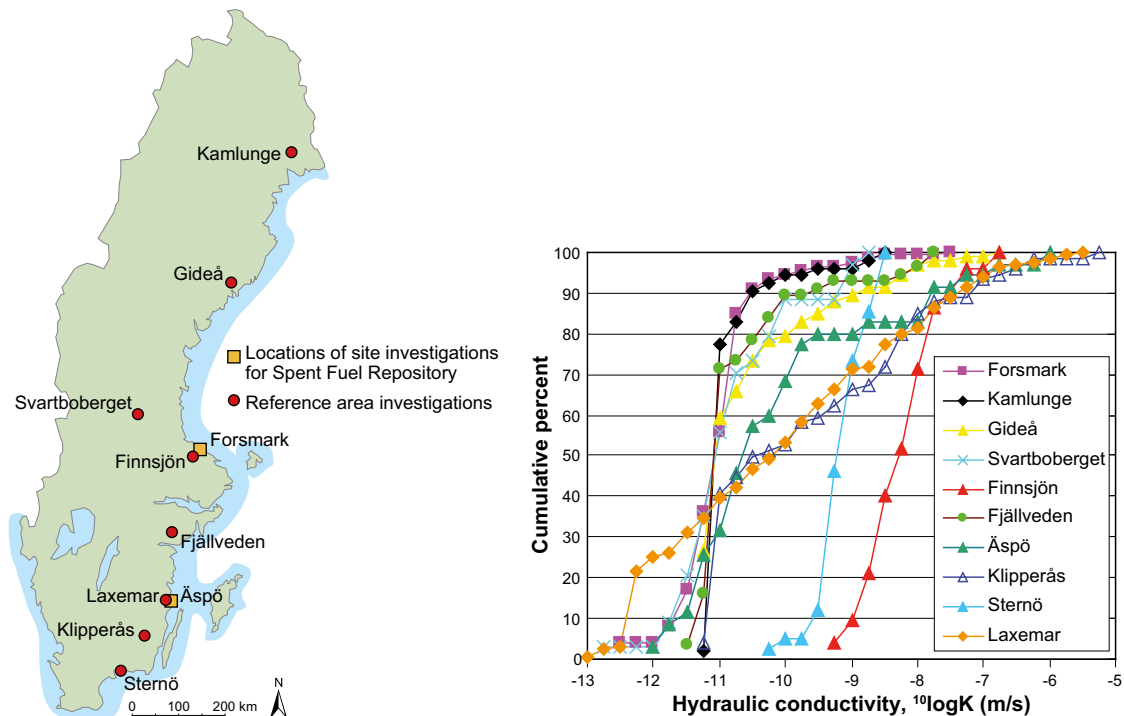


**Figure 4-12.** Left, map showing Sweden and locations of site investigations for the Spent Fuel Repository (yellow rectangles), and reference area investigations (red dots). Right, plot of cumulative distributions for measured hydraulic conductivity ( $K$ ) on a scale of 20–25 metres, for site investigation and reference areas. The data represents the bedrock between deterministic deformation zones in the depth interval 400 to 700 m (SKB 2011b).

#### 4.6.2 Rock composition and division into rock domains

The occurrence and distribution of rock types, that is, the site lithology, reveals important aspects of the homogeneity of a site. Furthermore, it is directly related to thermal- and mechanical properties.

In the SDM (Wahlgren et al. 2008), the lithology is described in terms of rock domains, defined on the basis of composition, grain size, homogeneity, and style and degree of ductile deformation.

Figure 4-13 displays the lithology and the position chosen for SFL in this safety evaluation. This location is primarily sited in the rock domain RSMA01 which is dominated by the medium-grained and finely porphyric Ävrö granite. Smaller portions of fine-grained diorite and granite bodies are also found. (Wahlgren et al. 2008). However, the southwestern-most parts of the repository are situated within the RSMM01 rock domain, dominated by Ävrö quartz monzodiorite. The RSMM01 rock domain has a much higher content of diorite and gabbro than RSMA01, which is more mafic in character than the main domain.

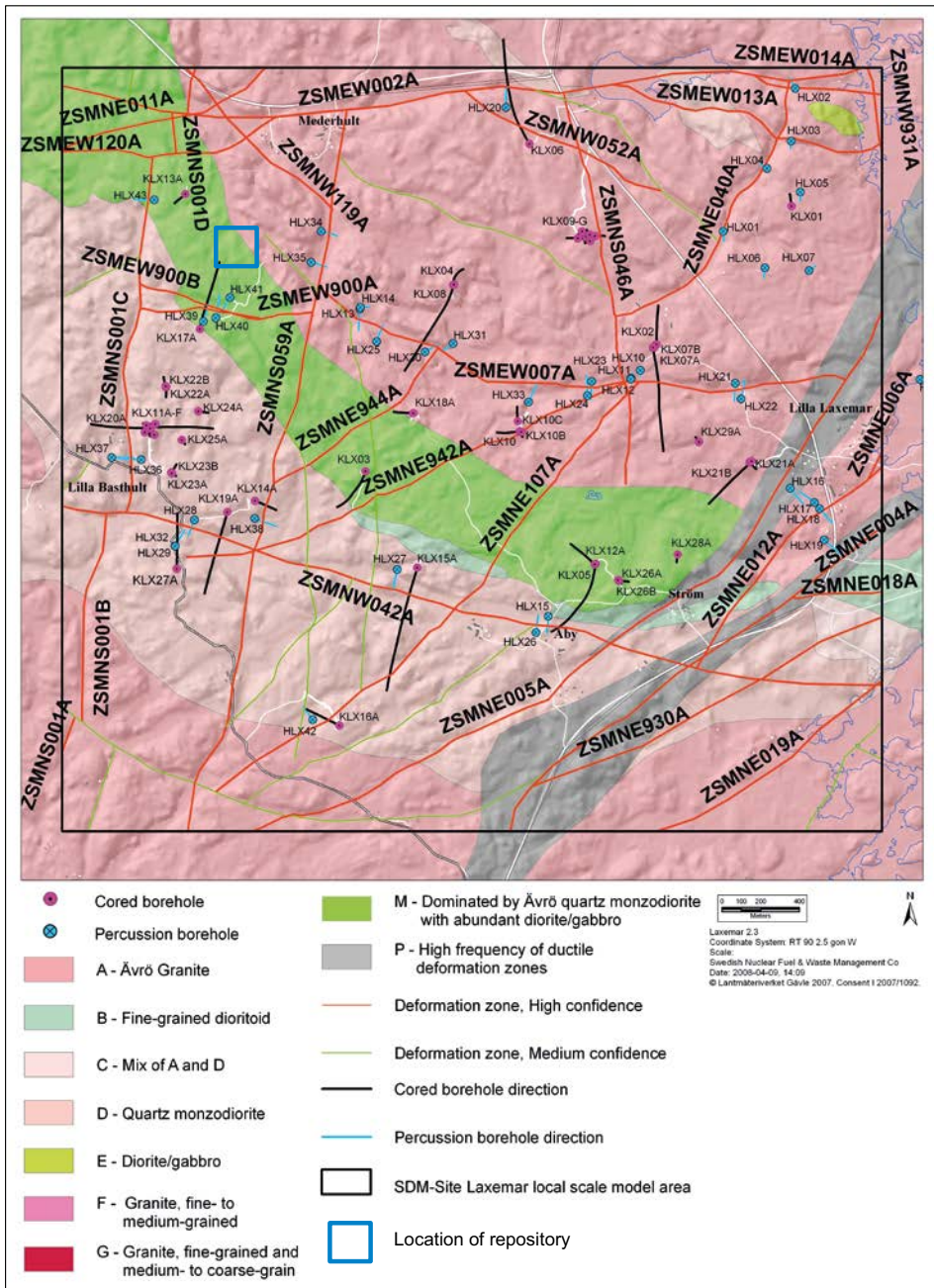


**Figure 4-13.** An overview of the lithology, deformation zones and rock domains modelled deterministically in the Laxemar local model area (Wahlgren et al. 2008).

### 4.6.3 Deformation zones and fracture domains

Deformation zones and fractures are themselves important characteristics of any site, as they affect mechanical stability of the bedrock, heat and groundwater flow and stress distribution, and therefore need to be considered in the choice of repository location. The stress distribution is also important for understanding the initial hydraulic properties of deformation zones and fractures. Any change in the stress field will create a change in the in-situ properties. Wahlgren et al. (2008) describe the site-specific deformation zone model that is assumed to contain all deformation zones of a length of 1 kilometre or greater present in the Laxemar region. Figure 4-13 also shows the deterministically treated deformation zones.

Fractures and minor deformation zones, not covered by the deformation zone models, are handled in a statistical way through discrete fracture network (DFN) models. The geological DFN model describes all fractures (open, partly open, sealed) (Wahlgren et al. 2008, La Pointe et al. 2008). Many of the sealed fractures are from mechanical or hydraulic aspects almost indistinguishable from the intact rock, hence hydrogeological DFN models may focus on the statistics of only the open and partly open fractures (Rhén et al. 2009).

The DFN models are presented as mathematical descriptions of fractures shorter than 1 km. The basic assumption is that all deformation zones of 1 km or larger are identified deterministically and included in the deformation zone model. A mathematical description is available for each fracture domain and for different depth intervals.

### 4.6.4 Bedrock temperature and thermal conditions

At initial state, the temperature in the repository and the bedrock at repository depth (–500 m) is assumed to be the same as the present-day bedrock temperature, i.e. about +14.9 °C (Sundberg et al. 2008). A linear dependence of temperature with depth, as established by Sundberg et al. (2008), is assumed, with a temperature of about +7.5 °C at the bedrock surface.

The thermal conditions of the bedrock in Laxemar vary for the different rock domains and are based on modelling realizations of lithology and thermal conductivity, followed by an upscaling to larger scales, according to the methodology described in Hökmark et al. (2009). The main result of the thermal modelling is a set of realisations describing the spatial distribution of thermal properties at the 2 m scale for the rock domains.

As noted above, the chosen volume for SFL in this safety evaluation is mostly located in rock domain RSMA01 and consists of three thermal subdomains. RSMA01 has the highest mean thermal conductivity of all three domains in Laxemar, with a certain amount of heterogeneity. Other parameters such as thermal anisotropy, heat capacity and thermal expansion coefficient have been measured *in situ* (SKB 2009).

As described in Section 4.4.1, the air temperature is expected to increase by a few degrees under global warming climate conditions, part of which would occur up until the time of repository closure at 2075 AD. However, in line with the notion that the initial conditions at repository closure should reflect present-day conditions, it is assumed that the bedrock temperatures at the time of repository closure are the same as those of today.

### 4.6.5 Rock mechanical conditions

The intact rock properties for the most dominant rock types in Laxemar show high strength, but a fairly large spread (Hakami et al. 2008). The position chosen for SFL in this safety evaluation is comprised mostly of the rock types Ävrö granodiorite and Ävrö quartz monzodiorite, which have a lower spread than the other rock types in terms of strength (SKB 2009). Average Young's modulus and Poisson's ratio values, which quantify the stiffness and ratio of transverse to axial strain, are relatively similar for all rock types, but a clearer difference can be noted in the tensile strength. Regarding fracture mechanical properties, the confidence in the model is moderately high due to the large number of tests performed (Hakami et al. 2008).

The Laxemar local model volume has been divided into several fracture domains according to similarities in fracturing (see Section 4.6.3). The rock mass properties in Laxemar have been estimated following both an empirical and a theoretical approach for the fracture domains as well as for the deformation zones (Hakami et al. 2008). The results from both approaches agree quite well for the fracture domains, but properties for deformation zones differ to a greater extent.

The model for the state of stress in Laxemar (Hakami et al. 2008) is based on primary site-specific local scale and regional scale data, an evaluation of the large-scale variability in rock stress due to major deformation zones and an evaluation of the small-scale stress variability. The stress model relates to the stresses between depths of 400–700 m with moderately high uncertainty for stress magnitudes (SKB 2009), but the confidence on the model estimates of the upper limits for the stresses is higher. The rock stresses are low in comparison with the rock strength.

#### 4.6.6 Bedrock hydraulic properties

The basis for assigning hydraulic properties comes from detailed information on the positions of deterministically modelled deformation zones and the water-conductive fractures in-between the deformation zones (SKB 2009). Moreover, information has been gathered from numerous different field investigations, such as detailed flow measurements in boreholes and interference pump tests in core- and percussion-drilled boreholes.

##### Hydraulic properties of deformation zones

Analyses of the hydraulic data have revealed that all deformation zones, regardless of orientation display a large variability in transmissivity, as well as a correlation between size and transmissivity, and all deformation zones show a weakly decreasing trend of transmissivity with depth (Figure 4-14). Further, the east-west trending deformation zones have a slightly higher mean transmissivity than all other oriented deformation zones. Supporting data for property assignments are presented in Rhén et al. (2009) and Rhén and Hartley (2009).

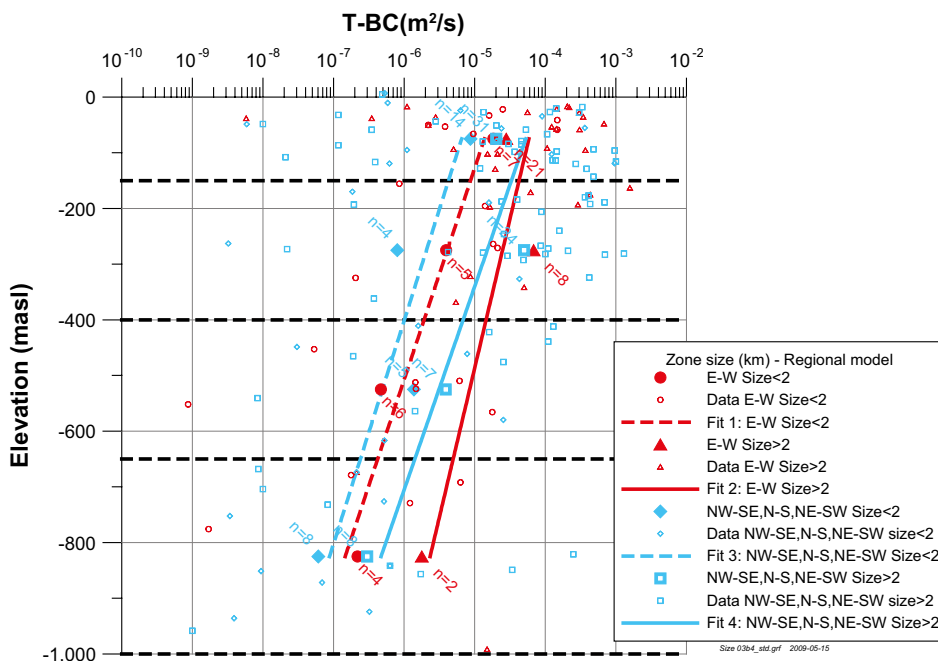


**Figure 4-14.** Deformation zone transmissivity ( $T$ ) related to deformation zone orientations in the horizontal plane and size, versus elevation. The best choice (BC) of the transmissivities evaluated from the available transient data is shown. Mean of  $\log_{10}(T)$ , plotted as well as the number of observations ( $n$ ), together with regression line and data (Figure 5-3 in Rhén and Hartley 2009).

### **Hydraulic properties of fracture domains**

The hydraulic properties in the fracture domains are primarily established via a tuning of the hydrogeological DFN models against site data in terms of parameters affecting the connectivity pattern and the relation between fracture size and transmissivity (Rhén and Hartley 2009). In SE-SFL the parameterisation for the DFN model established by Joyce et al. (2010) is used.

### **4.6.7 Geochemistry**

As part of the site investigations for the spent fuel repository, explorative analyses of measured groundwater chemistry and hydrogeochemical modelling have been used (Laaksoharju et al. 2009) to evaluate the geochemical conditions at Laxemar. The site investigation included an assessment of the origins of the groundwater and the processes that control the water composition.

Figure 4-15 shows the main geochemical characteristics of the present-day groundwaters in Laxemar as a function of depth, representing the initial state geochemical condition for SE-SFL. The groundwater types in Laxemar are based on the salinity content of the water (i.e. fresh, brackish, saline and highly saline). Brackish waters may be subdivided into brackish-glacial, brackish-marine and brackish non-marine, mainly based on  $\delta^{18}\text{O}/\delta^2\text{H}$  and marine indicators such as the Mg content and Br/Cl ratios.

The complex groundwater patterns currently present in Laxemar are a result of many factors such as: a) past changes in hydrogeology related to glaciation/deglaciation, land uplift and repeated marine/lake water regressions/transgressions, b) the present-day topography and proximity to the Baltic Sea, and c) organic or inorganic modifications of the groundwater composition caused by microbial processes and water/rock interactions. The sampled groundwaters reflect, to various degrees, processes relating to modern or ancient water/rock interactions and mixing.

Mixing processes to describe the initial conditions in Laxemar are described in Laaksoharju et al. (2009) and in Kalinowski (2009) based on at least four end-member waters; an old deep saline water (Deep Saline), an old marine water (Littorina Sea), a modern meteoric water (Altered Meteoric), and a glacial meltwater (Glacial). Mixing was considered to be the prime irreversible process responsible for the chemical evolution of the groundwater systems in Laxemar, leading to the present-day conditions. The successive disequilibrium states caused by mixing conditioned the subsequent water-rock interaction processes and, hence, the re-equilibration pathways of the mixed groundwaters.

Concerning the redox properties of the bedrock, studies on the fracture fillings from Laxemar indicate that the transition from oxidising to reducing conditions takes place in the upper 20 m, as deduced from the occurrences of recent low temperature Fe-oxyhydroxides and from the results of U-series disequilibrium analyses. The existence of Fe(II)-minerals (chlorite and pyrite) in the fracture fillings, even in the shallowest part of the system, indicates that  $\text{O}_2$ -rich waters introduced, for example during past glacial episodes, have not exhausted the reducing capacity of the fracture minerals (Laaksoharju et al. 2009).

Glacial signatures are most prominent at depths between 300–600 m (Figure 4-15b). It is likely that large volumes of glacial meltwaters will penetrate to repository depth in the SFL-focused volume also during future glacial episodes. However, the probability is low of the glacial meltwaters retaining their oxidising character for a long period of time and reaching repository depth, considering the buffer capacity of the fracture fillings, discussed above, and the significant Fe(II) content of the bedrock (even in the red-stained altered wall rock). This assumption is supported by detailed mineralogical studies from Laxemar and Äspö, all of which indicate no signs of this glacial meltwater having been oxidising at depths below 100 m and the current redox values (Figure 4-15f) of  $-270$  to  $-300$  mV<sup>6</sup> (Laaksoharju et al. 2009).

<sup>6</sup>Excluding the very poor-quality measurements noted as Category 5 in figure 4-15f.

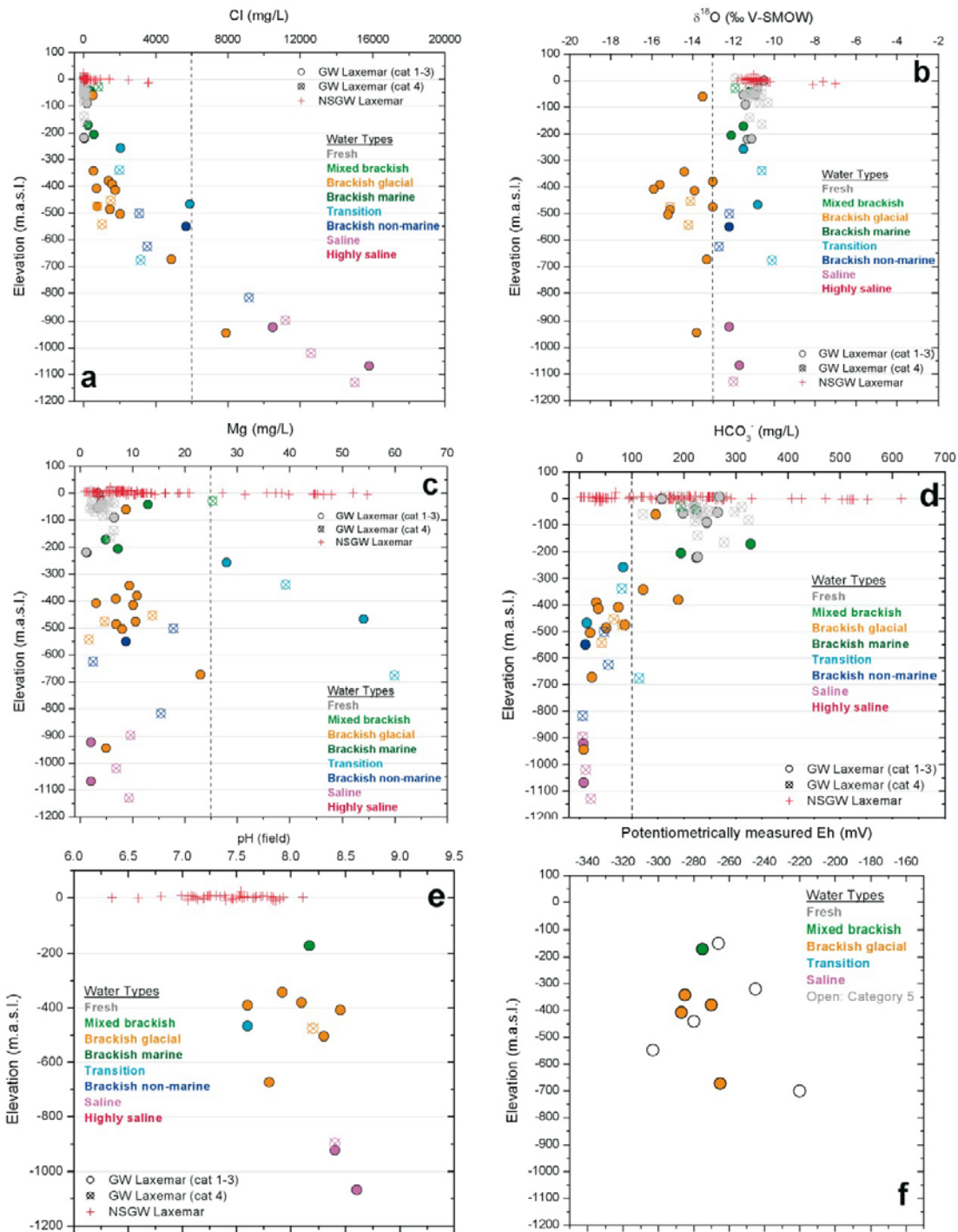


**Figure 4-15.** Distributions of key parameters versus depth in groundwaters from Laxemar: (a) chloride, vertical dashed line indicates maximum possible penetration depth for *Littorina* water (= 6000 mg/L Cl); (b)  $\delta^{18}\text{O}$ , vertical dashed line at  $\delta^{18}\text{O} = -13$  ‰ VSMOW indicates the upper limit for the classification of water with a glacial component; (c) magnesium, vertical dashed line at 25 mg/L indicates the lower limit for groundwater with a marine component; (d) bicarbonate, vertical dashed line at 100 mg/L indicates upper limit for most of the waters at repository depth; (e) pH, and (f) redox potential. The groundwater (GW) data are categorised in five categories relating to data quality and the near surface groundwater (NSGW) data are depicted by red crosses. From Figure 7-1 in Laaksoharju et al. (2009).

## 5 Safety functions

### 5.1 Role of safety functions in safety analyses

Safety functions are utilised in SKB's safety analysis methodology to qualitatively define what roles a repository component has for post-closure safety and can generally be used for several purposes. First, the safety functions can be an aid in evaluation of the safety significance of the evolution of the barriers over time. In that context, it should be noted that maintaining a safety function of a component may neither be necessary to maintain safety of the repository nor may it be sufficient for proving safety. Instead, safety needs to be evaluated in relation to applicable requirements including the risk criteria. Second, in SR-Site and SR-PSU, one main purpose of the safety functions was to serve as a basis for the selection of scenarios; in particular, for the less probable scenarios that should be included in the analysis according to the guidance to the regulations. Third, the safety functions can play a role in the optimisation of the repository by highlighting components for which an improvement of their performance may be advantageous. A further aspect is that the safety functions can be a basis for the development of technical design requirements as suggested for the Spent Fuel Repository (Posiva SKB 2017). Last, the safety functions may be an aid in defining site selection factors that should be considered in the siting of the facility.

A quantifiable indicator is coupled to each safety function and this can be used to evaluate the state of the safety function over time. The safety function indicators can help to identify important aspects of the evaluation or analysis that merit further analysis or require adjustments of the component design. In general, a criterion can be coupled to a safety function indicator that reflects a value above or below which the safety function is upheld. In SR-Site, such criteria were defined for safety functions for which a clear distinction could be made as to whether the safety function was fulfilled or not. This is possible if a feature or process related to the safety function experiences an abrupt change at the value of the safety function indicator criterion. For instance, the isolation provided by the copper canister in SR-Site upholds its function if the thickness of the copper is greater than zero. Another example from SR-Site is that the safety function of the buffer to filter colloids is upheld if the buffer density is maintained above a certain value. However, there are also safety function indicators that are not directly coupled to entities that experience abrupt changes. Instead, the safety function is coupled to gradual changes and gradual effects on its performance. An example of this from SR-Site is the safety function related to the ability of the bentonite backfill in the deposition tunnels to counteract expansion of the bentonite buffer from the deposition holes (SKB 2011a, Section 8.4). The related safety function indicator is buffer density and a high density is favourable. In such cases, it makes no sense to define quantitative safety function indicator criteria.

The identification of the safety functions generally begins with considering the safety principle<sup>7</sup> for the repository, which is then broken down to several safety functions. In SR-PSU, for instance, the safety functions were based on the characteristics of the repository's sub-components from the perspective of long-term safety. Given the safety principles and the initial state of the repository, potential aspects were considered that are important for the various components in the different vaults. These aspects were then discussed in terms of the functions of the repository components, i.e. the waste and packaging, engineered barriers, and closure components. Moreover, the functions of the geosphere and the surface were discussed. Based on these discussions several safety functions and associated indicators were then defined (SKB 2015a, Chapter 5).

---

<sup>7</sup> It can be noted that the term safety principle is not uniquely defined. In SE-SFL the term is used in the same way as in SR-PSU, namely, to denote the basic idea underlying the repository concept (SKB 2015a). The term has, however, also been used in SR-Site to denote the starting points underlying the development of the KBS-3 concept including, for instance, the choice to use natural materials that are long-term stable in the repository environment (SKB 2011a). The term safety principle is also used in IAEA's Safety Fundamental SF-1 to denote the ten safety principles that are associated with the fundamental safety objective to protect people and environment from harmful effects of ionizing radiation (IAEA 2018).

In SE-SFL, the main objective is to introduce a set of safety functions that can be used in the further development of the safety analysis and the design of the concept. The safety functions are only briefly discussed in the reference evolution when the analysis indicates that repository components might not fully function throughout the entire analysis period as desired. This is intended as a step in the further improvement of the concept in future work. Since there is no intention in SE-SFL to undertake a comprehensive scenario analysis (see Sections 2.2 and 2.5.8), the main purpose of the safety functions to aid the definition of less probable scenarios is not followed through here, but will need to be carried out in a subsequent full safety analysis.

## 5.2 Safety functions in SE-SFL

The safety functions for SE-SFL are defined based on the safety principle for SFL. In the concept study that was carried out before SE-SFL, the safety principle for SFL was proposed to be *retardation* (Elfving et al. 2013). The idea behind the proposed concept for SFL is thus to use a system of engineered and natural barriers to reduce the mobility and transport of radionuclides. Elfving et al. (2013) describe the design principles of the barriers for post-closure safety in the proposed repository concept. Based on this, an initial state has been defined in SE-SFL with repository components that can be attributed different safety functions with respect to post-closure safety. This includes the waste form, packaging and surrounding grout, engineered barriers, and closure components. In addition to the engineered barriers, the rock surrounding the repository as a natural barrier can also be attributed safety functions. The nature of the safety functions is deduced from the requirements that the internal processes and external conditions put on repository performance. Following the practice in SR-PSU no quantitative safety function indicator criteria have been defined, noting that the safety functions considered are generally coupled to gradual changes and gradual effects on repository performance.

Given the preceding discussion, the following safety functions and related indicators are defined for the two vaults, closure components and natural barriers in SE-SFL.

The waste form, packaging and surrounding grout are handled as a single entity when it comes to safety functions in SE-SFL. The following safety functions and indicators (in parenthesis) are attributed to the waste domain of BHA and BHK:

- Good retention (as determined by pH, redox potential, concentration of complexing agents in BHA, available sorption surface area, corrosion rate in BHK).

Good retention implies favourable conditions for sorption of radionuclides in concrete contained in the waste domains. This is achieved by high pH, low redox potential, low concentrations of complexing agents and high available sorption surface areas. High pH and low redox potential also inhibit the corrosion of steel and thus the release of induced activity in BHK. In practice, the waste packages and grout will also limit the flow of water through the waste domain, but this is not accounted for in SE-SFL in BHA or BHK and therefore is not included as a safety function.

Colloid formation and transport in the waste is included in the SE-SFL FEP catalogue. However, the process is not considered in SE-SFL, but will be handled in future safety analyses (**FEP report**, Section 4.2.2). As the process is not analysed, no safety function relating to colloid formation or transport in the waste domain is considered in SE-SFL.

For the bentonite barrier of BHA, the following safety functions and associated indicators (in parentheses) are identified:

- Low flow in the waste vault (hydraulic conductivity).
- Good retention (diffusivity, available sorption surface area).

Low flow in the waste vault implies that the hydraulic conductivity of the bentonite barrier needs to be limited to make diffusion the main transport process. Good retention is maintained if the diffusivity is low, and the area available for sorption is high.

In the FEP processing, it is stated that mechanical processes in the BHA barriers are not considered in SE-SFL. Consequently, no quantitative mechanical analysis of the bentonite barrier is performed within SE-SFL. Mechanical processes in the bentonite could however influence the post-closure performance of BHA and should be considered in subsequent safety analysis. It is also noted that phase changes/freezing is not considered since it is assumed that the depth of the repository is chosen to avoid permafrost. The production of gas is likely to be small in BHA and therefore no safety function related to gas is associated with the bentonite barrier in BHA. Since colloid transport is not considered in SE-SFL the capacity of the bentonite to filter colloids is not included as a safety function indicator related to good retention. If colloid transport in future analysis should show to be of importance such a safety function indicator could be considered.

For the concrete barrier in BHK, the following safety functions and associated indicators (in parentheses) are identified:

- Low flow in the waste vault (hydraulic conductivity).
- Good retention (low diffusivity, large available sorption surface area, high pH, and low redox potential).

Low flow in the waste vault implies that the hydraulic conductivity of the concrete barrier is low. This implies that the conductivity should be lower than that in the surrounding rock. If diffusive transport becomes dominant below some conductivity there is no reason to decrease the conductivity further. Good retention implies that the diffusivity is low, the available sorption surface area is high, the pH is high, and the redox potential low.

In the selection of the safety functions, it is considered that the formation of gas in BHK is not significant (Section 6.2.10). Due to the high pH that prevails in the concrete structure, microbial processes are also screened out. The amounts of colloids in the engineered barriers in the BHK and BHA vaults are assumed to be negligible since the concrete barriers and the concrete packaging will supply calcium ions, suppressing colloid formation (Swanton et al. 2010). Consequently, no related safety functions are defined. Mechanical loads can arise, for instance, by seismic activity and this has not been analysed in SE-SFL.

The closure components include the bentonite sealing of the tunnel sections adjacent to the waste vaults and the plugs separating the sealing from the access tunnels (Section 4.3.3 and **Initial state report**, Chapter 6). Moreover, the backfilling of the tunnel system at repository level with crushed rock or similar material is part of the closure components. The following safety function is defined for the closure components:

- Low flow in the seals (hydraulic conductivity).

In the FEP processing, mechanical and other degradation processes affecting the plugs and other closure components are disregarded (Section 4.3.3 and **Initial state report**, Section 4.1.2). Thus, safety functions related to the mechanical stability and degradation of the plugs and the access tunnel backfill are not defined. Since the limited groundwater flow in the seals is of importance, such safety functions might need to be considered in future safety analyses.

The bedrock is the natural barrier surrounding the waste vaults. The following safety function is defined for the bedrock

- Low flow in bedrock (low hydraulic gradient and conductivity).

The groundwater flow is controlled by the siting of the facility and is therefore likely to be an important site selection factor. In addition to the safety function of low flow, the bedrock has the role of protecting the engineered barriers, for instance by providing favourable chemical conditions. Another example is low seismic activity. However, these factors may be treated as site-selection criteria in a future site selection process.

In summary, a set of safety functions and associated indicators are suggested in SE-SFL that will need to be reconsidered in a full safety analysis. At that time, focus should be given to the aspects of the safety functions relating to the scenario selection process, since no scenario selection process has been carried out within SE-SFL.



## 6 Reference evolution of the repository and its environs

### 6.1 Introduction

As described in Section 2.5.6, a reference evolution of the repository and its environs that follows from the reference external conditions defined in step 3 of the methodology (Section 2.5.3), is established and analysed in this chapter. The purpose of defining and analysing the reference evolution is to gain an understanding of the likely overall evolution of the system under representative external conditions that may influence post-closure safety. To this end, identified FEPs that can affect the post-closure performance of the system are considered. Further, the safety functions defined in Section 5.2 are briefly discussed when the analysis indicates that the function of repository components might be significantly altered over time. This understanding of the overall evolution of the system and its safety functions serves as a basis for the selection and analysis of various evaluation cases, described in Chapters 7 and 8.

Three variants of the reference evolution are considered, described respectively in Sections 6.2–6.4. The *base variant* is a hypothetical situation where external (climatic) conditions are assumed identical to those at the present day during the complete analysis period of 1 million years. The second, *increased greenhouse effect variant* of the reference evolution, describes a future climate affected by anthropogenic activities. The third and final, *simplified glacial cycle variant*, describes an overall climate development that follows reconstruction of the last glacial cycle, with periods of temperate climate, periglacial conditions with permafrost, ice-sheet development and variations in shore level. These three climate variants are the basis for the three main evaluation cases for radionuclide transport and dose estimation in the **Radionuclide transport report**.

The starting point for the reference evolution is the initial state. The initial state is defined as the expected state of the repository and its environs at closure, under the assumption that the repository is designed and constructed in accordance with the proposed repository concept and placed at the example location at approximately 500 m depth in the position in Laxemar assumed for SE-SFL. At closure, the closure components are installed, including backfill and plugs for the vaults, tunnel system, shaft and boreholes.

The repository properties start to develop already during construction, including changes to the waste, concrete caissons, vaults, tunnels, and the bedrock surrounding the repository. For instance, the rock excavation and groundwater abstraction may lead to mechanical changes in the bedrock, and locally altered groundwater chemistry. Due to the atmospheric pressure in the tunnels, the groundwater flow field is altered which implies that water from shallower and greater depths, with possible differences in hydrochemistry, is drawn towards the repository. The radioactivity in the waste is decaying and the concrete structures of the waste domain are affected by the atmosphere in the vault. All these important processes during construction and operation affecting the initial state of the repository need to be considered in a full safety assessment. In SE-SFL, it is for simplicity assumed that the initial state conditions are those stated in Chapter 4 and no analyses of the evolution during construction and operation of the repository are performed to underpin the given assumptions.

### 6.2 Base variant of the reference evolution

#### 6.2.1 External conditions

The initial-state climate conditions upon repository closure at 2075 AD, assumed to be the same as present-day conditions, are described in Section 4.4. For the Laxemar area, the mean annual air temperature is about 6.4 °C and the annual precipitation is 553 mm (Table 3-1 in the **Climate report**).

The ongoing regressive shoreline displacement in Laxemar continues until approximately 40 000 AD (Figure 6-1). The SE-SFL repository example location is below a local hill in the landscape at an average peak elevation of 21.5 m above present mean sea level. This area became terrestrial around 8800 BC according to the reconstructed Holocene shore-level development at Laxemar (for details see Appendix B in the **Climate report**).

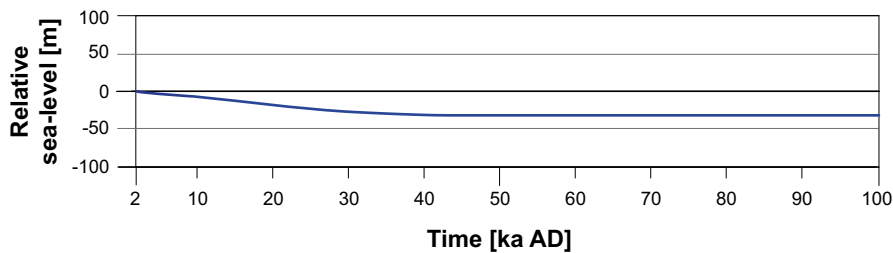


**Figure 6-1.** Relative sea level in Laxemar in the base variant of the reference evolution. The evolution is based on Pässe (2001) as well as an adaptation to glacial isostatic adjustment (GIA) data used for forecasts into the future. For detailed information, see Section 3.2 and Appendix A in the *Climate report*.

## 6.2.2 Development of surface systems

Long-term landscape development in the Laxemar area is dependent on two main and partly interdependent factors: climate variations and shoreline displacement (described in Section 6.2.1). These two factors in combination strongly affect several processes, which in turn determine the development of ecosystems and future conditions of importance for radionuclide transport, exposure, and resulting doses and risk. Examples of such processes are erosion and sedimentation, groundwater recharge and discharge, soil formation, primary production and decomposition of organic matter.

According to results from the hydrogeological modelling, including by Sassner et al. (2011) for Laxemar and by Odén et al. (2014) for Forsmark, discharge of deep groundwater will almost exclusively take place at low points in the landscape, i.e. in lakes, wetlands, and streams, and in near-shore areas of the sea. The presence of these landscape areas is shown in the map of the Laxemar region in Figure 6-2. Thus, the following description of landscape development is focussed on these areas, as these are where accumulation of potentially released radionuclides may occur.

The current state of the surface systems is described in Section 4.5. The evolution after closure will be characterised by the ongoing regressive shoreline displacement, which will gradually bring new areas of the sea floor above sea-level. This will expose sediments to wave erosion and resuspended fine-grained particles will be transported out of the area into the Baltic Sea, or re-settle on the sea bottom within the parts of the study area with the greatest water depths (Brydsten and Strömgren 2010, **Biosphere synthesis**). Accordingly, the relocation of sediments may have important implications for transport and accumulation in lakes and sea basins of radionuclides potentially originating from the repository. The shoreline displacement will also cause a continuing and predictable change in the abiotic environment, e.g. in water depth and nutrient availability. It is therefore appropriate to describe the ecosystems occurring around the main discharge areas for deep groundwater, with respect to their origin and development in relation to shoreline displacement. The discharge areas are characterised by long valleys with fine sediments, on top of which are also traces of peat (Sohlenius and Hedenström 2008).

This pattern is typical of a sea bay having undergone isolation into a lake, followed by ontogeny of the lake and its development into a wetland. As the lake ages, sediment and organic matter accumulate due to sedimentation and vegetation growth, and eventually most lakes are transformed to wetlands, except those of considerable depth and area. The wetland areas may at later stages be drained by humans and transformed into agricultural land. The future emerging land will follow the same pattern in terms of sediment deposition and the two large narrow sea basins surrounding the Äspö island today will gradually be transformed into large lakes. Due to their difference in depth, this will happen around 2500 AD and 5100 AD, respectively (**Biosphere synthesis**). Newly isolated lakes will occasionally be affected by flooding with brackish water from the Baltic Sea during periods of high sea water levels, in the same way that can be seen in low-elevation, present-day lakes in other areas such as Forsmark (Johansson 2008). The only present lake in the Laxemar area is the small and shallow lake Frisksjön. The rate of sedimentation in the lakes is dependent on lake volume (Brydsten 2004), whereas the colonisation by littoral plants only occurs in shallow water (depth < 2 m). Thus, the rate of lake infilling is mainly dependent on lake depth, area and volume (Brydsten and Strömgren 2010). Lake Frisksjön will, according to the modelled evolution, be transformed to a wetland around 9800 AD (**Biosphere synthesis**).

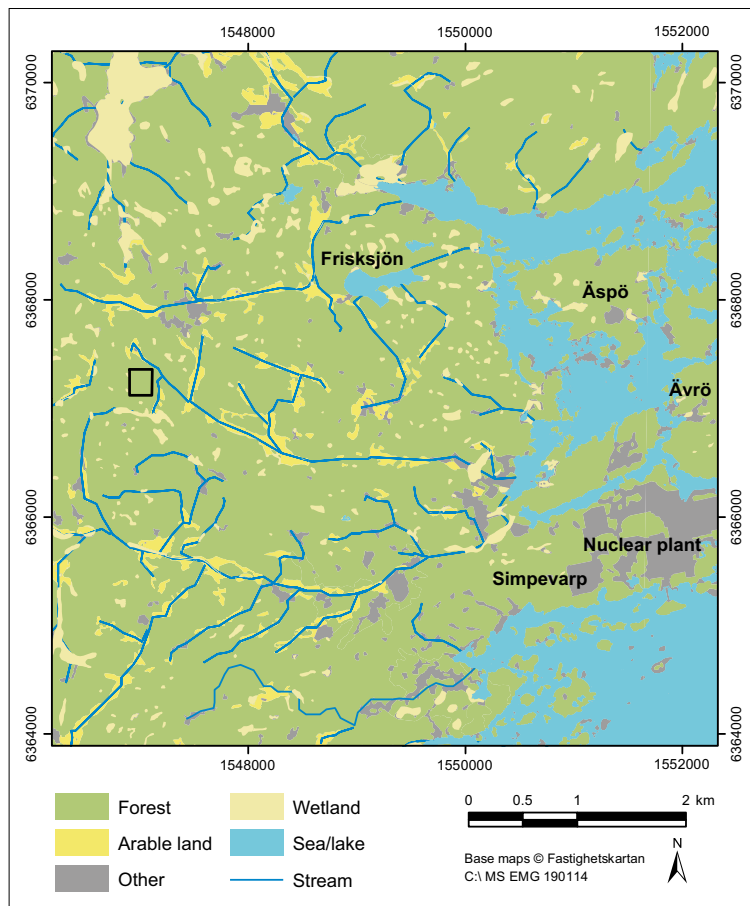


**Figure 6-2.** Map of the Laxemar area. The human land use in Laxemar today is dominated by agricultural areas along the valleys where fine sediments are found. Typically, these areas have streams that have been improved to drain the fine sediments and enable cultivation. The example location for SFL is indicated with a square.

As the sea close to the coast gets shallower, erosion will occur on wave-exposed bottoms. Some sheltered areas inside a developing, denser archipelago will show sediment accumulation for a short period (Brydsten 2009). The salinity of the Baltic Sea around Laxemar, currently 6.4 ‰, is expected to decrease by a few per-mille points during the initial 1 000 years, until it becomes limnic around 4000 AD (Gustafsson 2004). The ongoing shoreline regression causes a succession pattern in which shore vegetation will be replaced by forest vegetation. The types of dominating vegetation communities during this succession are mainly determined by the composition of the underlying regolith, e.g. coarse till or fine sediments.

Human land-use is a factor that could have a large impact on landscape development and, apart from drainage and agricultural land use, forestry and animal husbandry may also have large consequences for the vegetation distribution in the area. Large-scale irrigation is not currently practiced in the area but may possibly be implemented by future farmers, so the potential influence of irrigation has been studied by Grolander and Jaeschke (2019).

The potential for sustainable human exploitation of food resources in the area over the forthcoming millennia is not expected to differ much from the situation today. Similarly, the water supply available for humans is expected to be roughly unaltered during this period. Additional stream stretches will be added to the already present ones. In the future, the deep lakes around Äspö have the potential to become freshwater reservoirs when the salinity decreases. New wells may be dug in the regolith, in the area that is land today, or in new land having risen to > 1 m above sea level.

The description in this section, which involves shoreline regression and a succession resulting in new land areas beyond the present shoreline, is applicable in both the *increased greenhouse effect variant* (Section 6.3) and in the temperate periods that follow each glaciation period in the *simplified glacial cycle variant* (Section 6.4).

### 6.2.3 Thermal evolution

The present-day conditions are described in Section 4.6.4. The temperature effect of heat-generating waste on the repository components and the surrounding bedrock is negligible (see Section 6.2.8). Thus, in the *base variant* of the reference evolution, the thermal properties are expected to remain unchanged after closure.

### 6.2.4 Mechanical evolution

The mechanical conditions in the bedrock at the Laxemar site are presented briefly in Section 4.6.5, based on the SDM for Laxemar (SKB 2009, Hakami et al. 2008). In order to describe the mechanical evolution of the host rock for the SFL repository, a thermo-hydro-mechanical approach may be used; see for instance modelling of the Laxemar site for a Spent Fuel Repository (Hökmark et al. 2010). In these models, no temporal evolution of the bedrock properties is considered.

The stiffness of the bedrock affects the stresses experienced by the concrete backfill in the vault, where less stiff bedrock implies higher stresses on the vault. The stiffness in terms of the Young's modulus is, however, subject to uncertainty. Idiart et al. (2019a) therefore modelled the sensitivity of the BHK backfill to bedrock stiffness, resulting in low load transfers to the backfill except in the case of a very low Young's modulus of 25 GPa, which is unrealistic for Laxemar bedrock. Only with this least stiff bedrock would mechanical damage of the backfill be predicted to occur, starting at its interface with the waste domain.

Earthquakes could potentially affect the repository stability. The likelihood of, and potential damage from, earthquakes was studied for the Spent Fuel Repository in Laxemar and Forsmark (SKB 2010f). To quantitatively evaluate the effect of earthquakes, the spatio-temporal variability of the magnitude-frequency relation needs to be addressed over a glacial cycle, which is a major undertaking. Given the objectives of SE-SFL, and the fact that no site is determined yet, such an analysis has been omitted here.

The most severe mechanical changes in the bedrock occur during repository excavation. This may create an excavation-damaged zone around the repository, but the effects of this have not been studied in SE-SFL. The rock mechanical properties are strongly site-dependent, so a more specific analysis of the SFL rock mechanical evolution is not judged meaningful until a site for SFL is decided upon.

### 6.2.5 Regional hydrogeological conditions

The base variant of the reference evolution assumes present-day climate conditions and accounts for the shoreline displacement after the last glacial rebound as described in Section 4.4. Based on this climate evolution, Joyce et al. (2019) modelled the evolution of the hydrogeological system around the example repository location from 8000 BC to 60000 AD with a catchment-focussed and a facility-focussed model. Both models have the same dimensions (Figure 6-3) as the hydrogeological site descriptive model (SDM) that was constructed as part of SKB's Spent Fuel Repository programme (Rhén and Hartley 2009) and uses the conceptualization of the groundwater system following SKB's established methodology also used in both SDM-Site Forsmark and SDM-PSU (Rhén et al. 2003, Follin 2008, Öhman et al. 2012).

Both the catchment-focussed and the facility-focussed models implement an equivalent porous medium model (ECPM) based on an up-scaled discrete fracture network (DFN) representation (Section 3.3.1 in Joyce et al. 2019, Section 6.1 in SKB 2009, Rhén and Hartley 2009). In the facility-focused model, however, calculations are performed using a DFN representation in a volume around the repository (Joyce et al. 2019, Section 3.4.1). The individual regolith layers of the hydraulic soil domain as well as the repository structures are explicitly represented with a continuous porous medium model (CPM), except for the ramp and shaft which are treated as equivalent planar features in the DFN. In the catchment-focussed model, the grid is refined around the example volume within the Laxemar area evaluated in SE-SFL (Figure 6-3), denoted the facility volume. Within this facility volume, a further refined volume (600 m across and 60 m deep) is defined around the repository example location, with even higher grid resolution. The repository itself is, however, not explicitly represented in the model. The model accounts for density-driven flow, solute transport by advection and dispersion, matrix diffusion, and hydrogeochemical processes (Sections 2.2.6–2.2.9 in Joyce et al. 2019).

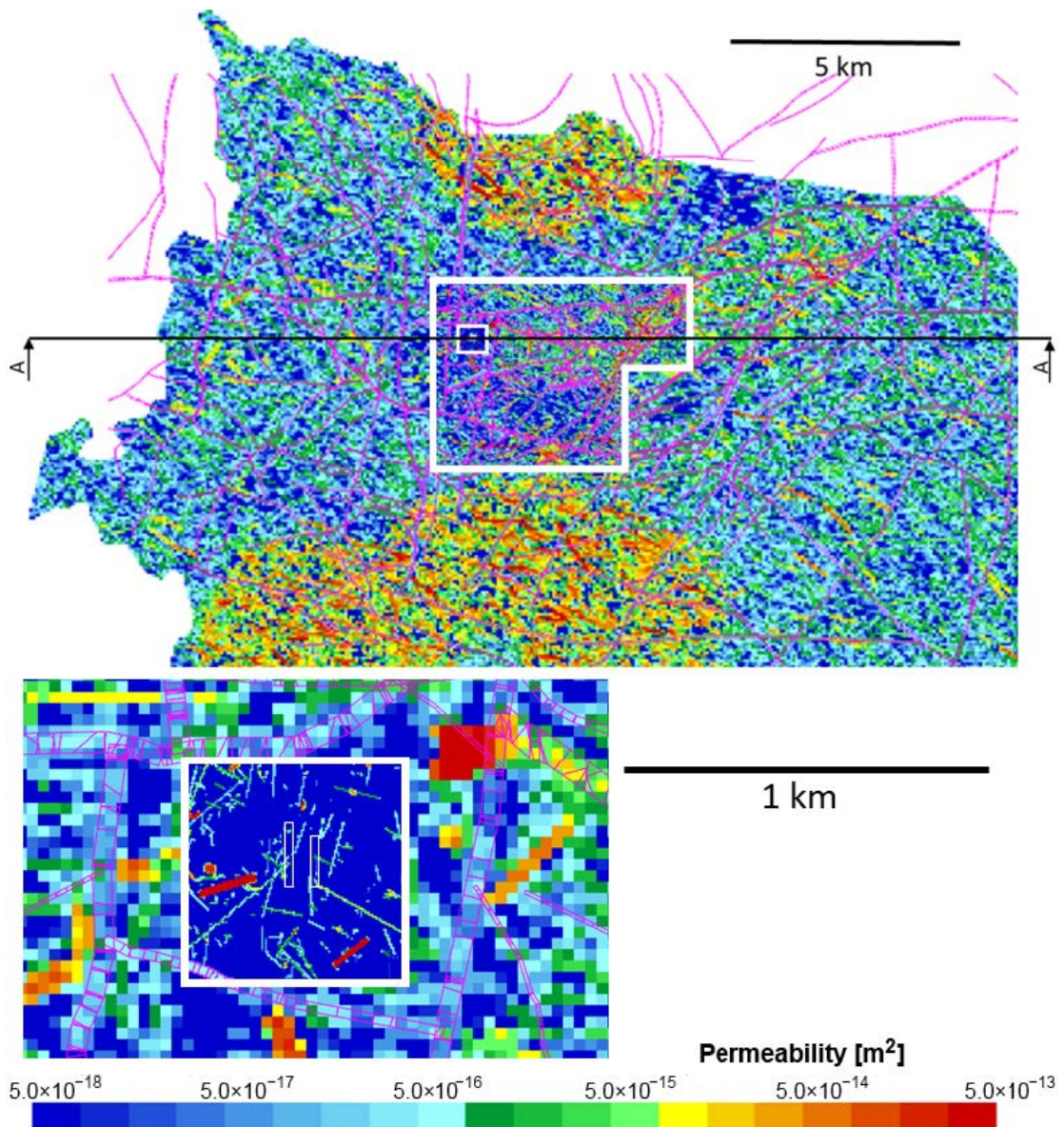


**Figure 6-3.** The entire catchment-focussed model domain, showing the horizontal permeability distribution for HRD realisation 1, for a horizontal cross-section at a depth of 500 m (top panel). The deformation zones are shown in purple, the facility and refined volumes are delineated with thick white borders. The refined volume in larger scale (bottom panel) where the example locations of the vaults are shown with very thin white borders; note, however, that they are not represented within the model. Figure adapted from Figure 4-102 in Joyce et al. (2019).

The catchment-focussed model is used to calculate groundwater-density and -pressure values at specified time slices for use in the facility-focussed model. As described in Section 6.2.7, three different cases are considered for the hydrogeochemical reactions (Sections 3.1 and 3.3.5 in Joyce et al. 2019). Five realisations with the facility-focussed model, representing the fractured bedrock between the deformation zones (hydraulic rock domains; HRDs) were simulated to test the sensitivity of the different results to stochastic variability of the fracture network. The first of these realisations is combined with deterministic hydraulic properties within the representation of the deterministically defined deformation zones larger than 1 km length (hydraulic conductor domains; HCD). The other four realisations are combined with stochastic realisations of the hydraulic properties within the HCD (Section 4.6.4 in Joyce et al. 2019). Hydrogeochemical processes are not modelled in the facility-focussed model, but their effects on flow are included through the imported spatially variable water density.

The facility-focussed model calculates a steady-state, density-dependent pressure solution for the considered time slice. Inside the facility volume, calculations are performed using an explicit DFN representation. The initial conditions as imported from the catchment-focussed model are interpolated onto the fractures and ECPM or CPM cells (Section 3.4 in Joyce et al. 2019). Pathways of particles from fractures intersecting the vaults to discharge locations are also calculated for use in the radionuclide transport modelling (see Section 7.3).

Results from the catchment-focussed and facility-focussed models are directly used to describe the regional geosphere hydrogeology. An additional model has been constructed for the repository near-field (Section 6.2.6). The near-field model uses a CPM representation of the repository and waste structures and an ECPM representation for the surrounding bedrock; see Abarca et al. (2019) for details.

The hydrogeological evolution in the bedrock surrounding the example location for SFL, as interpreted from the results of this modelling, is described below. The regional geochemical results are summarised in Section 6.2.7.

Using the five HRD realisations defined at 2000 AD, the facility-focussed model was used to calculate particle tracks and properties relevant for transport for a set of time slices from 8000 BC to 60000 AD. Overall, groundwater-recharge locations and extents vary very little after 2000 AD, responding mainly to the shoreline displacement (Section 4.6.2 in Joyce et al. 2019). The particle tracks for 2000 AD (Figure 6-4) show that the recharge area for particles passing through the repository is located above and slightly west of the repository. Thus, the recharge to the vaults (after saturation, Section 6.2.6) occurs almost directly from above. The particle tracks generally continue further down after passing through the repository and thus the model simulates insignificant cross flow between the vaults. Discharge locations are found mostly in depressions and stream valleys, and primarily to the north and east of the repository towards the sea.

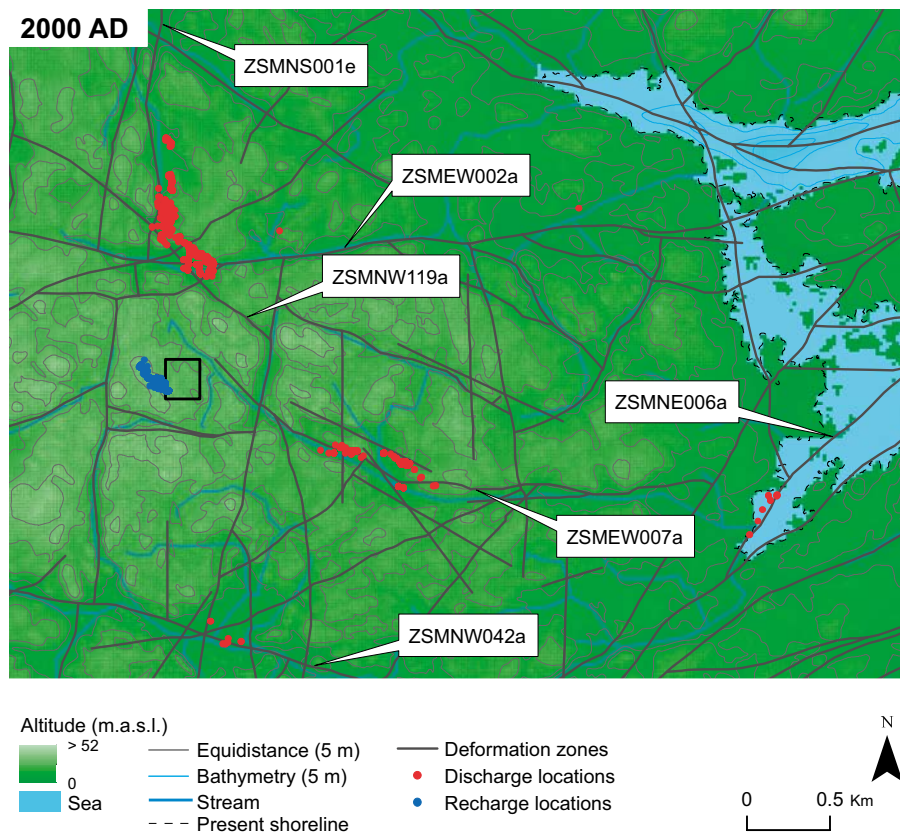


**Figure 6-4.** Particle recharge (blue) and discharge (red) locations at the ground surface for Case 1 of the facility-focussed model at 2000 AD. The model surface is coloured by elevation (land in green, sea in blue). Water courses (blue), deformation zones at  $-20$  m elevation (dark grey) and the repository example location (black) are added for context. The boxes with arrows show the names of the deformation zones with which the main discharge locations are associated. Adapted from Figure 4-130 in Joyce et al. (2019).

For illustration, Figure 6-5 shows a subset of 100 particle tracks from the waste vault BHA to the surface. Also discharge locations close to the repository show only very small changes after 2000 AD, but due to shoreline displacement, a few more distant discharge locations appear to the east (Section 4.6.2 in Joyce et al. 2019). Deformation zones have a significant influence on the particle tracks, resulting in a clustering of the discharge locations as apparent in Figure 6-4. However, a few particle tracks discharge far from other discharge locations. Overall, the five considered HRD realisations for 2000 AD result in similar recharge and discharge areas, but there are some differences and not all realisations discharge to all the areas (Section 4.6.4 in Joyce et al. 2019).

The distributions of the calculated transport-related properties of the particle tracks that result from the facility-focussed model are wide and show substantial tailing, except for the particle-track lengths which range over less than two orders of magnitude (Section 4.6.3 in Joyce et al. 2019). For illustration, the cumulative distribution functions (CDFs) of the travel time  $t$  and the F-factor at different times are plotted in Figure 6-6. The transport-related properties change relatively little after 2000 AD. The five HRD realisations that were simulated for 2000 AD result in substantial variation of the transport-related properties, especially for the F-factor (right panel in Figure 6-6). CDFs for other transport-related properties are found in Joyce et al. (2019), including equivalent flux, equivalent flow rate, and path length. The variation is attributed to the presence of large sub-vertical fractures with depth-dependent properties that intersect the vaults in some realisations, including realisation r1, the main realisation considered in SE-SFL (Section 7.4.3). The relatively large differences between the realisations indicate that the full variability of the bedrock properties may not be captured with only five realisations; a higher number of realisations may be warranted in future safety assessments.

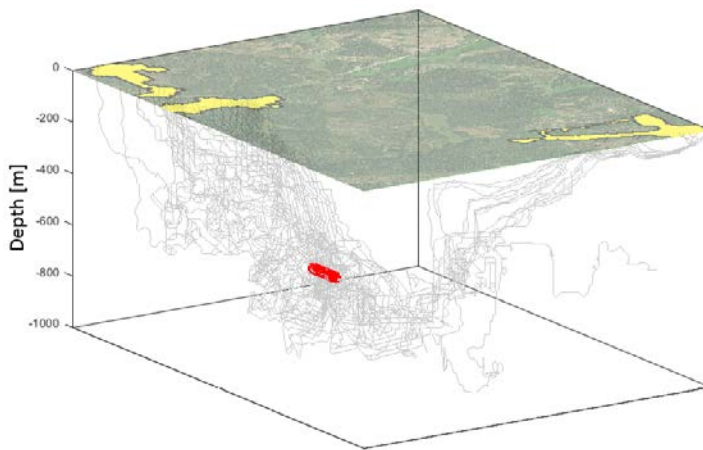


**Figure 6-5.** Subset of 100 particle tracks (grey traces) from waste vault BHA (red) to the surface. Yellow areas at the surface represent biosphere objects that are used in the biosphere modelling and into which most particles discharge. Figure identical to Figure 4-9 in the **Radionuclide transport report**.

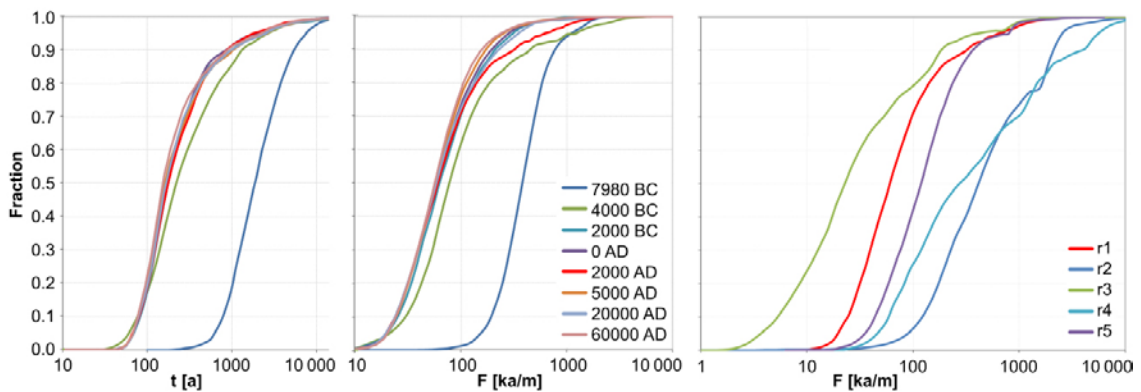


**Figure 6-6.** Distributions of travel times  $t$  (left) and flow-related transport resistances  $F$  (middle) for particles successfully reaching the model top boundary as released at the specified times, assuming no chemical reactions, and using the first HRD realisation r1, shown as normalised CDF plots with logarithmic x-axes. Flow-related transport resistance distributions for the different HRD realisations (right). Panels adapted from Figures 4-140, 4-139, and 4-144 in Joyce et al. (2019), respectively.

Possible drinking water wells located some distance away from the repository have a small effect on the particle tracks and transport-related properties (Section 4.7 in Joyce et al. 2019). Only one of the five modelled wells captured particles of water that had passed through the repository, and only 2.5 % of the total number of particles that reached the model top boundary were captured in this well.

### 6.2.6 Repository hydrological evolution

As described in Section 6.2.5, the regional hydrogeology shows only slight changes with time after 2000 AD according to the simulations. Therefore, the hydrogeological properties in the bedrock surrounding the repository are expected to be practically constant during the complete analysis period of 1 million years in the base variant. Thus, the temporal evolution of the hydrology around the vaults is determined by the hydraulic properties of the components within the repository itself. The backfill materials in BHK and BHA restrict the flow through the vaults and the waste. This is an important feature of the backfill in the two vaults, which is dictated by the safety function *low flow* in the waste vault (Section 5.2). The waste form, packaging and grout are also likely to restrict flow to some extent.

Modelling of the near-field hydrogeology has been performed to evaluate the groundwater flow through the SFL vaults and waste (Abarca et al. 2019), using an ECPM representation of the bedrock. As mentioned in Section 6.2.5, the model is coupled to the regional hydrogeology model by Joyce et al. (2019). In the near-field, a stationary flow field is calculated based on a snapshot of the regional hydrogeology simulation at 2000 AD. Boundary and initial conditions are inherited from the regional hydrogeological model, which also provides the hydraulic properties of the bedrock.

Assuming the hydraulic properties of saturated vaults at 2075 AD, the calculated total flow through the BHA vault of  $2.2 \times 10^{-2} \text{ m}^3/\text{a}$  is two orders of magnitude lower than the total flow through BHK of  $1.1 \text{ m}^3/\text{a}$  (Abarca et al. 2019). This difference correlates with the hydraulic conductivities assumed for the backfill materials, where the value for the bentonite backfill in BHA is in the order of  $1.0 \times 10^{-13} \text{ m/s}$  while that of the concrete backfill in BHK is  $8.3 \times 10^{-10} \text{ m/s}$  (Table 3-9 in Joyce et al. 2019, Table 3-2 in Abarca et al. 2019, and Section 4.3.2).

The bentonite backfill in BHA retains its hydraulic properties throughout the analysis period (see Section 6.2.9). In BHK however, groundwater will gradually leach the cement minerals in the concrete backfill, as studied in detail by Idiart and Laviña (2019), described in Section 6.2.10, and briefly summarised here since it determines the water flow. The leaching is controlled by diffusion, with a weathered zone developing at the bedrock-backfill interface, expanding inward, approaching the centre of the vault on a time scale on the order of 100 000 years. The material in the degraded zone is more permeable than the concrete initially installed and therefore affects groundwater flow through the BHK vault and waste. After the highly soluble alkali hydroxides, the first concrete mineral fraction affected by leaching is portlandite and after about 85 ka post-closure, the outermost quarter of the backfill has lost its portlandite. After portlandite dissolution and leaching, the calcium-silicate-hydrate gel (C-S-H) starts leaching out and is completely lost from the outer half of the backfill after ~700 ka.

Abarca et al. (2019) performed near-field hydrogeological modelling with a concrete degradation process discretised into three phases. The transition time points from one state to the other are chosen based on the concrete mineralogical evolution as studied by Idiart and Laviña (2019); see also Idiart and Shafei (2019) and Idiart et al. (2019a). Figure 6-7 shows the resulting flow rates, where the flow through the BHK vault increases as the permeability of the backfill increases. However, during the period when degradation is spatially limited to an outer zone of the backfill, the flow through the waste will decrease because the degraded, outer part of the backfill acts as a hydraulic cage, redirecting water around the waste instead of passing through it. The presence of a hydraulic cage in the SFR repository was shown to retard release of radionuclides from the waste domain (von Schenck 2018). When the BHK concrete backfill has degraded throughout its entire thickness, the flow increases through both the waste and the vault as a whole.

Heterogeneities in the bedrock are expected to induce local variations in the flow through the waste vaults. This is exemplified here in Figure 6-8, which shows the direction of the Darcy velocity field vectors and the permeability of the bedrock together with the magnitude of the Darcy flow inside the waste domains with intact concrete. The presence of local stochastic fractures affects the distribution of flow in the vaults.

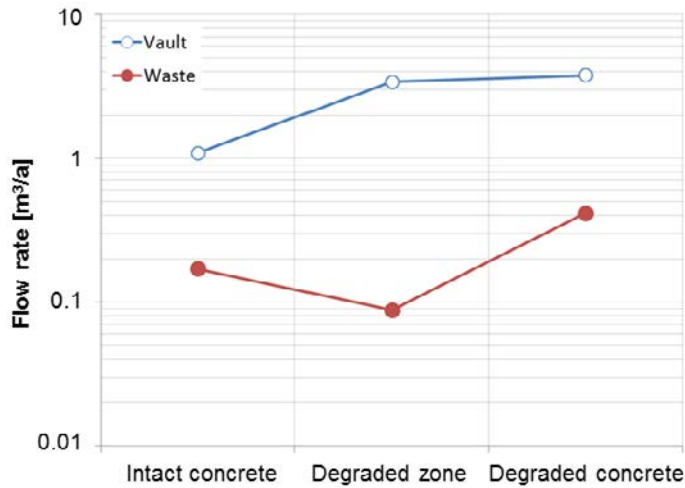


**Figure 6-7.** Average flows through the BHK vault and its waste domain during the three degradation states of the concrete backfill (data from Abarca et al. 2019).

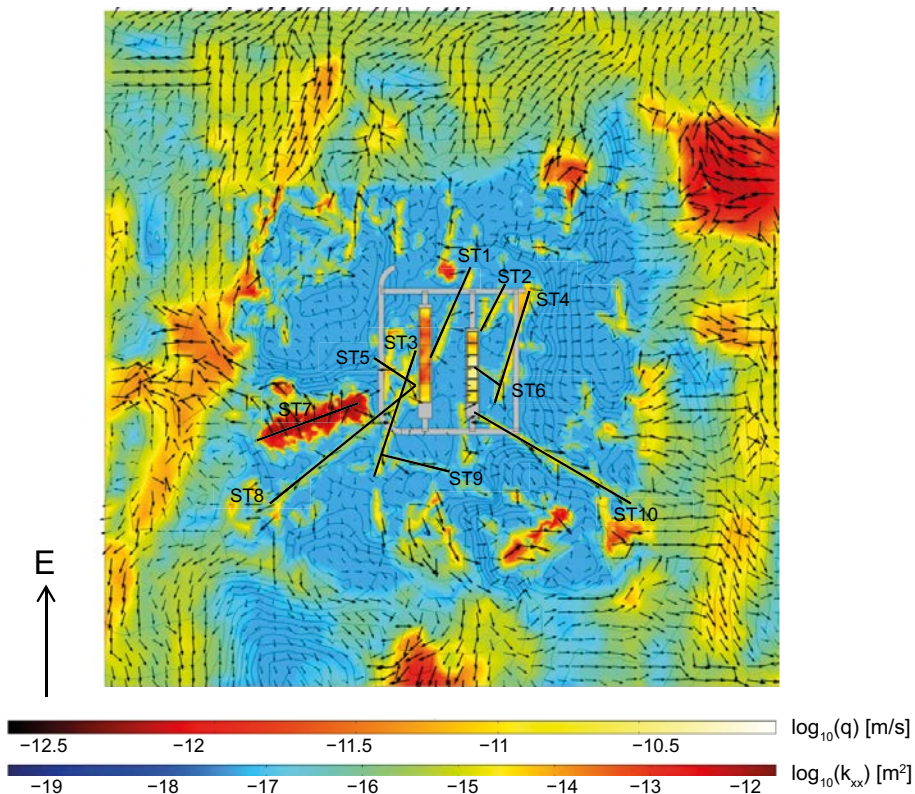


**Figure 6-8.** Hydrological properties around the repository, with Darcy velocities ( $q$ ) inside the waste control volumes (upper colour scale bar), and in the bedrock surrounding the repository at a depth of 500 m (black vector arrows in the horizontal plane). The bedrock permeability ( $k_{xx}$ ) is also indicated (lower colour scale bar). The dashed lines labelled ST1–ST10 indicate the approximate locations of stochastic fractures that have been the basis for the upscaling of the permeability that is used in the model’s ECPM representation (Figure 4-4 in Abarca et al. 2019).

At repository depth at the example location, the general direction of the flow in the bedrock is vertically downwards according to the hydrological modelling (Section 6.2.5). Thus, the groundwater flow downwards from BHK dominates over outflow to the sides of the vault (Section 4.3 in Abarca et al. 2019), which limits flow towards BHA.

### Water saturation of the vaults

The safety functions for the backfill are based on the properties of a fully water-saturated state. Backfill performance while the vault is unsaturated is not addressed, since no mass-transfer by water between the waste and the groundwater in the bedrock takes place in the unsaturated stage and activity release by gas is deemed inconsequential.

The repository hydrogeological modelling includes transient unsaturated flow simulations to estimate the time required to reach full saturation of BHA and BHK (Abarca et al. 2019). These preliminary simulations do not account for possible trapping of gas or drying-out of the surrounding bedrock during the operational phase of the repository. The resulting time evolution of the vault-average saturation is presented in Figure 6-9 and shows saturation times of 1 600–15 000 years for BHA, and 2–120 years for BHK, depending on the choice of the leakage coefficient  $\beta$ . Saturation of BHK is much faster than BHA due to the lower hydraulic resistance of concrete compared with bentonite.

During the few millennia when BHK is saturated and BHA is not, groundwater may be driven towards BHA due to pressure gradients amplified by gas production in BHK (Section 6.2.8). However, this period is relatively short compared with the full assessment time frame. The changes to hydrogeology resulting from the construction and operational phases have not been studied within SE-SFL.

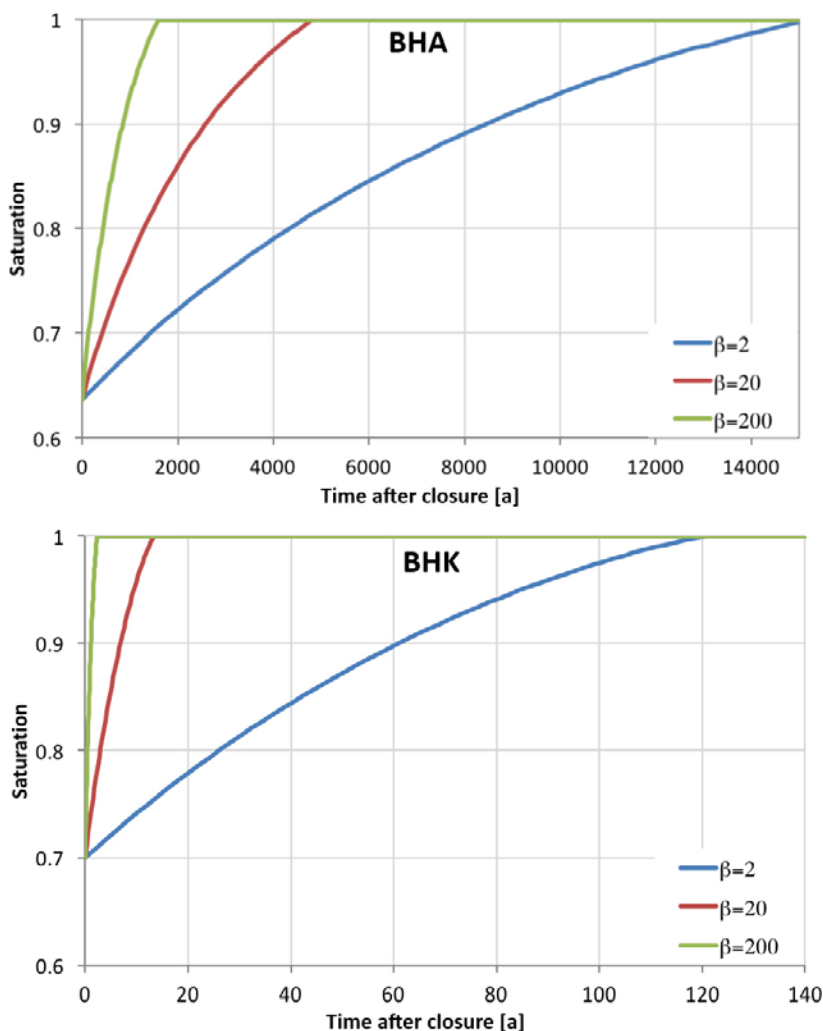


**Figure 6-9.** Temporal evolution of the volume-averaged effective saturation in BHA (top) and BHK (bottom) for leakage coefficient  $b = 2, 20$  and  $200 \text{ s/m}^3$ , assuming an initial degree of saturation of 61 % for the bentonite in BHA, and 70 % for the concrete backfill in BHK and for the waste domain in both vaults. Adapted from Figures 8-5 and 8-7 in Abarca et al. (2019).

Abarca et al. (2019) also modelled the spatial distribution of saturation during the saturation process (Figure 6-10). Results show that most of the water enters the vault through areas in contact with stochastic fractures. In BHA, the loading area (bottom right end in Figure 6-10) which is completely filled with bentonite, takes the longest time to saturate. The waste has a lower total porosity and thus saturates faster than the bentonite.

The saturation times from Abarca et al. (2019) can be compared with those for the backfill in the deposition tunnels in SR-Site, where different geometries and assumptions regarding input data and boundary conditions were investigated (Åkesson et al. 2010). Their results show a range of saturation times of 80–6000 years, which is in line with the results of Abarca et al. (2019) considering the differences in geometries. The interpretation of the results of Åkesson et al. (2010, Section 2.7) shows that the overall influence of the fractured bedrock characteristics on the resaturation time is much greater than the uncertainties related to the bentonite properties.

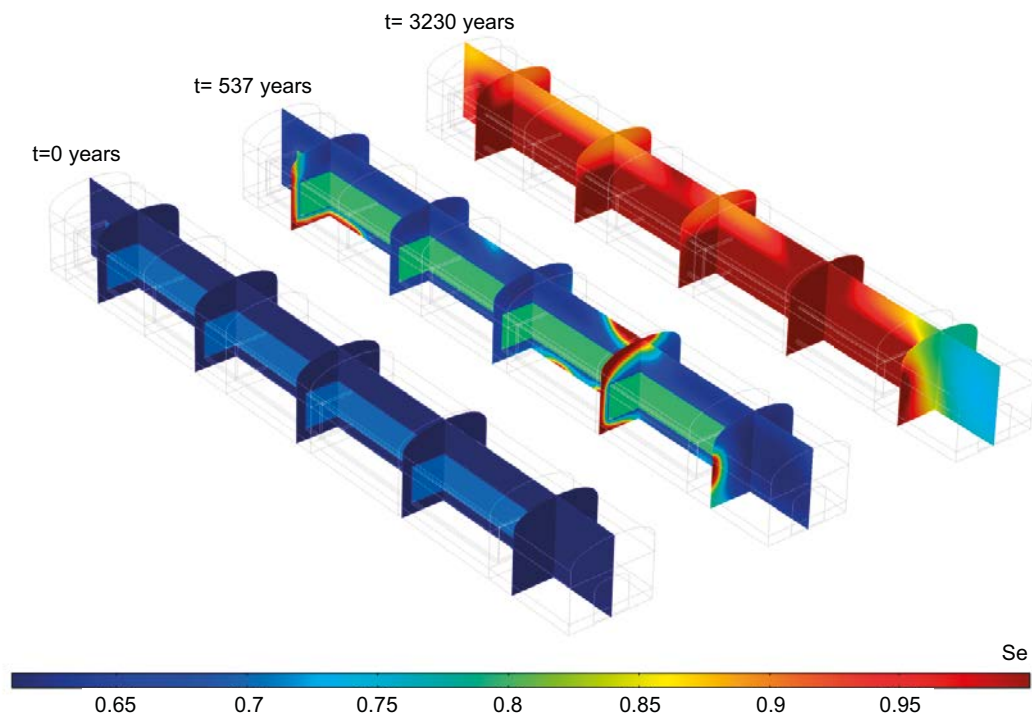


**Figure 6-10.** Saturation distribution, where red indicates 100 % saturation, in the BHA vault, at  $t = 0$ , 537, and 3 230 a after closure, for  $\beta = 20 \text{ s/m}^3$  (Abarca et al. 2019).

## 6.2.7 Geochemical evolution

The chemical properties of the groundwater in the bedrock are important since they can affect the chemical evolution in the vaults, including the pH and redox potential, which in turn affects the radionuclide release and speciation as discussed in Section 6.2.8. As described in Section 6.2.5, Joyce et al. (2019) used an ECPM model to simulate groundwater flow, transport of solutes, and a limited set of chemical reactions in the bedrock surrounding the example location. The simulations provide a detailed spatial description of the distribution of groundwater compositions. Following the work of Gimeno et al. (2010), three cases were studied in Joyce et al. (2019): Case 1 without chemical reactions; Case 2 assuming chemical equilibrium with calcite, quartz and iron(II) sulfide; and Case 3 assuming equilibration of groundwater with calcite, quartz and haematite (an iron(III) oxide mineral). Case 1 is included mostly as a reference since Cases 2 and 3 are judged more realistic. All three cases were simulated for the period from 8000 BC to 60 000 AD.

At 2000 AD, the shoreline has migrated eastwards from its initial location at 8000 BC. The glacial water present at 8000 BC in the upper part of the bedrock has to a large extent been flushed out by 2000 AD and been replaced by altered meteoric water (Case 1, Section 4.2 in Joyce et al. 2019). In the part of the bedrock that lies under the Baltic Sea, a fraction of water from the sea's earlier Littorina stage is still present. The fraction of glacial water that remains at 2000 AD is located at depths around 600–1 100 m, indicating that flushing at these depths is a rather slow process. The deep saline water is not much affected by flushing from the top and the fraction remains rather stable at depths below around 600 m. The inter-glacial water is present at depths around 600 m to 1 500 m with fractions of around 0.2 to 0.4. In some locations, the fractions have increased from the initial condition to about 0.5, which is attributed to diffusion of inter-glacial water out of the bedrock matrix (Joyce et al. 2019).

The total dissolved solids (TDS) concentration relates to the groundwater salinity and will decrease over the coming millennia according to the evolution shown in Figure 6-9, as simulated by Joyce et al. (2019). The TDS is not sensitive to the assumption of governing chemical reactions in the bedrock; Cases 2 and 3 differ only minimally from Case 1 where chemical reactions were not considered. Thus, the hydrogeological conditions are found to be more important for the time evolution of TDS than the effect of chemical reactions.

Penetration of dilute water is delayed by the retardation effect of diffusion into the bedrock matrix and by a buoyancy effect caused by the presence of water with higher salinity below repository depth (Section 4.3.2 in Joyce et al. 2019). A high salinity at great depth is expected from the understanding of the local hydrogeochemical properties and is explicitly enforced in the modelling via a boundary condition below the repository. This prevents the replacement of deep saline water with dilute water over very long time periods. These effects limit the changes in groundwater composition caused by penetration of meteoric water beyond 20 000 AD.

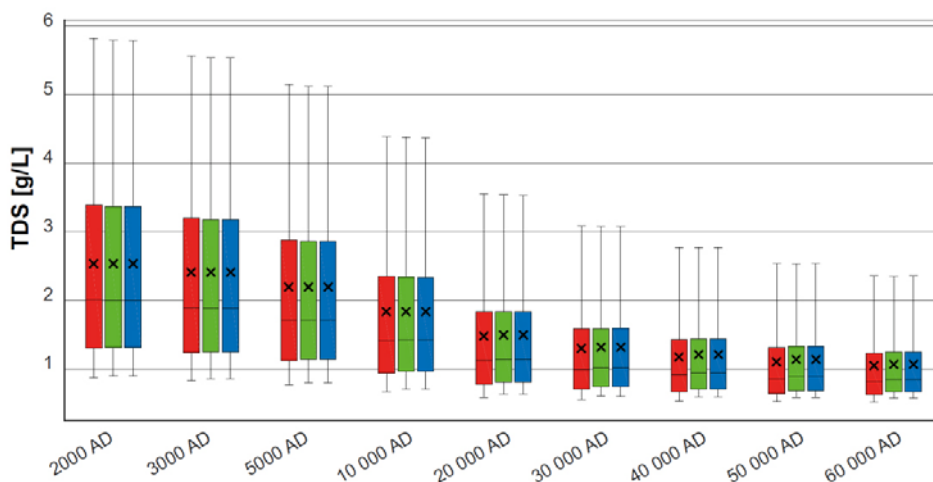


**Figure 6-11.** Time evolution of the total dissolved solids (TDS) concentration within the repository volume between elevations  $-530$  m and  $-470$  m for the three cases: Case 1 in red, no chemical reactions; Case 2 in green, equilibrium with quartz, calcite and iron sulfide; Case 3 in blue, equilibrium with quartz, calcite and hematite. The statistical measures are the median, the 25th and 75th percentiles (box), the mean (cross) and the 5th and 95th percentiles (whiskers). Taken from Figure 4-32 in Joyce et al. (2019).

A set of five DFN realisations was used in Joyce et al. (2019) to investigate the sensitivity of the results for Case 1 (without reactions) to the spatial distribution of hydraulic properties. The results, exemplified in Figure 6-12, show that the five realisations outline two distinct groups. Joyce et al. (2019) found that there is a correlation between the permeability and the modelled chemical results. Higher permeability in and around the repository volume, corresponding to low flow-related transport resistance  $F$  ( $r_1$  and  $r_3$  in the right panel of Figure 6-6) leads to more and deeper flushing of saline waters, with more fresh meteoric water entering from the top of the model.

Concentrations of important chemical components and parameters for Cases 2 and 3 are presented in detail in Joyce et al. (2019), and some of the results are reproduced here in Figure 6-13. Like the TDS concentrations, these results show that the differences between the three modelled reaction cases are in general small, even for sulfide and iron whose reactions differ between the two cases. This indicates that the hydrogeology has a larger effect than geochemistry on the groundwater chemical composition. Cases 2 and 3 differ only to a minor extent from the reaction-less Case 1, and except for iron and to some extent hydrogen sulfide (right panel of Figure 6-13), the differences between Cases 2 and 3 are minor. Even for sulfate, the differences are small, suggesting that its concentrations are mainly controlled by transport and mixing (Section 4.3.10 in Joyce et al. 2019)

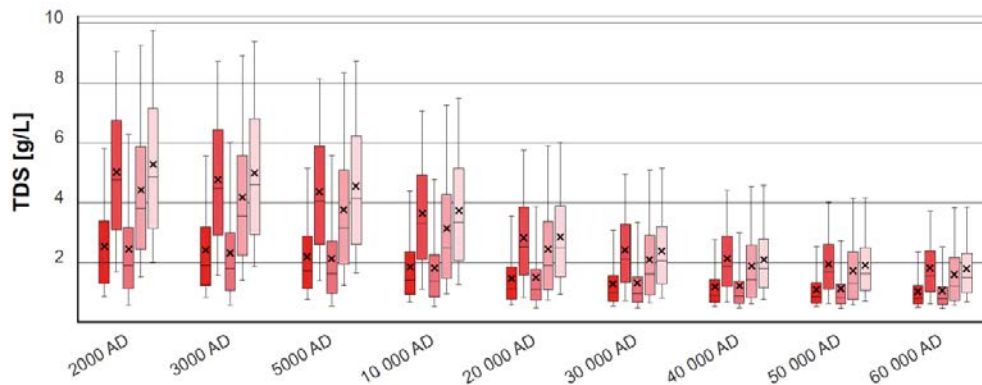


**Figure 6-12.** Statistical distributions of the time evolution of TDS concentration as compared between the five DFN realisations ( $r_0$  in dark red to  $r_5$  in light pink) of Case 1 (no chemical reactions) within the repository volume between elevations  $-530$  m and  $-470$  m. The statistical measures are the median, the 25th and 75th percentiles (box), the mean (cross) and the 5th and 95th percentiles (whiskers). Identical to Figure 4-106 in Joyce et al. (2019).

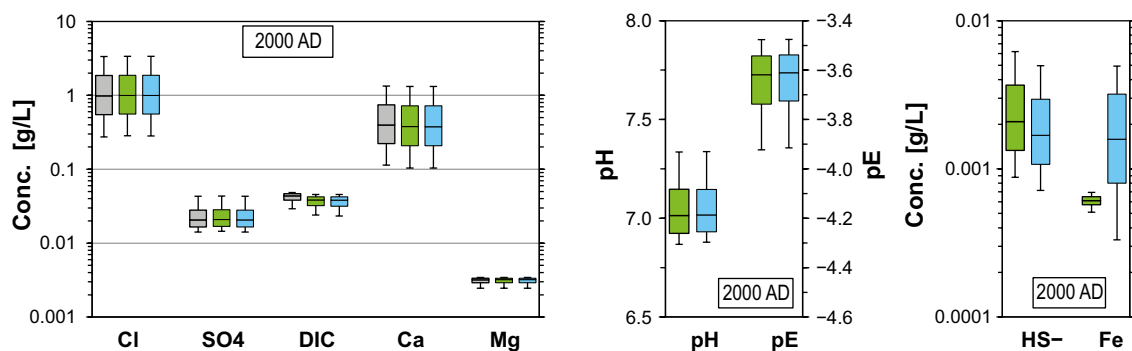


**Figure 6-13.** Groundwater chemistry at 2000 AD including concentrations of some chemical components where DIC is dissolved inorganic carbon and  $SO_4$  is sulfate (left), pH and pE values (middle), and hydrogen sulfide and iron concentrations (right) for the three cases: Case 1 in grey, without chemical reactions; Case 2 in green, equilibrium with quartz, calcite and  $FeS(s)$ ; Case 3 in blue, equilibrium with quartz, calcite and hematite. The statistical measures are the median, the 25th and 75th percentiles (box) and the 5th and 95th percentiles (whiskers). Data from Joyce et al. (2019).

The effect of the five DFN realisations on the results for important chemical components for Case 1 is exemplified in Figure 6-14. Also these results show that the five realisations outline two distinct groups related to a correlation between the DFN-realisation permeability (right panel in Figure 6-6) and the modelled chemical results, where realisations r1 and r3 give lower concentrations of chloride, sulfate and calcium, whereas DIC and Mg are somewhat higher. Full accounts of the results from the ECPM modelling and the sensitivity analyses are found in Joyce et al. (2019).

A comparison of the results shown in Figure 6-13 with the sensitivity analysis shown in Figure 6-14 leads to the conclusion that the representation of the bedrock fracture network has a large effect on the results for practically all geochemical parameters. This sensitivity to DFN realisation is large because of the relatively small volume of the repository.

The model results presented in Joyce et al. (2019) describe the groundwater chemistry in the bedrock around the repository without taking into consideration the possible effects that the repository itself may have on the hydro-geochemistry of its surroundings. Specifically, the following is not considered in SE-SFL:

- The effects of the migration of cement leachates, which could affect the migration characteristics of some radionuclides in the bedrock.
- BHK cement leachate effects on BHA. However, the groundwater flow (albeit calculated in absence of the repository) is predominantly vertical in the bedrock surrounding the repository vaults, which implies that the cement leachates from BHK move downwards and not towards the BHA vault.
- The migration of repository waters with a high content of dissolved organic matter. This might affect sulfide, iron, and redox conditions, which are of importance for the migration of redox-sensitive radionuclides.
- The migration of gases such as hydrogen, generated through corrosion in BHK, either dissolved or as gas phase (bubbles), generated within the SFL repository. A two-phase flow might influence the hydrogeology in the repository environs, and the presence of hydrogen could affect sulfide, iron, and redox conditions. Both two-phase flow and the redox conditions could affect the transport of radionuclides. In a first assessment of gas production (Silva et al. 2019a, b), the gas production in BHK was found not to influence the water flow noticeably (see further Section 6.2.8).

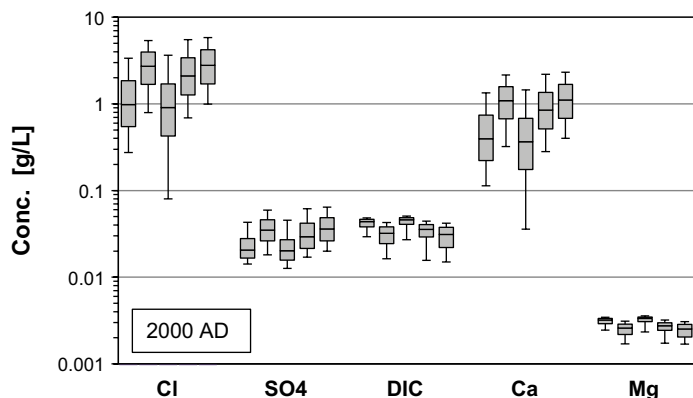


**Figure 6-14.** Concentrations of some chemical components for the five realisations of Case 1 (r1 to r5 from left to right for each component) at 2000 AD within the repository volume between elevations  $-530$  m and  $-470$  m. The statistical measures are the median, the 25th and 75th percentiles (box) and the 5th and 95th percentiles (whiskers). Data from Figures 4-107–4-111 in Joyce et al. (2019).

## 6.2.8 Evolution of the waste

This section discusses the events and processes of importance for the evolution of the waste, whereas the buffers are discussed in the following subsections. The waste is defined as the waste matrix (waste form) itself, as well as all radionuclides, any waste solidification or embedment material, the waste containers, and grout used around the waste. This section describes the reference evolution of the waste, the water composition around the waste, the speciation of radionuclides, corrosion of metals, organic complexing agents, microbiology, gas generation, heat generation, and gas transport in the waste vault. Processes in the waste also affect the surrounding concrete barriers and vice versa, so the chemical evolution of the concrete barriers is also discussed to some extent in this section, although the evolution of the barriers is described mainly in Sections 6.2.9 and 6.2.10.

The waste in SFL is described in Chapter 3.5 in the **Initial state report** and summarized in Section 4.2.1. The amounts of various materials are summarized in Section 4.2.5 and the radionuclide inventory is described in Sections 4.2.6–4.2.7.

### Waste containers

The waste packaging is described in Sections 4.2.3 and 4.2.4. In addition to the waste itself, the waste packaging materials are also of high importance for the evolution of the repository. The waste packaging contributes to the total amount of steel and concrete in the repository, resulting in a low redox potential and consistently high pH. The void inside each waste package is also of importance when assessing the concentrations of e.g. radionuclides and organic complexing agents. Tables 4-1 summarises the waste package dimensions including void volumes, and Table 4-4 shows the materials in the waste packaging for BHK and BHA.

The carbon steel packaging will to an extent hinder transport of water, gas, and radionuclides. However, the packages are not welded shut (Section 4.2.3 and 4.2.4), so some flow through them is expected, which may increase after some time due to loss of integrity caused by corrosion.

The presence of iron and steel gives rise to reducing conditions in the repository (see subsection Redox potential below), contributing to the safety function *good retention* in the waste domain, which comprises the waste form, packaging and surrounding grout (Section 5.2).

### Water composition

The inflowing groundwater has a slightly basic pH and contains significant amounts of  $\text{CO}_3^{2-}$ ,  $\text{SO}_4^{2-}$ ,  $\text{Ca}^{2+}$  and  $\text{Mg}^{2+}$ , see Section 6.2.7. When the groundwater is transported through the concrete in the waste domains, it equilibrates with the concrete and its composition changes to resemble a cement porewater, as presented in Table 6-1. The pH in the water in contact with the waste is expected to follow the concrete degradation stages as described in Section 6.2.10, i.e. the initial pH in the concrete-containing waste is set by alkali hydroxides to 13.3, which rapidly decreases to 12.5, corresponding to calcium hydroxide.

**Table 6-1. Chemical components in porewater of young and evolved cement.**

	Young cement porewater <sup>a</sup>	Evolved (leached) cement porewater <sup>b</sup>
$\text{SO}_4^{2-}$ [mg/L]	3.84	1.92
$\text{Cl}^-$ [mg/L]	2.13	71
$\text{Na}^+$ [mg/L]	644	69
$\text{K}^+$ [mg/L]	3237	3.9
$\text{Ca}^{2+}$ [mg/L]	36	800
Si as $\text{SiO}_2(\text{aq})$ [mg/L]	22.4	0.084
$\text{Al}_{\text{tot}}$ [mg/L]	1.08	0.054
$\text{OH}^-$ [mg/L]	1938	612
pH	> 13	12.5
Ionic strength [M]	0.12	0.061

<sup>a</sup> Lagerblad and Trägårdh (1994).

<sup>b</sup> Engkvist et al. (1996).

The chemical evolution of the concrete barriers over time is further described in Section 6.2.10. The key impacts of the cement on the aqueous composition are the high pH and the increased ionic strength.

### **Corrosion**

Steel is highly prevalent in SFL; the waste in BHK is made of steel and so are the waste packages in both vaults. Some waste in BHA is also expected to be metallic. The rate of steel corrosion depends on the metallurgical properties of the steel and on the chemical conditions, and depending on the value of these parameters, a wide range of corrosion rates can be observed. The most important factors are pH, the redox potential as mainly determined by the presence of oxygen (see subsection Redox potential below), and whether the material is carbon steel or stainless steel.

The metals start corroding aerobically already during (and even before) the repository operation phase, and also for a short time after closure before oxygen is depleted (Section 6.2.8). However, since these time periods are very short compared to the analysis period, and steel corrosion in air is slow, the corrosion in air before water saturation of the vaults is expected to be negligible.

Upon closure, water saturation of the vaults will occur gradually (Section 6.2.6). Oxygen from the gas phase will then dissolve in the water phase, where it will cause oxidic corrosion of any steel in contact with the rising water. The oxidic corrosion rates under alkaline (high pH) conditions was in SR-PSU assumed to be 20 nm/a for stainless and 100 nm/a for carbon steel (Tables 5-3 and 5-4 in SKB 2014h). The oxygen amounts in the vaults upon closure are only enough to corrode the outermost tens of nanometers of the steel materials (assuming corrosion distributed evenly over all steel surfaces in the vaults). Based on the oxidic corrosion rate, oxygen depletion is expected to take a few years in BHK, and even less in BHA due to oxygen adsorption on bentonite, a process found to be significant by Giroud et al. (2018).

The short, oxidic period will be followed by reducing conditions prevailing during the remainder of the assessment period (Pekala et al. 2015). During this period, steel will corrode anoxically, using water as oxidant and producing hydrogen gas. Many different oxides, hydroxides, and oxyhydroxides of iron are expected to occur as products and intermediates of anoxic steel corrosion, but eventually,  $\alpha\text{Fe}_3\text{O}_4$  (magnetite) is the predominant product because of its thermodynamic stability.

Certain corrosion products, as well as other dissolved waste materials including radionuclides, are likely to reach their solubility limit and precipitate, e.g. in the form of oxides. However, this has not been studied specifically for SE-SFL. Precipitated corrosion products can be good sorbents for radionuclides that are present in the water as cations. Many radionuclides, including Fe, Ni, and Mo, can also be co-precipitated together with corrosion products. However, the radionuclide-immobilising potential of corrosion products has not been studied specifically for SE-SFL.

Under these anoxic, alkaline conditions prevailing in SFL, the corrosion rate for carbon steel is expected to be of the order of 50 nm/a, taken from SR-PSU (SKB 2014h) and based on values from the scientific literature. For stainless steel, the corrosion rate ranges between 0.4 nm/a as reported for simulated repository conditions by Sakuragi et al. (2016) and 10 nm/a (SKB 2014h).

As concrete degrades due to chemical leaching (Section 6.2.10) the pH value will slowly decrease in the waste domain of the two vaults, down to a minimum of pH 10.5 in the inner parts of BHK (Section 6.2.10). In the literature survey by King (2008) it is consistently shown that the anoxic corrosion rate of carbon steel decreases with pH up to pH 10. The corrosion rate of carbon steel at pH 10.5 has been shown to range between 40 nm/a (Tables 3 and 4 in King 2008) and 100 nm/a (Smart et al. 2001), depending on water composition. Thus, the corrosion rates for alkaline conditions are judged to be valid over the entire assessment period of one million years. In BHA, the very low-permeability bentonite backfill may reduce the leaching rate of the waste-domain concrete, leading to a slower pH decrease, but this has not been studied within SE-SFL.

Corrosion of steel is an important process in BHK because the waste consists of metal (primarily stainless steel) with neutron-induced activity, and radionuclides are released from the metal through corrosion. Consequently, the annual activity release from BHK is determined by the corrosion rate as well as by the distribution of different types of metallic parts, the component thicknesses, their associated radionuclide inventories, and the radionuclide half-lives. The inventory of stainless steel in BHK

is larger than that of carbon steel (Table 4-3). The activity is expected to be evenly distributed within each metal part, since the neutrons that induce the activity have a penetration depth, depending on temperature and neutron energy, of several centimetres in steel, which is larger than the metal thickness. In addition to the corrosion-released activity, a remaining fraction of the initial activity in BHK that represents surface contamination is expected to be released into the water phase immediately upon water saturation.

The rate at which the metal corrodes is important also because it determines the time until all steel is corroded, at which point the redox potential in the vaults increases noticeably (subsection Redox potential below). Finally, the rate at which the metal corrodes is directly proportional to the rate at which hydrogen gas is produced (subsection Gas transport below).

### **Sorption on cementitious materials**

Cementitious materials, including the grout inside and between the waste packages and the cement in the concrete structures around the waste (Sections 4.3), are good sorbents for many chemical species. Similarly, bentonite supports sorption of many radionuclides (Section 4.3.2). A certain fraction of corresponding radionuclides, quantified by radionuclide-specific sorption coefficients  $K_d$ , will thus be immobilised by sorption in the waste domain. The cementitious materials in the waste domain of both vaults are expected to degrade similarly to the concrete backfill in BHK, as described in Section 6.2.10. The sorption coefficients change gradually as concrete degrades, since they respond to both decreasing pH and altered concrete mineralogical composition.

### **Organic complexing agents**

Complexing agents can bind radionuclides and enhance their solubility, weakening their sorption and facilitating transport out from the repository. No organic material that might form metal-organic complexes will be present in BHK, since the waste consists exclusively of metallic parts. In BHA, the characteristics of the waste are not fully specified, but the inventory of cellulose has been estimated as further discussed in Chapter 3.7 in the **Initial state report** and briefly in Section 4.5.5 herein.

Cellulose is a precursor to isosaccharinate (ISA) that is formed gradually by hydrolysis of cellulose in a  $\text{Ca}^{2+}$ -rich, alkaline environment. Soon after saturation (about 100 years), the concentration of dissolved ISA in BHA is expected to reach a value where complexation of radionuclides with ISA starts to adversely affect their sorption in the bentonite barrier (Table 3-24 in the **Initial state report**). The maximum dissolved concentration of ISA in a cementitious environment is about 20 mM, limited by the solubility of  $\text{Ca}(\text{ISA})_2$ , which is reached after about 1 000 years.

As ISA is produced, some of it will be transported out of the vault; for the SFR repository, von Schenck and Källström (2014) performed reactive transport modelling and found that about 90 % of ISA would remain in SFR after 20 000 years. ISA sorbs onto cement, which enhances its retention in the vault, but then the cement-sorbed fraction is unavailable for complexation with radionuclides (Keith-Roach et al. 2014). Furthermore, ISA degrades over time, by microbial and chemical (abiotic) means. ISA was found to be chemically stable at high pH over a period of 12 years (Glaus and Van Loon 2008). Bacterial degradation is possible under alkaline conditions (Bassil et al. 2015), but this microbial process is suppressed to negligible rates at pH values above ~11 (Section 3.5.8 in Keith-Roach et al. 2014), which holds for several hundred thousand years after closure in BHA (Section 6.2.9). The out-transport and degradation of ISA are thus limited.

Colloids, like complexing agents, have the potential to enhance radionuclide solubility. Radionuclides can associate to mobile colloids, reducing the tendency of the radionuclides to sorb and increasing their transport out of the vault. The amounts of colloids in the engineered barriers in the BHK and BHA vaults are assumed to be negligible since the concrete barriers and the concrete packaging will supply calcium ions, suppressing colloid formation (Swanton et al. 2010). Colloid formation in bentonite is also a potential mechanism for mass loss, as further discussed in Section 6.2.9.

## **Redox potential**

The evolution of the redox conditions in SFL is highly relevant for the evaluation of post-closure safety. Redox conditions influence the speciation of redox-sensitive elements such as selenium, technetium, neptunium and plutonium, and a change in oxidation state influences their solubility and sorption behaviour. The evolution of the redox conditions in SFL described here is based on a preliminary assessment by Pękala et al. (2015).

The redox potential  $E_h$  is determined by anoxic corrosion of steel by water, assumed to produce  $\text{Fe}_3\text{O}_4$  and hydrogen gas (subsection Corrosion above). This results in a reducing potential of around  $-0.8$  V so long as concrete still contains portlandite and supplies a high  $\text{pH} \geq 12.5$  (Pękala et al. 2015). Section 6.2.10 describes concrete degradation which, after about 500 000 years, has lowered the pH to about 10.5 in the inner parts of the BHK vault, directly increasing the potential to about  $-0.7$  V. These modelling results are in line with experimentally measured potentials of a  $(\text{Fe}_3\text{O}_4 + \text{Fe})$  system of around  $-0.65$  V and  $-0.6$  V at pH values around 12.5 and 10.5, respectively (Bruno et al. 2018).

After a long time, all the steel in BHK will corrode, estimated at 640 000 years after closure by Pękala et al. (2015). At this point, the redox conditions are determined by remaining materials and the potential of the incoming groundwater, which in turn depends on bedrock mineral composition. In absence of metallic Fe, the main long-term corrosion product,  $\text{Fe}_3\text{O}_4$ , could set a reducing  $E_h$  of around  $-0.4$  V based on its thermodynamic equilibrium with Fe(III). However, this oxidation reaction lacks driving force because of a lack of oxidants such as oxygen and its long-term kinetics are very slow so its redox-determining capacity is uncertain. The groundwater would set a potential in the waste domain between  $-0.30$  V and  $-0.42$  V, respectively including or excluding sulfate-sulfide and carbonate-methane equilibration (Pękala et al. 2015). Consequently, the potential after all steel has corroded is expected to be between  $-0.3$  V and  $-0.4$  V.

The same processes occur in BHA, but because of the smaller amount of metal present, the time required to corrode all the steel is shorter (Pękala et al. 2015). Minor differences in pH evolution between the BHA and BHK waste domains (Sections 6.2.9 and 6.2.10), have an additional but limited influence on the evolution of the redox potential.

## **Radionuclide speciation**

The major factors affecting radionuclide speciation are the acidity (pH), redox potential ( $E_h$ ), and concentration and type of other chemicals in the system, including the presence of complexing agents. The pH is fundamentally important as it defines the solution's balance between protons and hydroxyl ions which are crucially involved in a multitude of chemical reactions. Alkaline conditions prevail in the waste domains in SFL, due to the large amount of cementitious materials (Sections 6.2.9 and 6.2.10). A high pH increases the abundance of anionic species both through deprotonation and due to complexation with hydroxyl ligands.  $E_h$  is of critical importance for redox-sensitive elements, where the low  $E_h$  in SFL favours reduced oxidation states. A key example of a redox-sensitive element in the waste is iron, which via corrosion oxidises from Fe(0) to Fe(II) and/or Fe(III), depending on the  $E_h$  and pH conditions. Molybdenum is another important example which can be reduced from Mo(VII) as  $\text{MoO}_4^-$ , via  $\text{Mo(VI)O}_4^{2-}$ , to  $\text{Mo(IV)O}_2$ . Thermodynamic modelling is required to account for all the different interactions occurring within a complex system such as the waste vaults of SFL. The speciation control exerted by pH,  $E_h$ , dissolved ions and the presence of complexing agents is important because it determines a) the overall solubility of each element present with respect to chemical precipitation in the solution, b) the interactions of the element with surface sorption sites, and c) the potential for the species to migrate with groundwater flow.

The speciation of five elements, Se, Mo, Te, U and Pu, were studied by thermodynamic modelling specifically for SFL (Pękala et al. 2015). Aqueous Mo, a major dose-contributing radionuclide, is under all conditions expected to be present as Mo(VI) in both waste vaults and its speciation dominated by the molybdate oxy-anion ( $\text{MoO}_4^{2-}$ ). For the actinides, the  $E_h$  and pH has a less pronounced effect on speciation and thus on retardation parameters such as  $K_d$ .

## **Microbiology**

Biological processes can take place from  $-20\text{ }^{\circ}\text{C}$  up to above  $113\text{ }^{\circ}\text{C}$  where, in general, all life processes stop. Life is also possible within a wide pH range, from pH 1 up to above pH 12.

The most important limiting conditions are access to water and the high pH in the repository once it is filled with water, since most of the waste is either encapsulated in concrete/cement or at least in close contact with it. The system is buffered first with alkali hydroxides for a short time and then with portlandite (calcium hydroxide) which sustains a high pH over a long time (Water composition subsection above). It has been demonstrated that microorganisms could grow and be metabolically active under aerobic as well as anaerobic alkaline conditions, at pH 10–11 (Pedersen et al. 2004) and even higher pH (Yumoto 2007). However, since growth is slow, the number of bacteria and their metabolic activity will both be low. The main reason for this is that the pH will remain above 11 to suppress microbial growth over long time periods (Sections 2.6.9 and 2.6.10). C-14-containing organic species might be used as nutrients for methanogens but no evidence in the literature suggests that such species are metabolically active at the pH assumed in the waste. Over long timescales, the pH decreases and could potentially become low enough for methanogens to be metabolically active. However, this happens at a time scale beyond 100 000 years, hence virtually all C-14 has decayed and methanogenesis becomes irrelevant in the dose assessment.

## **Gas transport**

The main gas-generating process in the SFL waste involves hydrogen formation by anoxic corrosion of metals in the waste and containers, predominantly steel, but some aluminium is also planned for disposal to BHA (Tables 4-2 and 4-3). Metabolic activity will be low in the high-pH environment formed by concrete leachate (see Microbiology subsection above). Therefore, the transport of radionuclides transformed into gaseous form due to microbial processes is expected to be very small in both waste vaults.

Potential effects of hydrogen gas production in BHK on water-saturation conditions and the local groundwater flow were studied by Silva et al. (2019a, b). Multiphase flow modelling of the waste vault and the bedrock surrounding the vault (Silva et al. 2019a) was performed, and the model was subsequently extended to the bedrock-regolith interface (Silva et al. 2019b), accounting for the coupling between local groundwater flow and generated hydrogen and the effects of bedrock heterogeneity.

Gas generation is expected to cause an overpressure in the BHK vault of around 2 bar within the first 100 years after saturation (Silva et al. 2019a). This is somewhat slower than the timescale for water-saturation of BHK which is complete within about a decade (Section 6.2.10). The gas gradually escapes from the vault due to its buoyancy, mainly upwards but also in the direction of groundwater flow, depending on the groundwater flow rate. Bedrock fracture zones may possibly intersect the vault, serving as effective gas escape routes. Once all steel is corroded and hydrogen gas production ceases at about 600 000 years after closure, the overpressure decreases to  $\leq 0.5$  bar within about 10 000 years, depending somewhat on the hydrostatic flow conditions (Silva et al. 2019a). The hydrogen gas flux at the bedrock-regolith interface is controlled by the gas production rate and the permeability distribution of the host bedrock, suggesting a linear relationship between gas flow rates and gas production rate (Silva et al. 2019b).

In conclusion, gas generation has a negligible effect on the groundwater flow and water-saturation conditions in BHK and the bedrock surrounding the vault (Silva et al. 2019a). Moreover, the resulting overpressure is found to be sufficiently small, even in the case of very high gas production rates, to not influence the hydraulic behaviour of the concrete barriers in BHK or the groundwater flow situation (Silva et al. 2019a, b).

Gas production and transport from the BHA vault has not been studied due to the smaller amount of metal in its waste (see Figure 4-3). However, this will need to be studied for subsequent SFL safety assessments, since large overpressures might affect the bentonite buffer integrity.

## Heat generation

The metallic waste in the BHK vault will generate significant heat during the first few hundred years after repository closure (Figure 6-13, von Schenck 2018). Significantly less heat is generated by BHA waste as compared with the waste in BHK due to lower initial activity, so the heat contribution from BHA is considered negligible. Heat generation in BHK is initially dominated by the decay of Co-60. After a few hundred years, the decay of longer-lived Ni-59 and Ni-63 determines the heat release. The expected power output as function of time is shown in Figure 6-15.

The volume-averaged temperature increase due to the heat source is at most about 1 °C for the BHK waste and the concrete structure and less than 1 °C for the concrete backfill. After five hundred years, the average temperature increase is less than 0.2 °C for BHK. The increase in temperature in the bentonite backfill of BHA, due to heat transfer from BHK, is less than 0.1 °C. The temperature effect of heat-generating waste on the repository components and the surrounding bedrock is thus negligible. Therefore, the temperature in the repository is determined almost entirely by the temperature of the surrounding bedrock.

### 6.2.9 Evolution of engineered barriers in BHA

The components of the engineered barrier system of BHA are described in Section 4.3.2. The main purpose of the concrete in the waste domain is to reduce the corrosion rate due to high pH and to enhance sorption of radionuclides. The main engineered barrier in BHA is the bentonite backfill that has as its primary purpose the inhibition of advection, ensuring that transport of species between waste and bedrock is dominated by diffusive transport. A second purpose is good retention of radionuclides. These properties are articulated in the safety functions *low flow* in the waste vault and *good retention* (Section 5.2). Furthermore, bentonite can decrease microbial activity (Persson et al. 2011, Bengtsson et al. 2017), although this is not studied specifically within SE-SFL.

The evolution of the backfill is marked by two states. In the unsaturated state after repository closure, resaturation with groundwater (Figure 6-9) leads to swelling of the bentonite which leads to properties that inhibit advection and ensures good retention. Initially, local swelling by wetting from the rock may be unevenly distributed in space, potentially causing inhomogeneous swelling. However, as the swelling progresses, it results in backfill homogenisation and mechanical interactions between the backfill and the waste compartment. Subsequently, when the backfill is in the saturated state, the chemical evolution is important, including interactions with the local groundwater and pore waters of the waste compartment. Potential release of colloids to the groundwater is a further important process. In the following, these various processes and their effect on the evolution of the engineered barriers in BHA are described.

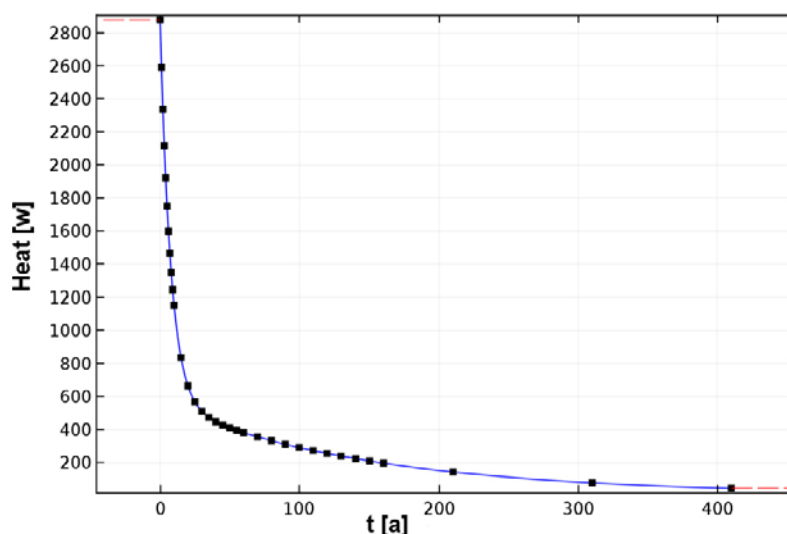


**Figure 6-15.** Power output from BHK waste as function of time. Constant extrapolation is assumed beyond 400 years.

### ***Initial evolution after closure***

During the resaturation period upon repository closure, a well-performing plug (see Section 4.3.3) is needed to ensure that the performance of the bentonite backfill and sealing is upheld, with respect to density, swelling pressure, and hydraulic conductivity. Until the backfill and sealing have developed a sufficient swelling pressure, there is a risk of piping and associated erosion effects in these components. This may lead to a lowered density in certain parts of the backfill which would affect related parameters, such as hydraulic conductivity. The swelling and related homogenisation of the backfill is crucial to fulfil performance targets related to backfill density.

### ***Piping and erosion***

Water inflow into the BHA vault will take place mainly through bedrock fractures. However, if the inflow is localised to fractures that carry more water than the swelling bentonite can adsorb, there will be a water pressure in the fracture acting on the backfill. Since the swelling bentonite is initially a gel, which increases its density with time as the water goes deeper into the bentonite, the gel may initially be too soft to stop the water inflow. The results may be piping in the bentonite, i.e. formation of a channel and a continuing water flow with associated erosion of bentonite particles. There will consequently be a competition between the swelling rate of the bentonite and the flow and erosion rate.

The mass loss and redistribution from piping and subsequent erosion has not been studied in detail in SE-SFL. However, a simple calculation is performed in Appendix 1, based on an empirical formula by Sandén and Börgesson (2010). According to this calculation, the cautiously estimated maximum loss of bentonite is about 7230 kg for piping from a single fracture. This represents a volume of ~4.7 m<sup>3</sup>, or less than 0.01 % of the total backfill volume. At the Laxemar site, it is rather likely that the inflow will come from several fractures; for 10 fractures, the global erosion would be around 16 180 kg. In general, high local erosion is worse than high global erosion, since the local effects set the limit on the ability of the bentonite backfill to swell and homogenise. Given the cautious estimate and the small fraction of bentonite mass eroded, it is considered unlikely that erosion via piping would have any significant impact on the performance of the barrier in BHA.

### ***Swelling and swelling pressure***

The swelling pressure in the bentonite is expected to seal all gaps and ensure that there is tight contact between the bedrock and the backfill, which is the state that the safety functions are based on. In order to verify that the intended conditions after swelling will be reached, it is necessary to assess carefully the swelling process with focus on four parameters: 1) backfill homogenisation, 2) mechanical interaction between the backfill and the waste compartment, 3) movement of the waste compartment inside the vault, and 4) homogenisation after loss of bentonite mass. The swelling processes have not been studied specifically for SE-SFL. This was a deliberate omission at this stage of the programme. These processes have been analysed in depth within SR-Site and reliance is placed on that analysis here, although caution must be taken due to differences in bentonite dimensions and other interacting materials (e.g. copper canister in SR-Site, concrete waste packages in SE-SFL). These processes need to be quantified specifically for SFL in future safety assessments.

Extrusion of bentonite into the bedrock fractures may to some extent block them, hindering water flow. This process is likely to occur, but only to a small extent since erosion of the buffer is slow. This process has not been studied in SE-SFL but should be considered in future safety assessments.

### ***Backfill homogenisation***

Upon saturation with water, bentonite swells and its dry density decreases if there is space to expand. Due to friction within the material, hysteresis effects, and the backfill geometric properties including bentonite pellets near the ceiling (Section 4.3.2), the swelling and homogenisation that comes with the wetting of the bentonite is not complete and there will remain density differences and swelling pressure differences in the backfill. These processes have been studied in depth within SR-Site (Åkesson et al. 2010). Although significant differences exist between the Spent Fuel Repository studied there and SFL, their analysis can be used to illustrate how these processes can be handled and give an indication about the system's behaviour. Based on the interpretation of the results of Åkesson et al. (2010), it is assumed

that there will be substantial density gradients in the backfill in BHA after completed saturation and swelling. The magnitude of the gradients has not been assessed specifically for SFL. However, since the target density is high, a well-performing backfill in the entire vault is still expected.

In addition to the variations in density arising during swelling, voids may occur because of failures to install backfill correctly, errors in the disposition of installed backfill, loss of bentonite due to piping erosion, or long-term erosion of bentonite (described below in this section). In SR-Site, homogenisation after bentonite loss was analysed in detail. Due to the difference in geometries these results are not directly applicable to the analysis of SFL. It is, however, deemed very unlikely that the quality control after installation would fail to detect an omission of several tonnes of bentonite. In conclusion, although BHA is currently assumed to resist performance reduction due to bentonite mass loss via various mechanisms, homogenisation after loss of mass needs to be considered in future assessments.

### ***Mechanical interaction between backfill and waste compartment***

Because water will enter the vault from discrete fractures in the wall, it cannot be expected that the wetting of, and the build-up of swelling pressure in, the bentonite backfill will be uniform over the entire volume. This will lead to several waste-domain-backfill mechanical interaction possibilities, depending on the main direction of water uptake and swelling:

1. Swelling from the bottom may lead to a lifting of the waste compartment and a compression of the dry pellets in the ceiling filling, an elevated final position of the waste compartment, lower bentonite density in the lower part, and higher density in the upper parts.
2. An initial water uptake and swelling in the pellets in the ceiling filling may lead to a lower final density in that part because the compressibility of the pellets is lower when saturated. This effect should, however, be limited. Swelling from the top does not move the waste compartment since it is supported by pillars but fracturing or deformation may be possible.
3. Swelling from one side would mean that the waste compartment is pushed towards the other side which then induces a shortened diffusion distance to the bedrock.
4. Because the vault is large, water is expected to enter through several fractures which could be in different locations in the vault. This means that all the processes above can go on at the same time at different locations in the vault. As a result, the waste compartment may twist and bend, possibly leading to cracks and fractures.

The mechanical interaction between the bentonite backfill and the waste compartment has not been analysed specifically for SE-SFL. However, because the waste compartment is not credited with mechanical integrity and movements are expected to be small compared with the vault dimensions, it can be justified leaving consideration of this process to future full assessments.

In addition to the effects of an uneven resaturation process, the waste compartment could sink through the bentonite and thus decrease the distance between the waste compartment and the bedrock. The granite pillars will support the waste compartment if both are intact, but the backfill swelling might break the waste compartment or tilt the pillars. Pieces of a broken waste compartment could sink between pillars. Deviatoric creep and deviatoric stresses (or shear stresses) can become problematic as the clay internal friction and cohesion decrease with time, decreasing the clay's resistance against waste-compartment sinking. However, this process was judged highly unlikely for a canister in a deposition hole in the Spent Fuel Repository (Åkesson et al. 2010). Compared with the copper canisters in the Spent Fuel Repository, the BHA waste compartment has a much lower density which decreases the probability for sinking, but on the other hand, its geometry is larger and less constrained which may increase the probability.

A more detailed and quantitative analysis of the bentonite mechanical properties will be necessary in future safety assessments.

### ***Backfill chemical evolution***

After deposition, there will be a hydraulic gradient caused by the suction in the unsaturated bentonite blocks and the hydrostatic pressure in the surrounding bedrock. After saturation of the near field, the interaction of groundwater with the bentonite backfill may result in an evolving distribution of some

aqueous species in the bentonite porewater, as well as the redistribution of accessory minerals and the cation exchanger. Altered bentonite chemistry could potentially affect sorption of radionuclides. The backfill chemistry depends on the interaction of the water-saturated bentonite with both the local groundwater and with the pore water in the waste compartment.

### **Bentonite-groundwater interaction**

During the period of bentonite saturation, advection of solutes to the bentonite porewater is the main mechanism of transport between the groundwater and the backfill. However, as the saturation slows down, diffusion becomes more important. Since there is no thermal gradient, the chemical evolution during the saturation of the bentonite backfill is expected to be modest. The ion-exchange in the bentonite will be very limited since the original material has a much higher content of cations than the saturating water. Thus, for the initial period of saturation, the actual porewater composition corresponds to a mixture between the local groundwater and porewater already present in the bentonite. Given a longer time, diffusion of species (e.g. chloride) between the backfill and the groundwater will alter the porewater composition, but this effect is expected to be small and without consequences for the barrier performance.

Once saturated, there will be diffusive exchange of species between the groundwater and the bentonite porewater, dominated by cation exchange in the bentonite. The direction of exchange is determined by the relative composition of the two waters. Assuming MX-80 bentonite and present-day Laxemar groundwater, Ca will replace Na as the dominant cation in the bentonite. Due to the large amount of porewater in the backfill and the relatively small flow of groundwater, exchange equilibrium will probably never be reached. The composition of the exchanger will have a very limited effect on the hydro-mechanical properties of the bentonite as long as the target density is maintained. In addition to the ion-change, there may be precipitation and/or dissolution of accessory minerals such as calcium carbonates and sulfates. Since there are no thermal gradients, the extent of this process is expected to be small and not affect the backfill performance. A more detailed quantification of these processes is not deemed necessary in SE-SFL, but might need to be reconsidered in a future analysis.

### **Bentonite-waste-package-pore-water interaction**

The advantageous physical properties of the backfill, e.g. high swelling pressure and low hydraulic conductivity, are determined by the ability for water uptake between the montmorillonite mineral layers (swelling) in the bentonite. However, montmorillonite can transform into other minerals of the same principal atomic structure but with less or no ability to swell in contact with groundwater. The transformation processes usually involve several basic mechanisms, which under the repository physicochemical conditions include congruent dissolution, reduction/oxidation of iron in the mineral structure, atomic substitutions in the mineral structure, octahedral layer charge elimination by small cations, and replacement of charge-compensating cations in the interlayer.

Transformation from smectite (montmorillonite) to illite, which is the most common alteration observed in natural sediments, is well documented in both nature and laboratory conditions. However, this requires high potassium concentrations and elevated temperatures of about 130 °C (Section 3.5.9 in SKB 2010e). Since the temperature will always be low in BHA, no transformation of this type is expected, even in a million-year perspective.

The stability of montmorillonite, which contains silica, depends on pH, since silica solubility increases significantly at pH above 9. The interaction between the bentonite backfill and the alkaline concrete waste compartment is thus important (Section 3.5.9 in SKB 2010e). In a study that is ongoing during the preparation of present report, the long-term (i.e. 100 000 years) stability of montmorillonite under repository conditions, i.e. at 15 °C and exposed to an alkaline plume originating from the waste domain, is modelled with a 1D description of the BHA vault cross section. The 1D reactive transport model considers both kinetically controlled and thermodynamic-equilibrium chemical reactions. Solute transport is diffusion-driven, based on a Fickian approach with a single bulk porosity. The degradation of the concrete domains determines the alkaline water interacting with the bentonite backfill. The dissolution of montmorillonite is set as a kinetically controlled reaction. The implemented dissolution considers the dependency on pH, temperature, and the proximity to thermodynamic equilibrium. In the full analysis, all chemical reactions in the cement-based materials are considered under thermodynamic equilibrium.

Preliminary results from the ongoing study are in broad agreement with simulations for the Silo in SFR with similar assumptions. The results for the Silo show that montmorillonite depletion is confined to a few decimetres next to the concrete-bentonite interface (Cronstrand 2016).

There are uncertainties in the models and assumptions used in the ongoing study which will need to be further explored in a future assessment. When the development can be quantified, the effect of the bentonite transformation on the safety functions *low flow in the waste vault* and *good retention* need to be analysed. Such an analysis is needed to be able to assess how the slowly progressing degradation of the bentonite buffer affects the flow and retention properties. The transformations take place from the bentonite-concrete interface outwards, thus the transport resistances at the bentonite-bedrock interface is probably not affected to the same degree. The montmorillonite is transformed into other minerals, and the performance of these in relation to the safety function *good retention* would also need to be evaluated to be able to draw conclusions regarding the temporal evolution of the safety functions.

### **Colloid release from backfill**

Should low-salinity water with less than a few millimolar sodium or calcium concentrations intrude through the bedrock and into bentonite clay, as can possibly happen during a prolonged temperate climate or due to glacial freshwater intrusion, colloidal-size smectite particles in the clay can form a sol and flow away. Clay can be lost and the protecting properties of the bentonite backfill can decrease, which has been described in detail in the Buffer, backfill and closure process report for the safety assessment SR-Site (Section 3.5.11 in SKB 2010e). No quantification of mass loss from colloid release from backfill has been performed in SE-SFL and such an analysis is therefore needed in future safety analyses.

### **6.2.10 Evolution of engineered barriers in BHK**

The components of the engineered barrier system of BHK are described in Section 4.3.1. Concrete is an important barrier material in both repository structures and backfill, which is articulated in the safety functions *low flow in the waste vault* and *good retention*. The concrete provides an alkaline environment in the repository that reduces the steel corrosion rate and the microbial activity. This in turn limits the release of induced activity and the production of gases. Additionally, concrete has a high sorption coefficient for many radionuclides, as described for the waste domain in Section 6.2.8. Finally, mass transport by means of advection and diffusion is limited, which is important in limiting the release of radionuclides. In this section, the long-term evolution of the concrete barriers in the base variant of the reference evolution is described. The focus is on evaluating transport-related properties of the concrete barriers, such as porosity, effective diffusivity, and hydraulic conductivity that in turn govern the ability of the barriers to retain radionuclides.

Computational modelling has been used to calculate the long-term evolution of the BHK backfill as groundwater interacts with the concrete. (Idiart and Shafei 2019, Idiart et al. 2019a, Idiart and Laviña 2019). The focus has been on evaluating properties relating to radionuclide transport such as porosity, effective diffusivity and hydraulic conductivity, as functions of time, while making a distinction between the outer and inner part of the backfill. The pH evolution has also been studied in detail, as it has a bearing on the sorption of radionuclides onto cement and affects the corrosion rate of steel. A fully coupled reactive transport modelling approach has been employed by Nardi et al. (2014), where groundwater flow evolves as hydraulic transport parameters change due to chemical processes such as dissolution and precipitation. Abarca et al. (2019) studied how the hydrological properties throughout the vault relate to concrete degradation.

### Mineralogical properties

The properties of the BHK concrete backfill change because of chemical leaching by incoming groundwater. Thus, the mineralogical composition changes with time, influencing porosity, hydraulic conductivity, and effective diffusivity in the concrete backfill. The evolution of the flow-related properties of the vaults is discussed in Section 6.2.6, including the discretisation into three stages of degradation for the flow modelling. Groundwater flow through the BHK waste is limited, and according to the hydrogeological modelling (Sections 6.2.5 and 6.2.6) it mainly flows vertically through the vault, exiting through its bottom and not towards BHA (Abarca et al. 2019). Advective travel times through the cross-section of the vault are in excess of 5000 years. Furthermore, the initial effective diffusivity in the concrete is low, limiting the extent of groundwater-concrete diffusive interactions. Consequently, the water-induced degradation of the BHK backfill will be slow.

Concrete leaching in the BHK vault starts at the concrete-backfill-bedrock interface where groundwater enters the vault. The leaching front then moves slowly through the backfill, towards the concrete structures holding the grouted waste. The degradation sequence is outlined in Figure 6-16, showing the mineral volume fractions in a 1D profile extending horizontally from the bedrock-backfill interface.

At 100 000 years after closure, degradation is limited to the outer zone where dissolution of the concrete portlandite mineral is observed to a depth of approximately 1 m from the interface (Idiart and Laviña 2019). This zone becomes more permeable and therefore conducts water around the intact inner part of the backfill (Section 6.2.6). The dissolution of portlandite and ettringite is followed by decalcification of calcium silica hydrate (C-S-H) and the dissolution of other hydrates. Calcite and hydrotalcite precipitate to some extent in the degraded zone. Portlandite completely dissolves in the outer half of the backfill after approximately 180 000 years, and in the inner half after about 340 000 years. C-S-H starts decalcifying after portlandite is depleted, although this process is even slower than portlandite dissolution. In the outer half of the backfill, C-S-H is not completely dissolved until after ~800 000 years. This is significantly longer than the concrete degradation time in the SFR repository, where all C-S-H in the 2BMA vault will be dissolved after ~60 000 years (Figure 6-27 in SKB 2015a). The main reason for this difference is that BHK is fully backfilled with concrete upon repository closure, unlike 2BMA of SFR where the macadam-based backfill will be interpenetrated by a large water volume in contact with the concrete, increasing the concrete leaching rate. After 1 million years of interaction with groundwater, the concrete backfill in BHK is almost fully degraded (Figure 6-16). Partially decalcified C-S-H is the main hydrate close to the waste domain, and calcite dominates in the rest of the concrete backfill.

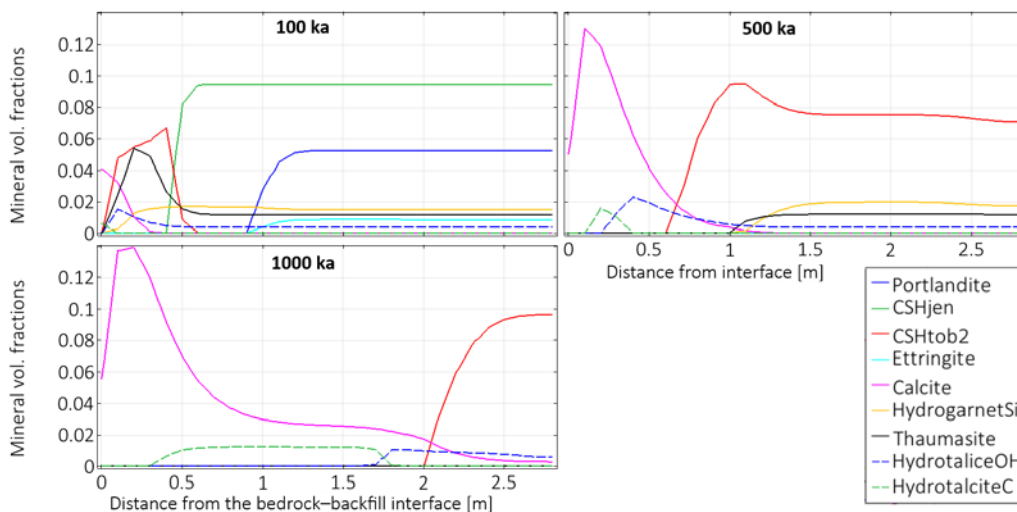


**Figure 6-16.** Mineral volume fractions after 100 000, 500 000, and 1 000 000 years after closure in a 1D profile extending horizontally from the bedrock-backfill interface. Adapted from Figure 6-2 in Idiart and Laviña (2019).

### Chemical and transport-related properties

In addition to flow-related properties, the degradation also affects the chemical environment in the vault, which affects sorption of radionuclides in the concrete backfill, as well as the corrosion rate of steel (Section 2.6.8). Figure 6-17 shows the temporal evolution of the pH of the porewater solution in the concrete backfill as a function of distance from the bedrock-concrete interface. The incoming groundwater has a pH slightly above neutral, whereas the initial pH of the concrete pore water is above 13 but within ~30 000 years decreases to 12.5 due to portlandite dissolution. Subsequent decalcifying of C-S-H phases changes the pH to approximately 10.5 at about 400 000 years after closure. This still highly basic pH value is retained in the inner parts of the backfill for the full assessment period of one million years. In addition to the backfill material, both the grout embedment and the concrete packaging contribute to the high pH in the waste domain.

The mineralogical degradation also gives rise to changes in porosity and diffusivity in the backfill material. This is shown in Figure 6-18. As a result of the dissolution process, porosity increases notably from the initial value of 0.11 to up to 0.30. The concrete mix contains an aggregate volume fraction of 0.70. Therefore, a porosity of 0.30 corresponds to a situation where all the hardened cement paste is completely removed.

Fresh groundwater flows into the BHK vault predominantly from above according to the hydrogeological modelling (Sections 6.2.5 and 6.2.6), and the top part of the backfill therefore experiences more aggressive leaching than the bottom part of the backfill where the flowing water is chemically equilibrated with the concrete (Idiart et al. 2019a). This is reflected in faster changes of porosity, diffusivity and sorption coefficients in the inflow (top) part of the backfill than in the outflow (bottom) part, although this effect was not studied by Idiart and Laviña (2019) and is thus not seen in Figure 6-18.

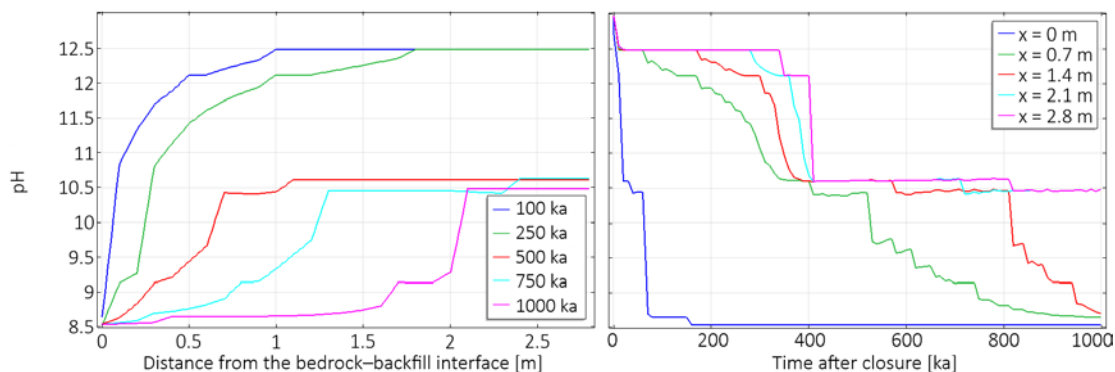


**Figure 6-17.** pH distribution in time and space of the BHK backfill, shown as a function of distance from the bedrock-backfill interface at different points in time after repository closure (left), and as a function of time for different points in space (right). Adapted from Figure 6-3 in Idiart and Laviña (2019).

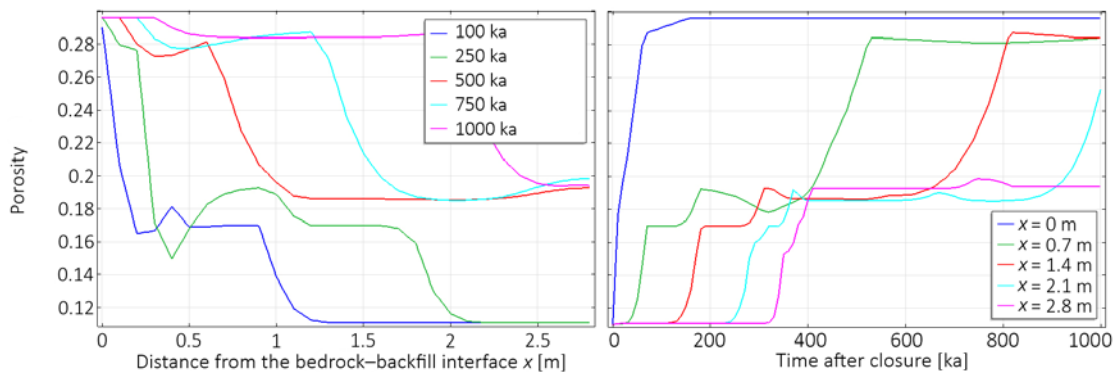


**Figure 6-18.** Porosity distribution in time and space of the BHK concrete backfill shown as a function of distance from the bedrock-backfill interface at different points in time after repository closure (left), and as a function of time for different points in space (right). Adapted from Idiart and Laviña (2019).

### **Mechanical properties**

In addition to chemical damage from leaching, the concrete backfill of BHK may also be affected by mechanical stress from the surrounding bedrock. The damage caused by hydro-chemo-mechanical processes in the concrete has been investigated by Idiart et al. (2019a). At 500 m depth, with the repository orientated in the direction of the major horizontal stress, simulations indicate that limited mechanical damage may occur internally in the concrete backfill, at the corners of the waste domain (Hakami et al. 2008). As noted in the paragraphs above, leaching of concrete by groundwater leads to chemical damage in the backfill, close to the bedrock. The degraded material is softer than intact concrete with a greater capacity to sustain deformations from the bedrock, and as such, the outer, degraded concrete has a partly protective effect on the inner, intact concrete and waste domain.

The presence of sufficiently large amounts of sulfate in groundwater may trigger additional chemo-mechanical degradation in concrete. Sulfate ions react with calcium aluminates in the cement paste leading to the formation of expansive ettringite and gypsum in the bulk material, accompanied by a reduction in the total porosity (Lothenbach et al. 2012). In the event of substantial expansion, the concrete structure could be severely cracked and spalled, with a negative impact on the transport properties and degradation rate (Brown and Taylor 1999, Idiart et al. 2011). Sulfate concentrations of up to 6 mM have been measured in boreholes at a depth of 500 m in the Laxemar area (Kalinowski 2009). According to the simulations of Idiart et al. (2019a), this concentration is sufficiently high to cause ettringite-induced chemo-mechanical degradation, with the possible risk of a significantly increased hydraulic conductivity and diffusion coefficient, locally but across the entire barrier thickness, within 14 500 years. However, the results are associated with high uncertainties due to conservative assumptions, including the choice of a conservative mechanical-damage model. Furthermore, the porosity decrease due to ettringite is partly compensated by a porosity increase due to mineral leaching. A reduction in the overall concrete leaching rate due to ettringite formation is possible but has not been quantified within SE-SFL.

#### **6.2.11 Evolution of plugs and other closure components**

The closure components are the bentonite seals of the waste vaults, the plugs, and the backfill of the tunnel system with crushed rock (Section 4.3.3). The bentonite seals and plugs serve to limit groundwater flow through the vaults, whereas the tunnel plug keeps the sealing material in place during the period after vault backfilling but before transport-tunnel backfilling is complete. The evolution of the crushed rock is expected to have negligible impact on the repository performance and is therefore not analysed further in SE-SFL. The evolution of the bentonite seal will be similar to that of the bentonite backfill in the vault, except that it is only in contact with concrete at the end where the plug is installed. The evolution of the seal is therefore expected to be similar to that for bentonite described in Section 6.2.9.

The closure-component solution is in accordance with previous investigations and concepts developed by SKB for the Spent Fuel Repository (Luterkort et al. 2012). The evolution of the plugs has not been specifically studied in SE-SFL. However, since the design is assumed to be similar to the design for the Spent Fuel Repository, the assessment presented in Åkesson et al. (2010) should be valid.

### **6.3 Increased greenhouse effect variant of the reference evolution**

The *base variant* of the reference evolution described an evolution of the repository and its environs under unchanging present-day climate conditions. The *increased greenhouse effect variant* includes the effect of global warming, resulting from anthropogenic influence on climate combined with natural climate variability (see Section 4.2 in the **Climate report**). This variant involves a climate development at Laxemar with an initially considerably warmer and wetter future climate compared with the present situation, followed by present-day climate conditions.

### 6.3.1 Evolution of external conditions

The *increased greenhouse effect variant* of the reference evolution follows from the reference external conditions of the *increased greenhouse effect climate case* (Section 4.2 in the **Climate report**). This climate case corresponds to the IPCC intermediate-emissions scenario RCP4.5 in which radiative forcing is stabilised shortly after 2100 AD, assuming a future with relatively ambitious reductions in carbon-dioxide emissions (Section 4.2 in the **Climate report**). To this end, it assumes temperate climate conditions with a considerably warmer and wetter climate than at present during the first 23 000 years after closure. After 25 075 AD, and for the remaining part of the analysis period of one million years, present-day temperate climate conditions are assumed.

As described in Section 2.5.3, the future climate developments chosen for SE-SFL are intentionally simplified. The temperature and precipitation increase for the *increased greenhouse effect climate case* is implemented using a simplified step function where the mean annual near-surface air temperature is instantaneously increased by 2.6 °C around 2100 AD (Section 4.2 in the **Climate report**). The resulting elevated temperature of +9.0 °C is then kept constant until year 25 075 AD, after which the temperature is lowered to the present-day temperature (Figure 6-19). During the period of increased temperature, the precipitation increases by 20–30 % as compared with the present.

In the *increased greenhouse effect climate case*, the initial future time period includes a rising sea level caused by the warming climate (Section 4.2 in the **Climate report**). The sea-level rise is a result of melting ice sheets and glaciers, thermal expansion of warming ocean water, and by gravitational and rotational effects associated with the ice-sheet melt. However, even if this sea-level rise affects the coast-line of the Laxemar region, the area above SFL will not be submerged under the Baltic Sea in the *increased greenhouse effect variant* of the reference evolution since this area constitutes an elevated part of the Laxemar landscape and is subject to ongoing regressive shoreline displacement (Section 4.2 in the **Climate report**).

A climate evolution with temperate, albeit varying, climate conditions for the coming one million years is considered unrealistic. More realistically, present human greenhouse-gas emissions are likely to cause an air temperature increase at Laxemar with a maximum occurring around 3000 AD. Thus, the temperature could get even higher, than implemented in this variant which implements a simplified temperature increase over a shorter period. After that, the temperature is likely to slowly return to lower values over many millennia. Glaciation is eventually possible but will occur later than in the *base variant*. Compared with the realistic climate evolution, this simplified climate variant thus entails a somewhat lower maximum temperature but it extends over a longer period of time, which for instance allows for a longer period of infiltration of dilute meteoric water. As described in Section 2.5.3, the results of the SE-SFL evaluation will serve as basis for coming safety assessments that will include the definition of a full set of future climate developments describing a more complete climate variability on long and short timescales.

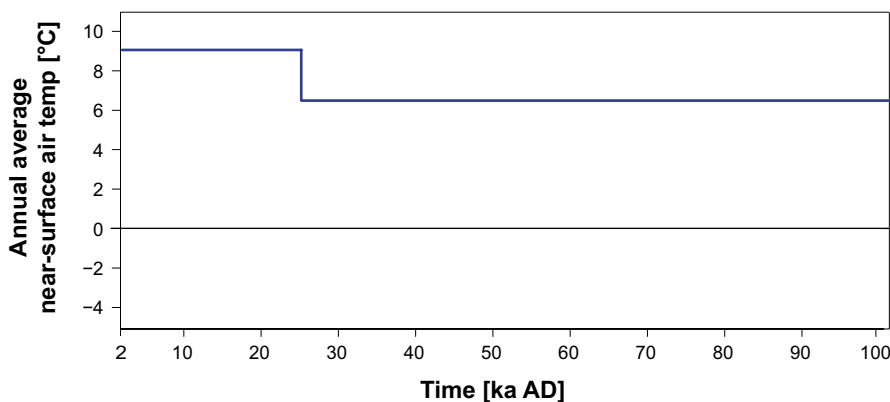


**Figure 6-19.** Evolution of annual average air temperature for the first 100 000 years of the SE-SFL increased greenhouse effect climate case. Reproduced from Figure 4-2 in the **Climate report**.

### 6.3.2 Development of surface systems

Most properties of the various types of considered agricultural ecosystems are expected to be marginally affected by a moderate change in regional climate (Chapter 4 in SKB 2014f). Moreover, the expected effect of warmer-climate plant- and crop-related parameters (e.g. biomass, net primary production and leaf area index) has small effects on the calculated dose (Section 10-6 in SKB 2014f). Precipitation is predicted to increase more during the colder season than during the warmer season. Due to increased temperatures and associated evapotranspiration, the runoff decreases during summer, whereas its annual mean is predicted to change only slightly in the Laxemar area (Persson et al. 2015). Similar results are reported by Losjö et al. (1999) for the neighbouring Äspö area, assuming a somewhat warmer and slightly less wet climate than for SE-SFL. Consequently, in a warmer climate where precipitation does not compensate for higher evapotranspiration during the vegetation period, the plant water deficit will increase.

The increased water demand of the plants can either be supplied by an increased groundwater uptake through capillary rise, or it can be supplied by irrigation water. The irrigation water can be taken either from surface water or groundwater, and the effect of both was studied by Grolander and Jaeschke (2019). Surface water in the form of streams is readily available in the region and is thus expected as the likely irrigation-water source. This climate variant includes an increased atmospheric concentration of stable CO<sub>2</sub>, which can stimulate photosynthesis and possibly decrease plant uptake of carbon from groundwater, including C-14.

Possible effects on surface systems of more frequent extreme weather, including storms and surges, are not included in this reference evolution variant.

### 6.3.3 Thermal evolution

The increased air temperature during the initial period of this variant of the reference evolution results in slightly increased bedrock temperatures. The effect of the increased air temperature on the bedrock temperature is, however, not further analysed in SE-SFL. As described in Section 6.2.3, the temperature follows a linear dependence on depth into the bedrock; a change in surface temperature of a few degrees is judged to be of negligible significance for the performance of the repository at its depth of 500 m.

### 6.3.4 Mechanical evolution

During the *increased greenhouse effect variant*, the host bedrock of the SFL repository will be subjected to a higher air temperature and higher amount of precipitation according to Section 6.3.1. The thermally induced load in the host bedrock of the SFL repository due to an increase of the air temperature will only marginally affect the *in-situ* stress conditions of the bedrock mass. The higher amount of precipitation is not likely to affect the mechanical evolution of the bedrock mass either. Therefore, the results of the mechanical evolution of the host bedrock for the *base variant* as described in Section 6.2.4 are assumed to be the same for the *increased greenhouse effect variant*.

### 6.3.5 Regional hydrogeological evolution

Increased irrigation as discussed in Section 6.3.2 is associated with water pumping or withdrawal from surface waters. Pumping would have consequences for the hydrogeology, leading to local groundwater drawdown at the pumping wells during the growing season. For the mean annual groundwater flows at repository depth, the effects are judged to be insignificant, and changes in irrigation are therefore not considered in the hydrogeological reference evolution. Irrigation can, however, affect the relative importance of different exposure pathways for humans.

The hydrogeological modelling of Joyce et al. (2019) assumes steady-state groundwater flow at the different time slices, which therefore represent mean values over several years. The small future changes in the annual runoff predicted by Persson et al. (2015) indicate small changes in the mean annual groundwater flows, given that surface water flows in the Swedish setting generally are controlled by groundwater inputs.

A limited decrease in total groundwater recharge is expected in a warmer and wetter climate, due to decreased snow accumulation and thus of spring snowmelt. Calculations by Losjö et al. (1999) predict a 10 % decrease in recharge for a climate that is slightly warmer and slightly less wet than assumed in the *increased greenhouse effect variant*. The effect of the warmer and wetter climate on groundwater flows is thus predicted to be small. Therefore, the results for groundwater flows for present-day climate conditions as described in section 6.2.5 are judged to be valid also for the *increased greenhouse effect variant*. Also, increases in air temperatures have such a small effect on the groundwater temperature that changes in groundwater density and viscosity are negligible.

### **6.3.6 Repository hydrological evolution**

The repository hydrology for present-day climate conditions as described in Section 6.2.6 is assumed to be valid also for the *increased greenhouse effect variant*, given that the regional hydrogeological evolution is judged to be similar to the base variant of the reference evolution (Section 6.3.5).

### **6.3.7 Geochemical evolution**

The hydrochemical evolution is closely linked to the hydrogeology as is indicated by the modelling results of Joyce et al. (2019) that are described in Section 6.2.7. The increased air temperature that is assumed to prevail until 23 000 years after closure is judged to have only a minor effect on the groundwater flow (Section 6.3.5). Therefore, it is expected that the hydrochemical conditions will also evolve in a similar way as modelled for the *base variant* of the reference evolution. Consequently, no separate hydrochemical modelling is carried out for the *increased greenhouse effect variant* of the reference evolution.

### **6.3.8 Evolution of the waste**

As noted in Section 6.3.3, the temperature depends linearly on depth. Changes in temperature generally affect chemical processes, including corrosion, complexation, sorption, speciation, and solubility. However, the temperature dependence is very weak for all such processes relevant in SFL, so the minor temperature differences that may arise in the repository would have negligible effects on the chemical evolution of the waste. Furthermore, the groundwater chemistry in the *increased greenhouse effect variant* is similar to that in the *base variant* (Section 6.3.7). Thus, the evolution as described in Section 6.2.8 is deemed applicable also to this variant of the reference evolution.

### **6.3.9 Evolution of engineered barriers in BHA**

The evolution of the BHA barriers during a period of increased greenhouse effect is not expected to deviate from the evolution described in the base variant, since the hydrogeological and hydrochemical evolutions are judged to be similar. Possible effects of more dilute groundwater, i.e. bentonite colloid release from the backfill, are described in in Section 6.2.9.

### **6.3.10 Evolution of engineered barriers in BHK**

The repository hydrogeology for the *increased greenhouse effect variant* is expected to be the same as for present-day climate conditions (see Section 6.3.6). Furthermore, the bedrock hydrogeochemical conditions are expected to be largely unaffected (see Section 6.3.7). Simulations of the hydro-chemical degradation of concrete in BHK have found only minor effects when exposing the concrete to more dilute groundwater (Idiart and Shafei 2019). As a consequence, the evolution of the concrete backfill in BHK described in Section 6.2.10 applies also for the *increased greenhouse effect variant*.

### **6.3.11 Evolution of plugs and other closure components**

The evolution of the plugs and other closure compartments is expected to be the same as in the base variant of the reference evolution (Section 6.2.11), given that the evolution of the engineered barriers is not expected to change either in BHA or in BHK.

## 6.4 Simplified glacial cycle variant of the reference evolution

The *base variant* of the reference evolution described an evolution of the repository and its environs under unchanging present-day climate conditions whereas the *increased greenhouse effect variant* included the effect of global warming. The *simplified glacial cycle variant* of the reference evolution includes simplified glacial-cycle cold-climate conditions, manifested through lower air temperatures, permafrost growth, and ice-sheet overridding at the Laxemar site. The ice sheet induces subsidence, so the glacial period is followed by submerged conditions in which the site of the SFL is covered by sea.

As with the other two variants of the reference evolution, the *simplified glacial cycle variant* represents a hypothetical situation, defined in a simplified manner and subsequently evaluated with respect to post-closure safety of the repository.

### 6.4.1 Evolution of external conditions

The *simplified glacial cycle variant* of the reference evolution follows from the reference external conditions of the *simplified glacial cycle climate case* which assumes that an early period of periglacial climate domain, with permafrost at the site, occurs ~17 000 years after repository closure (Section 4.3 in the **Climate report**). This time corresponds to the next future period when the solar radiation will be at a minimum at high northern latitudes. A second period of periglacial conditions starts ~50 000 years after repository closure, again corresponding to a second period of low summer solar irradiation, which is followed by a period of glacial climate, with an ice sheet overridding the repository site. During the glacial period, the ice sheet is assumed to grow thick enough to result in substantial isostatic bedrock depression, identical to the situation reconstructed for the Laxemar site for the last stadial period of the Weichselian glacial cycle around 20 000 years ago (during Marine Isotope Stage 2) in SR-Can (SKB 2006c). The reconstructed maximum ice-sheet thickness over Laxemar during this period is almost 2 500 m, resulting in isostatic depression and associated submerged conditions following deglaciation of the site. This sequence of events is illustrated in Figure 6-20, including the shoreline displacement and ice-sheet thickness.

As in the *increased greenhouse effect variant*, the changes in annual mean temperature in the *simplified glacial cycle variant* are also implemented as a simplified step function. The stepwise climate description is chosen to match the simplistic assumptions made in the calculations of landscape development. The air temperature evolution of this climate case is illustrated in Figure 6-21.

### 6.4.2 Development of surface systems

The yearly vegetation period in the periglacial domain is short. Nevertheless, primary production may be high in some environments, e.g. in shallow lakes (Andersson 2010). The terrestrial vegetation consists of sedges, herbs, and shrubs. At more exposed and drier localities, lichens dominate, whereas wet ground is dominated by mosses. The precipitation will likely be lower than during temperate conditions, due to limited evapotranspiration (Kjellström et al. 2009). The low evapotranspiration means that wet ground is prevalent, because surplus water is unable to infiltrate into the ground (French 2007, Bosson et al. 2010). This may result in larger areas of wetlands compared with a temperate climate but, on the other hand, the peat formation rate is lower, partly because the terrestrial plant productivity is low. A short and colder vegetation period in combination with lower precipitation make agricultural practise very difficult and is therefore disregarded under permafrost conditions (Löfgren 2010).

Taliks are unfrozen areas in permafrost regions, often occurring under lakes or rivers (see Hartikainen et al. 2010). Taliks, which are unfrozen throughout the entire permafrost layer, are the only spots in the periglacial landscape through which radionuclides released from the repository can be transported to the surface, and only if they are through taliks which are open (unfrozen) both at their top and bottom ends. Given that lakes and streams are often locations for human settlement and land use, taliks can potentially be locations where humans are exposed to radionuclides during periods of periglacial conditions. However, the generally low food productivity in the permafrost region requires utilisation of a larger area to supply the resources needed by even a small community, which means that radionuclide discharge through a talik may affect a comparatively small part of the food consumed by humans living in the talik area.

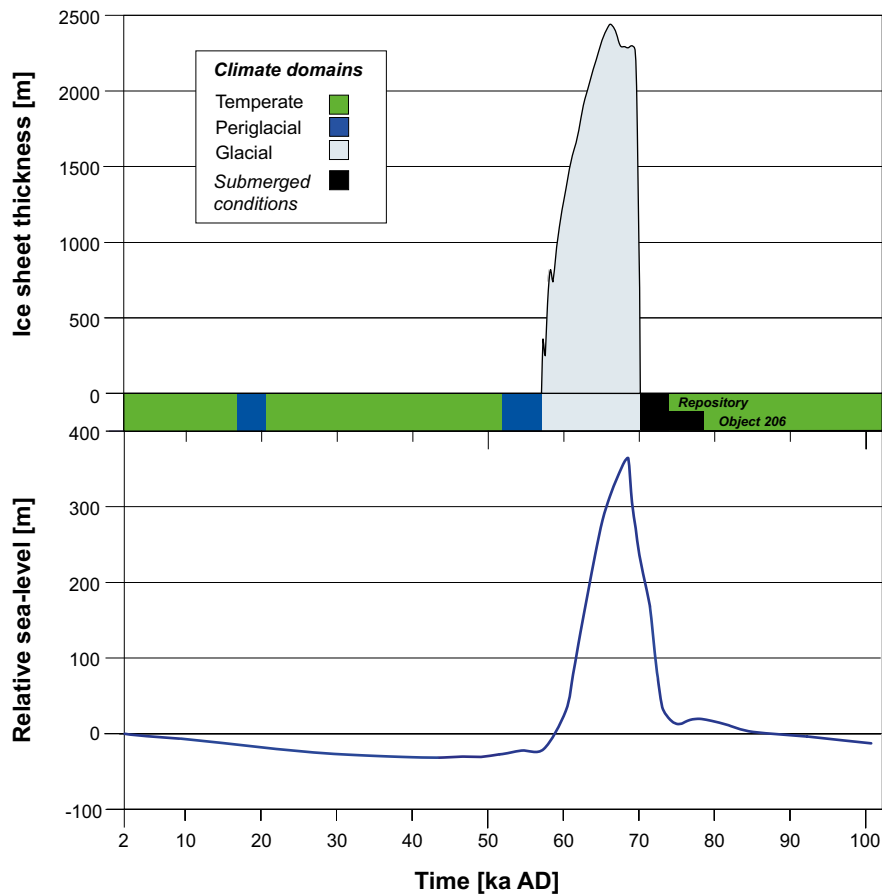


**Figure 6-20.** Evolution of climate and climate-related conditions 100 000 years into the future for the simplified glacial cycle climate case for Laxemar, shown as a succession of climate domains and submerged periods (top panel). The durations of the glacial climate domain and the subsequent submerged conditions are derived from the glacial maximum stadial (corresponding to MIS 2) in the Laxemar Reference glacial cycle of SR-Can (SKB 2006c). The submerged period following deglaciation shows the duration of water-covered conditions for the locally elevated (21.5 m above present sea level) area immediately above the repository and for biosphere object 206 which receives most of the discharge from the repository. The relative sea-level curve (bottom panel) has its zero line at the present sea level. In SE-SFL, the evolution from 2000 AD to 102 000 AD is repeated every 100 000 years until one million years after repository closure to represent the effects of repeated Late Quaternary glacial–interglacial cycles. Reproduced from Figure 4-3 in the *Climate report*.

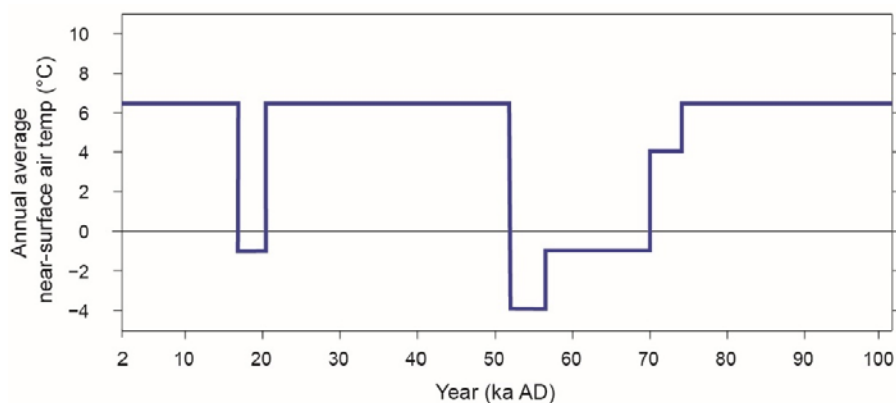


**Figure 6-21.** Evolution of annual average air temperature for the first 100 000 years of the SE-SFL simplified glacial cycle climate case. The figure shows the temperature evolution for the area above the repository. Reproduced from Figure 4-4 in the *Climate report*.

### 6.4.3 Thermal evolution

The decreasing temperature and, in particular, the presence of permafrost and perennially frozen ground may impact the backfill and closure-component materials. Since the *simplified glacial cycle climate case* is based on the reconstruction of the last glacial–interglacial cycle, the maximum permafrost depth in the reconstruction is taken as the maximum depth in this climate case in SE-SFL. SKB (2006c) concluded that the maximum permafrost and frozen ground depth at Forsmark and Laxemar occurs prior to the first major glacial advance, at about 50 ka after closure. At that time, the modelled permafrost depth reaches about 250 m at Forsmark and about 160 m at Laxemar. The frozen depth is, at the same time, a few tens of metres to a few metres shallower. More recent modelling of Forsmark (Hartikainen et al. 2010) has confirmed the maximum depth of about 250 metres for the reconstruction of the last glacial–interglacial cycle in Forsmark. Thus, freezing is excluded at the repository example location, at the 500 m depth evaluated in SE-SFL.

### 6.4.4 Mechanical evolution

In the event of a glacial cycle, the host bedrock of the SFL repository will experience variations in the mechanical load to which it is subjected, both through the additional weight of ice sheet and through the flexural response of the Earth’s lithosphere (Lund et al. 2009). The flexure of the lithosphere will induce horizontal stresses of the same magnitude as the vertical stress due to the weight of the ice. In addition to the increased stresses, the ice sheet will increase the hydrostatic pressure in the bedrock below the ice.

A key factor in the assessment of the mechanical evolution of the host bedrock during a glacial cycle is the magnitude of the glacially induced pore pressures, since the stress-modelling results are sensitive to assumptions regarding these magnitudes. The temporal evolution of the glacially induced principal stresses at 500 m depth at Laxemar, as well as the evolution of the ice-sheet thickness, is shown in Figure 6-22 (Hökmark et al. 2010). There are only marginal variations of the glacial-load-induced stresses in the upper 1 km of the bedrock, and the values presented in Figure 6-22 are assumed to be valid throughout the 0–1 km interval.

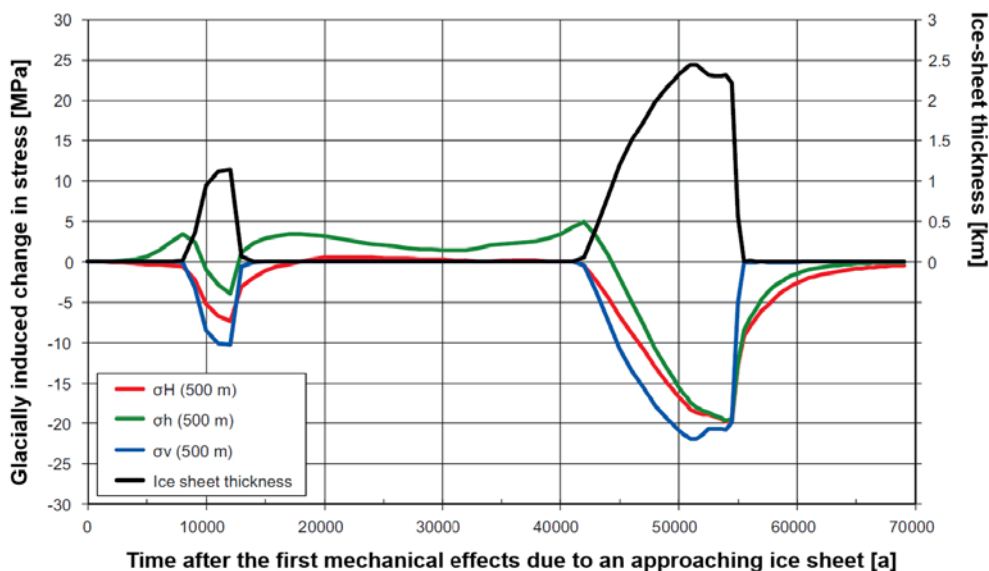


**Figure 6-22.** Development of glacially induced changes in the three principal stresses at 500 m depth obtained from ice-crust-mantle analyses (Lund et al. 2009), responding to the ice sheet thickness during the reference glacial cycle at Laxemar.  $\sigma_v$  (blue) is the vertical stress and  $\sigma_h$  (green) and  $\sigma_H$  (red) are the smallest and largest horizontal stresses, respectively. Note that the x-axis does not represent absolute time but starts when the first stresses appear according to the reference glacial cycle. Figure adapted from Figure I-7 in Hökmark et al. (2010).

The results of the assessment of the mechanical evolution of the host bedrock during a glacial cycle are typically grouped into three categories: stress-induced transmissivity changes, hydraulic jacking, and stability of fractures. None of these processes have been studied specifically for SE-SFL, but they will need to be quantified for future safety analyses.

#### 6.4.5 Regional hydrogeological evolution

The climate evolution in the *simplified glacial cycle variant* includes periods of temperate, periglacial, and glacial conditions (Section 4.3 in the **Climate report** and Section 6.4.1), where the future evolution is reconstructed from the last glacial cycle in Laxemar. The evolution of the hydrogeological conditions is closely linked to the climate evolution of these different climate periods. The hydrogeology of a present-day temperate climate as modelled by Joyce et al. (2019) and described in Section 6.2.5 is applicable for the temperate period of the *simplified glacial cycle variant*, and in particular the groundwater flow results for 2000 AD are assumed valid for the terrestrial (non-submerged) periods when temperate conditions govern the site.

For the periglacial, glacial, and submerged periods, results from previous detailed modelling studies on the effect of permafrost and glaciation on the hydrogeology at the Laxemar and Forsmark sites (Vidstrand et al. 2010a, b, 2013, 2014a, b) are used as input for SE-SFL. During permafrost conditions, the ground is frozen to a certain depth, below which unfrozen bedrock is encountered. In SE-SFL, the repository is assumed to be located deep enough to always reside in the unfrozen bedrock (Section 6.4.3). In frozen soil and bedrock, advective groundwater flow is negligible. However, during periglacial conditions, significant flow may occur in some unfrozen parts of the bedrock, which in certain cases can lead to local water flow even greater than under temperate conditions. Such flow could recharge from beneath a local ice sheet and discharge into taliks if present in the landscape beyond the margin of the ice sheet, as shown in Figure 6-23. Permafrost growth may lead to salt freezing out and therefore to a temporarily higher salinity in liquid water inclusions or beneath the frozen ground (Section 6.4.7). However, Hartikainen et al. (2010, Section 5.1) found this effect to be small in Forsmark, and it is judged inconsequential for the groundwater flow in SE-SFL.

According to the reconstruction of the Weichselian glacial cycle (SKB 2006c, Section 4.2.1), Laxemar is covered by warm-based ice for most of the glacial periods. Cold-based conditions occur only when the ice sheet advances over areas with permafrost and only in the region closest to the margin (Figure 6-23). This situation is included in the description of the evolution for the *simplified glacial cycle variant* of the reference evolution. During warm-based (wet-bed) glacial conditions, the gradient of the ice-sheet surface and the basal conditions influence the groundwater flow pattern and magnitude. In the cold-based regions closest to the ice-sheet margin, groundwater recharge is negligible; however, recharge still occurs in the warm-based areas farther away from the margin (Figure 6-23). The Weichselian ice-sheet reconstruction shows that compared with during the ice-sheet retreat, the ice-front profile is steeper during advance, increasing groundwater recharge and overall flow (Section 4.5 in the **Climate report**, Appendix 2 in SKB 2010b). At the time of peak glaciation, the ice-sheet gradients are generally expected to be low. During submerged conditions, the groundwater flow becomes very low due to the low hydraulic head gradients.

#### **Groundwater flow rate variation during glacial cycles**

The groundwater flow *pattern* resulting from the calculations of Joyce et al. (2019) for 2000 AD is assumed to persist during all climate periods, whereas the flow *magnitudes* vary with shoreline displacement, bedrock freezing, and ice-sheet advance or retreat. The flow decreases during submerged conditions and increases during the 2 000-year periods when the ice-front advances and retreats over the repository. The maximum flow occurs when the ice-front is above the repository during its advance.

The lengths of travel paths through the bedrock also vary with ice-sheet advance and retreat; a lengthening of the discharge flow paths occurs when flow magnitudes are highest, given the assumptions of permafrost during ice-sheet advance. The permafrost hinders the groundwater flow to the surface close to the ice-sheet margin. The effects of the groundwater flow on the barrier system are mainly connected to the flow magnitude and not directly linked to the flow directions. Possible anisotropic bedrock mechanics that affect flow directions, and possible effects of flow patterns on the hydrochemistry, may need to be considered in future assessments.

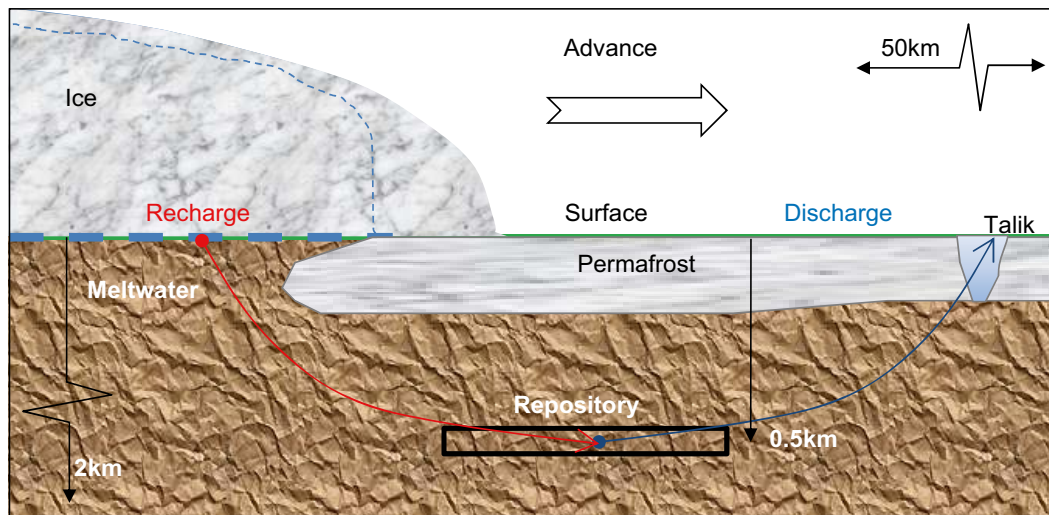


**Figure 6-23.** Illustration of the hydrogeology around the repository beneath an advancing ice sheet margin with permafrost and taliks in the periglacial area in front of the margin. The location of the groundwater surface is shown with a dashed blue line. Adapted from Figure 1-2 in Vidstrand et al. (2010b).

#### 6.4.6 Repository hydrological evolution

For the *simplified glacial cycle variant*, the evolution of groundwater flow around the vaults is expected to follow the regional hydrogeological evolution described in Section 6.4.5. Accordingly, the groundwater flow *pattern* resulting from the *base variant* for 2000 AD is assumed to persist during all climate phases, and the flow *magnitudes* are taken to vary with shoreline displacement, ground freezing, and ice-sheet advance or retreat. This affects the flow rates through the waste, backfill, and bedrock.

#### 6.4.7 Geochemical evolution

##### **Periglacial conditions**

Periglacial climate conditions will lead to permafrost at the repository site (Sections 6.4.1 and 6.4.2), which will affect groundwater flow patterns, as described in Section 6.4.5. Exclusion of salts due to groundwater freezing may lead to temporarily increased groundwater salinities, mainly due to salt transport occurring more slowly than the freezing zone advances. The possible effects of permafrost were modelled in 2D for the Forsmark site by Hartikainen et al. (2010) within the SR-Site safety assessment (SKB 2011a). The results indicate that freezing can induce salt exclusion and transport when perennially frozen ground development exceeds 200 m depth. For the more intense permafrost case, based on a dry variant of the repetition of the last glacial cycle and an air temperature 8 °C lower, calculated groundwater salinities increased to about 4 mass-% (Hartikainen et al. 2010).

However, salt transport by density-driven mixing processes is expected to be contained within more permeable deformation zones and these processes are fast when compared with expected permafrost growth rates. Consequently, no effects from salt exclusion are expected except if a vault is intercepted by deterministic deformation zones (Vidstrand et al. 2006). The effect of salt exclusion due to permafrost has not been evaluated specifically within SE-SFL.

Gimeno et al. (2019) performed hydrogeochemical modelling of the groundwaters in the SE-SFL bedrock volume during glacial and periglacial climate conditions, based on previously calculated salinities for the area (Vidstrand et al. 2010a). Groundwater compositions were similar to, but with lower variability than, those found in the wider Laxemar area (Gimeno et al. 2010). The effect on salinity of freezing and thawing was not accounted for in the modelling.

The generation of gases inside the SFL repository can lead to gas-phase activity releases (Section 6.2.8) and may result in gas pockets entrapped under a permafrost layer. The main elements in the produced gases are hydrogen and carbon. The half-life of H-3 is significantly shorter than the time from closure

until the first permafrost and should therefore not be a concern. Also, C-14 decays significantly and the amount of C-14 releases due to gas generation should only be related to a fraction of the total C-14 inventory. The consequences of gas trapped under permafrost have not been evaluated in SE-SFL but may be warranted in future safety assessments.

### Glacial conditions

The characteristics of glacial conditions at the repository site are described in Sections 6.4.1 and 6.4.2 and the effects on groundwater flow are described in Section 6.4.5. Increased groundwater flow, combined with the low salinities of glacial meltwaters, are expected to result in periods during which the groundwater salinities in the repository environs are substantially lower than during temperate periods. However, the hydrogeological models predict that the deep groundwater will undergo upconing in front of the advancing or retreating ice margin and cause higher salinities, see for example Vidstrand et al. (2013a). In general, the passage of the ice margin is relatively fast and the periods of increased salinity are expected to be short as well. The upconing effect is diminished if the ice sheet advances over permafrost-affected ground (Vidstrand et al. 2010a, 2013, Gimeno et al. 2010).

Similarly to periglacial conditions, as discussed in the previous subsection, the groundwater chemical conditions during a glacial advance and retreat were modelled for the wider Laxemar area and for SE-SFL, respectively (Gimeno et al. 2010, 2019), both based on the salinities calculated by Vidstrand et al. (2010a).

Figure 6-24 shows the resulting groundwater salinities, represented by total dissolved solids (TDS) concentrations, at repository depth (500 m) as dependent on the ice advance over frozen ground and retreat with submerged ground conditions beyond the ice-sheet terminus (Gimeno et al. 2010, 2019). When the repository is behind the ice margin, under the ice, groundwater salinity is expected to be decreased by a factor of about ten (Figure 6-29). This is accompanied by a slight groundwater pH increase to a value of  $\sim 9$ , and an  $E_h$  decrease to around  $-0.3$  V throughout the entire ice-covered time period (Gimeno et al. 2019).

The modelled volume for SFL considered in Gimeno et al. (2019) is a part of the modelled volume for Laxemar considered in Gimeno et al. (2010), and therefore the results obtained in the former are within the range of the latter, as seen for the TDS in Figure 6-28. The largest differences are due to spatially varying hydrogeological conditions within the bedrock volume. Most notably, simulation stage 1a of the ice movement shows the salinity-increasing effect of upconing in Gimeno et al. (2010), whereas this effect is not seen in the corresponding stage for the SE-SFL volume because the SE-SFL is already under the ice and at some distance from the ice front. However, this difference is purely due spatial heterogeneity which is averaged out in Gimeno et al. (2010).

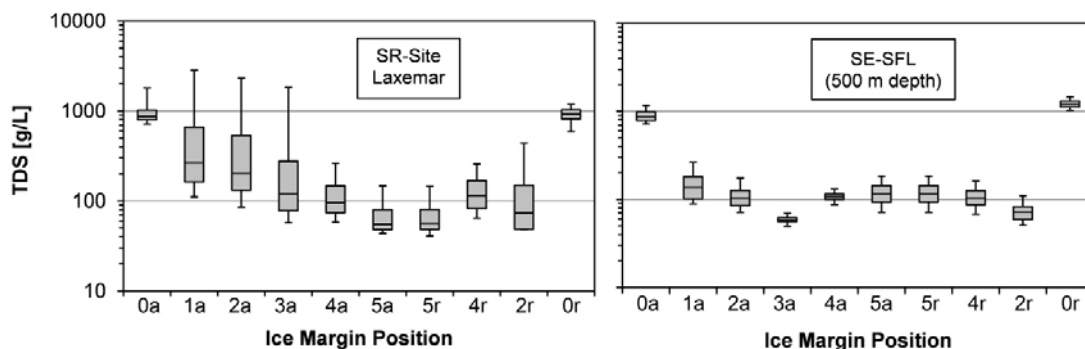


**Figure 6-24.** The calculated TDS concentrations for the different stages of the glacial period, where the x-axis shows the six time periods of advancing ice (0–5a) over frozen ground (permafrost), followed by four time periods of ice retreat (r) with submerged conditions in front of the ice margin. Results for groundwaters within the candidate Spent Fuel Repository volume at 500 m depth at Laxemar (left, Gimeno et al. 2010), and within the SE-SFL bedrock volume at 500 m depth (right, Gimeno et al. 2019). The statistical measures are the median, the 25th and 75th percentiles (box), and the 5th and 95th percentiles (whiskers).

A sensitivity analysis on the DFN realisations, corresponding to that reported in Joyce et al. (2019) has not been performed for the glacial or periglacial conditions; see also Section 6.2.7. By comparison with the results for the base variant and *increased greenhouse effect variant*, it may be concluded that the uncertainty contribution from DFN realisations to groundwater chemical composition might be a factor of about three.

#### 6.4.8 Evolution of the waste

As discussed in Section 6.3.8, chemical processes such as corrosion are temperature dependent, albeit weakly. The small repository-temperature decrease of less than a few degrees is not enough to cause noticeably altered corrosion rates. Corrosion rates are also insensitive to the slight variations in groundwater chemistry. Consequently, the evolution as described in Section 6.2.8 for the base variant is assumed to be valid also for the present *simplified glacial cycle variant*.

In the shallower SFR repository, glaciation is predicted to possibly cause an influx of oxygen-rich glacial meltwater, leading to oxidising conditions (Duro et al. 2012). For the SFL repository at 500 m below ground, however, the reducing capacity of the bedrock is expected to deplete the oxygen in the glacial water before it reaches the repository. The sorption coefficients  $K_d$  are expected to decrease only slightly during the short periods of increased flow discussed in Section 6.4.5. The same chemical conditions, including a reducing environment in the repository, are thus assumed in the *simplified glacial cycle variant* as in the base variant.

#### 6.4.9 Evolution of engineered barriers in BHA

The evolution of the BHA barriers during a period of glaciation is generally not expected to deviate from the evolution described in the base variant. The possible effects of more dilute groundwaters (Section 6.4.7) have been described in section 6.2.9. The increased groundwater flow magnitudes associated with the ice-front passage may have some adverse effect on bentonite erosion. Furthermore, periods of lower salinity may trigger colloidal release, a process discussed in Section 6.2.9. However, the time periods with elevated flows are limited. Upconing of groundwater with high salinity might occur when the front of the ice sheet passes the site (Section 6.4.7). Given the density assumed for the saturated bentonite in the BHA backfill, high groundwater salinity is needed to noticeably influence the bentonite performance (Section 2.2.3 in SKB 2010e). The sensitivity of the bentonite to salinity and increased flows, and the resulting effects, will need to be addressed in future safety assessments.

The repository is assumed to be deep enough not to be affected by permafrost (Section 6.4.3), and thus freezing of the buffer is not analysed. In a future safety assessment, such an analysis might be required, depending on the suggested siting and depth of the facility. The effects that freezing would have on bentonite have been studied in detail by Birgersson et al. (2010).

#### 6.4.10 Evolution of engineered barriers in BHK

The groundwater flow rate at the interface between the bedrock and concrete backfill will, in general, affect how efficiently dissolved cement minerals are removed and hence influence the concrete degradation rate.

Glaciation may introduce dilute groundwater into the repository. Simulations of concrete degradation in BHK have found only minor effects when exposing the concrete to glacial groundwater (Idiart and Shafei 2019).

As shown in Figure 6-22, the formation of an extensive ice sheet can impact the in-situ stresses at the repository level. This is because the glaciation-induced stresses tend to increase the ratio of vertical to minimum horizontal stresses. As a result, substantial effective stresses may result, approaching the uniaxial tensile and compressive strengths, respectively. Simulations indicate that mechanical damage may occur in the concrete backfill, close to the waste domain, and locally at the interface between the backfill and the bedrock (Idiart et al. 2019a).

#### **6.4.11 Evolution of plugs and other closure components**

The bentonite in the vault seals and plugs might be affected by groundwater of low salinity originating from glacial meltwaters. As described in Section 6.2.9, bentonite colloids might be formed and cause chemical erosion of the bentonite. The low salinity might also affect the degradation of the concrete in the plugs. In Section 6.4.10, the conclusion is that the concrete in the barriers of BHK is only little affected by waters of low salinity. This suggests that the concrete in the plugs is also insensitive to glaciation. However, the degradation of plugs and other closure components has not been analysed within SE-SFL and in a future safety assessment such analyses might be warranted.

## 7 Evaluation of post-closure safety for the repository design at the example location

### 7.1 Introduction

To quantify the potential for the proposed repository concept to meet applicable criteria on the maximum annual effective dose to humans after closure, evaluation cases are defined in SE-SFL (Section 2.5.8). Mathematical models are used to calculate radionuclide releases from the repository, transport from the repository to the surface system, uptake and transport in the biosphere, and the resultant doses to humans (2.5.9). In support of the discussion in Chapter 9, the performance of the repository design at the example location is described in this chapter (Section 7.5). The description is based on the analysis of the results of the radionuclide transport and dose calculations for the base case, i.e. the *present-day evaluation case*. This evaluation case is defined for the base variant of the reference evolution (Section 6.2) and its implementation is described in Section 7.4. Further, the modelling approach, including radionuclides considered in the analysis and the models utilized in SE-SFL to calculate radionuclide transport and dose are described in Sections 7.1–7.3. A detailed presentation of the modelling and analysis of the results is given in the **Radionuclide transport report**.

The sensitivity of the resulting releases and doses to specific assumptions made in the base case is evaluated in a set of evaluation cases. The set of evaluation cases included in SE-SFL is described in Section 8.2. All evaluation cases, except for the base case, are described and analysed in Chapter 8, in further support of the discussion on the potential of the proposed repository concept in Chapter 9.

### 7.2 Radionuclides included in the analysis

The prioritisation and selection of radionuclides to consider in the SE-SFL radionuclide transport modelling is mainly based on their half-lives and radiotoxicities from ingestion (Crawford 2018, Chapter 3 in the **Radionuclide transport report**). Radiotoxicity is here defined as the committed effective dose from ingestion of the radionuclide and is calculated for all radionuclides as a function of time starting from the assumed time of repository closure (2075 AD). Note that the radionuclides with the highest activity inventory are not necessarily those that contribute most to the total radiotoxicity. For example, Tc-99 dominates the activity inventory of BHA upon closure but has a low degree of bioaccumulation in the human body and lower energy radiation than, for example, Pu-239 and has thus a lower total radiotoxicity.

The radiotoxicity of the total inventory upon closure is plotted versus half-life in Figure 7-1 for each radionuclide in the waste for BHA and BHK. The vertical red line corresponds to a half-life of 10 years which delineates the cut-off for radionuclide relevance in SR-Site and SR-PSU (SKB 2010g, SKB 2015c, Chapter 3). All non-decay-chain radionuclides to the left of this dividing line are excluded from the analysis also in SE-SFL since their activity will decrease by more than four orders of magnitude within the first 100 years after closure. However, radionuclides belonging to decay chains may have decay products (e.g. Po-210, Ra-228) produced by ingrowth that contribute noticeably to the dose. Co-60 represents the second largest radionuclide inventory in BHK at repository closure, and the inventories of other radionuclides are in some cases derived from Co-60 via correlation factors (Lindgren et al. 2007, IAEA 2009). Hence, this radionuclide is included in the analysis despite having a half-life shorter than 10 years.

Radionuclides with a total radiotoxicity of less than 0.1 Sv (horizontal green line in Figure 7-1) are excluded based on negligible contribution to annual doses. The value of 0.1 Sv is arbitrary but is loosely based on the lowest annual dose from which cancer induction due to chronic exposure is thought to be statistically verifiable in population cohort studies (e.g. Brenner et al. 2003). Note that Figure 7-1 shows the total toxicity inside the repository at closure; the values after only ~100 years would be entirely different for many radionuclides (see Figure 2.1), and the data correlate only very weakly with the eventual doses to humans in the biosphere (Section 7.5.3).

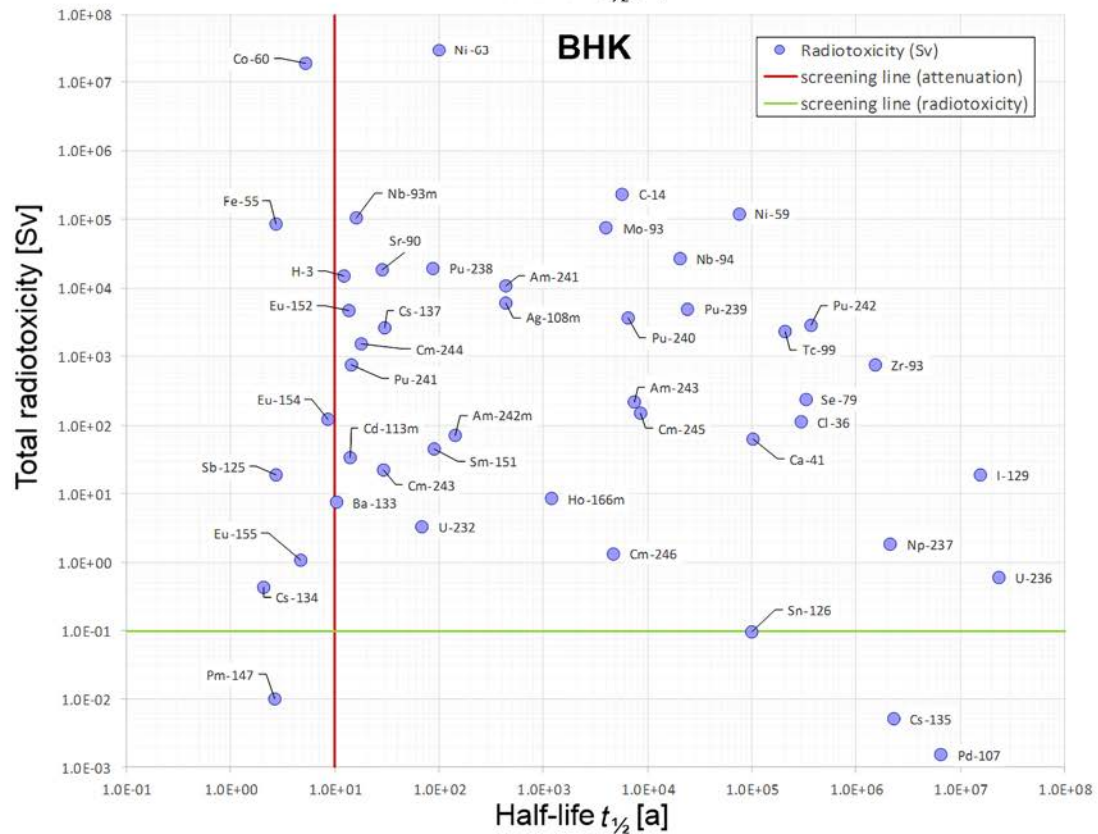
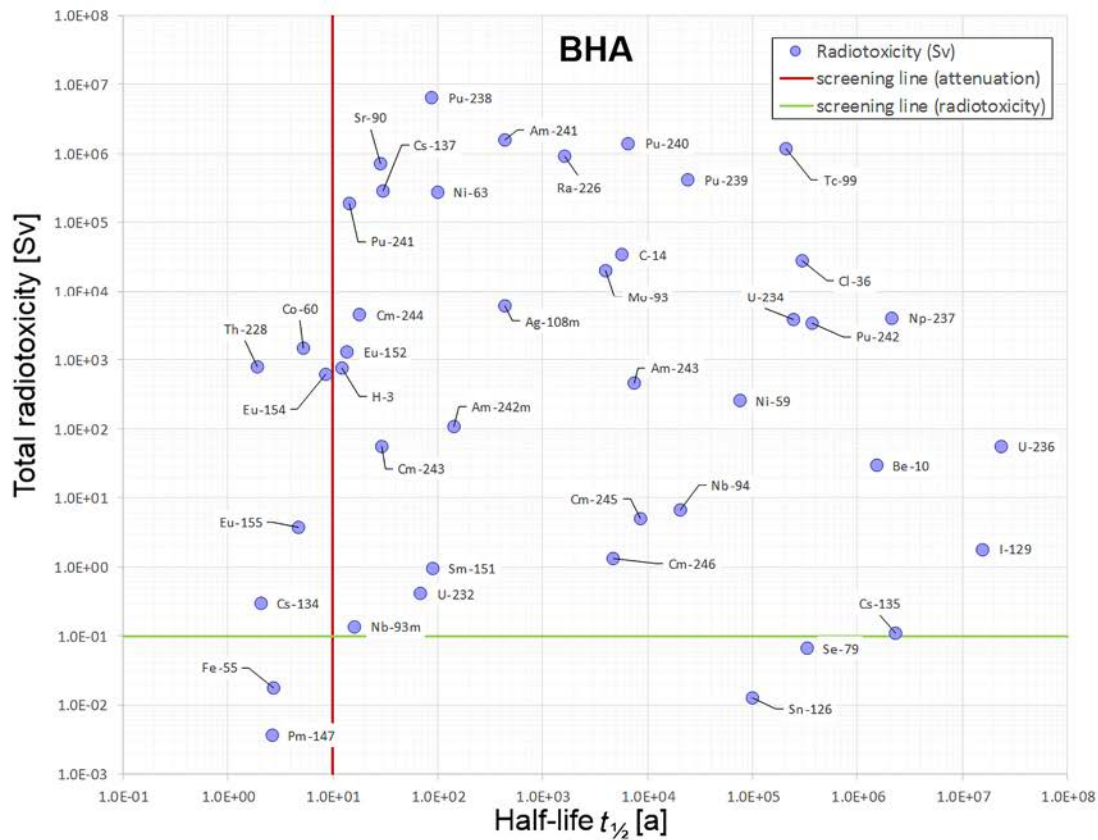


**Figure 7-1.** Total radiotoxicity at 2075 AD versus half-life for all radionuclides present in the waste to be deposited in BHA (top) and BHK (bottom). The red and green screening lines are the same as those used previously in SR-Site and SR-PSU, as described in the text. Figure identical to Figure 3-1 in the **Radionuclide transport report**.

Since the operational plans for the ESS are not yet finalised, only limited information is available on the amount and composition of its waste. Due to these uncertainties, the ESS waste amounts are not considered in SE-SFL. Instead, the ESS radionuclides that are not found in the BHK and BHA inventories, including decay chains, are included in a dedicated evaluation case to assess which of the two vaults is most suitable (Chapter 6.5 in the **Radionuclide transport report** and Section 8.4.3). These radionuclides are Si-32, Ti-44, La-137, Gd-148, Eu-150, Tb-157, Tb-158 and Re-186m.

## 7.3 Modelling approach

### 7.3.1 Model chain and data flow

The SE-SFL radionuclide transport modelling methodology is based on the experiences from SKB's previous safety assessments SR-Site and in particular SR-PSU (SKB 2015c) but includes some simplifications since SE-SFL is only an initial evaluation of post-closure safety and not part of a licensing application. Radionuclide transport and dose modelling is performed with a set of models representing different parts of the repository and its environs: the near-field, the geosphere, and the biosphere. Figure 7-2 presents a schematic diagram of the main flow of data within the SE-SFL model chain. The chain starts with the near-field model that describes the release, transport and retention of radionuclides in the waste domain and the surrounding engineered barriers. Moreover, the activity release at the waste vault-bedrock interface is calculated. The geosphere model describes the subsequent transport and retention of radionuclides in and through the bedrock towards the surface. Finally, the biosphere model consists of sub-models (not shown) describing transport and accumulation in the surface ecosystems, natural and cultivated, and determines the resulting doses to humans. The details of the respective models are described in Sections 7.3.2–7.3.4. The definition of the term dose as used in SE-SFL is given in Section 2.5.9.

The radionuclide transport calculations are carried out as dynamic simulations, where the output from one model, in terms of the annual activity release for each radionuclide, is used as input for the next (Chapter 2 in the **Radionuclide transport report**). The modelling tools are coupled indirectly, i.e. the model chain has not been executed in continuous mode, but rather for one entity at a time followed by a manual or semi-automatic transfer of files to the calculation tool for the subsequent model. To ensure functional coupling between the three models, the models have been designed to use compatible definitions of the parameters, so that the inputs and outputs are not only numerically compatible but also represent the same features, events, and processes (FEPs). Testing and verification of the models have been performed, both within and between them.

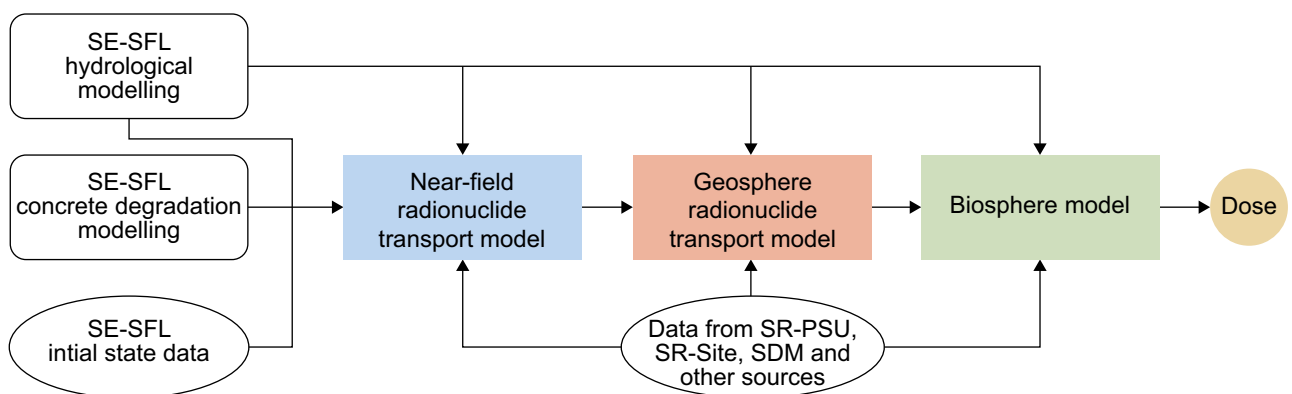


**Figure 7-2.** Schematic representation of the SE-SFL radionuclide transport model chain and main sources of input for the respective models. Adapted from Figure 1-3 in Shahkarami (2019).

As in SR-PSU, transient releases from the geosphere are fed directly into the biosphere transport model in SE-SFL. This enables the dose calculation to take account of the release history and the evolution of the biosphere system. This is different from SKB's earlier long-term safety assessments where geosphere releases were converted directly to doses via separately calculated landscape dose-conversion factors.

The transport modelling as described in the **Radionuclide transport report** relies on many other reports. Material properties and conditions in the repository and its environs assumed in the modelling are chosen based on the initial state (Chapter 4 and the **Initial state report**) and the reference evolution (Chapter 6, **Climate report, FEP report**). Many studies were performed specifically for SE-SFL to provide parameters for the various system components. These include definition of methods and input data for the near-field (Wessely and Shahkarami 2019, Shahkarami 2019), the geosphere (Shahkarami 2019, Trinchero et al. 2018), and the biosphere (**Biosphere synthesis**, Grolander and Jaeschke 2019, Johansson and Sassner 2019). Some input was also taken from SR-PSU and SR-Site, for example data relating to sorption, material properties, corrosion, and the Laxemar site-descriptive modelling.

As indicated in the top left of Figure 7-2, further input parameters were supplied by dedicated modelling studies of the hydrogeological properties around the repository (Abarca et al. 2019, Joyce et al. 2019, Gimeno et al. 2019), performed as steady-state calculations for a limited number of time-points with corresponding geosphere conditions. Further, the evolution of the concrete and bentonite engineered barriers are described in six reports by Idiart and co-workers (Idiart and Coene 2019, Idiart and Shafei 2019, Idiart and Laviña 2019, Idiart et al. 2019a, b), including modelling with coupling between flow and degradation properties.

### 7.3.2 Near-field

The near-field models are built in the compartment (block) simulation tool Ecolego<sup>8</sup>. To account for the different designs and wastes in the two vaults, a separate model has been constructed for each waste vault (Wessely and Shahkarami 2019). The models rely on a compartmental conceptualization of the waste packages and engineered barriers in the form of the backfill, and address the diffusive and advective transport of radionuclides in the repository near-field. Thus, the near-field components are divided into compartments with internally homogenous properties, and radionuclides and other materials are assumed to be well mixed within each compartment. The radionuclide inventory in each compartment depends on local processes as well as exchange processes with connected compartments, i.e. transport, briefly described in this section. Both vault models include five backfill sub-compartments on each of the six sides of the waste compartment (Figures 7-3 and 7-4).

#### **BHA**

The waste in BHA is deposited in metal containers and stabilized with grout. The containers are emplaced in a concrete structure and the vault is backfilled with bentonite, as shown schematically in Figures 4-4 and 7-3. A detailed description of the BHA geometry is given in the **Initial state report** and the parameterisation of the BHA compartment model is given in Shahkarami (2019). The single, central waste compartment includes the concrete structure, the waste, the waste packages, and the grout. Like all other compartments, the waste compartment is assumed internally homogeneous and well mixed in terms of materials and radionuclide inventory.

The groundwater flow rates through BHA are very low thanks to the very low hydraulic conductivity of the bentonite backfill (Section 6.2.6). Simulations of the near-field hydrology (Abarca et al. 2019) have furthermore shown that the groundwater flow through BHA at the example location is mainly directed along the length of the vault whereas the vertical flow component is small. Thus, in the near-field model, advective water flow is simplified by assuming that it only enters through one short end and leaves through the other, i.e. water flows axially along the length of the vault.

<sup>8</sup> <http://ecolego.facilia.se/ecolego/show/Ecolego+Wiki>.

Therefore, the six backfill compartments (shown in pink in Figure 7-3) on each side of the central waste compartment comprise an inflow compartment at one short end of the vault; an outflow compartment at the opposite short end; and four side compartments representing the backfill above, below and beside the waste compartment. Each of the backfill compartments consist of five equally sized sub-compartments, where the outermost boundary sub-compartments connect to the geosphere model at the bedrock-vault interface.

In the model, radionuclide transport by advection occurs only from the inflow compartment, through the waste compartment, and then out from the vault through the outflow compartment. Transport by diffusion occurs between all compartments and is modelled as one-dimensional transport with net activity flow towards or away from the waste compartment depending on the concentration gradients at any given time.

The bentonite barrier is assumed to retain its properties throughout the entire assessment period, including sorption, diffusion, and hydraulic conductivity (Section 2.3 in the **Radionuclide transport report** and Section 6.2.9). Radionuclides in the BHA near-field model are conservatively assumed to be immediately available for transport upon repository closure (see further Section 7.4.2).

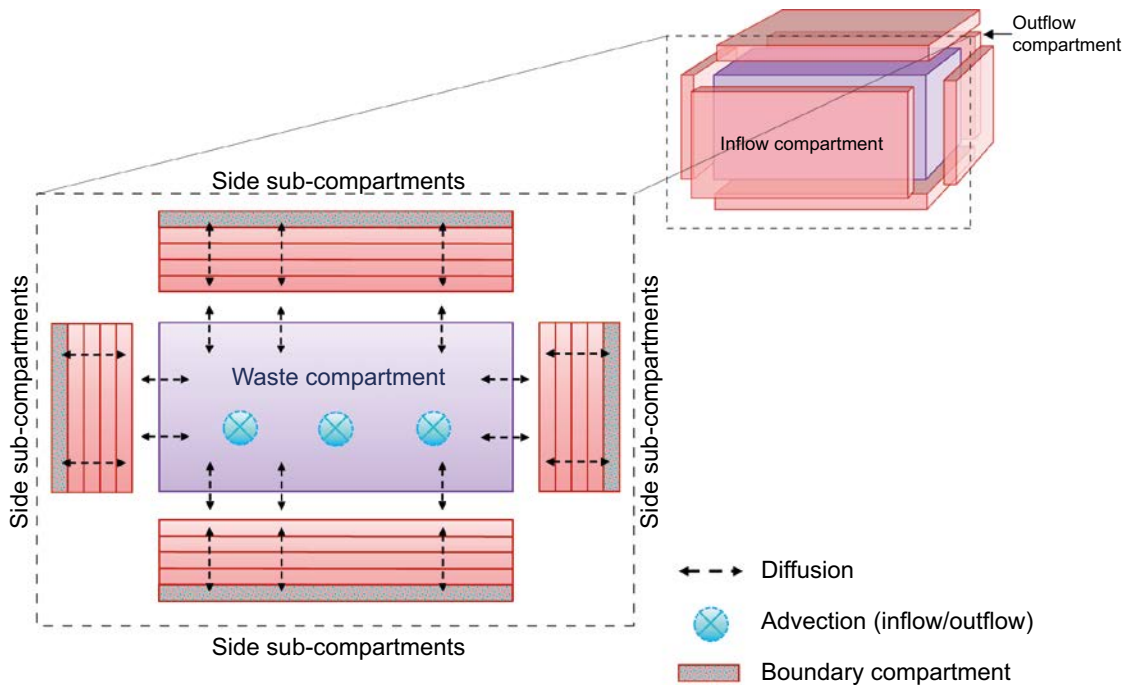


**Figure 7-3.** Schematic diagram of the compartment model of BHA, seen from the short end into the length of the vault. The bentonite backfill, shown in pink, is discretised into six compartments which in turn consist of five sub-compartments. The outflow backfill compartment is on the far end, behind the waste compartment, and the inflow compartment is in front of the waste compartment (Figure 4-3 in the **Radionuclide transport report**).

## BHK

The waste in BHK mostly consists of metallic parts with induced activity, stored in steel tanks and stabilized with grout. The steel tanks are emplaced in concrete structures and the vault is backfilled with concrete. The tanks are conservatively assumed not to provide any transport resistance. A detailed description of the BHK geometry is given in the **Initial state report** and the parameterisation of the BHK compartment model is detailed in Shahkarami (2019).

The compartmental representation of BHK is like that of BHA. The vault is assumed to be a cuboid with one waste compartment and three groups of concrete backfill compartments (Figures 4-3 and 7-4). The waste compartment represents the six concrete caissons, the waste, the waste packages, and the grout, and is assumed to be homogeneous in terms of materials and radionuclide inventory. Each of the six backfill compartments consist of five equally sized sub-compartments with one-dimensional diffusive transport within each sub-compartment. The outermost boundary sub-compartments connect to the geosphere model at the bedrock-vault interface.

BHK has higher groundwater flow rates than BHA due to a higher hydraulic conductivity of the concrete than the bentonite (Section 6.2.9). Furthermore, simulations of the near-field hydrology (Abarca et al. 2019) have shown that the groundwater flow is mainly directed vertically down through the BHK vault. Therefore, advective inflow of groundwater is in the model assumed to only occur through the inflow compartment representing the concrete backfill above the waste, and radionuclides are then transported out from the vault by advection mainly through the outflow compartment beneath the waste. The model also assumes a small advective transport component outwards in the horizontal plane, allowing for advective transport also through the side compartments.

The transport modelling in BHK differs from BHA in two main ways. First, the BHK modelling assumes a time-dependent degradation of the concrete barriers, resulting in altered flow rates and transport properties, for example, for sorption and effective diffusion coefficients (details on implementation in Section 7.4.2 and parametrization in Shahkarami 2019). Second, the main fraction of the metallic waste in BHK is assumed to be slowly dissolved by corrosion, represented by  $R_c^i$  in Equation 7-1. This results in slow, gradual release of radionuclides into the water phase, providing an activity-release retardation in BHK. In BHA on the other hand, all radionuclides are assumed to be dissolved and available for transport at closure.

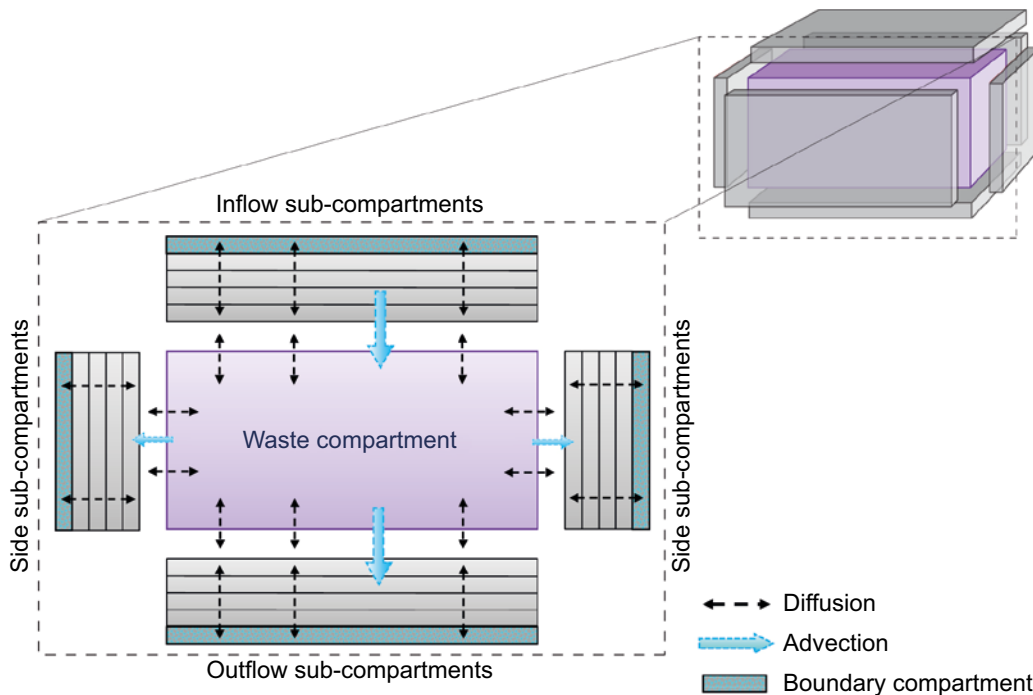


**Figure 7-4.** Schematic illustration of the BHK model including the discretised backfill, consisting of compartments and sub-compartments. The grey colour denotes the concrete backfill (Figure 4-4 in the **Radionuclide transport report**).

### Activity transport equation

An activity transport equation was set up (Equation 7-1), as adapted from Fetter (1999) to the compartment approach. The components, i.e. waste and backfill compartments, are represented by continuous porous media. The equation calculates the change over time ( $\partial/\partial t$ ) of a compartment's activity inventory concentration  $c$  (Section 4.2.2 in the **Radionuclide transport report**).

$$\begin{aligned} \left(\frac{\partial}{\partial t} + \lambda^i\right) (V_j(\varepsilon_j^i + K_d^i \rho_{\text{bulk}})c_j^i) - \sum_p V_j(\varepsilon_j^p + K_d^p \rho_{\text{bulk}})Br_p^i \lambda^i c_j^p \\ = \sum_k (N_{kj}^i - N_{jk}^i) + R_c^i \end{aligned} \quad 7-1$$

where:

$c_j^i$  = Activity concentration (time-dependent) of species  $i$  in the pore water in compartment  $j$  [Bq/m<sup>3</sup>]

$V_j$  = Volume of compartment  $j$  [m<sup>3</sup>]

$\varepsilon_j^i$  = Diffusion-available porosity for species  $i$  in compartment  $j$  [-]

$\lambda^i$  = Decay constant of species  $i$  [s<sup>-1</sup>]

$\rho_{\text{bulk}}$  = Bulk density of the sorbing material, i.e. concrete or bentonite [kg/m<sup>3</sup>]

$K_d^i$  = Sorption coefficient for species  $i$  [m<sup>3</sup>/kg]

$Br_p^i$  = Branching ratio from parent radionuclide  $p$  to radionuclide  $i$  [-]. This differs from unity only for parent nuclides  $p$  that have more than one decay mode.

$N_{kj}^i$  = Activity transfer rate of species  $i$  from compartment  $k$  to  $j$  [Bq/s].  $N_{kj}^i$  is a sum of the transport by diffusion and advection and is thus a function of the effective diffusivity, water flow, and the activity concentrations  $c_j^i$  and  $c_k^i$ .

$R_c^i$  = Rate of release the activity of species  $i$  by corrosion of metallic waste [Bq/s]

$(\varepsilon^p + K_d^p \rho_{\text{bulk}})Br_p^i \lambda^i c^p$  = Rate of activity in-growth of decay product  $i$  per unit volume from parent radionuclide  $p$  [Bq s<sup>-1</sup> m<sup>-3</sup>]

Equation 7-1 is solved separately for all relevant radionuclides  $i$  including decay-chain radionuclides. The left-hand side represents the accumulation of the species in the water and solid by radioactive decay and ingrowth, as well as by sorption as discussed below.  $\varepsilon_j^i$  is the diffusion-available porosity defined as the portion of the total porosity available for diffusive transport of species  $i$ . Solubility limits are conservatively disregarded and so is reprecipitation of dissolved radionuclides.

On the right-hand side of Equation 7-1, the terms in the sum represent transport to and from adjacent compartments. The final term represents the release from the waste by corrosion (only considered in BHK).

### Sorption, advection, diffusion and dispersion

Sorption represents the immobilisation onto solid materials that a dissolved species may undergo, as do many of the radionuclides in SFL. Sorption onto cementitious and clay materials in the near-field is explicitly considered in form of the linear volumetric sorption coefficient  $K_d$  [m<sup>3</sup>/kg] (Section 2.5.5 in Shahkarami 2019). Fully reversible instantaneous sorption is assumed.  $K_d$  represents the ratio between the adsorbed mass onto the solid phase and the mass in the fluid:

$$K_d^i = \frac{c_s^i}{c_{\text{aq}}^i} \Big|_{\text{eq}} \quad 7-2$$

where  $c_s^i = m_i/m_s$  [kg/kg] is the concentration of species  $i$  in the solid phase, expressed as the mass of species  $i$  per unit mass of porous, solid medium  $s$  onto which it sorbs; and  $c_{\text{aq}}^i$  [kg/m<sup>3</sup>] is the concentration in the fluid phase, expressed as mass of species  $i$  per unit volume of the fluid. Some radionuclides are assumed not to sorb at all, corresponding to  $K_d = 0$ .

The radionuclide transfer  $N_{kj}^i$  [Bq/s] between compartments in Equation 7-1 is a sum of advective and diffusive transport. The forward advective transport from compartment  $j$  to  $k$  is calculated as:

$$N_{jk}^i = \begin{cases} 0, & Q_{jk} < 0 \\ c_j^i Q_{jk}, & Q_{jk} \geq 0 \end{cases} \quad 7-3$$

where the activity concentration  $c_j^i$  [Bq/m<sup>3</sup>] in solution is moderated by sorption, and  $Q_{jk}$  [m<sup>3</sup>/s] is the water flow rate from  $j$  to  $k$ , which is related to the water Darcy flux  $u_D$  [m/s] and the compartment's dimensions and is taken from the repository-scale hydrogeology (Abarca et al. 2019).

The compartments are represented by porous media, and radionuclides released from the waste are transported by molecular diffusion in the pore water. The diffusion contribution to the transfer terms  $N_{kj}^i$  in the near-field model transport equation is:

$$N_{jk}^i - N_{kj}^i = \frac{c_j^i - c_k^i}{R_{kj}^i + R_{jk}^i} \quad 7-4$$

where the transport resistance  $R_{jk}^i$  in turn depends on the material-specific effective diffusivity  $D_e$  and porosity  $\varepsilon_j^i$  as well as the spatial properties diffusion length  $l_{jk}$  and contact area  $A^{jk}$  between the two compartments (Section 4.2.1 in the **Radionuclide transport report** and Shahkarami 2019).

Mechanical (hydrodynamic) dispersion is not explicitly represented in the compartmental approach. However, the spatial discretisation of the system in the near-field model introduces a numerical dispersive effect with respect to transport. The numerical dispersion corresponds to a Péclet number of 10, which is comparable with the expected influence of mechanical dispersion (Section 3.2.2 in Shahkarami 2019). A more detailed account of the near-field transport processes can be found in Chapters 3 and 4 in Wessely and Shahkarami (2019).

### Coupling to the geosphere

Release of radionuclides from the near-field to the surrounding host rock serves as a source term to the geosphere transport model, where the groundwater flows through fractures (Section 7.3.3). The connection to the geosphere is, as a simplifying assumption, modelled as transport only entering the fractures, while for example disregarding sorption onto the bedrock wall at the vault-bedrock interface. Advective transport into the fractures comes from the outflow boundary compartment in BHA and outflow and side boundary compartments in BHK (Figures 7-3 and 7-4). The advective activity transport from these boundary compartments is analogous to inter-compartment advection (Equation 7-3), with an advective flow  $Q_b$  out from the backfill taken from Abarca et al. (2019).

Diffusive transport to the fractures is different from inter-compartment diffusion for two reasons. First, the fractures are much thinner than the compartments, resulting in additional diffusive resistance. In the model, this is approximated by a plug through which the nuclides are transported, with the same thickness and cross-sectional area as the fracture. Second, the fractures are much more permeable to groundwater flow than the backfill, accounted for by the introduction of the fracture equivalent flow rate  $Q_{eq}$  and diffusive resistance  $R_{eq} = 1/Q_{eq}$ . The forward diffusion  $N_{bf}^i$  of radionuclide  $i$  from boundary compartment to fracture is thus calculated by adding two corresponding resistance terms in the denominator of the diffusion transfer equation (derivation in Section 4.2.1 in Wessely and Shahkarami 2019):

$$N_{bf}^i = \frac{c_b^i - c_f^i}{R_b^i + R_{plug}^i + R_{eq}^i} \quad 7-5$$

The activity release from the waste vault is distributed among a multitude of transport paths that originate in fractures at the waste vault-bedrock interface (Section 2.9.2 in Shahkarami 2019). The distribution of the total radionuclide release over the many trajectories is calculated using distribution factors (Section 2.10 in Shahkarami 2019). The distribution factors are assumed constant, whereas the source terms (release rates) vary over time.

### 7.3.3 Geosphere

The main assessment code for the geosphere transport, FARFCOMP, is based on a compartment concept and is a new implementation of the same conceptual model that underlies FARF31 (Lindgren et al. 2002) used within SR-Site (SKB 2010g, 2011a). FARFCOMP is built in Matlab and was developed

to get a clearer, more flexible, faster and more consistent solution method compared with codes used previously by SKB for solving the geosphere transport equation. The code is described in detail in Appendix B in the **Radionuclide transport report**.

The geosphere is modelled as an idealised fracture-rock-matrix system with discrete parallel fractures through which the radionuclides are transported, as schematically illustrated in Figure 7-5. The fractures are situated in a porous rock matrix. Fractures have a total length  $z_{tot}$  and are discretised along their length with resulting compartment length  $\Delta z$  and volume  $V_f$ . The rock matrix is discretised along the axis perpendicular to the fractures into compartments with volume  $V_m$ . The rock-matrix compartments are further divided into  $N_m$  sub-compartments whose depths  $d$  increase with distance from the fracture, i.e. a finer spatial resolution close to the fracture. Although the model is calculated in one dimension, it is shown as three-dimensional boxes in Figure 7-5 to aid interpretation. Advection and dispersion (solid and dashed blue arrows in Figure 7-5) transports radionuclides through the fracture, whereas diffusion (yellow arrows in Figure 7-5) moves them into and out of the rock matrix.

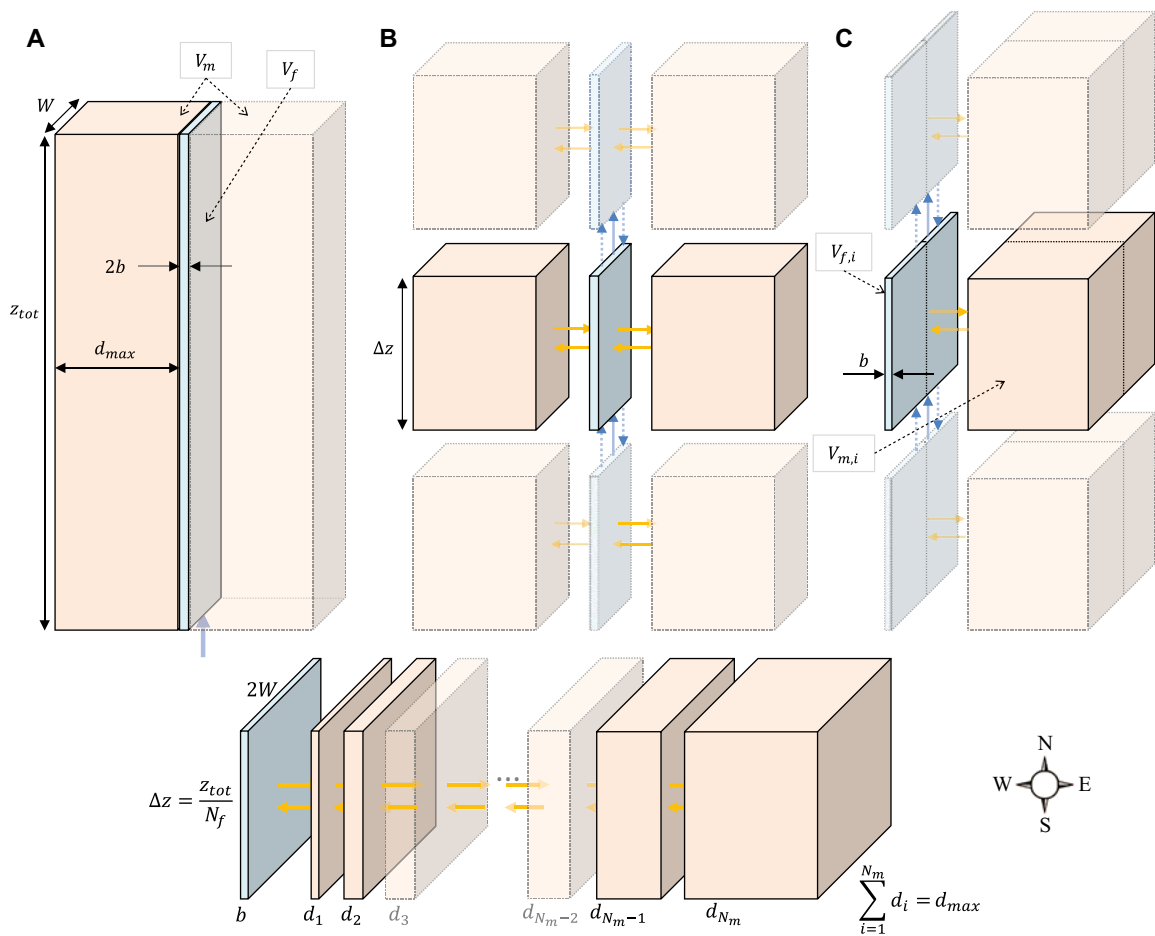


**Figure 7-5.** Schematic view of the idealised fracture-rock-matrix system implemented in the geosphere model (A). Discretising the simple volumes in panel A into sections along the fracture (B). Rearranging the volumes to one side so that only one rock matrix volume needs to be considered per discretised fracture volume (C). Schematic view of the rock matrix discretisation (D).  $V_f$  and  $V_m$  are the volumes of the modelled fracture and porous rock matrix, respectively.  $z_{tot}$  is the total length of the fracture and  $\Delta z$  is the length of fracture compartment  $i$ . Advective (solid blue arrows) and dispersive (dashed blue arrows) transport occurs along the fracture and diffusion (yellow arrows) transports radionuclides into the rock matrix.  $d_1$  is the depth of the first matrix compartment adjacent to the fracture compartment and  $N_m$  is the number of rock-matrix compartments. (Figures B-3 and B-4 in the **Radionuclide transport report**).

In the regional hydrogeology model for SE-SFL, groundwater flows through discrete fractures (Joyce et al. 2019). The flow field generated by the hydrogeology model is used to determine potential paths taken by a tracer particle, for example, a radionuclide, where a multitude of particles are injected in fractures that intersect the near-field vaults. The simulation then moves the particles towards the surface through the fracture network, where the path selection is stochastic and statistically weighted according to the water flux at fracture intersections. Each individual particle is followed, tracing out its transport path, that is, trajectory, which is built up of a series of connected fracture segments. Trajectories that do not connect to the biosphere are neglected. One reason for particles not reaching the surface is that the flows are so low that numerical artefacts occur. Thus, neglecting such pathways conservatively disregards transport with high potential for retention and results in a larger part of the near-field release making it to the biosphere. Flow-related data are recorded for each trajectory: the total advective travel time  $t_w$  of a water particle passing through the fracture network, the sum of the flow-related transport resistances over all fracture segments (F-factor), and water fluxes at the fracture-vault intersection. These data are used in the model calculations of geosphere radionuclide transport (Equations 7-6 and 7-7).

### Activity transport equation

The geosphere model uses the release of radionuclides from the near-field models as source term. The geosphere model then solves the radionuclide transport separately for each trajectory, whose properties are assumed constant during each simulation in most evaluation cases. Eventually, by calculating a weighted sum over all trajectories, the radionuclide release into the biosphere is determined. This approach thus accounts for release from all possible pathways within the geosphere as well as macro-scale dispersion arising from the presence of multiple flow-paths.

A contaminant source exists at the origin of each fracture. The groundwater velocity  $v$  in each fracture is assumed constant within each simulation but can vary between simulations representing different points in time such as in the *simplified glacial cycle evaluation case* (Section 8.6.2). The transport processes in such system can be described by the following two coupled, one-dimensional equations, one for the fracture and one for the porous matrix. The coupling is provided by the continuity of concentrations along the interface.

$$\frac{\partial C_f^i}{\partial t} = -v \frac{\partial C_f^i}{\partial z} + D_L \frac{\partial^2 C_f^i}{\partial z^2} - \lambda^i C_f^i + \sum_{p \in P_n} \lambda^i C_f^p B r_p^i + \left. \frac{D_e^i}{b} \frac{\partial C_m^i}{\partial x} \right|_{x=0} \quad 7-6$$

$$R_m^i \frac{\partial C_m^i}{\partial t} = \frac{D_e^i}{\varepsilon_m} \frac{\partial^2 C_m^i}{\partial x^2} - R_m^i \lambda^i C_m^i + \sum_{p \in P_i} R_m^p \lambda^i C_m^p B r_p^i \quad 7-7$$

In the above equations:

- $C_f^i$  = Activity concentration of radionuclide  $i$  in the flowing water  $f$  of the fracture [Bq m<sup>-3</sup>]
- $C_m^i$  = Pore-water activity concentration of radionuclide  $i$  in the matrix  $m$  next to the fracture [Bq m<sup>-3</sup>]
- $t$  = Time [a]
- $v$  = Mean water velocity in the water-bearing fracture [m a<sup>-1</sup>]
- $z$  = Distance in the flow direction [m]
- $D_L$  = Longitudinal dispersion coefficient [m<sup>2</sup> a<sup>-1</sup>]
- $b$  = Half-aperture of the fracture [m]
- $D_e^i$  = Effective diffusivity of radionuclide  $i$  in the rock matrix [m<sup>2</sup> a<sup>-1</sup>]
- $x$  = Distance into the rock matrix [m]
- $\lambda^i$  = Decay rate for radionuclide  $i$  [a<sup>-1</sup>]
- $P_i$  = Set of indices of parents of radionuclide  $i$  [-]
- $B r_p^i$  = Branching ratio from parent radionuclide  $p$  to radionuclide  $i$  [-]
- $R_m^i$  = Capacity factor for radionuclide  $i$  in rock matrix  $m$  [-], defined as:

$$R_m^i = \frac{\varepsilon_m + K_{d,m}^i \rho_m}{\varepsilon_m} \quad 7-8$$

- $\varepsilon_m$  = Porosity of the rock matrix  $m$  [-]  
 $K_{d,m}^i$  = Sorption coefficient in rock matrix  $m$  for radionuclide  $i$  [ $\text{m}^3 \text{kg}^{-1}$ ]  
 $\rho_m$  = Bulk density of the rock matrix  $m$  [ $\text{kg m}^{-3}$ ]

The initial and boundary conditions are:

$$C_f^i|_{t=0} = 0 \quad 7-9$$

$$C_m^i|_{t=0} = 0 \quad 7-10$$

$$C_f^i|_{z \rightarrow \infty} = 0 \quad 7-11$$

$$Q_{\text{tube}} \left( C_f^i - \frac{D_L}{v} \frac{\partial C_f^i}{\partial z} \right) \Big|_{z=0} = F_{\text{in}}^i \quad 7-12$$

$$C_m^i|_{x=0} = C_f^i \quad 7-13$$

$$\frac{\partial C_m^i}{\partial x} \Big|_{x=d_{\text{max}}} = 0 \quad 7-14$$

- $Q_{\text{tube}}$  = Volume flow of water in the fracture [ $\text{m}^3 \text{a}^{-1}$ ]  
 $F_{\text{in}}^i$  = Inlet activity flow of radionuclide  $i$  to fracture [ $\text{Bq a}^{-1}$ ]  
 $d_{\text{max}}$  = Maximum penetration depth into the rock matrix [m]

The desired quantity is the output release  $F_{\text{out}}^i$  for radionuclide  $i$  at the end of the fracture where  $z = z_{\text{tot}}$ :

$$F_{\text{out}}^i = Q_{\text{tube}} \left( C_f^i - \frac{D_L}{v} \frac{\partial C_f^i}{\partial z} \right) \Big|_{z=z_{\text{tot}}} \quad 7-15$$

- $F_{\text{out}}^i$  = Output release of radionuclide  $i$  from the fracture [ $\text{Bq a}^{-1}$ ]  
 $z_{\text{tot}}$  = Total length of the fracture [m]

### **Sorption, advection, diffusion, and dispersion**

Sorption on the pore surfaces inside the porous rock matrix, expressed by  $K_{d,m}^i$ , enters the transport Equation 7-7 in form of the capacity factor  $R_m^i$  (Equation 7-8). However, sorption in the fracture, on its surfaces or possible fracture infill, is disregarded in the geosphere model, a conservative assumption consistent with SKB's earlier transport modelling (SKB 2010g).

Radionuclides are transported through the fracture by advective water flow. Mechanical dispersion along the individual trajectories is explicitly modelled by means of a constant Péclet number,  $Pe = 10$ , which quantifies the ratio between advective and dispersive transport. Dispersion in the geosphere is thus of the same magnitude as in the near-field, although it is explicit in the geosphere model and an implicit result of the discretisation in the near-field.

The rock matrix next to the fracture is porous, and radionuclides can be withdrawn from the flowing groundwater and enter the stagnant water in the pores of the rock matrix by molecular diffusion. This exchange is included in Equation 7-7 and assumes sorption-modulated Fickian diffusion with a constant effective matrix diffusivity  $D_e^i$  and finite penetration depth  $d_{\text{max}}$  (Shahkarami 2019).

### **Coupling to the biosphere**

In the SE-SFL radionuclide transport modelling chain, the activity release from the geosphere serves as a source term to the biosphere model. The geosphere model results in an activity release from each trajectory and those trajectories terminate at different locations. However, the results of the regional hydrogeological modelling (Joyce et al. 2019) indicate that most of the total potential release from the SFL repository typically ends up close to one of three biosphere objects. Therefore, it is assumed that the total radionuclide release from the geosphere is discharged entirely into a single biosphere object, a pessimistic assumption in most evaluation cases including the base case.

### 7.3.4 Biosphere

The biosphere radionuclide transport model, like the near-field model, is built in Ecolego, and is based on the corresponding model used in SR-PSU (Saetre et al. 2013). The model consists of several sub-models for transport in the biosphere, i.e., natural and cultivated ecosystems, as well as modules for the calculation of effective radiation doses to humans. The continuous release from the geosphere is used as the radionuclide source term for the biosphere calculations. The model then calculates transport, accumulation, decay and ingrowth of radionuclides with different geochemical behaviour, using radionuclide-specific data applicable specifically to the biosphere. The details of the biosphere model can be found in the **Biosphere synthesis**.

#### ***Biosphere objects***

Discharge areas for deep groundwater at the example location in Laxemar were identified from two hydrological modelling studies (Werner et al. 2006, Sassner et al. 2011), both showing discharge areas being located along streams and at the coastline, as well as in lakes, mires and coastal bays. These areas where released radionuclides can reach the biosphere are referred to as biosphere objects, geographically bounded so as to represent clearly defined ecosystems with reasonably homogenous properties (SKB 2014f, Lindborg 2010). Figure 7-6 shows the nine Laxemar biosphere objects considered in SE-SFL, which include two semi-enclosed sea bays (201, 208), lake Frisksjön (207), the Gäster mire (203), and five agricultural biosphere objects representing areas of arable land of different size and location in the landscape (204, 206, 210, 212 and 213).

The biosphere model accounts for biosphere objects changing over time. For example, shoreline displacement can result in the transformation of a sea basin into an isolated lake, as is assumed for objects 201 and 208 (Figure 7-6). This natural succession of biosphere objects is described in detail in the **Biosphere synthesis**.

In the SR-Site and SR-PSU biosphere modelling, it was found that the dose consequences from biosphere objects receiving the release through groundwater discharge were generally higher than doses from down-stream areas having received radionuclides by dispersion through the landscape (SKB 2010h, 2014f). The SE-SFL biosphere modelling therefore analyses multiple potential discharge areas but disregards down-stream exposure.

#### ***Radionuclide transport model***

Radionuclide transport in the biosphere objects in SE-SFL is simulated based on the same compartmental calculation model used in SR-PSU (Saetre et al. 2013), which includes additional discretisation of the two bottom regolith layers compared with SR-Site (SKB 2010h). The model assumes that the distribution of radionuclides in the biosphere can be represented by a limited number of internally homogenous and interconnected compartments. This is a highly simplified representation, but because the time and spatial scales for SE-SFL are in the order of hundreds of thousands of years and hundreds of hectares, respectively, it is considered reasonable to represent the ecosystem using temporally and spatially averaged conditions.

Two types of ecosystems are modelled: terrestrial ecosystems including mires (Figure 7-7A), and aquatic, comprising sea, lakes and streams (Figure 7-7B). The distribution of radionuclides in terrestrial ecosystems is represented by eight compartments associated with regolith layers, representing from the bottom: lower, glacial clay, post-glacial sediment, peat, and upper regolith, where the three latter compartments also include counterparts with organic radionuclide species. The aquatic ecosystem lacks peat but includes two compartments associated with the water, representing the water phase and particulate organic matter ( $PM_{org}$ ), respectively. Both ecosystem types include a compartment associated with primary producers (Prim Prod). Radionuclides flow between compartments and also out of the system and can even move from an aquatic system to terrestrial through ingrowth of wetland vegetation.

Many of the biosphere objects in the Laxemar area are presently cultivated, so the agricultural model in SE-SFL has been updated to enable evaluation of continuous cultivation in a discharge area, including drainage to a ditch (Figure 7-7C). Since long-term accumulation of organic matter is expected to be limited in agricultural ecosystems, this model does not have separate compartments for radionuclides stored in organic matter.

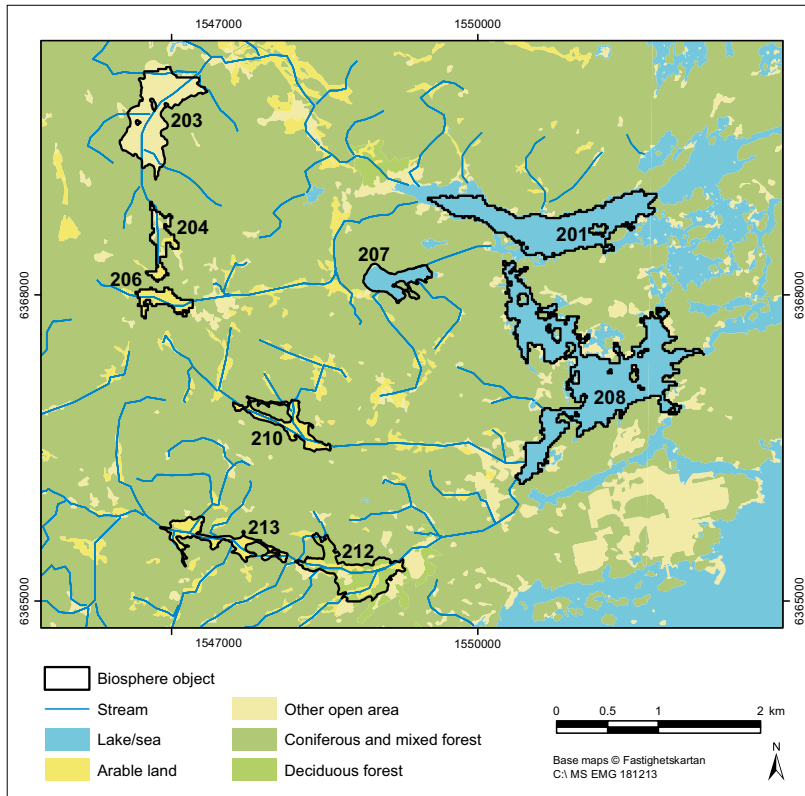


**Figure 7-6.** The nine biosphere objects projected onto the present land-use map in the Laxemar area. The objects represent different ecosystems and locations in the landscape, and deep groundwater is expected to be discharged into all of them. The outlined area of biosphere objects 201 and 208 correspond to the future lake basins that are somewhat smaller than the sea basins present today (**Biosphere synthesis**).

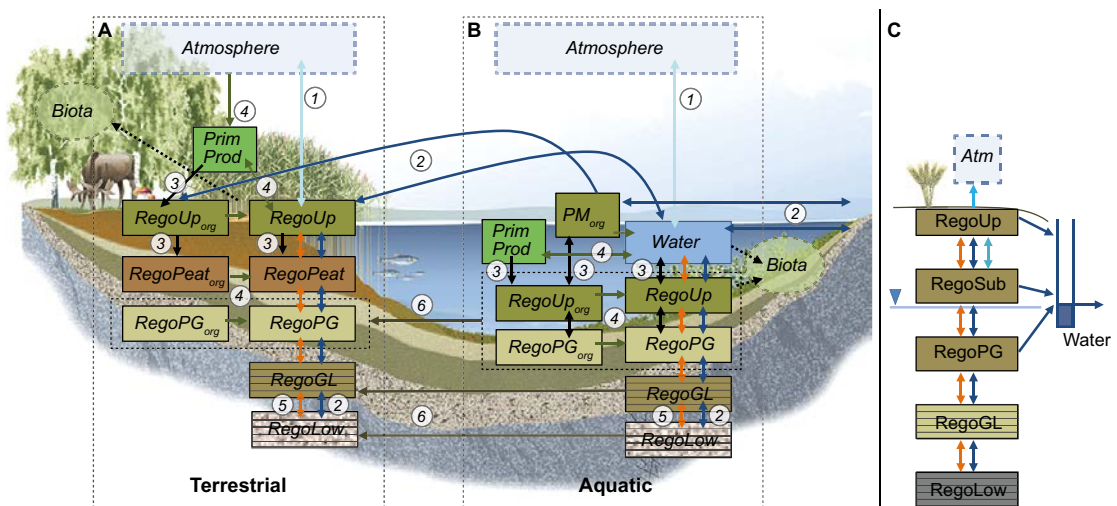


**Figure 7-7.** Schematic representation of the biosphere radionuclide transport model for simulating transport and accumulation in a discharge area with two natural ecosystems delimited by thin dotted black lines (A, B) and a discharge area with a permanent agricultural ecosystem (C). Each box within the three ecosystems corresponds to a radionuclide inventory associated with a physical compartment. Note that in SE-SFL, the lower regolith layers are represented by five sub-compartments each. Arrows represent radionuclide fluxes between compartments and fluxes into and out of the system. Radionuclide fluxes are linked to mass fluxes of solutes (orange), gas (1, light blue), water (2, dark blue) and solid matter (3, black), to transitions between inorganic and organic forms of radionuclides (4, green), to diffusion in soil pore water (5, red), and to ingrowth of wetland vegetation (6). The atmosphere also serves as a source and sink of radionuclides. The water from the three uppermost regolith compartments in (C) is in the model drained to a ditch. The activity concentrations in atmosphere and crop are calculated assuming equilibrium. Figure adapted from the **Biosphere synthesis**.

Non-coupled versions of the biosphere sub-models for mire and aquatic ecosystems are also explored to study the radionuclide concentrations in these ecosystems under stationary conditions. See Chapter 4.4.2 in the **Radionuclide transport report** for a full description of all compartments and transport processes in the biosphere model.

In the model, radionuclides are released from the geosphere to the deepest regolith layer (RegoLow) of a biosphere object. The dynamic change in the radionuclide content of each compartment is related to the flow of water, solid matter or gas, as well as diffusion, photosynthesis, mineralisation and radioactive decay and in-growth. The endpoints of the transport modelling are radionuclide concentrations in environmental media, that is, ground- and surface waters, the various layers of the regolith, mire vegetation, and the atmosphere. Humans, plants and animals are then assumed to be in contact with the radionuclides through these media. All the processes that are incorporated in the model are discussed in the **Biosphere synthesis**, where the relevant transport equations are also given.

### Human exposure

Radionuclide concentrations in soil, water, air and organisms are used when calculating the dose to humans. Doses arise from external exposure (radiation from the ground, air and water), inhalation of radionuclides and, most importantly, through ingestion of radionuclides through food and water (Figure 7-8), depending on the type of ecosystem. Natural, marine ecosystems (sea bays) can be used for food and as a source for organic fertilizers, but not for cultivation. The possibility to use the biosphere object for agriculture and water supply increases when the shoreline has migrated past it.

The selection of exposure pathways is based on the findings in SR-PSU (SKB 2014f). Potentially important pathways were identified and mapped to one or more exposed human groups. The exclusion of pathways with insignificant dose contributions in SR-PSU (e.g. adventitious ingestion of sediments) was confirmed to be reasonable also in SE-SFL (**Biosphere synthesis**).

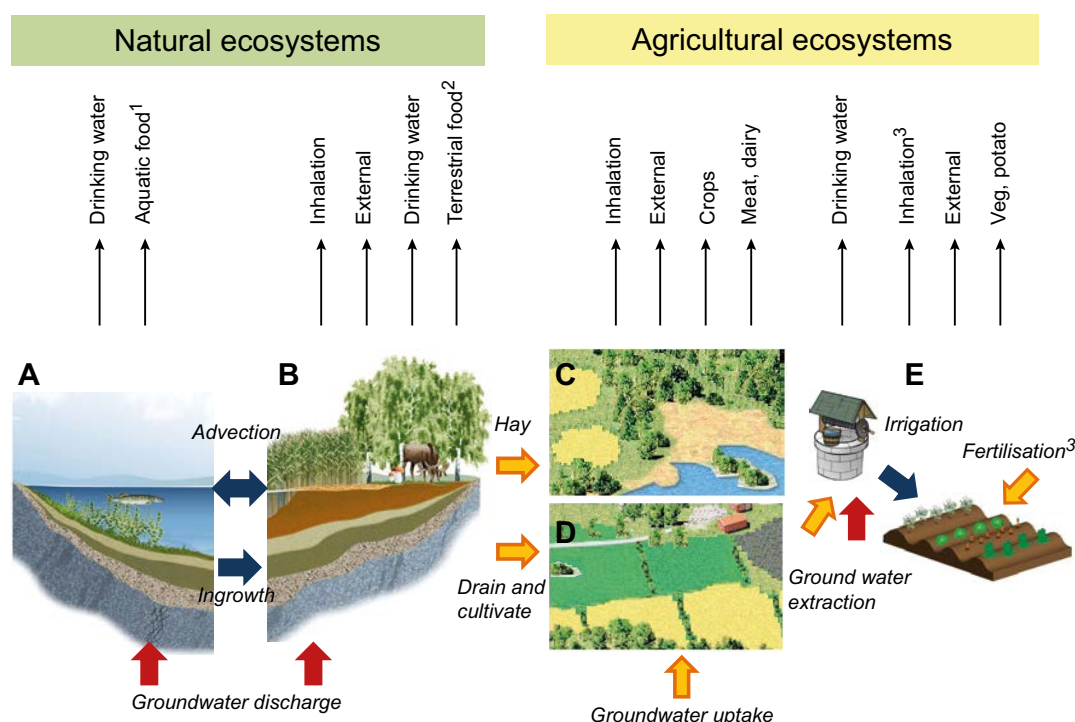


**Figure 7-8.** Exposure pathways included in the dose calculations for exposed populations using natural resources and/or living in biosphere objects. Hunter-gatherers use natural aquatic (A) and mire (B) ecosystems. The other three exposed populations represent different uses of arable land, namely infield-outland agriculture (C), draining and cultivating a mire (D) and small-scale horticulture on a garden plot (E). Bold arrows represent input of radionuclides from the bedrock (red), from natural ecosystems or deep regolith deposits (orange), or water-bound transfer of radionuclides within the biosphere (blue). The thin arrows (top) represent exposure routes, where the superscripts: 1 = fish and crayfish, 2 = game, berries and mushrooms, and 3 includes radionuclides from combustion of biofuel. Figure from the **Biosphere synthesis**.

Four types of human populations were identified as most exposed to dose through all major exposure pathways, and thus included in the analysis of SE-SFL, just as in SR-PSU (SKB 2014f):

**Hunter-gatherers (HG)** – A hunter and gatherer community, assumed to consist of 30 individuals that utilise a forage area of approximately 200 km<sup>2</sup> of undisturbed biosphere. The major exposure pathways are from fishing, hunting, and gathering berries and mushrooms in discharge areas, and from drinking surface freshwater. Typical land use and habits are taken from historical records.

**Infield–outland farmers (IO)** – Self-sustained agricultural community, assumed to comprise 10 individuals, where infield farming of crops is dependent on nutrients from a wetland area (outland), assumed forage area 0.1 km<sup>2</sup> = 10 ha. Radionuclides in wetland hay reach the cultivated soil through fertilization with manure. The major exposure pathways are from growing food and raising live-stock, and from drinking water from a dug well or from surface water.

**Family farmers (DM/Agr)** – Self-sustained industrial agricultural community, assumed to comprise 10 individuals, on a former lake or wetland. Both crops and fodder are cultivated on organic soils, requiring an assumed area of 6 ha. Radionuclides reach the cultivated soil through plant uptake from groundwater (DM and Agr) and may have accumulated for an extended time prior to drainage (DM). The major exposure pathways are from growing food and raising livestock and from drinking water from a dug well or from surface water.

**Garden-plot households (GP)** – A household, assuming 5 individuals that are self-sustained with respect to vegetables and root crops produced through small-scale horticulture on a 270 m<sup>2</sup> area garden plot. Radionuclides reach the cultivated soil through fertilization (with algae or biomass ash) and irrigation. The major exposure pathways are from growing food and from drinking water from a dug well or from surface water.

The HG community uses undisturbed ecosystems, whereas the other three groups actively cultivate the land. For HG and DM/Agr, exposure occurs within the boundaries of the biosphere object, whereas the IO and GP groups can be exposed while living outside the biosphere object by utilizing resources from inside it, e.g. organic fertilizers, biofuel or irrigation water.

## 7.4 Present-day evaluation case

### 7.4.1 Rationale

The *present-day evaluation case* constitutes the base case for the evaluation of post-closure safety for the proposed repository concept for SFL at an example site (Section 2.5.8). It is simplified and stylised for ease of interpretation and straightforward comparison with the other evaluation cases with alternative assumptions or temporal evolutions. The base case assumes constant, present-day climatic and other external conditions throughout the full assessment period, whereas the internal conditions evolve according to the base variant of the reference evolution (Chapter 6.2). It is further assumed, as in all evaluation cases in SE-SFL, that the repository is constructed according to the proposed design concept. Most cases assume that the repository is constructed at the example location, but the effects of constructing the repository below the sea are separately explored in the *initially submerged conditions evaluation case* (Section 8.4.2).

Importantly, since SE-SFL is not part of a licensing application, the base case is not intended to establish a main scenario as defined by the regulatory guidelines (SSM 2008a). Similarly, for the remaining evaluation cases, the term scenario is not used since a broader approach is applied in their selection than that proposed by the authorities (SSM 2008a).

The following sections describe the implementation of the three respective domain radionuclide transport models, including assumptions made and parameter values used. Most of the assumptions in the transport and dose modelling in SE-SFL are based on corresponding assumptions in SR-PSU and/or SR-Site, with some additional simplifications in the near-field due to the preliminary nature of SE-SFL. For a detailed description of the assumptions made in the radionuclide transport and dose modelling for the base case, see Section 5.2 in the **Radionuclide transport report**.

## 7.4.2 Handling in the near-field

The radionuclide transport calculations in the near-field require information on flow-related and non-flow-related migration properties and their development in time. The repository is assumed to become instantly saturated with groundwater upon closure and remains so for the full assessment period. Diffusion and advection will move the dissolved radionuclides away from the waste, through the engineered barriers (backfills), to the surrounding bedrock. See Chapter 2 of Shahkarami (2019) for a complete description of the data used and Chapter 5.2.3 in the **Radionuclide transport report** for more details on the implementation.

### **Radionuclide release from the waste**

#### **BHA**

There is limited knowledge about the BHA radionuclide inventory due to its legacy nature (Section 4.2.7). Thus, it is pessimistically assumed that all BHA radionuclides are dissolved in the porewater of the waste compartment and are available for transport immediately after repository closure. This is even though some of the radionuclides are likely to be contained within solid and non-soluble materials (Section 2.3.1 in Shahkarami 2019).

#### **BHK**

The waste in BHK mainly contains metallic components with neutron-induced activity (Section 4.2.1). The activity is assumed to be evenly distributed within each metallic component, since the neutrons that induce the activity have a penetration depth, depending on temperature and neutron energy, of several centimetres in steel, which is larger than the metal thickness. The release of this activity is controlled by corrosion according to the reference evolution (Section 6.2.8).

The corrosion rate is assumed to remain constant at 10 nm/a, based on the parameterisation of corrosion rates of stainless steel under alkaline, anoxic conditions in SR-SPU (Table 5-4 in SKB 2014h, Shahkarami 2019). Given the assumptions of constant corrosion rate and no solubility limitations, the time required for complete corrosion of a metallic component depends only on its thickness. In the near-field modelling, the range of component thicknesses is discretised into four categories: all components thicker than 20 mm are conservatively assumed to be exactly 20 mm (corresponding to a corrosion time of 1 000 000 years), components 10–20 mm thick are assumed exactly 10 mm (corrosion time 500 000 a), components 1–10 mm thick are assumed exactly 1 mm (corrosion time 50 000 a), and components thinner than 1 mm are assumed to be instantly dissolved upon repository closure (instant-release fraction). An alternative assumption on the corrosion rate is investigated in the *lower steel corrosion rate evaluation case* (Section 8.3.2).

### **Flow-related properties**

The water-flow properties described here have a direct effect on the advective transport rate for radionuclides in the near-field transport model. Since the hydrogeological system in the bedrock surrounding the repository is assumed to be constant during the complete analysis period of 1 million years (Section 6.2.6), the future evolution of the near-field hydrogeology is determined by the hydraulic properties of the repository itself and its components. The bentonite backfill in BHA and the concrete backfill in BHK are both designed to retard the release of radionuclides from the near-field but they are assumed to evolve differently in time, as follows.

#### **BHA**

The bentonite is assumed to have constant transport properties over the whole simulation period; potential effects of bentonite erosion, homogenisation, degradation, and chemical evolution are evaluated in the reference evolution (Section 6.2.9). These effects are mostly relatively small, and so are neglected in SE-SFL but require further exploration in future safety assessments. Thus, for BHA, the near-field flows are constant during the complete SE-SFL analysis period.

In the near-field transport model for BHA, water flow through waste and backfill is simplified; flow is assumed only in the direction along the vault (Section 2.6.3 in Shahkarami 2019 and Section 7.3.2). A hydraulic conductivity of the bentonite backfill of  $1.0 \times 10^{-13}$  m/s is assumed (Table 3-9 in Joyce et al. 2019, Table 3-2 in Abarca et al. 2019) and the resulting flow through the entire vault is  $2.2 \times 10^{-2}$  m<sup>3</sup>/a (Section 6.2.6). The water flow from the waste compartment towards the backfill outflow compartment is taken as the sum of the flows through the vault control volumes in the hydrological modelling by Abarca et al. (2019), amounting to  $1.6 \times 10^{-3}$  m<sup>3</sup>/a. This flow rate is applied for the entire analysis period of one million years.

## BHK

The reference evolution of the concrete considered in the *present-day evaluation case* (Section 6.2.10), cautiously assumes an effective hydraulic conductivity of  $8.3 \times 10^{-10}$  m/s, as was adopted for concrete structures in SR-PSU (SKB 2014h). Concrete with a lower hydraulic conductivity, as well as lower effective diffusivity, is under development within SR-PSU and the effect of such a concrete is evaluated in the *alternative concrete backfill in BHK evaluation case* (Section 8.3.3).

Unlike the bentonite in BHA, the concrete backfill is assumed to degrade over time, mainly driven by dissolution and leaching of cement hydrates (Idiart and Laviña 2019). The degradation affects the hydraulic conductivity, and thus groundwater flow in the waste vault (Section 6.2.6). In the near-field transport model for BHK, the degradation-induced time evolution of the groundwater flow is assumed to follow the degradation sequence of the near-field hydrology modelling by Abarca et al. (2019). That is, the gradual degradation described in the reference evolution (Section 6.2.10) is simplified via a discretisation into three consecutive states. These three degradation states, and the time periods over which they are applied in the transport modelling, are:

- *Intact concrete*: The concrete backfill is intact and essentially unaffected by leaching. This state holds for 85 ka after repository closure, until the portlandite has leached out of the outer quarter of the backfill.
- *Degraded zone*: Leaching of cement minerals has resulted in degraded, significantly more permeable concrete in the outer half than in the inner, intact half of the concrete backfill. This is assumed to prevail during the subsequent ~700 ka until the calcium-silicate-hydrate gel (C-S-H) in the outer half of the backfill has leached out.
- *Degraded concrete*: The full backfill volume has now degraded, resulting in substantially higher hydraulic conductivity compared with the intact concrete state, assumed to last for the remainder of the total analysis period of one million years.

Hydraulic conditions corresponding to these three respective states were used to model the water flows for advection (and, implicitly, dispersion) in three separate calculations of the near-field hydrogeology (Abarca et al. 2019).

During the intact-concrete period, the total flow through the BHK waste vault is two orders of magnitude higher than the flow through BHA (Section 2.6.3–2.6.4 in Shahkarami 2019), correlating with the hydraulic conductivities of  $1 \times 10^{-12}$  m/s for bentonite backfill in BHA and  $8.3 \times 10^{-10}$  m/s for intact concrete in BHK. In the degraded-zone state, a higher hydraulic conductivity of  $1 \times 10^{-7}$  m/s in the symmetrically defined outer half of the BHK concrete backfill leads to a hydraulic-cage effect. It acts as a bypass, redirecting water around the waste (Abarca et al. 2019 and Section 6.2.6), resulting in a water flow that compared with the intact concrete period is lower through the waste, but higher through the BHK vault as a whole. The resulting average flow rates through vault and waste compartment are shown in Figure 6-7, and the rates specifically through outflow and side compartments are shown in Figure 7-9.

The near-field transport model for BHK assumes that water flow enters the vault from above and leaves through the floor and sides of the vault (Section 2.6.4 in Shahkarami 2019 and Section 7.3.2). Initially, the water flow from the waste compartment to the outflow (i.e. floor) compartment is 0.696 m<sup>3</sup>/a, and 0.020 m<sup>3</sup>/a to the side compartment (Figure 7-9). During the subsequent degraded-zone period, the hydraulic-cage effect cuts the flow by about half. Finally, during the degraded-concrete period, the water flow from the waste to the outflow and side compartments shows a clear increase compared with intact concrete.

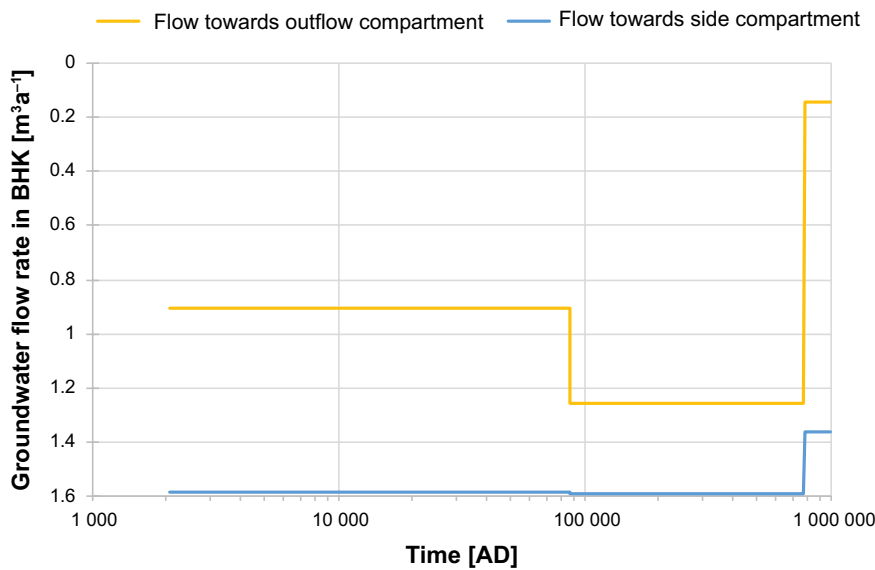


**Figure 7-9.** Groundwater flow rates from the waste towards the outflow backfill and side backfill compartments in BHK, according to the discretised concrete-degradation time evolution applied in the near-field transport model. Data described in Sections 2.6.4 in Shahkarami (2019).

### Porosity and diffusion

In the waste compartments of both vaults, a constant effective diffusivity  $D_e$  of  $2.0 \times 10^{-9}$  m<sup>2</sup>/s, is conservatively assumed for all radionuclides (Sections 2.6.1 and 2.6.2 in Shahkarami 2019). For the concrete structures surrounding the waste in both BHA and BHK, the porosity is assumed to increase with time in a similar manner as the development assumed for the BHK concrete backfill outflow compartments, shown in Figure 7-10 (Section 2.5.1 in Shahkarami 2019). This is a conservative assumption for BHA, since the low-permeability bentonite is likely to delay concrete leaching in the BHA waste domain compared with BHK (Section 6.2.8).

### BHA

Unlike the concrete in BHK, the porosity and effective diffusivity of the bentonite backfill in BHA are assumed to be constant over the full assessment period (Sections 2.7.1 and 2.8.1 in Shahkarami 2019). Both the effective diffusivity and the diffusion-available porosity are assumed to be lower for radionuclides assumed to speciate into anionic compounds compared with those that form cations or neutral species. The diffusion-available porosity  $\varepsilon$  for cations and neutral species is 0.43 and for anions it is 0.17. The effective diffusivity in the bentonite backfill in BHA for both anions ( $D_e = 1.0 \times 10^{-11}$  m<sup>2</sup>/s) and cations and neutral species ( $D_e = 1.2 \times 10^{-10}$  m<sup>2</sup>/s) exceeds that of the intact concrete backfill in BHK.

As described in Section 7.3.2, diffusive transport from the boundary compartments to the seeping water in the fractured rock is determined by the diffusive resistance  $R_b$  against transport between neighbouring compartments, the plug resistance  $R_{\text{plug}}$  and the equivalent flow rate  $Q_{\text{eq}}$  (Equation 7-5). The value of  $Q_{\text{eq}}$  is 0.187 m<sup>3</sup>/a for BHA, and due to a high plug resistance at the bentonite-fracture interface, the rate of diffusive transport from BHA to the bedrock is lower than from BHK. Nevertheless, transport out from BHA is still dominated by diffusion since advective transport out from BHA is even lower due to high hydraulic resistance and low advective flow  $Q_b$  (Abarca et al. 2019).

### BHK

Just like the flow-related properties, the porosity and effective diffusivity of concrete evolve in time due to chemical degradation of the material. A simplified development of the porosity and effective diffusivity of the inner and outer parts of the BHK concrete backfill (Table B-2 in Idiart and Laviña 2019), is used in the near-field model (Sections 2.7.1 and 2.8 in Shahkarami 2019). In addition to the spatially symmetric degradation assumed for the flow-related properties, the porosity and effective diffusivity

are assumed to increase faster due to concrete degradation where incoming groundwater meets the backfill than where water leaves the backfill (Section 6.2.10). Therefore, during the degraded-zone and degraded-concrete states, the concrete properties representing the more degraded outer backfill in Idiart and Laviña (2019) are used for the inflow compartment in the near-field radionuclide transport model for BHK, and the inner-backfill properties from Idiart and Laviña (2019) are used for the less affected outflow and side compartments (Figure 7-10). The concrete structures holding the waste in both vaults are assumed to follow the outflow-compartment development.

Diffusive transport inside BHK changes with the porosity and effective diffusivity. Diffusion out to the vault-geosphere interface additionally depends on the equivalent flow rate  $Q_{eq}$  and plug resistance  $R_{plug}$  (Equation 7-5). The  $R_{plug}$  for concrete is smaller than the other terms in the denominator of Equation 7-5 so it is conservatively neglected in the BHK near-field modelling. The rate of diffusive transport from BHK to the bedrock is significantly higher than from BHA, both for anions and cations, due to the high plug resistance at the bentonite-fracture interface in BHA compared with the internal resistance in the border concrete compartment in BHK.

During the initial, intact-concrete period for BHK, the total equivalent flow rate  $Q_{eq}$  summed over all fractures that intersect the vault is  $0.251 \text{ m}^3/\text{a}$ , as compared with  $0.187 \text{ m}^3/\text{a}$  for BHA (Sections 2.9.2 and 2.9.6 in Shahkarami 2019). To account for the simulated increased flow in the outer concrete during the degraded-zone period in BHK (Abarca et al. 2019),  $Q_{eq}$  is increased to be the difference between the water flow in the degraded part and the intact part of the concrete. The resulting total equivalent flow rate is  $4.52 \text{ m}^3/\text{a}$  during this period (Section 2.9.6 in Shahkarami 2019). Further, the diffusion length is divided by two to account for the reduced amount of intact concrete during this period. These two changes result in an increased rate of diffusive transport from BHK to the bedrock as compared with the intact period. During the final, degraded-concrete period, a decrease of the diffusive transport rate is observed.

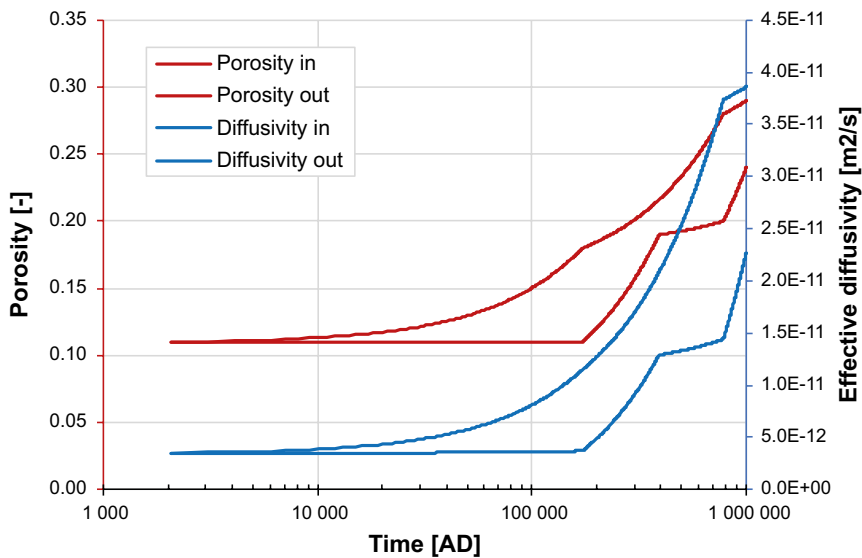


**Figure 7-10.** Development of porosity and effective diffusivity due to concrete degradation in the BHK backfill, in the inflow compartment (solid lines) and the outflow compartments (dashed lines). The data are linearly interpolated between the time points given in Table B-2 in Idiart and Laviña (2019), i.e. at repository closure (2075 AD), and at 170, 390, 780, and 1 000 ka after closure. The data are described in Sections 2.7 and 2.8 of Shahkarami (2019).

### **Sorption-related properties**

Some radionuclides form chemical species that can sorb onto cementitious materials and bentonite in the waste vaults. A certain fraction of these radionuclides will thus be immobilized on the solid phase, allowing time for radioactive decay and ingrowth before the radionuclide content is transported out of the waste vault. The handling of three sorption-related parameters is described in the following: sorption coefficients  $K_d$ , retardation coefficients  $R$ , and sorption reduction factors.

The degree of sorption is represented by the sorption coefficient  $K_d$  [ $\text{m}^3 \text{kg}^{-1}$ ] that expresses the ratio between the adsorbed mass concentration onto the solid phase and the mass concentration in the fluid (Tables 2-18 and 2-31 in Shahkarami 2019 and Section 7.3.2 above).

The unitless retardation coefficient  $R$  is a measure of the barrier's capability to retard the transport of radionuclides by means of sorption. It is closely related to the capacity factor for the geosphere given in Equation 7-8.

$$R = 1 + K_d \times \frac{m}{V\varepsilon} \quad 7-16$$

Here,  $K_d$  is the sorption coefficient [ $\text{m}^3 \text{kg}^{-1}$ ],  $m$  is the mass [kg] of the sorbing material,  $V$  is its total volume [ $\text{m}^3$ ], and  $\varepsilon$  is its unitless porosity. The retardation coefficient describes by how much the transport of a radionuclide subjected to sorption is retarded compared with the velocity of the flowing water in the pore spaces, i.e. with the transport velocity of a non-sorbing radionuclide. The inverse of the retardation coefficient can be interpreted as the fraction of a radionuclide in the barrier that is dissolved within the pore volume of the barrier material. The minimum value of  $R$  is unity and occurs when sorption does not occur ( $K_d = 0$ ).

### **BHA**

Cellulose is present in some of the BHA waste, e.g. in wood, paper and cotton tissues. It is a precursor to the complexing agent isosaccarinate (ISA) that is formed by hydrolysis of cellulose in a  $\text{Ca}^{2+}$ -rich alkaline environment (Section 6.2.8). To account for the solubility enhancement due to complexation, sorption of specific radionuclides in BHA is reduced by dividing the  $K_d$  values by a sorption reduction factor ranging from 1 to 10 000 (Table 2-20 in Shahkarami 2019).

The sorption reduction factors are taken from SR-PSU for solubility-limited concentrations of ISA in portlandite-buffered water (SKB 2014h). The sorption reduction factors are applied in BHA during the complete analysis period of one million years. As such, it is conservatively assumed that complexation is not affected by the evolution in the waste vault, and that the amount of complexing agents is not reduced by degradation or out-transport. The effect of this assumption is evaluated in the *no effect of complexing agents in BHA* evaluation case (Section 8.3.1).

The retardation coefficient for each radionuclide in BHA is constant throughout the assessment period since the barrier is assumed to remain fully intact. However, the retardation coefficient varies over four orders of magnitude between the assessed radionuclides, from  $R = 1$  (e.g. Mo) to  $R = 28\,000$  for Nb, including the effect of sorption reduction factors. Sorption coefficients and sorption reduction factors of the BHA radionuclides that contribute most to the near-field releases in the *present-day evaluation case* are given in Table 7-1.

### **BHK**

In BHK, no organic material that might form metal-organic complexes will be present. However, the sorption coefficients in BHK are affected by the changes in the chemical conditions in the waste vault, where concrete chemical degradation is associated with a pH evolution (Section 6.2.10). Thus,  $K_d$  values are assumed to vary over time, based on the simplified pH development (Table B-1 in Idiart and Laviña 2019), as described in the reference evolution (Section 6.2.10). Four  $K_d$  values are used for each radionuclide, corresponding to points in time when  $\text{pH} > 12.5$  (state I),  $\text{pH} \approx 12.5$  (state II),  $\text{pH} \approx 12$  (state IIIa), and  $\text{pH} \approx 10.5$  (state IIIb), respectively (Shahkarami 2019). Between these time points,  $K_d$  is estimated by linear interpolation between them. As described in the previous sub-sections, the concrete chemical degradation is assumed to occur faster where incoming groundwater meets the backfill than where it leaves the vault. Therefore, the evolution of pH and thus of  $K_d$  is faster in the inflow compartments than in the waste, outflow, and side compartments of BHK (Table 2-19 in Shahkarami 2019).

The sorption of Ca serves as an interesting example. It starts with a modest  $K_d$  of 0.035 m<sup>3</sup>/kg in state I but then, mainly because of lower pH due to concrete leaching,  $K_d$  decreases to about 0.003 m<sup>3</sup>/kg in states II and IIIa. Then in state IIIb, it increases again to 0.047 m<sup>3</sup>/kg due to changes in the concrete mineral composition (Table 2-18 in Shahkarami 2019). Sorption coefficients of the BHK radionuclides that contribute most to the near-field releases in the *present-day evaluation case* are given in Table 7-1.

The retardation coefficients  $R$  depend on  $K_d$ , but also on the porosity  $\varepsilon$  (Equation 7-16). Consequently,  $R$  for all sorbing nuclides decreases gradually with time as  $\varepsilon$  increases due the concrete pore-volume increase via leaching (Figure 7-10), which is superimposed on the effect of changing  $K_d$  values associated with pH (Figure 5-4 in the **Radionuclide transport report**).

**Table 7-1. Properties of the radionuclides that are among the top-three contributors to either the near-field releases, geosphere releases, or dose, from BHA or BHK. Sorption coefficients ( $K_d$ ) in bentonite, in cement (states I and IIIb), and in the geosphere, and sorption reduction factors. The corresponding information for all radionuclides and cement degradation states is given in Sections 2.5.5, 2.5.6, 2.7.4, 2.7.5, 2.7.6, and 3.3.5 in Shahkarami (2019).**

Radionuclide	Half-life [a]	$K_d$ bentonite [m <sup>3</sup> /kg]	$K_d$ cement state I [m <sup>3</sup> /kg] /state IIIb [m <sup>3</sup> /kg]	$K_d$ geosphere [m <sup>3</sup> /kg]	Sorption reduction factor in BHA
Ag-108m	438	0	0 / 0	0.00065	1
C-14-org	5730	0	0 / 0	0	1
C-14-ind	5730	0	0 / 0	0	1
Ca-41	103 000	0.005	0.035 / 0.047	0	1
Cl-36	301 000	0	0.001 / 0.001	0	1
Mo-93	4 000	0	0.003 / 0	0	1
Ni-59	76 000	0.3	0.03 / 0.2	0.0021	1
Tc-99	211 000	63	3.0 / 3.0	0.099	10 000

### 7.4.3 Handling in the geosphere

The geosphere properties evolve according to the reference evolution (Chapter 6), as do the near-field properties. The SE-SFL geosphere modelling uses flow-related migration properties taken from the hydrogeological modelling (Joyce et al. 2019) whereas the non-flow-related migration properties are taken from the safety analysis work for the Laxemar area within SR-Site (SKB 2010f). For a few radionuclides that were not included in SR-Site, data were taken from SR-PSU and, for a handful of radionuclides, properties were approximated from element analogues (Section 3.3 in Shahkarami 2019).

#### **Flow-related migration properties**

In the *present-day evaluation case*, the groundwater flow is assumed constant. Of the five realisations of the discrete fracture network model, the first realisation is used, which includes deterministic hydraulic properties within deterministically defined deformation zones (Section 6.2.5 and Joyce et al. 2019). The results are calculated without consideration of hydrogeochemical effects, noting that these effects are very small (Section 6.2.7). In this fracture network realisation, the repository is comparatively well connected to the geosphere compared with the other realisations with stochastic hydraulic properties (Section 4.4.1 in Joyce et al. 2019), which implies that the flow paths are more numerous and/or have higher flows that can transport radionuclides. The choice of fracture network can thus be described as cautious, and the effect of this choice is evaluated in the *alternative realisations of stochastic bedrock fractures evaluation case* (Section 8.5.1). Furthermore, the effects of a different bedrock with more favourable hydraulic properties is investigated in the *lower groundwater flow evaluation case* (Section 8.4.1).

In the particle-tracking calculations, ten particles were released into each of the rock fractures intersecting the BHA and BHK vaults and tracked through the fracture network to the surface (Joyce et al. 2019). At most ~50 % of the particles were expected to successfully reach the surface, assuming similar number of fractures with flow towards the surface or into the vault. Of the 9590 particles released, 4459 were tracked to the surface. Most of the remaining particles flowed into the repository and were not further tracked, and the last, small fraction of particles were halted somewhere in

the geosphere due to e.g. constricted flow paths or poor connectivity. For every particle track that reached the surface, flow-related properties were summed along the sections of the trajectory: travel time  $t_w$  [a], F-factor [ $\text{a m}^{-1}$ ] and a volume-specific flow-wetted area  $a_w = \text{F-factor}/t_w$  [ $\text{m}^2/\text{m}^3$ ]. This represents the travel-time-weighted average relative area along the flow pathway.

A summary of the flow-property statistics along the pathways is given in Table 7-2. The differences between the vaults relate to their respective placements in an heterogeneously fractured bedrock. More details can be found in Joyce et al. (2019).

**Table 7-2. Statistics for flow-related migration properties for the DFN realisation used in the base case. Data from Joyce et al. (2019).**

Waste Vault Statistic	Travel time $t_w$ [a]	F-factor [ $\text{a m}^{-1}$ ]	Relative flow-wetted area $a_w$ [ $\text{m}^2 \text{m}^{-3}$ ]	Trajectory length $L$ [m]
<b>BHA</b>				
Average	$8.98 \times 10^2$	$2.13 \times 10^5$	$6.25 \times 10^2$	$2.43 \times 10^3$
Median	$2.43 \times 10^2$	$7.88 \times 10^4$	$3.20 \times 10^2$	$2.18 \times 10^3$
Min	$3.28 \times 10^1$	$9.46 \times 10^3$	$2.20 \times 10^1$	$1.38 \times 10^3$
Max	$5.12 \times 10^4$	$4.78 \times 10^6$	$4.19 \times 10^3$	$1.32 \times 10^4$
<b>BHK</b>				
Average	$2.09 \times 10^2$	$6.59 \times 10^4$	$3.93 \times 10^2$	$2.28 \times 10^3$
Median	$1.45 \times 10^2$	$4.75 \times 10^4$	$3.24 \times 10^2$	$2.09 \times 10^3$
Min	$3.55 \times 10^1$	$7.86 \times 10^3$	$2.50 \times 10^1$	$1.45 \times 10^3$
Max	$3.93 \times 10^3$	$2.47 \times 10^6$	$2.09 \times 10^3$	$1.37 \times 10^4$

Note that 2424 particle pathways reached the surface from BHA, whereas the corresponding number from BHK is 2035.

### **Non-flow-related migration properties**

The non-flow-related migration properties used in the geosphere transport modelling are summarised in Table 7-3. The sorption coefficients and half-lives of the radionuclides that give the largest contributions to geosphere releases in the *present-day evaluation case* are given in Table 7-1. In the model calculations, radionuclides are allowed to penetrate up to a distance  $d_{\text{max}} = 4.5$  m into the rock matrix, corresponding to half the average spacing between conductive fractures at the Laxemar site (Figure 7-5). The sensitivity to these parameters is studied in the *alternative geosphere retention properties* evaluation case (Section 8.4.3).

**Table 7-3. Non-flow-related migration properties. Data described in Sections 2.4 and 3.3 in Shahkarami (2019).**

Parameter	Value
Rock matrix porosity [%]	0.19
Effective diffusivity cations and non-charged species [ $\text{m}^2/\text{s}$ ] <sup>a</sup>	$2.7 \times 10^{-14}$
Effective diffusivity anions [ $\text{m}^2/\text{s}$ ] <sup>b</sup>	$8.5 \times 10^{-15}$
Maximum penetration depth in the rock matrix [m]	4.5
Rock matrix density [ $\text{kg}/\text{m}^3$ ]	2700
Geosphere sorption coefficient [ $\text{m}^3 \text{kg}^{-1}$ ]	Radionuclide-specific
Radionuclide half-life [ $\text{a}^{-1}$ ]	Radionuclide-specific
Decay chain and branching ratio	Radionuclide-specific

<sup>a</sup> Ac, Am, Ar, Ba, Be, Ca, Cd, Cm, C-org, Cs, Eu, Gd, Ho, K, Ni, Np, Pa, Pb, Pd, Pu, Ra, Sm, Sr.

<sup>b</sup> Ag, C-inorg, Cl, Co, H, I, La, Mo, Nb, Po, Re, Se, Si, Tb, Tc, Th, Ti, U, Zr.

Note that some radionuclides are assumed to belong to different species categories (anion vs. cation/neutral) for different purposes, for example in the geosphere vs. in bentonite vs. in concrete, depending on assumptions regarding conditions such as redox potential, pH, and water composition. For several radionuclides, highly conservative assumptions regarding speciation and transport properties are warranted due to the presence of large uncertainties (Section 3.3.1 in Shahkarami 2019).

#### 7.4.4 Handling in the biosphere

The SE-SFL biosphere radionuclide transport model accounts for landscape development and surface hydrology for the relevant ecosystems (Section 7.3.4). The model relies on several ecosystem parameters and definitions of the exposed human groups as described in the following.

##### **Landscape development**

The development of surface systems is included in the repository reference evolution (Section 6.2.2). As noted in Section 7.3.3, the total radionuclide release from the geosphere into the biosphere model is pessimistically assumed to be discharged homogeneously into a single biosphere object. Object 206 was chosen, because it received a major part of the tracked particles in most of the regional hydrogeology simulations. Since this is an agricultural ecosystem rather than natural, the ongoing shoreline displacement and landscape development are neglected. Hence, the ecosystem properties are assumed to be constant during the entire analysis period, including the present regolith layer thicknesses (Nyman et al. 2008). An alternative state of the discharge area is also assessed in this evaluation case, namely a mire ecosystem that could have developed in the lake basin of 206 in the absence of human intervention. For more details, see Chapter 3 in Grolander and Jaeschke (2019). The effects of choice of discharge area are studied in the *alternative discharge area evaluation case* (Section 8.5.2).

##### **Surface hydrology**

Hydrological flow rates for the two ecosystem states of object 206 are obtained from two separate water-balance models based on its present conditions. Two corresponding regolith profiles are used. In one, the upper soil layers in the agricultural field are assumed to be unsaturated and drained by ditches surrounding the cultivated land (Figure 7-7C). In contrast, in the mire ecosystem state, all regolith layers are assumed to be saturated and excess ground and surface water is discharged into a central stream.

##### **Ecosystem parameters**

In SR-PSU, parameter values reflected the present and future conditions of the Forsmark area. The present-day regional climate for Laxemar is similar to that at Forsmark, 1.4 °C warmer average annual temperature and with an average of 53 mm more annual precipitation (Chapter 3 in the **Climate report**). Consequently, most parameter values derived for terrestrial ecosystems in Forsmark (Grolander 2013) are relevant also for SE-SFL (Chapter 8 in Grolander and Jaeschke 2019). However, the values of a few terrestrial ecosystem parameters have been updated in SE-SFL to reflect the conditions in Laxemar, including the length of the irrigation season for a garden plot and the wind velocity at 10 m height. The sensitivity to climatic properties is evaluated in the *alternative regional climate* (Section 8.4.4), *increased greenhouse effect* (Section 8.6.1), and *simplified glacial cycle evaluation cases* (Section 8.6.2).

Moreover, not all element distribution and transfer factors (i.e.  $K_d$  and concentration ratio (CR) values) derived for Forsmark are considered applicable to the Laxemar site, as the geochemical properties of the two sites differ (Chapter 6 in Grolander and Jaeschke 2019). In SE-SFL, values for element-specific parameters are based on data from Laxemar when available. Due to a model update, a handful of new parameters are introduced in SE-SFL, including soil respiration, the fraction of inorganic chlorine in primary producers, and the concentrations of three essential elements: Ca, Cl and K, in plants, fungi and soil pore water. In addition, parameters for eight new elements (Be, Gd, K, La, Re, Si, Tb, and Ti) are included in SE-SFL, and values for these are approximated from element analogues.

##### **Exposed populations**

Exposure pathways include ingestion of food and drinking water, inhalation from respiration, and direct external radiation. Ingestion of food is expected to be the most important exposure pathway, and consequently the exposed population of primary interest is self-sustaining farmers. For the agricultural ecosystem state, the land-use and productivity of a family farm (Agr) from the turn of the nineteenth century is assumed (Section 7.3.4, Saetre et al. 2013, Grolander 2013). For the mire ecosystem state, all the land-use variants from SR-PSU are studied, including hunter-gatherers (HG), infield–outland

farmers (IO), and a garden-plot household (GP). Potential exposure from draining the mire and cultivating it for 50 years is also assessed (DM), using the same assumptions for land use and productivity as for the Agr group. Historical data have been used to define parameter values that reflect typical land use, habits and agrarian productivity for all human groups, except for GP for which present-day habits have been assumed (**Biosphere synthesis**).

#### **7.4.5 Simplifications in comparison to the reference evolution**

The three climate variants of the reference evolution are defined to be simplified compared to the most realistic projections of future climate developments (Chapter 6). Additionally, certain aspects of the reference evolution that are judged to be of minor importance or have been handled by cautious assumptions in order to account for uncertainties are further simplified and sometimes omitted in the transport calculations, as described for the *present-day evaluation case* in the following subsections. Most of the assumptions made in SE-SFL are based on corresponding assumptions made in SR-PSU or SR-Site, or both. The level of detail applied in the SE-SFL geosphere and biosphere models is similar to that in previous safety assessments, but the near-field model is less detailed in certain aspects.

Simplifications compared with the other two variants of the reference evolution, *increased greenhouse effect* and *simplified glacial cycle*, are described in connection with the corresponding evaluation cases in Sections 8.6.1 and 8.6.2. The set of evaluation cases representing the reference evolution will need to be further developed to reflect all aspects that must be included in a main scenario in a future full safety analysis, as described in the general guidance to SSM's regulations (SSM 2008a).

#### **Corrosion**

Corrosion of steel leads to formation of iron oxides and hydroxides (Section 6.2.8). Since the exact distribution of corrosion products and their solubilities is uncertain, an unlimited solubility is assumed. This means that the iron from the steel does not reprecipitate in any form once corroded, and the possible concentration build-up in the aqueous solution is assumed to not slow down further corrosion.

Although radionuclides can sorb onto solid corrosion products of iron and steel, this sorption is disregarded in SE-SFL as a consequence of assuming no reprecipitation of corrosion products. This also excludes co-precipitation of radionuclides inside corrosion-product precipitates.

During the first few years after closure, oxygen is still present in the vaults and leads to oxidic corrosion of steel. Since this time period is very short relative to one million years, the oxidic corrosion is disregarded. Instead, a constant corrosion rate is assumed throughout the entire analysis period (Section 7.4.2). A wide range of corrosion rates can result from variations in conditions and material properties, but in SE-SFL, as in SKB's earlier safety assessments, it is assumed that the rate is determined only by whether the material is carbon steel or stainless steel, whether the pH is basic or near-neutral, and whether oxygen is present or not (oxidic or anoxic corrosion).

#### **Complexing agents**

Cellulose degrades, forming ISA in BHA. The transport of ISA out from the vault, and degradation of ISA inside it, has not been studied specifically for SE-SFL. However, both processes are expected to be limited (Section 6.2.8), so it is cautiously assumed that all formed ISA stays in the vault, intact and available for complexation with radionuclides. The concentration of ISA is thus assumed to be at the solubility limit for  $\text{Ca}(\text{ISA})_2$  throughout the whole assessment period, and sorption reduction factors are selected to reflect such conditions.

#### **Backfill development**

In the reference evolution (Sections 6.4.9 and 6.4.11), several processes potentially affecting the bentonite backfill and plugs are discussed. First, intrusion of dilute waters and glacial meltwaters might possibly lead to chemical bentonite erosion which, if sustained over sufficiently long times, could impair the performance of the barrier functions. Second, the bentonite barrier performance could further be influenced by chemical interactions with the concrete in the BHA waste domain leading to clay mineral transformation. Third, the selected bentonite thickness may be important for its function.

Fourth, changes in groundwater salinity and redox conditions at repository depth may affect barrier performance. Fifth, extrusion of bentonite from BHA into the bedrock fractures may block them. None of these five processes have been quantified within SE-SFL and they are thus disregarded but will need to be addressed in future safety assessments. Consequently, in the near-field transport modelling, the bentonite is assumed to retain its properties over the entire analysis period

In the radionuclide transport modelling, the concrete is assumed to follow the degradation sequence adopted in the near-field hydrology modelling by Abarca et al. (2019). That is, the gradual degradation described in the reference evolution (Section 6.2.10) is discretised into three states with corresponding values for flow rates (Figure 7-9). Also, the porosity and effective diffusivity are estimated for the same three states, but with linear interpolation in-between (Figure 7-10).

The sorption coefficients,  $K_d$ , also develop as concrete degrades and the gradual change described in the reference evolution (Section 6.2.8) is discretised for the near-field transport model. Four different  $K_d$  values are applied for each radionuclide, corresponding to time points of different pH values, with linear interpolation in-between (Section 7.4.2).

### **Hydrological properties**

The time from closure until saturation of the vaults with water is a few millennia for BHA (Figure 6-16) and about a decade for BHK (Figure 6-20), according to simple estimates (Section 6.2.6). Given the one-million-year time scale of the analysis of post-closure safety, the saturation process is approximated to be instantaneous upon closure for purposes of radionuclide transport modelling.

The water flows through BHK follow the degradation sequence of the concrete backfill and have been discretised into three distinct states, as described in the previous subsection.

The waste form, packaging and grout are likely to restrict water flow albeit to an uncertain extent, thus, the waste form itself is conservatively assumed to provide no hydraulic resistance. Similarly, for the steel packaging; since it starts to corrode already during the operational phase, its transport resistance after closure is uncertain so it is conservatively disregarded as a barrier for transport of water, gas, and radionuclides.

### **Bedrock fracture network**

The construction of the discrete fracture network (DFN) involves generation of fractures, which was performed once including deterministic hydraulic properties and four times with different stochastic properties by Joyce et al. (2019). Not all five realisations of the DFN are used for the transport modelling, however, so the full variability of the bedrock properties is not captured in the transport modelling. Different realisations result in different discharge locations, so the choice of using only the first DFN realisation r1 leads to a clustering of discharge locations near biosphere object 206. From this follows the conservative assumption that all radionuclides reaching the biosphere enter biosphere object 206 (Section 7.4.4). The choice of using only realisation r1 further affects the bedrock groundwater chemistry, since TDS concentrations for r1 are lower than the average over all five realisations (Figure 6-10).

### **Shoreline displacement**

The ongoing shoreline displacement has, for simplicity, been neglected in the *present-day evaluation case*, since it has been judged not to have any significant implications for the performance of the repository, including effects on hydrogeology, hydrochemistry or ecosystems. The sensitivity to ecosystem changes of the *present-day evaluation case* are limited, since both the area above the repository and the associated discharge area (biosphere object 206) are already above the sea level at repository closure. In contrast, the *simplified glacial cycle evaluation case* (Section 8.6.2) includes the effects of submerged conditions and shoreline displacement after the inland ice sheet has retreated.

## 7.5 Function of the repository design at the example location

In support of the discussion on the potential of the proposed repository concept (Chapter 9), the performance of the repository design at the example location is described here. The description is based on an analysis of the results of the radionuclide transport and dose calculations for the base case, i.e. the *present-day evaluation case*. A more detailed description and analysis is given in Section 5.2 of the **Radionuclide transport report**.

The safety principle for the proposed repository concept, *retardation*, is achieved by upholding the safety functions *good retention* and *low flow* in the waste vaults and the bedrock sufficiently for an adequate period (Chapter 5). Effective retardation ensures that annual near-field releases are only small fractions of the total activity inventory at repository closure. This time-dilution via sustained, slow release is important to post-closure safety and applies to all radionuclides. Additionally, releases and resulting doses are further decreased by retention and radioactive decay, which is most effective for radionuclides with short half-lives relative to their retention time in the near-field (or geosphere).

### 7.5.1 Retention in the near-field model

The annual near-field activity release from BHA and BHK is dominated by the radionuclides that dominate the initial (available) inventory and have half-lives longer than a few thousand years, i.e. Tc-99, C-14 and Cl-36 from BHA (Figure 7-11 left panel) and C-14 and Ni-59 from BHK (Figure 7-11 right panel). Several radionuclides that contribute significantly to the initial inventories of BHA and BHK (e.g. Ni-63) do not contribute significantly to the release due to their short half-lives and strong sorption onto cement and bentonite in the near-field. Further, the slow release by corrosion that is represented in the BHK near-field model significantly reduces the annual near-field activity releases for non-sorbing radionuclides such as C-14 compared with an instantly available source.

Initially, C-14 dominates the total annual activity release from BHA, but from about 4000 AD and for the remaining part of the analysis period of one million years, Tc-99 dominates (Figure 7-11 left panel). These two radionuclides together give a release that is at least one order of magnitude higher than any of the other radionuclides at all points in time. The total annual activity release from BHK is dominated by C-14 during the first ~25 ka after closure, resulting in a maximum total release at about 6000 AD (Figure 7-11 right panel). During this period, the significantly lower releases of Ag-108m, Mo-93 and Ca-41 also reach their maxima. From about 100 ka after closure, Ni-59 dominates the release from the BHK near-field with a maximum at about 400 ka after closure.

Beyond 10 ka after closure, the ingrowth of decay products leads to an increase over time of the near-field activity releases from BHA of specific radionuclides. For example, Ra-226 shows two release maxima, the first from Ra-226 present in the BHA waste at closure, which reaches a release maximum at approximately 3000 AD, and the second due to ingrowth at approximately 600 ka after closure. Ra-226 sorbs to a lesser extent than U and Th-isotopes in the near-field and thus is more mobile than its parent radionuclides.

In BHK, the release of activity due to corrosion results in increasing activity available for transport until about 10 ka after closure for e.g. C-14 (see Figure 5-9 in the **Radionuclide transport report**). Therefore, the maximum activity release for C-14 in BHK occurs later than that from BHA, and the decrease in the activity release following the maximum is less rapid in BHK than in BHA due to sustained, slow release by corrosion (Figure 7-11). Compared with the activity release for a non-sorbing radionuclide such as C-14, even a low  $K_d$  leads to retention and a later maximum annual release for Mo-93 than C-14. For radionuclides with long half-lives that sorb more strongly onto cementitious materials, such as Ni-59, the annual-release maximum is reached significantly later.

The relative accumulated activity release from the near-field (Figure 7-12) for a specific radionuclide is determined by the radionuclide half-life, sorption onto cement in the grouted waste and onto bentonite (BHA) or cement (BHK) in the backfill. The near-field release from BHA is further influenced by the weakened sorption onto cement and bentonite due to complexing agents, and the effective diffusivity in bentonite, which is lower for anions than cations and neutral species. In BHK, two additional factors that significantly affect the near-field release are the slow release by corrosion and the fraction of radionuclides that is instantly available for transport.

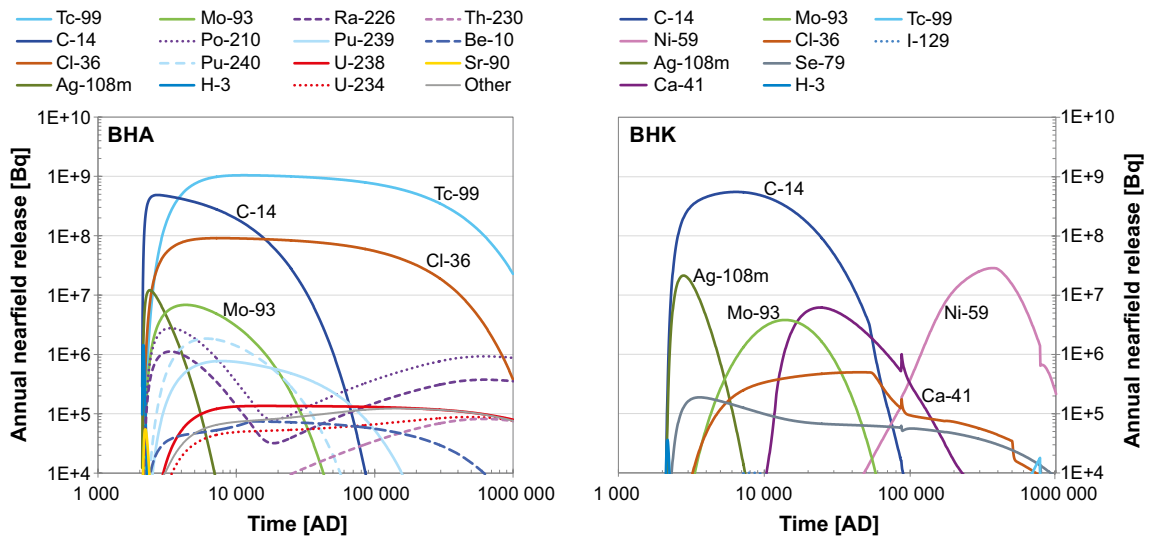


**Figure 7-11.** Annual near-field activity release from BHA (left panel) and BHK (right panel) in the present-day evaluation case. Radionuclides with a maximum annual release greater than  $1 \times 10^4$  Bq are shown individually, whereas remaining radionuclides are grouped in the “Other” series. The small, sharp features at  $\sim 85\,000$  AD and  $\sim 800\,000$  AD are artefacts from the abruptly changed water flows in BHK described in Section 7.4.2. Figure corresponds to Figures 5-7 and 5-10 in the **Radionuclide transport report**.

The radionuclide retention in the near-fields of BHA and BHK is substantial. For the non-sorbing C-14, the fraction that decays while retained in the near-field is 93 % of the initial inventory in BHA, whereas the corresponding value for BHK is 98 % (Figure 7-12). The total retention of C-14 is thus similar in the near-fields of BHA and BHK. However, the effect is achieved by different mechanisms, with retardation in bentonite backfill and limited diffusive transport into bedrock fractures being the main factor in BHA and slow release by corrosion in BHK. Retention is even more efficient for Mo-93 with more than 99 % decay in the near-field. This is because Mo-93 has a low but non-zero  $K_d$  for cement and a half-life that is somewhat shorter than that of C-14.

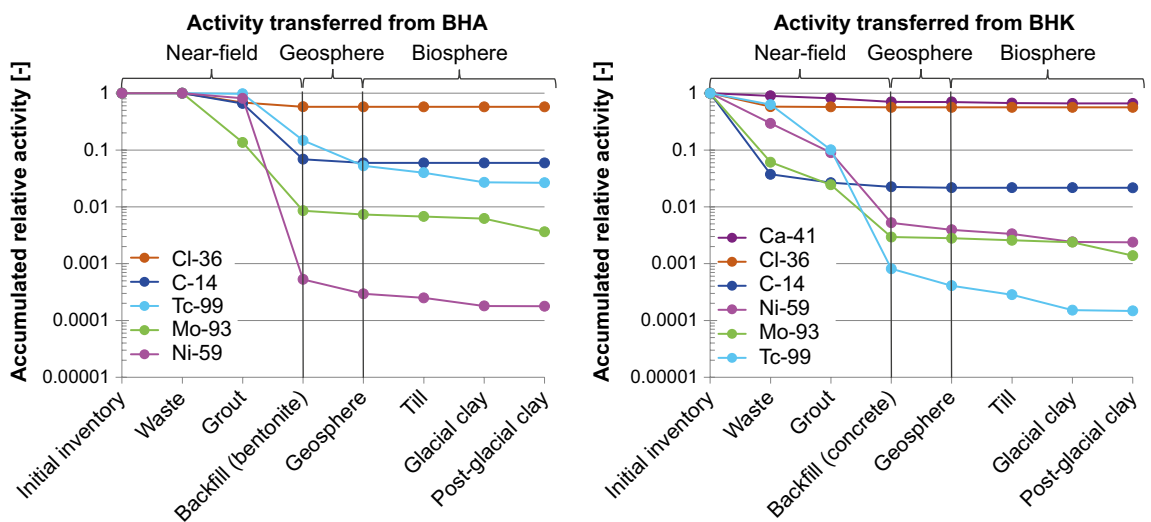


**Figure 7-12.** Relative activity transferred along the pathway from the initial inventory in BHA (left panel) and BHK (right panel) to the biosphere, accumulated over the entire analysis period of one million years. Figure corresponds to Figure 5-23 in the **Radionuclide transport report**.

Of the radionuclides that contribute significantly to the near-field release and eventual dose, decay of retained activity is least important for the long-lived and low-sorbing Cl-36; only about 40 % of the initial inventory in either waste vault decays in the near-field. However, retention in the near-field is still important since it leads to distribution of the release in time, which reduces the annual release to a small fraction of the inventory. For Cl-36, the maximum annual near-field release is five orders of magnitude lower than the initial inventory. Cl-36 furthermore contributes significantly less to the near-field releases from BHK than from BHA (Figure 7-11), with a difference of about two orders of magnitude in the maximum annual release. This is mainly due to about two orders of magnitude lower initial inventory in BHK. For Tc-99, with a half-life similar to that of Cl-36 (211 ka as compared to 301 ka for Cl-36), retention in the BHA and BHK near-fields is stronger than for Cl-36 due to sorption. Tc-99 retention in the backfill is significantly stronger in BHK than in BHA, since sorption of Tc-99 in BHA is assumed to be strongly reduced (by a factor of 10 000) due to formation of non-sorbing complexes with cellulose-degradation products.

Ni-59 has a significantly longer half-life than C-14 and Mo-93 and a relatively high  $K_d$  value for cement and bentonite. This, in combination with the slow, diffusive near-field transport, yields very strong retention in BHA and activity decay by three orders of magnitude in the bentonite backfill (Figure 7-12 left panel). Retardation of Ni-59 by sorption is effective also in BHK. This results in a near-field activity release that is significantly reduced (Figure 7-12 right panel) and occurs later compared with C-14 (Figure 7-11 right panel). That is, decay in the metal and decay during sorption onto cement in the grout, reduces the accumulated activity release by about two thirds in each step. Further, decay due to sorption in the concrete backfill reduces the activity released from the grouted waste by more than an order of magnitude.

The slow release by corrosion, represented in the BHK near-field model, significantly reduces the annual near-field activity releases in comparison with an instantly available source. If instead it were assumed that the total initial inventory in BHK is available for transport at closure, the maximum annual release for the non-sorbing C-14 would be two orders of magnitude higher than in the base case (data not shown). For strongly sorbing radionuclides, the effect of corrosion is less important. Thus, the assumption that all Ni-59 is available for instant release would only increase the maximum annual release by a factor of three as compared with the base case (data not shown).

## 7.5.2 Retention in the geosphere model

The release from the geosphere is modified compared with the near-field release due to dispersion, sorption, and decay during the transport through the geosphere. Radioactive decay significantly reduces the geosphere releases of radionuclides with a short half-life in comparison with the travel time through the geosphere (e.g. H-3 and Sr-90), and those with potential for sorption in the rock matrix (e.g. Ag-108m and several Pu isotopes). The geosphere release of Tc-99, which has a relatively long half-life, is reduced by a factor of between two and three (Figure 7-12) due to the combined effect of retardation and radioactive decay in the rock matrix. On the other hand, the effect of geosphere transport on the release of mobile radionuclides with a half-life of a few thousand years (C-14 and Mo-93) is limited, and for Cl-36, the reduction in the releases as a consequence of geosphere transport and decay is even less important (Figure 7-13).

Taken together, retardation and decay in the geosphere in the base case have a marginal effect on the release of non-sorbing radionuclides, and the effect on long-lived, sorbing radionuclides is larger but still limited.

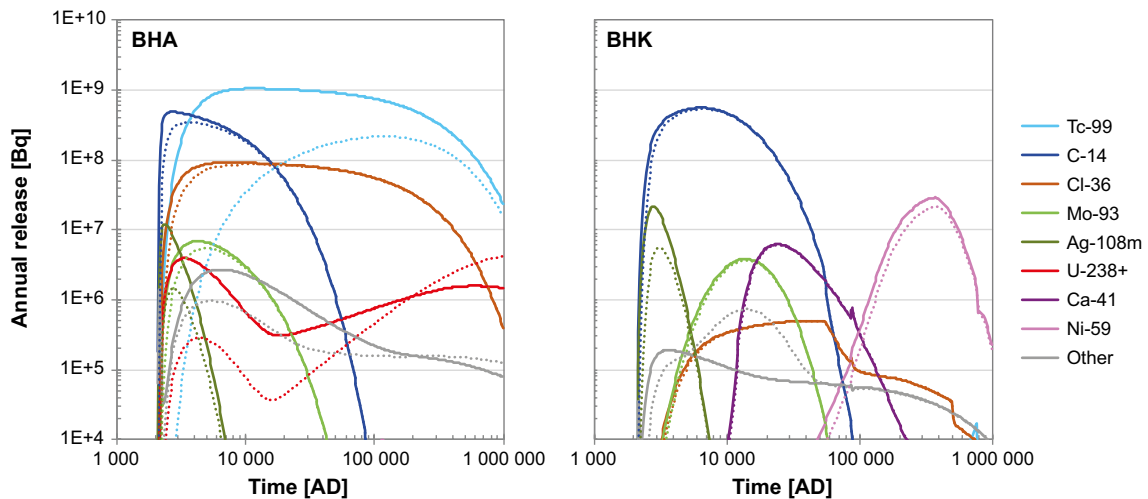


**Figure 7-13.** Annual releases from the near-field (solid lines) and the geosphere (dotted lines) from BHK and BHA in the present-day evaluation case. Note that the difference between the near-field and the geosphere release from BHK is barely visible for Cl-36, Ca-41 and Mo-93. The top three radionuclides for maximum near-field activity release and the top three radionuclides for maximum annual dose from BHA and BHK are shown separately in the figure and the rest are grouped in the Other series. The sum of the release from radionuclides in the U-238 decay chain (U-238, U-234, Th-230, Ra-226, Pb-210, Po-210) is also shown as U-238+. Figure corresponds to Figure 5-12 in the **Radionuclide transport report**.

### 7.5.3 Retention in the biosphere model and annual doses

In the base case, the total annual dose from each waste vault exceeds the dose corresponding to the regulatory risk limit, 14  $\mu\text{Sv}$ , by less than an order of magnitude. The annual doses from several individual radionuclides are within an order of magnitude of this limit: C-14 and Mo-93 for both BHA and BHK, and Tc-99, Cl-36 and the uranium series for BHA (Figure 7-14). Draining and cultivation of a mire in the discharge area is the land use that causes the highest doses. This is primarily because radionuclides can accumulate in peat over a long period of time prior to exposure, and because the dose-contributing radionuclides predominantly yield dose through ingestion of food. However, for release from BHA, the importance of exposure from well water increases with time, as the activity of Tc-99 and decay products from the uranium series reach the biosphere.

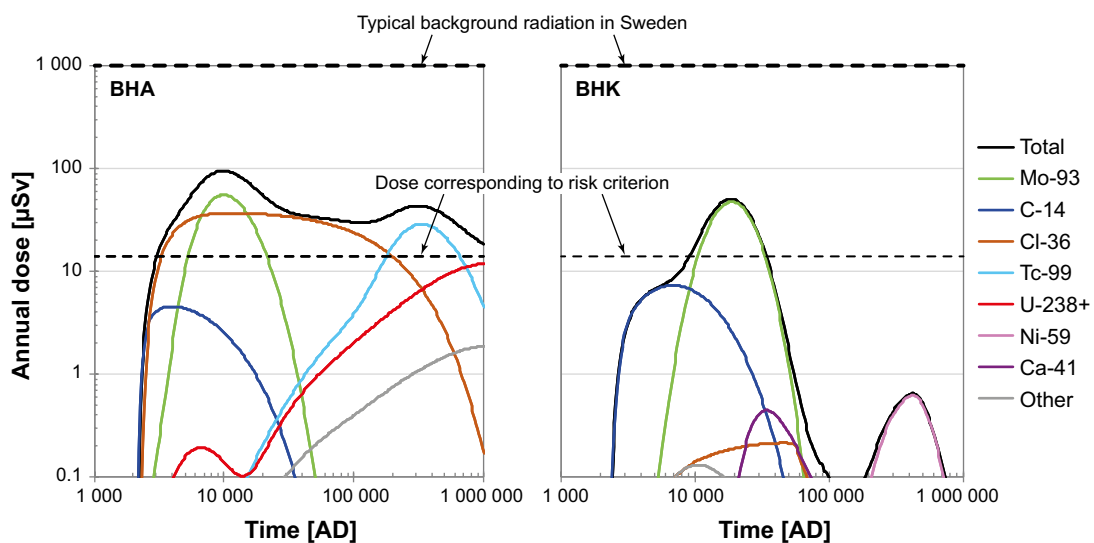


**Figure 7-14.** Annual doses from BHA and BHK from draining and cultivating the mire ecosystem in biosphere object 206. The total dose (black line) is shown together with the contributions from individual radionuclides (coloured lines). Dashed black lines show the dose corresponding to the regulatory risk limit (14  $\mu\text{Sv}$ ). Figure corresponds to Figure 5-18 in the **Radionuclide transport report**.

The temporal dynamics of nuclide-specific doses is primarily driven by the release from the geosphere, as reflected by similarly shaped curves in Figure 7-13 and Figure 7-14. However, the variation in annual dose for a given release spans more than three orders of magnitude for nuclides with the highest geosphere releases, where, for example, Mo-93 gives larger doses relative to its activity release compared with Ni-59 (Figure 7-15 and 7-16). The mechanisms behind the nuclide-specific behaviour in the biosphere system and the dose response can be divided into five factors; retention and decay, accumulation, leaching from cultivated soil, plant uptake, and radiotoxicity.

Radionuclide retention and decay in the regolith influence the timing and the fraction of the geosphere release that reaches the upper part of the regolith profile. Several environmental factors affect retardation and retention. Of these, sorption in the lower part of the regolith profile is a key property, and radionuclides that display strong sorption relative to their rate of radioactive decay will have insignificant amounts reaching the surface. Sorption properties in the upper section of the regolith profile determine the potential for accumulation in regolith that may be exposed by drainage. Moreover, sorption in the drained soil determines the rate of leaching, which decreases the soil activity during cultivation. Plant uptake is assumed to be proportional to soil concentrations, but the proportionality constant varies between radionuclides. Finally, the dose that is caused by a given intake of activity is determined by how a radionuclide is metabolised and by the type and energy of its ionising radiation, both contributing to its radiotoxicity.

All these factors vary by several orders of magnitude among radionuclides that have a substantial geosphere release, as reflected by a large spread in the relationship between the maximum geosphere release and the maximum annual doses in Figure 7-15. The relative influence of the main biosphere processes that influence the relationship between geosphere release and dose from ingestion of crops is shown for radionuclides with an annual geosphere release exceeding 10 000 Bq in Figure 7-16. The figure shows how the dose is affected by the five main biosphere processes, for nine important radionuclides of which three include decay-chain daughters.

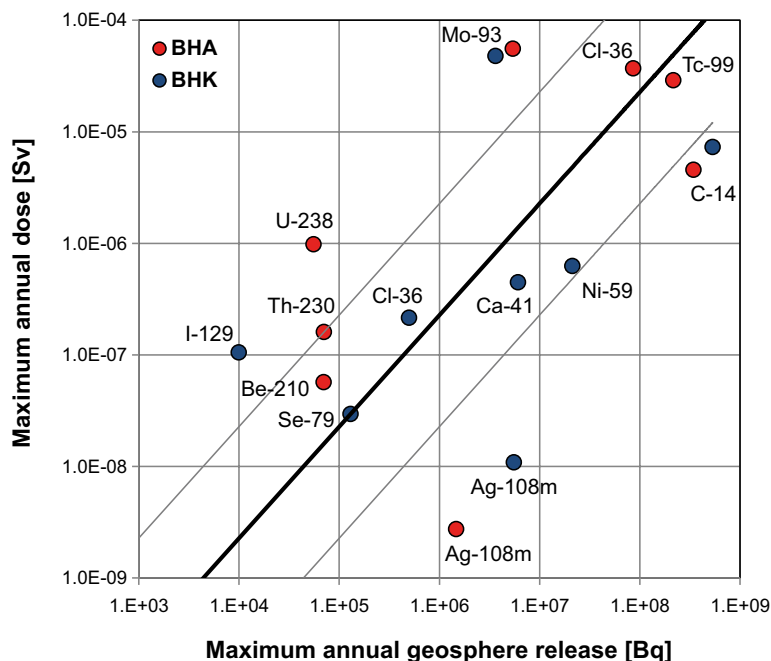


**Figure 7-15.** Maximum annual dose as a function of maximum annual release from the geosphere. All displayed radionuclides have a maximum annual release of at least  $10^4$  Bq from either BHA (red) or BHK (blue). Decay-product radionuclides whose dose primarily reflects the release or accumulation of the parent radionuclide (rather than the release of the decay product itself) have been excluded from the graph for clarity (Ra-226, Po-210, Pb-210, Pu-239 and Nb-93m). The line represents the median relationship between the maximum dose and the maximum release ( $2 \times 10^{-13}$  Sv/Bq) and the grey lines show 10:1 and 1:10 ratios of this relationship. Figure corresponds to Figure 5-21 in the *Radionuclide transport report*.

Taking Ca-41 and Mo-93 as an example, while the proportion of the release that decays during the transport through the regolith layers is similar between the two, molybdenum accumulates much more effectively in peat, reflected in a longer orange bar in Figure 7-16 (logarithmic scale). The leaching rate from the cultivated soil is similar for the two radionuclides, as is the availability for uptake by plants. However, the radiotoxicity of Mo-93 is significantly higher. Together, these factors result in the dose being about two orders of magnitude larger for Mo-93 than Ca-41, given an identical geosphere release (Figures 7-15 and 7-16). In the biosphere modelling, leaching from cultivated soil, plant uptake, and toxicity are properties that are assumed to be marginally affected by conditions in the discharge area, and patterns from present-day calculations can in this sense be viewed as valid for a broad range of environmental conditions. Conversely, decay due to retention and accumulation depends on the properties of the discharge area, e.g. size of object, soil depth and groundwater discharge. Thus, the reported differences between radionuclides cannot easily be generalised to other discharge areas. The sensitivity to variations in object properties is examined in the *alternative discharge area evaluation case* (see Section 8.5.2).

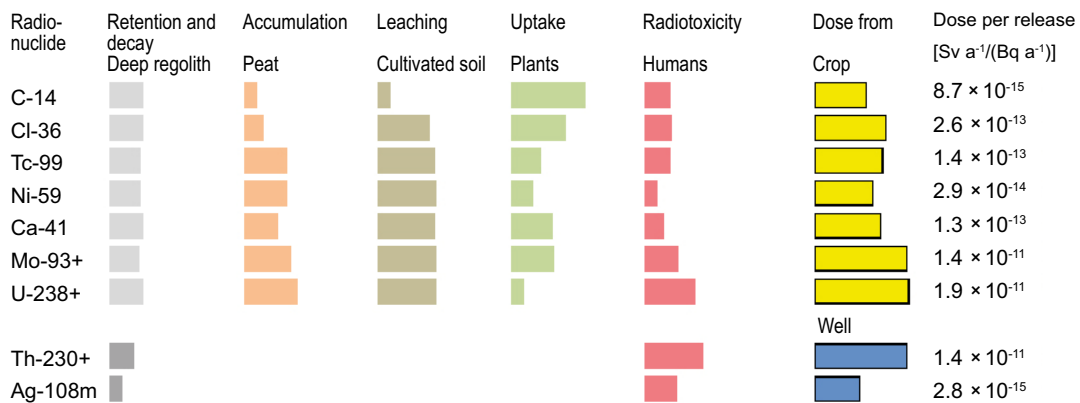


**Figure 7-16.** The influence of radionuclide properties on the dose for the dominating exposure pathway from a unit release. Coloured bars without contours represent the relative importance on dose of various processes: retention and decay in deep regolith (longer bar means less decay), accumulation in peat, leaching in cultivated soil (longer bar means less leaching), plant uptake, and radiotoxicity in humans. Properties are scaled so that the length of the bars corresponds to an additive positive dose response (on a logarithmic scale). Radionuclides are organised according to the major pathway of exposure; ingestion of crops (yellow, upper) and ingestion of drinking water from a dug well (blue, lower). Note that the effects of the first two processes: retention and decay and accumulation, result from the interaction between radionuclide-specific properties and object-specific properties, whereas the three remaining properties are primarily driven by radionuclide-specific properties. Plus sign (+) indicates that the dose includes the contribution of decay products. Figure corresponds to Figure 5-22 in the **Radionuclide transport report**.



## 8 Potential of the repository concept to meet applicable criteria

### 8.1 Introduction

In support of the Discussion in Chapter 9, the function and performance of the repository design at the example location is described in Section 7.5. The description is based on the analysis of the results of the radionuclide transport and dose calculations for the base case, i.e. the *present-day evaluation case*, described in Section 7.4. Further, the modelling approach, describing the radionuclides represented in the analysis and the models utilized in SE-SFL to calculate radionuclide transport and dose are described in Sections 7.1–7.3.

In further support of the discussion on the potential of the proposed repository concept to meet the regulatory criteria (Chapter 9), the base case is complemented with a set of evaluation cases described and analysed in this chapter.

The set of evaluation cases for SE-SFL is described in Section 8.2. The rationale and main assumptions made in each evaluation case are described, and the resulting activity release and dose are analysed in Sections 8.3–8.7. Complete descriptions of the assumptions and analyses of the results are given in Chapters 5–7 in the **Radionuclide transport report**.

### 8.2 Selection of evaluation cases

A total of fourteen evaluation cases are defined in SE-SFL to assess the conditions under which the repository concept has the potential to fulfil regulatory criteria with respect to radiological safety or to assess the sensitivity of assessment endpoints to selected uncertainties (Section 2.5.8, Figure 8-1). As noted in Section 2.5.8, the set of evaluation cases is linked to the objectives of SE-SFL but is not necessarily complete with regards to regulatory requirements.

For ease of interpretation and straightforward comparison with the evaluation cases based on alternative assumptions or temporal evolutions, a base case is defined in SE-SFL. The base case assumes constant, present-day climatic and other external conditions throughout the full assessment period (Section 7.4). Although the internal conditions are based on the reference evolution (Section 6.2), some simplifications are introduced and these are discussed in Section 7.4.5. It is further assumed that the repository is constructed at the example location in Laxemar, and, as in all evaluation cases in SE-SFL, it is assumed that the repository is constructed according to the proposed design concept.

The base case is complemented with a set of cases that evaluate the sensitivity of the resulting activity release and dose to specific assumptions made regarding conditions in the repository and the repository environs are included in the analysis (Figure 8-1). These cases were chosen to illustrate conditions in the repository and the repository environs that are likely to improve the repository performance in comparison with the base case. Cases that illustrate the effects of uncertainties in bedrock properties, discharge area and the effect of a drilled well, as well as uncertainties relating to the future climate evolution, are included in the evaluation. The rationale for each evaluation case is given in Sections 8.3–8.7. A very brief description of the implementation in the three respective transport models of each evaluation case is given in the overview Table 8-1.

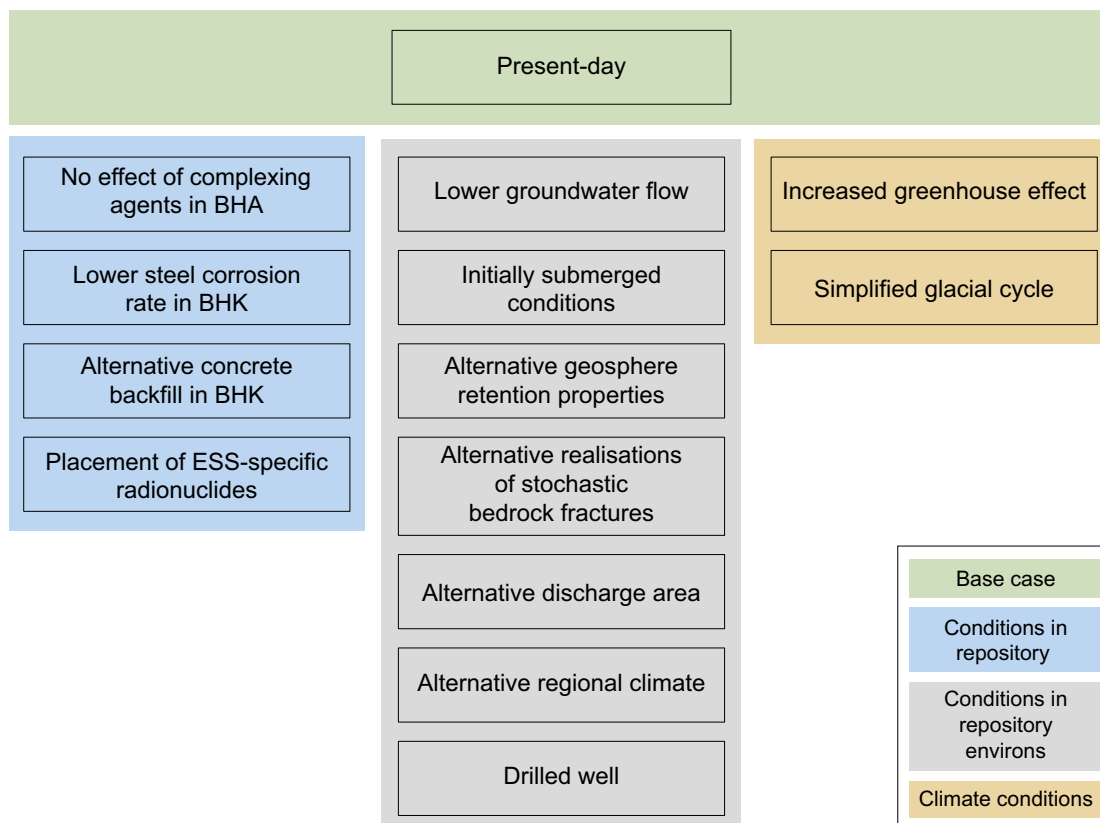


**Figure 8-1.** Evaluation cases included in the evaluation of the potential for the proposed repository concept to meet applicable criteria on the maximum annual effective dose to humans after closure, grouped and colour-coded according to type of scenario driver (conditions in the repository, the repository environs or large-scale climate conditions).

**Table 8-1. Summary of evaluation-case implementations in the three transport models.**

Evaluation case	Near-field	Geosphere	Biosphere	Remarks
No effect of complexing agents in BHA	Sorption reduction factors not applied	As in base case	As in base case	No effect on non-sorbing radionuclides
Lower steel corrosion rate in BHK	Factor 10 lower steel corrosion rate	As in base case	As in base case	
Alternative concrete backfill in BHK	Concrete porosity and diffusivity halved. Permeability decrease by scaling advective flow by factor 0.1	As in base case	As in base case	Similar concrete properties as in Lagerblad et al. (2017), Mårtensson and Vogt (2019), Idart et al. (2019b)
Placement of ESS-specific radionuclides	ESS radionuclides considered in BHA and BHK, respectively	As in base case	As in base case	
Lower groundwater flow	Flow rates in waste and backfill scaled by factor 0.1, 0.01 and 0.001, respectively	Advective travel time and F-factor scaled by factor 10, 100 and 1000, respectively	As in base case	Potential to meet regulatory targets for 100- and 1000-fold lower flow.
Initially submerged conditions	Initial period of 100-fold lower groundwater flow rates	Initial period of 100-fold lower groundwater flow rates	Biosphere object starts as sea basin, becomes a lake due to shoreline displacement	Three variants with initial periods of different length
Alternative geosphere retention properties	As in base case	Alternative bedrock sorption coefficients and diffusivities	As in base case	Bedrock data from Forsmark and Olkiluoto, respectively

Evaluation case	Near-field	Geosphere	Biosphere	Remarks
Alternative regional climate	As in base case	As in base case	Increased groundwater flow in biosphere object, corresponding to three other regions of Sweden, respectively	Correspond to increased precipitation and/or lower temperature
Alternative realisations of stochastic bedrock fractures	BHA situated in its base-case eastern position, or in the western, normally BHK's, position. Affects connectivity to geosphere: $R_{plug}$ and $Q_{eq}$	5 realisations of stochastic DFN with different $t_w$ and $a_w$	As in base case	10 variants: 2 BHA positions $\times$ 5 DFN realisations. Performance of BHK not assessed
Alternative discharge area	As in base case	As in base case	Discharge into biosphere objects with different properties, 9 in Laxemar and 6 in Forsmark	
Drilled well	As in base case	Release to the well = base-case geosphere release $\times$ fraction of particles that reach the well in the hydrogeological particle tracking	Garden plot household exposed through drinking water, and ingestion of vegetables and potatoes from a well-irrigated kitchen garden	Sufficiently small group (5 individuals) for use of more lenient risk criterion of $10^{-5}$ . U-238+ from BHA is dose-dominating
Increased greenhouse effect	As in base case	As in base case	Increased atmospheric $CO_2$ and decreased discharge rate of ground and surface water. Increased plant water deficit	Water deficit of plants covered by increased groundwater uptake or by irrigation, respectively
Simplified glacial cycle	Groundwater flow rates scaled by scaling factor that varies in time, following the progression of the glacial cycle	Groundwater flow rates scaled by the same scaling factor as in the near-field	Periglacial: discharge to lake via a through talik. Glacial: discharge to sea basin beyond the ice margin. Glacial retreat: flushing of radionuclides from regolith and erosion of upper regolith layers	No account of: mechanical effects, groundwater flush to depth

## 8.3 Conditions in the waste vaults

### 8.3.1 No effect of complexing agents in BHA

#### *Rationale and handling in the model*

In the base case, it is assumed that complexing agents are formed from cellulose in the BHA inventory. The complexing agents are assumed to form complexes with the radionuclides, making them more soluble and reducing their sorption onto cement and bentonite. The amount of cellulose in the BHA inventory is not well known and therefore the cautious assumption is made in the base case that the concentrations of complexing agents are high in the BHA vault. This case evaluates the effect of assuming that no complexing agents are present, or that they have no effect, in the waste domain in BHA. The case can be used as a basis to discuss the effects of different types of uncertainties related to complexing agents.

In the base case, the effect of complexing agents is accounted for by applying sorption reduction factors, which are specific for each element (see Table 7-1), for sorption onto cement and bentonite in BHA. The sorption coefficients are divided by the sorption reduction factors, weakening sorption. In this evaluation case, no sorption reduction factors are applied in the near-field model (Section 6.2 in the **Radionuclide transport report**). Figure 8-2 shows the retardation coefficient  $R$  in bentonite, as defined in Equation 7-16, describing how many times slower the transport of a sorbing radionuclide is compared with the water velocity in the pore spaces. Figure 8-2 also illustrates the effect of neglecting the effect of complexing agents for all assessed radionuclide species, as compared with the base case where complexing agents are taken into account. The reduced sorption due to complexing agents significantly decreases the retardation of several radionuclides, such as Tc-99 and U-238.

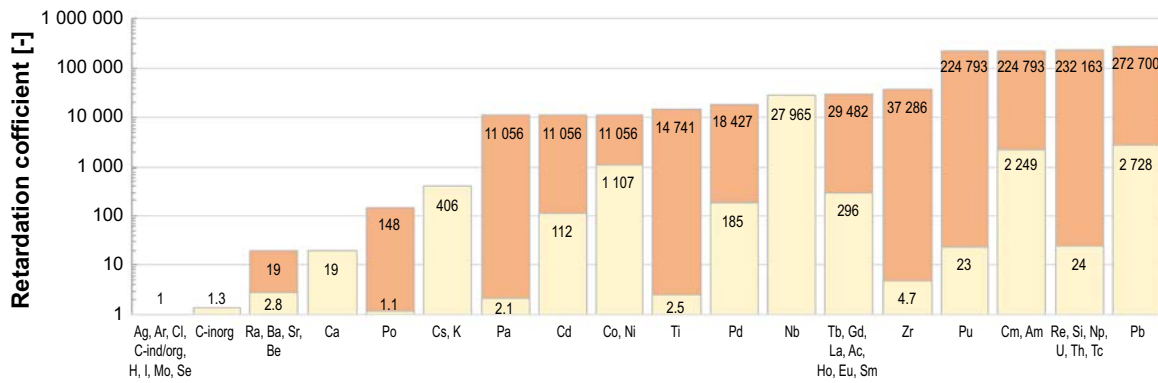


**Figure 8-2.** Retardation coefficient  $R$  in the BHA bentonite barrier for all assessed radionuclides grouped and sorted by the value of the coefficient. Beige fields represent retardation coefficients of the base case and the full height bars represent retardation coefficients without the assumed effect of complexing agents (with the increase in the coefficient shown in orange). The figure is identical to Figure 6-1 in the **Radionuclide transport report**.

### Summary of results

The occurrence or absence of complexing agents has no effect on the radionuclides (Mo-93, C-14 and Cl-36) dominating the dose resulting from BHA for about 50 000 years after closure (Figure 8-3 right panel). Hence, the maximum annual dose is the same as in the base case since it is determined by Cl-36 and Mo-93.

The assumption that there is no effect of complexing agents in BHA leads to a substantial decrease in near-field release for highly sorbing radionuclides affected by the sorption reduction factors applied in the base case. Most notable are the reductions in the releases of Tc-99 and tetravalent actinides, such as U-234 and U-238 (grouped into U-238+ in left panel in Figure 8-3). For the period after about 50 000 years after closure, doses decrease by several orders of magnitude in comparison with the base case due to the increased near-field sorption of Tc-99 and the tetravalent actinides. For this period, Cl-36 is the only radionuclide that significantly contributes to the dose (right panel in Figure 8-3).

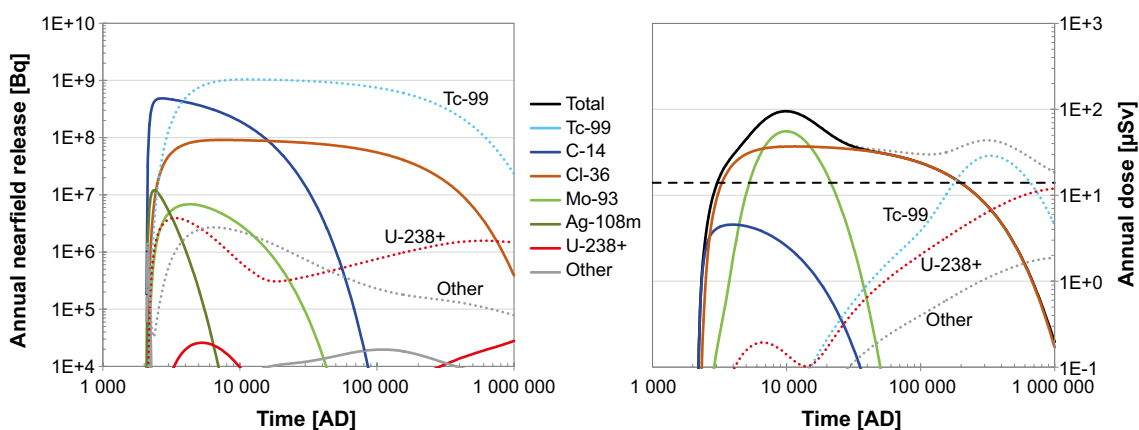


**Figure 8-3.** Annual near-field activity release (left panel) and annual dose (right panel) from BHA for the no effect of complexing agents evaluation case (solid lines). The corresponding near-field releases and annual dose for the base case are shown as dotted lines. The top three radionuclides for maximum near-field activity release and the top three radionuclides for maximum annual dose from BHA are included in the figure. The sum of the release/dose from radionuclides in the U-238 decay chain (U-238, U-234, Th-230, Ra-226, Pb-210, Po-210) is also shown as U-238+. The dose corresponding to the risk criterion is indicated with a dotted black line in the right panel. Figure identical to Figure 6-2 in the **Radionuclide transport report**.

### 8.3.2 Lower steel corrosion rate in BHK

#### *Rationale and handling in the model*

The waste planned for BHK is mostly in the form of scrap metal and most of the activity originates from neutron irradiation of the construction material of reactor components close to the core (Herschend 2014). The release of this induced radioactivity from the waste is assumed to be controlled by a constant corrosion rate. Since most of the waste planned for BHK is stainless steel, the corrosion rate of 10 nm/a used for stainless steel under alkaline anoxic conditions in SR-PSU (Table 5-3 in SKB 2014h) is also applied in the base case of SE-SFL (Section 7.4.2). There are also fractions of the radionuclide inventory that are present in very thin metallic parts (< 1 mm), assumed to be available for instant release (Section 7.4.2). This is a pessimistic assumption as even very thin metal may give retention on timescales of 100 000 years given the low corrosion rates.

The corrosion rate used in the base case is higher than recently reported long-term corrosion rates, such as 0.4 nm/a for stainless steel in simulated repository conditions (Sakuragi et al. 2016), or 1.0 nm/a, which is the lower end of the range for stainless steel corrosion under alkaline anoxic conditions recommended for use in PSAR for SR-PSU. This lower end is used here to represent a significantly lower (by a factor 10) corrosion rate than in the base case (Section 6.3 in the **Radionuclide transport report**).

#### *Summary of results*

Reducing the corrosion rate to this lower end of the range (i.e. by a factor of ten as compared with the base case) reduces the maximum annual activity release from the near-field, which is dominated by C-14, by a factor of four and the accumulated activity release by about a factor 5 (right panel in Figure 8-4). The maximum annual dose is in the base case dominated by Mo-93 and the total dose decreases by a factor of four due to the reduced corrosion rate. The dose reduction is controlled by the near-field response of Mo-93 with the accumulated activity release decreasing by a factor of 4 (left panel in Figure 8-4).

The effects of the corrosion rate on near-field releases and doses varies among radionuclides depending on the inventory in the instant-release fraction and in the thicker metal fractions that are influenced by corrosion, and on retention and decay rates. Consequently, the potential for reduced releases and doses from BHK associated with the uncertainty in corrosion rate needs to be evaluated in relation to the assumptions about, and uncertainty in, the initial distribution of the radionuclide inventory between the instant release and thicker metal fractions.

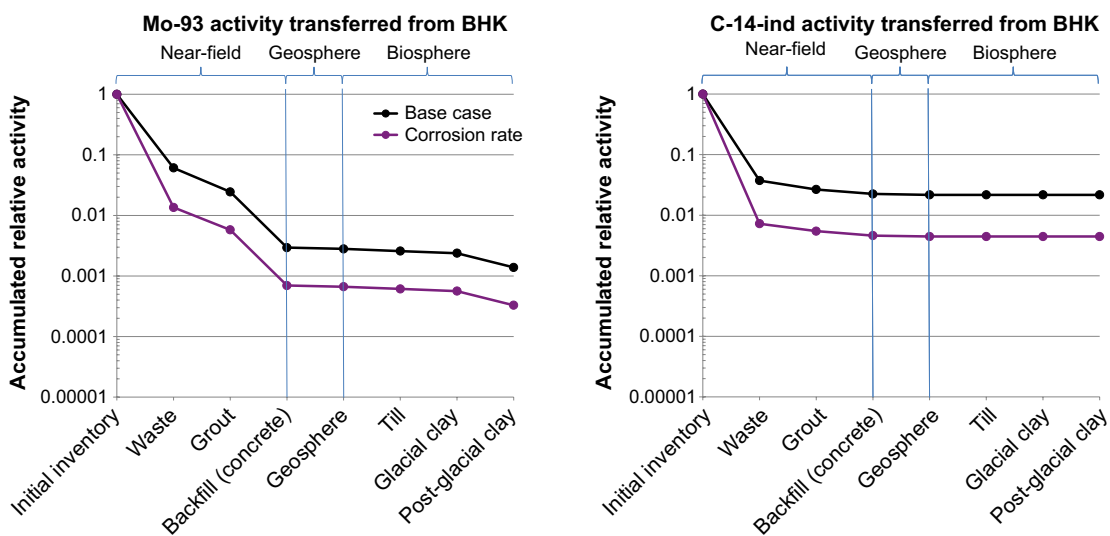


**Figure 8-4.** Activity of Mo-93 (left panel) and C-14 (right panel) transferred along the way from the initial inventory in BHK to the biosphere, accumulated over the entire analysis period of one million years, and normalised by the initial inventory. The relative activity transferred is shown for the base case (black), and for a ten times lower corrosion rate (yellow). Figure adapted from Figure 8-2 in the **Radionuclide transport report**.

### 8.3.3 Alternative concrete backfill in BHK

#### *Rationale and handling in the model*

The quality of the concrete used as backfill material in BHK is a design consideration. Idiart et al. (2019b) modelled the long-term evolution of transport parameters that are affected by degradation for five potential concrete compositions. The results show that it should be possible to achieve a concrete that has more favourable properties than the properties assumed for the concrete composition in the base case, which represents the construction concrete employed in the existing SFR repository. The effect of improved concrete transport properties for the BHK backfill is illustrated in this evaluation case, as further described in Section 6.4 in the **Radionuclide transport report**.

The concrete backfill is assigned an initial porosity and effective diffusivity that are half of the values used in the base case. A lower hydraulic conductivity is accounted for by reducing the advective flow through intact concrete within and out of the near-field by a factor of 10. These parameter values are comparable with the properties of a concrete containing limestone and dolomite additions which has been developed by Lagerblad et al. (2017) and used in the construction of large components representative of the caissons in 2BMA in large-scale experiments in the Äspö Hard Rock Laboratory (Mårtensson and Vogt 2019) and analysed by Idiart et al. (2019b).

The timing of leaching events and cement degradation is assumed to be the same as in the base case (Section 7.4), as are sorption coefficients  $K_d$  in cement. However, the values of the water flow through the waste domain and the backfill are scaled by a factor of 0.1 and the porosity and diffusivity are scaled by a factor of 0.5 while the concrete is intact or partly degraded. When the concrete is assumed to be completely degraded at about 780 000 AD, the water flow, porosity, and diffusivity are cautiously assumed to be the same as in the base case.

#### *Summary of results*

The resulting maximum annual dose from BHK is only 3 % of that in the base case (Figure 8-5 right panel), primarily due to increased retention and decay in the near-field (Figure 8-5 left panel and Figure 8-6). The decrease in the near-field release of the sorbing Mo-93 is larger than for the non-sorbing C-14 (right panel in Figure 8-6), and the dose-dominating radionuclide switches from Mo-93 in the base case to C-14 in the *alternative concrete backfill in BHK evaluation case* (Figure 8-5). In general, radionuclides with a high proportion of decay in the near-field (in the base case), i.e. due to high sorption and/or high decay rate, are most affected by a more favourable concrete composition.

An additional effect of the assumed lower porosity and diffusivity is that it should suppress cement leaching (Idiart et al. 2019b) compared with what is assumed in the base case. This implies that the degraded-zone period would occur later, if at all, within the time frame of the analysis. Consequently, the late time releases of Ca-41 and Ni-59 would decrease even further, although these radionuclides are not dose-dominating. Overall, this case results in a significantly improved long-term performance of BHK.

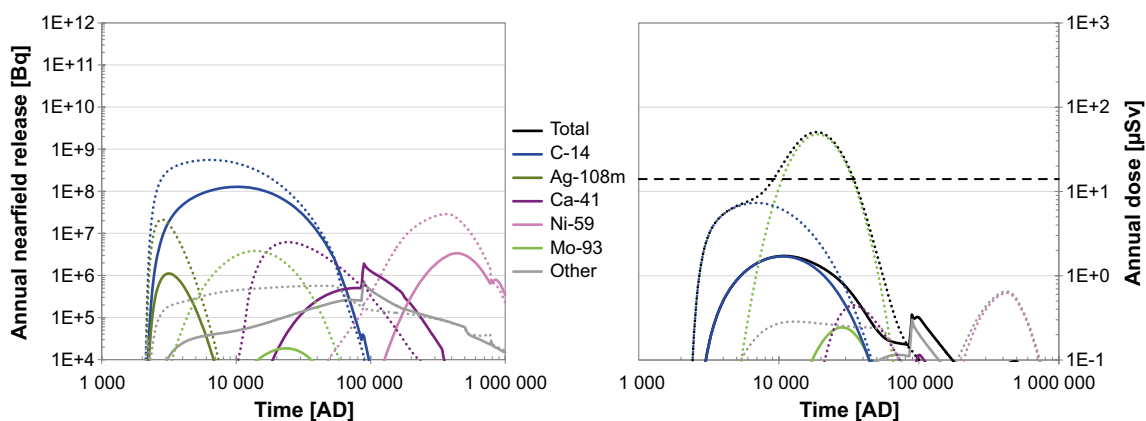


**Figure 8-5.** Activity release from the near-field (left panel) and annual dose (right panel) for the evaluation case with alternative concrete backfill in BHK. For comparison, the respective curves for the base case are also shown (dotted lines). The dose corresponding to the risk criterion is indicated with a dotted black line. Figure identical to Figure 6-6 in the **Radionuclide transport report**.

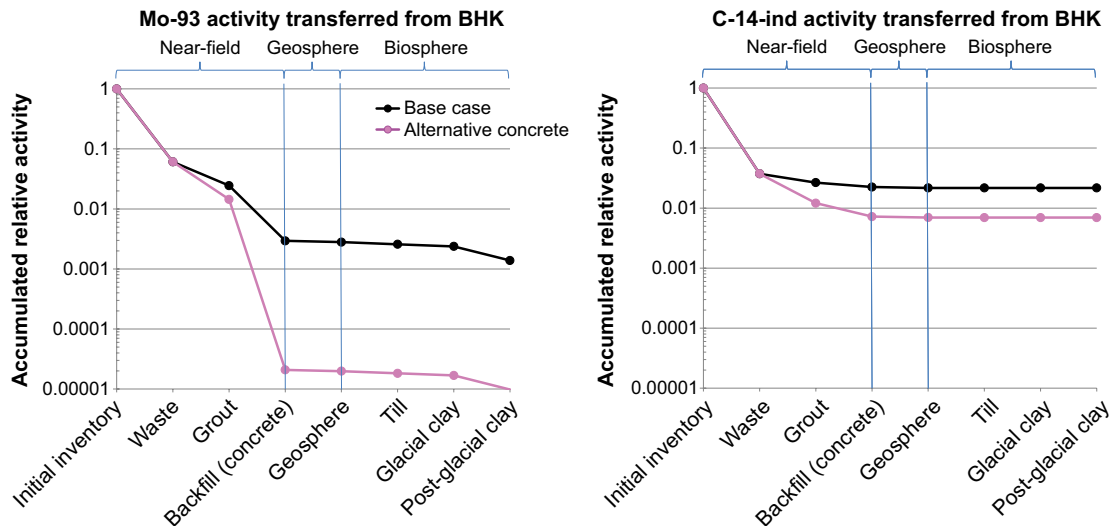


**Figure 8-6.** Activity of Mo-93 (left panel) and C-14 (right panel) transferred along the route from the initial inventory in BHK to the biosphere, accumulated over the entire analysis period of one million years, and normalised by the initial inventory. The relative activity transferred is shown for the base case (black), and for the case with alternative concrete (magenta). Figure adapted from Figure 8-2 in the **Radionuclide transport report**.

### 8.3.4 Placement of ESS-specific radionuclides

#### **Rationale and handling in the model**

As described in Section 7.2, radioactive waste from the ESS facility is included in SE-SFL. Owing to uncertainties in the inventory data for this waste, it is evaluated in a separate evaluation case. This is intended to investigate whether a clear advantage exists for using either the BHA or the BHK barrier concept for radionuclides specific to the ESS inventory.

As it is assumed that the released radionuclides have no effect on their environment or on any other radionuclide, a radionuclide's activity release, and thus its dose contribution, scales proportionally to its inventory. Since the actual ESS inventory is still largely unknown, a unit initial activity inventory of 1 Bq is here assumed for each of the radionuclides. The transport modelling thus provides information on annual releases of the radionuclides relative to this assumed inventory, but not on the absolute releases. For comparison, all radionuclides included in the base case are also included in the calculations with a unit initial activity inventory of 1 Bq.

The ESS-specific radionuclides are assumed to be available for transport at repository closure, in the same way as the legacy waste in BHA in the base case. In order to illustrate if one of the two barrier concepts, BHA or BHK, is more suitable for these radionuclides, five variants of this evaluation case were modelled, as described below.

The speciation of the ESS-specific radionuclides in the repository environment is not well known. Since the effective diffusivity in bentonite is different for anions compared with cations and neutral species, the evaluation for the ESS-specific radionuclides was performed twice, under the assumption that they are anions and cations, respectively. The radionuclide charge state does not affect transport through concrete. Further, sorption coefficients, and sorption reduction factors due to the presence of complexing agents, are not well known for the ESS-specific radionuclides. Therefore, element analogues were used to select values. For all the ESS-specific radionuclides, the sorption capacity in cement and bentonite in BHA is assumed to be influenced by the presence of complexing agents formed from cellulose in the legacy waste. As described in the *no effect of complexing agents in BHA evaluation case* (Section 8.3.1), the amount of cellulose in the legacy waste is not well-known and, therefore, the evaluation for the ESS-specific radionuclides was performed once more, assuming no effect of complexing agents in BHA. Since no complexing agents are assumed to be present in the waste in BHK, sorption reduction factors are not applied there for this variant or any other evaluation case. For details, see Section 6.5 in the **Radionuclide transport report**.

## Summary of results

Under the assumption that there is no effect of complexing agents in the waste vault used for disposal of the ESS-specific radionuclides, this evaluation suggests that both barrier concepts are efficient in retarding the transport out of the repository for most ESS-specific radionuclides. For the relatively short-lived and sorbing radionuclides Si-32, Eu-150, Gd-148, Tb-157 and Tb-158, the maximum near-field activity release (per initial activity) is insignificant as compared with that of the main contributors (e.g. C-14) to the near-field activity release in the base case. However, for the long-lived La-137 and Re-186m, both barrier concepts are to some extent less efficient.

In the presence of cellulose, the sorption capacity in BHA is assumed to be reduced for most of the ESS-specific radionuclides. The result is substantially higher near-field releases for these radionuclides.

The ESS-specific radionuclides show a broad distribution in radiotoxicity, which will require consideration along with the complete radionuclide inventory from ESS once it is more firmly established. The total activity releases and doses must then be assessed to determine the final dose consequences and decide which repository concept is most suitable for the ESS inventory.

## 8.4 Conditions in the repository environs

### 8.4.1 Lower groundwater flow

#### *Rationale and handling in the model*

The *lower groundwater flow evaluation case* evaluates the effect of lower groundwater flows in the geosphere than those estimated for the SE-SFL example location in Laxemar. The rationale behind the evaluation case is that the Laxemar area shows a wide distribution of hydraulic conductivities, so flow rates around the near-field could potentially be minimised by identifying a body of rock for the repository that has more favourable hydraulic characteristics. Furthermore, it is likely to be possible to find an entirely different site that has generally lower flow rates than the example location in Laxemar. Decreased flow influences the radionuclide transport both directly, and indirectly through slower degradation of the barriers. In the present case, only the direct effects on radionuclide transport are analysed.

In the near-field model, the base-case flow rates  $Q$  in the waste and backfill compartments are multiplied by a scaling factor (see Section 7.2 in the **Radionuclide transport report**). Three variants are included; variants A, B, C with scaling factors of 0.1, 0.01, and 0.001, respectively. The equivalent flow rate  $Q_{eq}$  (Section 7.3.2), affecting diffusive transfer from the near-field to the geosphere, also decreases (Section 7.2.1).

In the geosphere model, the total advective travel time  $t_w$  [a] for a water particle, and the sum of the flow-related transport resistances  $F$  [ $a\ m^{-1}$ ], are increased via division by the scaling factor. The trajectory lengths are assumed to be unaffected by changes in flow conditions.

Radionuclides from the repository are discharged to the same biosphere object as in the base case, namely biosphere object 206. It is assumed that the groundwater discharge from the bedrock to the biosphere is primarily driven by recharge of meteoric water, and thus a reduction of groundwater flow at repository depth is not expected to have any significant effect on this flow. Thus, the hydrological and ecological conditions, as well as the exposed groups, from the present-day calculations are also used in this evaluation case.

#### **Summary of results**

Resulting annual doses are shown in Figure 8-7. A sufficient reduction in flow has the potential to substantially reduce the doses, to the point of meeting the regulatory risk criterion in the case of a flow reduction of 100-fold or more.

#### **BHA**

Lower groundwater flow at repository depth than in the base case leads to reduced releases and doses from BHA. Radionuclide transport through the near field of BHA occurs mainly through diffusion. Therefore, the reductions of the BHA near-field releases are modest in response to a decrease in the

groundwater flow rate. With 10 times lower flow rate, the maximum near-field releases of the assumed anionic species of Mo-93 and Cl-36 are 66 % of that in the base case. The corresponding maximum near-field releases of the cationic Tc-99, C-14 and Ag-108m are 41 % of that in the base case. Decreasing the groundwater flow rate further to levels 100 times lower than in the base case, the importance of decay in the geosphere increases. The radionuclide retention times in the geosphere increasingly exceed their half-lives and the radionuclide-specific responses are accentuated (Figure 8-7). For Tc-99, which sorbs in the geosphere, retention in the geosphere is more than seven orders of magnitude higher than in the base case (Figure 8-8 right panel). The maximum dose from BHA is reduced to 6 % of that in the base case (left panel in Figure 8-7). The dose contributions of Mo-93, C-14 and, in particular, Tc-99 decrease and the dose from Cl-36 becomes of greater relative importance as the groundwater flow rate decreases (Figure 8-7 left panel).

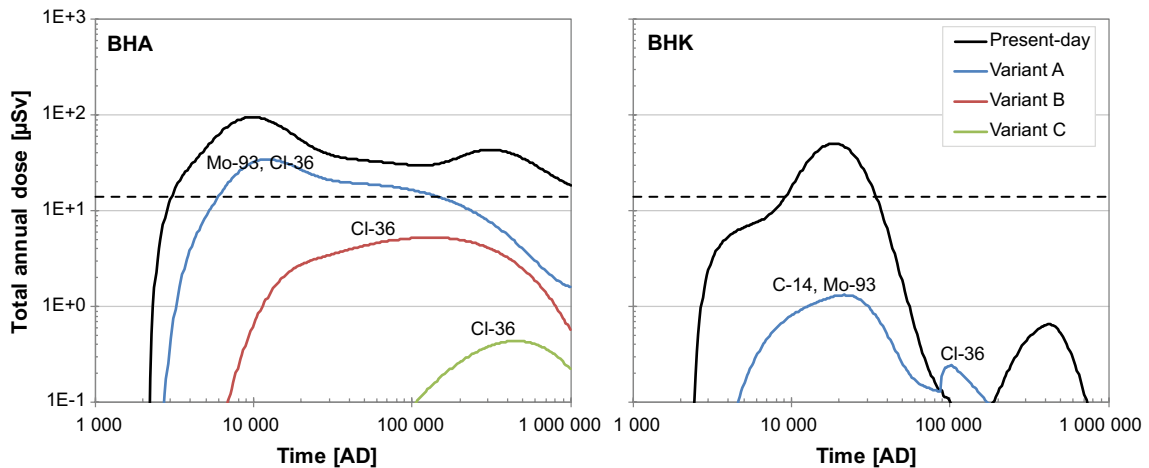


**Figure 8-7.** Annual dose from BHA (left) and BHK (right) in the lower groundwater flow evaluation case. Blue, red and green lines correspond to the dose from calculations where the groundwater flow in the repository and the geosphere is reduced by a factor of 10, 100 and 1000, respectively. The dose in the base (present-day) case is shown for reference (black line). The dose corresponding to the regulatory risk limit is shown with a dashed line. Figure identical to Figure 7-2 in the *Radionuclide transport report*.

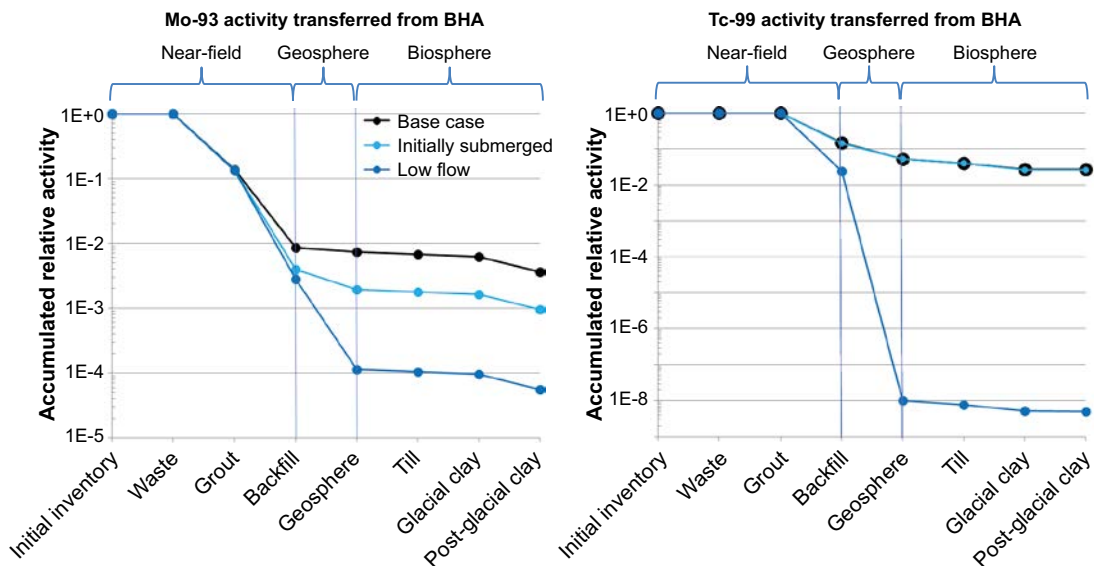


**Figure 8-8.** Activity of Mo-93 (left panel) and Tc-99 (right panel) transferred along the way from the initial inventory in BHA to the biosphere, accumulated over the entire analysis period of one million years, and normalised by the initial inventory. The relative activity transferred is shown for the base case (black), the variant with 10000 years of initially submerged conditions (light blue) and for the variant of the lower groundwater flow evaluation case with 100 times lower groundwater flow rate than in the base case (dark blue). Figure adapted from Figure 8-1 in the *Radionuclide transport report*.

## BHK

Lower groundwater flow rates have a greater impact on the doses from BHK compared with BHA, and 10 times lower flow rates are enough to decrease the dose from BHK to 3 % of that in the base case (right panel in Figure 8-7). The reason is mainly that transport within and out from the near field in BHK is limited by advection in the base case, whereas transport in BHA is mainly limited by diffusion and diffusive transport into surrounding fractures which is less sensitive to groundwater flow rates.

With ten times lower groundwater flow rates, the lower doses from BHK are mainly thanks to increased retention and decay in the near field, whereas retention and decay in the geosphere have a moderate effect (Figure 8-9). Lower groundwater flow rates affect the releases more for radionuclides strongly affected by decay, caused by a short half-life and/or strong sorption. Thus, the near-field release from BHK of the sorbing radionuclide Mo-93 (left panel in Figure 8-9) decreases more with lower flow rates than release of the non-sorbing C-14 (right panel in Figure 8-9).

With even lower groundwater flow rates, the relative importance of decay in the geosphere increases as the radionuclide retention times in the geosphere increasingly exceed their half-lives (not shown). The BHK near-field release eventually becomes dominated by diffusion with increasingly lowered groundwater flow rates.

The BHK near-field releases and doses in the *lower groundwater flow evaluation case* (Figures 8-5 and 8-6) are similar to the results for the *alternative concrete backfill in BHK evaluation case* (Figures 8-7 right panel and 8-9). The similarities are largely explained by the reduction in near-field advective flow by ten times in both evaluation cases. Geosphere retention and decay is, however, only affected in the *lower groundwater flow evaluation case*, and the decreased porosity in the *alternative concrete backfill in BHK evaluation case* has a different near-field effect on sorbing and non-sorbing radionuclides. Given the initial inventory in BHK, these two effects are of similar magnitude, resulting in similar total annual doses in the two evaluation cases (right panels in Figures 8-5 and 8-7).

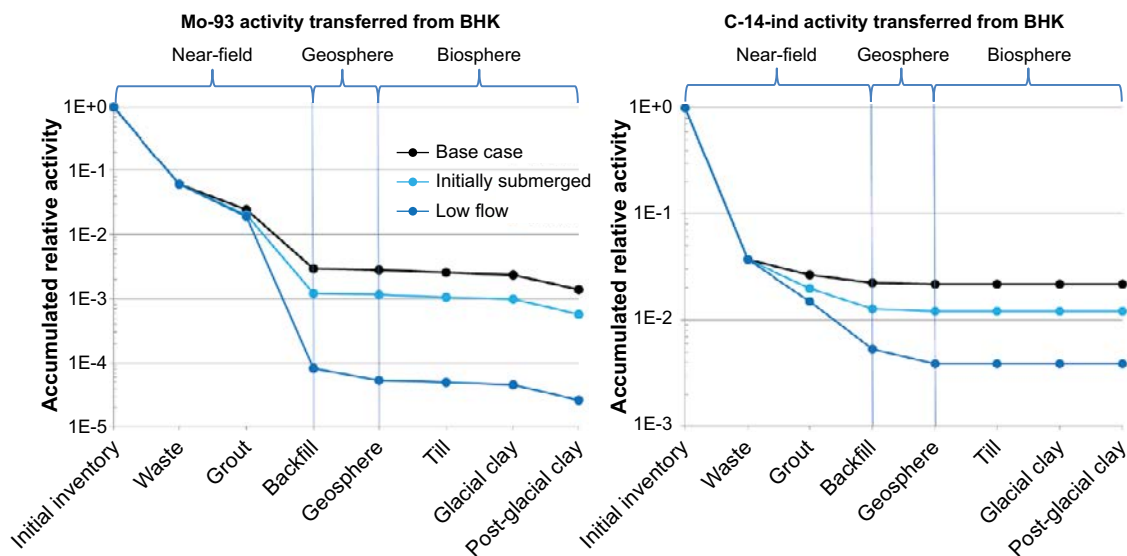


**Figure 8-9.** Activity of Mo-93 (left panel) and C-14 (right panel) transferred along the way from the initial inventory in BHK to the biosphere, accumulated over the entire analysis period of one million years, and normalised by the initial inventory. The relative activity transferred is shown for the base case (black), the variant with 10 000 years of initially submerged conditions (light blue), and for the variant of the lower groundwater flow evaluation case with 10 times lower groundwater flow rate than in the base case (dark blue). Figure adapted from Figure 8-2 in the *Radionuclide transport report*.

## 8.4.2 Initially submerged conditions

### Rationale and handling in the model

The *initially submerged conditions evaluation case* analyses the effect of locating SFL at a position that is currently below the seabed. A prolonged period of submerged conditions is likely to retard the advective transport from the repository due to low groundwater flow. This reduction is here assumed to correspond to 100 times lower groundwater flow rates during an initial period after repository closure. After a specified period, shoreline displacement causes a transition to the present rate. Three variants are included in this evaluation case, reflecting different durations between repository closure and when the area above the repository and the discharge area start to emerge from the sea. In the three variants, the groundwater flow starts to be influenced by the surface environment at the start of the simulations, after 5 000 years, and after 10 000 years, respectively.

The reconstructed shoreline displacement for the last glacial–interglacial cycle is used to describe the development of the landscape in this evaluation case, and radionuclides from the repository are discharged into biosphere object 206. This area is presently located at an altitude of 12.3 m above the mean sea level. For this evaluation case it is assumed that the groundwater flows in the surface environment of basin 206 start to become influenced by the surrounding terrestrial landscape when the average water depth is 6 metres (Chapter 3 in Grolander and Jaeschke 2019). From this state it takes 4 300 years according to the shoreline displacement reconstruction until the basin becomes an isolated lake (Section 6.2.1).

In the near-field and geosphere models, the groundwater flow pattern is assumed to be the same as in the base case. The changes in groundwater flow associated with the shoreline development are represented by a scaling factor, which modulates the magnitude of the groundwater flow relative to the present-day groundwater flow rate (lower panels of Figure 8-10). As in the *simplified glacial cycle* (Section 8.6.2) and *lower groundwater flow* evaluation cases (Section 8.4.1), the groundwater flow rates are scaled uniformly in the geosphere and near-field models. All other near-field and geosphere parameters are the same as in the base case.

In this evaluation case, radionuclides are discharged to the same biosphere object as in the base case, namely biosphere object 206. During the submerged period, the discharge is restricted to the central area of the sea basin that is object 206, which is later transformed into a lake-mire complex. For a detailed description of the assumptions made, see Section 7.3 in the **Radionuclide transport report**.

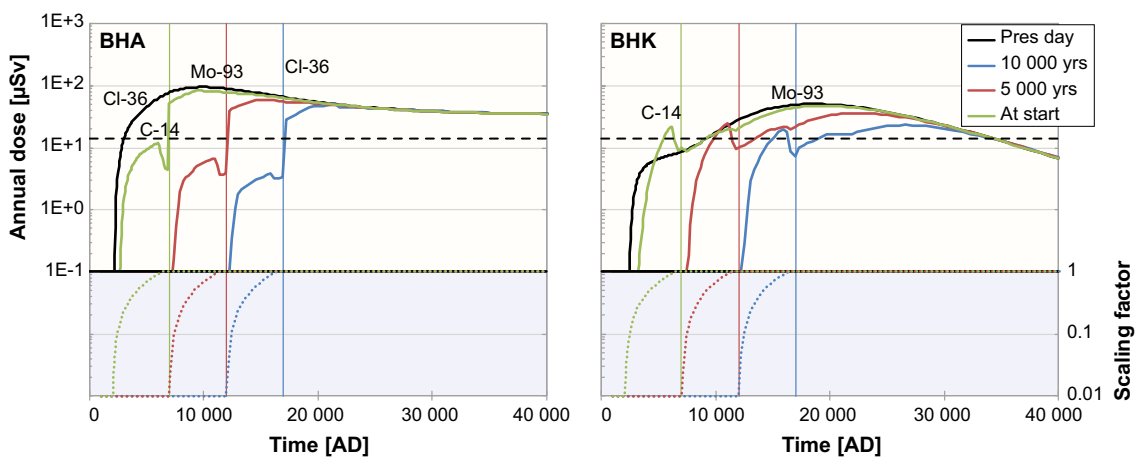


**Figure 8-10.** Annual dose from BHA (left) and BHK (right) in the three variants of the initially submerged conditions evaluation case. The terrestrial landscape starts to influence flow conditions in the waste vaults and the bedrock at the start of the simulation (green), after 5 000 years (red), or after 10 000 years (blue). The annual dose in the base case is shown for reference (black line). Dose-contributing radionuclides are indicated above the curves (early dose due to Cl-36 from BHA occurs in the base case only). Vertical line indicates when the biosphere object is 1 m above sea level, allowing cultivation of the drained mire. Lower panels show the hydrological scaling factor for the near-field and the geosphere release. Figure identical to Figure 7-6 in the **Radionuclide transport report**.

## Summary of results

This evaluation case entails 100 times lower flows, as in variant B of the *lower groundwater flow evaluation case*. In both cases, near-field releases from BHK experience a greater reduction than releases from BHA during the submerged period (not shown), because advection is the dominant mass transport process in BHK when the concrete is intact. Releases from the near-field of BHA are, on the other hand, diffusion-controlled. However, as the flow scaling factor returns to unity, radionuclides that have accumulated in BHK are flushed out, leading to release peaks, mainly due to C-14, that are similar to the base case but delayed in time. This flushing results in short annual-dose peaks, that in the earliest variant are higher than the corresponding dose in the *present-day evaluation case* (right panel in Figure 8-10). Generally, for both repository vaults, the effects of an initially submerged period diminish as the discharge area rises above sea level (Figure 8-10).

The evaluation shows that the maximum release rates to the biosphere may be delayed by the duration of the submerged period, and that radioactive decay may reduce the dose substantially in the terrestrial period following the submerged period due to shoreline displacement. For Mo-93 and C-14, which decay moderately during the submerged period, the maximum and accumulated near-field annual release rate from BHK is lower than in the base case (Figure 8-9). However, decay of Tc-99 and Cl-36 (half-life  $> 2 \times 10^5$  a) is limited during the submerged period, and, as is exemplified for Tc-99 from BHA (Figure 8-8), the accumulated release is hardly affected at all. Once the groundwater flow rate increases, the maximum near-field and geosphere release rates for these radionuclides are similar to those in the base case (Cl-36 shown in Figure 7-4 in the **Radionuclide transport report**). The resulting effect of an initially submerged period is not dramatic; the maximum annual dose from a repository that is submerged for 10 000 years is reduced by a factor two, as compared with release to a land location (base case).

### 8.4.3 Alternative geosphere retention properties

#### *Rationale and handling in the model*

In the geosphere transport calculations in the base case, the sorption coefficients  $K_d$  and bedrock diffusivities were cautiously chosen (Sections 3.3.1 and 3.3.3 in Shahkarami 2019). For instance, the  $K_d$  value of the dose-dominating radionuclide Mo-93 is set to zero in the absence of site-specific data from the Laxemar (and Forsmark) data set. However, site-specific data from Olkiluoto suggest that Mo-93 sorption does occur (Hakanen et al. 2014). The sensitivity of the resulting dose to the assumptions made in the base case is illustrated in the two variants of this evaluation case, where alternative geosphere retention properties, i.e.  $K_d$  values and rock diffusivities, are taken from the safety assessment for SKB's Spent Fuel Repository in Forsmark (SR-Site; SKB 2010i), or from the safety assessment for Posiva's repository for spent fuel in Olkiluoto, Finland (Posiva 2013). The differences between these data sets and the data used in the base case can be attributed to both site-specific conditions and differences in the reasoning behind the selection of  $K_d$  values. More details on this evaluation case can be found in Section 7.4 in the **Radionuclide transport report**.

$K_d$  values for the base case (Laxemar) are closer to the corresponding values for Forsmark than to those for Olkiluoto.  $K_d$  values in the Forsmark variant are about half of those used in the base case for Ag, Ni, Tc, U (including some of its decay products) and some other less important radionuclides. The differences reflect the general site-specific differences between Forsmark and Laxemar in terms of groundwater chemistry (pH, redox potential, salinity) and mineral composition. In the Olkiluoto variant, on the other hand, the  $K_d$  values are higher than in the base case for Ni, Mo, Ra, Tc and some less important radionuclides and lower for Ag, U and a few more elements. The differences in  $K_d$  values between Olkiluoto and Forsmark largely result from site-specific measurements (or lack thereof for some elements in Forsmark), and some higher  $K_d$  values in Olkiluoto can be explained by a greater presence of micaceous minerals (i.e. biotite, chlorite, muscovite) that offers increased cation sorption. Bedrock diffusivities are also higher in the Olkiluoto data set, by a factor of 7 for anions and a factor of 2 for cations and non-charged species.

### Summary of results

Using the Forsmark set, with  $K_d$  values about half as large as in the base case, has a limited effect on geosphere releases of sorbing nuclides, and since the main dose contributors, Mo-93, Cl-36 and C-14, are non-sorbing in both the Forsmark set and the base case, the effects on total annual doses during the first 100 000 years is marginal.

The increased diffusivity in combination with changing the  $K_d$  value for Mo-93 from zero in the base case to non-zero in Olkiluoto, decreases the Mo-93 release and its maximum dose from BHA by a factor of three (left panel in Figure 8-11). This makes Cl-36 the main contributor to the maximum annual dose instead of Mo-93 and the maximum total annual dose decreases by a factor of two. In addition, the second maximum in annual doses from BHA is significantly reduced due to the increased diffusivity and higher sorption of Tc-99 in the Olkiluoto data set than in the base case. BHK releases and doses display similar but smaller effects for Mo-93, and also for Ni-59 (right panel of Figure 8-11).

The sensitivity of the relative geosphere release to changes in diffusivity and  $K_d$  values is larger for radionuclides with a higher proportion of decay in the geosphere. Thus, the choice of retardation parameters is most important for relatively strongly retarded and dose-contributing radionuclides like Tc-99. Geosphere releases and annual doses from most high-retention radionuclides are very low due to decay in the near-field and the geosphere, and substantial geosphere  $K_d$  value reductions are needed for the geosphere release of these radionuclides to become noticeable. Furthermore, a shift between non-sorbing ( $K_d = 0$ ) and sorbing ( $K_d > 0$ ) behaviour could also influence geosphere releases and doses substantially and should be carefully considered for some cases, particularly Mo-93.

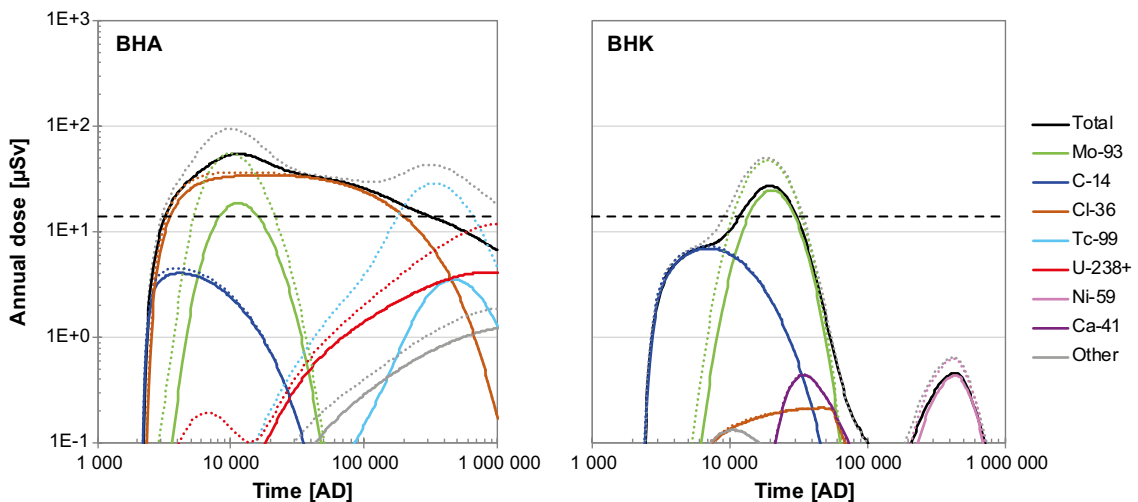


**Figure 8-11.** Annual doses from BHA (left panel) and BHK (right) with the Olkiluoto retention parameter set (solid lines) and for the base case (dotted lines). Figure identical to Figure 7-10 in the **Radionuclide transport report**.

## 8.4.4 Alternative regional climate

### Rationale and handling in the model

The *alternative regional climate evaluation case* illustrates to what extent the external conditions driven by the regional climate at the repository site may affect the calculated dose. External conditions are derived from temperature and precipitation regimes at three additional locations along the Swedish coast (Figure 8-12). The near-field and geosphere conditions are not expected to be affected by variations in regional climate within the temperate domain. However, groundwater recharge and discharge at the surface is expected to respond to changes in climate. Thus, post-closure safety for alternative regional climates is evaluated by adjusting the groundwater flow in biosphere object 206.

The North and Central regional climate variants correspond to locations along the Baltic sea coast, and the Southwest climate corresponds to a location facing the Swedish west coast (i.e. on the shores of Kattegatt/Skagerrak). As in the base case, the variant climatic conditions are assumed to prevail during the entire analysis period of 1 million years after repository closure. More details on this evaluation case can be found in Section 7.6 in the **Radionuclide transport report**.

### Summary of results

The results suggest that a climate associated with higher rates of groundwater recharge and discharge (i.e. a climate with higher precipitation and/or lower annual temperature) is likely to result in a lower annual dose than in the base case. Thus, representing the climate of a future repository with the conditions in Laxemar is a cautious assumption for present conditions compared with sites located in different parts of Sweden. However, the response to variations in regional climate is modest, and depends on the radionuclide composition of the release. Thus, it is unlikely that selection of a location with a favourable climate within the borders of Sweden would reduce the annual dose from SFL by more than a factor two as compared with Laxemar (the base case). Moreover, if the release of Mo-93 from the repository remains at the postulated levels (which results in a major contribution to dose), a reduction of around 35 % is a more realistic upper estimate of what could be accomplished by selection of a site along the southwest or central Swedish coast.

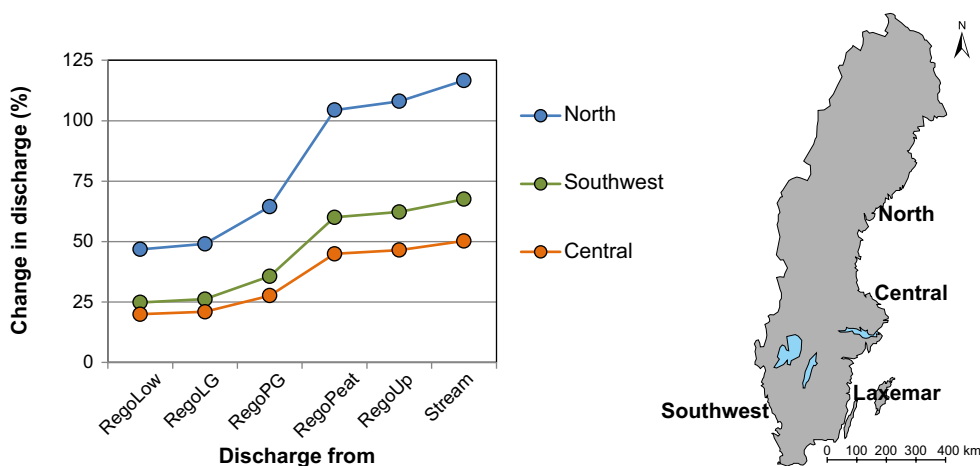


**Figure 8-12.** Groundwater discharge pattern as a function of regolith layer and regional climate. The rates are calculated for a time-independent mire (object 206) and are expressed as the relative increase (change) compared with those in Laxemar, i.e. Laxemar corresponds to 0 % change. The regional climate variants are examples along the Swedish coast. Figure modified from Grolander and Jaeschke (2019).

## 8.5 Uncertainties in bedrock properties, discharge area and effect of drilled well

### 8.5.1 Alternative realisations of stochastic bedrock fractures

#### *Rationale and handling in the model*

The groundwater flow through the bedrock is modelled using a discrete fracture network (DFN) approach (Joyce et al. 2019). The network contains deterministic fractures and also fractures generated stochastically from the derived fracture network statistics. The stochastically generated DFN realisations differ both with respect to the number of fractures intersecting each vault and their properties near the repository, and with respect to the characteristics of the flow pathways from repository depth to the surface. In this evaluation case, the sensitivity of the performance of BHA (including the bedrock as a natural barrier) to variations in the discrete fracture network was examined.

Five DFN realisations were performed and, for each realisation, the BHA repository was assumed to be located either at its original position (East) or at the BHK position (West). In the first realisation, which was selected for the base case, the repository is comparatively well connected to the geosphere. The first realisation includes deterministic properties of the deformation zones, the other four realisations treat the hydraulic properties of the deformation zones stochastically. All realisations account for a depth dependency of the properties. Although the number of realisations may be insufficient to fully assess the variability that is associated with the stochastic properties of the DFN, they should still give a reasonable indication of the likely spread of effects on transport and dose that can be expected between individual realisations.

For the western position, the conditions at the outer geometry of the BHA vault are approximated with those outside BHK (Section 7.5 in the **Radionuclide transport report**). Within the BHA waste vault, transport is dominated by diffusion, and therefore the advective flow through the near-field was not modified in the alternative DFN realisations. Thus, in total, ten DFN variants were studied and each of these variants has its unique set of connectivity parameters ( $R_{\text{plug}}$  and  $Q_{\text{eq}}$ , Section 7.3.2) and a unique distribution of flow pathways (characterised by the two parameters  $t_w$  and  $a_w$ , Section 7.3.3). In Figure 8-13 results for the East position are illustrated in terms of the connectivity parameter  $Q_{\text{eq}}$  and the flow pathway travel time  $t_w$ . All other near-field and geosphere parameters are the same as in the base case.

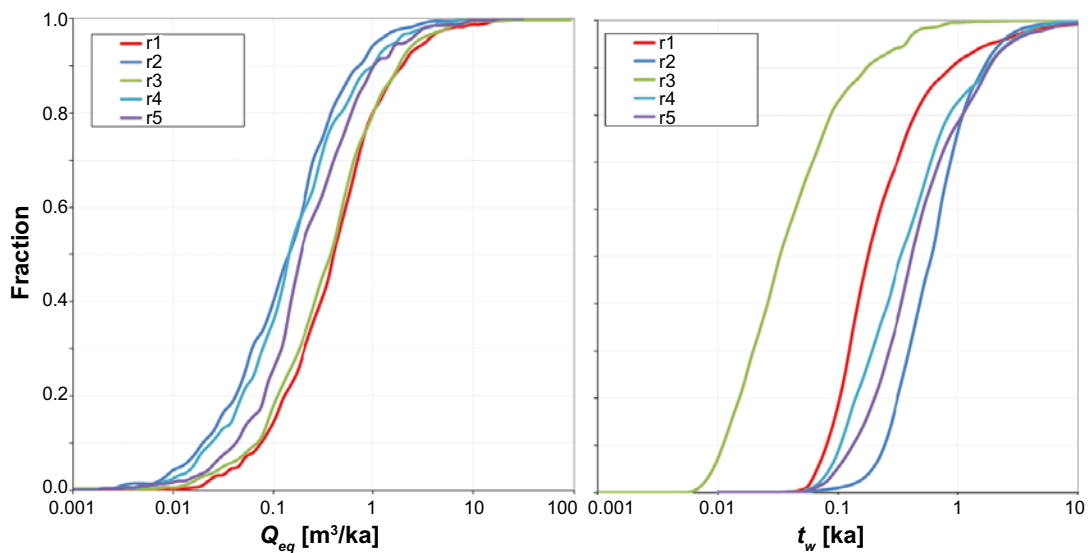


**Figure 8-13.** Connectivity and flow pathway characteristics from BHA in the East position (as in the base case) for the five DFN realisations. The graphs show the cumulative distribution functions for  $Q_{\text{eq}}$  (left) and  $t_w$  (right) of particles reaching the surface. The red curve corresponds to the base case realisation. In realisations 1 and 3, large sub-vertical fractures intersecting the vaults cause significantly higher  $Q_{\text{eq}}$  values and significantly lower  $t_w$  values. Figure identical to Figure 7-11 in the **Radionuclide transport report**.

## Summary of results

Stochastic variation in the discrete fracture network has a substantial effect on the geosphere release of mobile radionuclides such as C-14, Cl-36 and Mo-93 and even more so on the release of Tc-99 (Figure 8-14 left panel). The fracture network affects both the connectivity between the waste vault and the flow pathway to the surface and the characteristics of that flow pathway. For Cl-36, the difference in the connectivity is the primary source of variation in the geosphere release, whereas differences in the flow pathways through the bedrock is by far the most important source of the variation for release of Tc-99. Because Tc-99 sorbs in the rock matrix, the relationship between the rate of advection towards the surface and diffusion into the fracture is a key factor determining the activity reaching the biosphere. The geosphere transport of non-sorbing radionuclides is also affected by the travel time and the volume-specific flow-wetted area, but non-sorbing radionuclides with substantial near-field releases are far less sensitive to variations in DFN properties. The limited sensitivity of non-sorbing radionuclides and the selection of properties assigned to the DFN in the base case, together ensure that uncertainties with respect to the fracture network realisation are not likely to have a significant influence on the results of this safety evaluation. Nevertheless, large sub-vertical fractures intersecting a waste vault can influence both the connectivity of the vaults and provide direct pathways to the surface, and hence the occurrence and properties of such features is of key interest in a site characterisation.

### 8.5.2 Alternative discharge area

#### Rationale and handling in the model

In the biosphere model, the dose to the most exposed group of future human inhabitants is calculated. Since the location of a potential future repository and the areas where groundwater from the repository will reach the surface are unknown, the *alternative discharge area evaluation case* is designed to study how total and nuclide-specific annual doses are affected by properties of the discharge area. Further, to what extent the simplifications made in the base case (i.e. terrestrial ecosystems in biosphere object 206) influence the projected doses is also studied. The representativeness of object 206, which is used in all other evaluation cases, is examined and discussed.

All near-field and geosphere parameters are the same as in the base case (Section 7.6 in the **Radionuclide transport report**). Thus, the magnitude and temporal pattern of the release from the geosphere and repository into the lower regolith (till) of each biosphere object is the same as the release

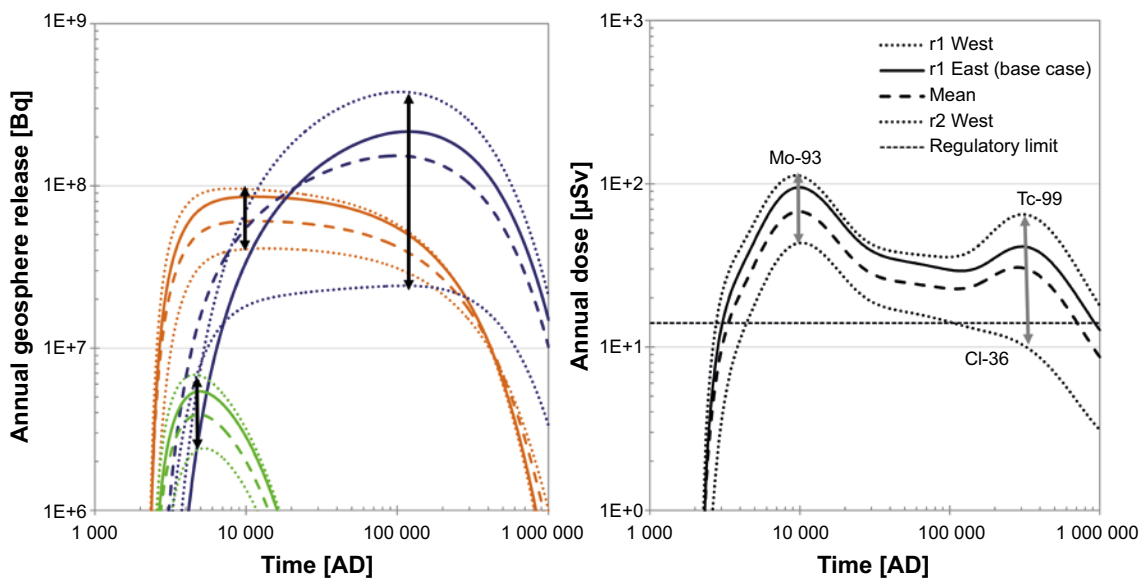


**Figure 8-14.** Annual geosphere releases and annual doses from BHA in the alternative realisations of stochastic bedrock fractures evaluation case. The realisations with the largest and smallest values are indicated with dotted lines, the means over ten DFN variants are shown with a dashed line, and the release and dose in the base case is shown with a solid line. Vertical arrows indicate the approximate range of maximum values. Left: Release of individual radionuclides; Cl-36 (brown), Mo-93 (green) and Tc-99 (dark blue). Right: Annual dose; dominant dose-contributing radionuclide indicated with text. Figure identical to Figure 7-14 in the *Radionuclide transport report*.

into object 206 in the base case (Figure 7-11). This means that all radionuclides from BHA and BHK that reached the bedrock surface in the radionuclide transport model were respectively released into each of the biosphere objects used in the *alternative discharge area evaluation case*.

As in the base case, the ongoing shoreline displacement and landscape development is not considered, and biosphere objects are simulated as static objects only, in a fixed ecosystem state. That is, present-day conditions are assumed for the entire assessment period of 1 million years. The effects of landscape development on annual doses are explored in the **Biosphere synthesis**. Further, the calculations of potential effects are limited to the primary discharge area, and exposure in down-stream objects is not evaluated. Nine potential discharge areas of deep groundwater (i.e. biosphere objects) in Laxemar and six areas in Forsmark were used in the analysis. The selected biosphere objects vary with respect to geometrical properties (object and watershed surface area), the depths of water, the regolith stratigraphy, and associated groundwater flow.

The Laxemar objects (Figure 7-6) are five current agricultural ecosystems (object 204, 206, 210, 212 and 213), one mire (203), one lake (207), one sheltered (208) and one relatively open (201) coastal bay. The five agricultural objects and the three aquatic objects were also described as static mire ecosystems (that could have or would develop in the absence of human intervention). All Laxemar biosphere objects are likely discharge areas for deep groundwater, and thus the set illustrates the potential effect of alternative locations of a hypothetical SFL repository within the Laxemar area or of differences in transport pathways from the repository to the surface system.

The local and regional topography affects the geometry of ecosystems and the surface hydrology. With the Forsmark biosphere object set, the effects of a release to a landscape with a flatter topography are examined (Figure 3-13 in Grolander and Jaeschke 2019). The set consist of six presently submerged biosphere objects located above the SFR repository (SKB 2014f), but in this evaluation they are all cautiously assumed to be fully developed mires.

### **Summary of results**

There are several factors that affect the projected dose from a discharge area, including the type of ecosystem, the properties of the area, and the development of the area. Figure 8-15 illustrates the maximum annual doses for BHA and BHK from the most important radionuclides, resulting from the same discharge into different biosphere objects as defined from data from Laxemar and Forsmark. The highest maximum annual doses typically result from accumulation of radionuclides in a mire, from which they are subsequently exposed and mobilised by drainage and cultivation, i.e. a scenario evaluated in the base case (biosphere objects with green and orange background in Figure 8-15). On the other hand, release to an open sea basin can result in doses that are several orders of magnitude lower (biosphere objects with blue background in Figure 8-15), partly due to a reduction of the activity during slower transport through the regolith (e.g. Tc-99 and Mo-93), and partly due to dilution in the open water (all radionuclides). The doses from lake ecosystems are also typically lower than from terrestrial ecosystems (biosphere objects with light blue background in Figure 8-15). However, for medium- and large-size discharge areas, the exposure from a lake can yield a higher dose from C-14 than from draining a mire, due to accumulation in aquatic foods.

The total maximum annual dose from both BHA and from BHK varies by more than an order of magnitude among the mire systems. However, for releases from BHA, the relative contribution of individual radionuclides (e.g. Tc-99) may also vary substantially. In general, doses from all radionuclides are lower in large objects (c.f. objects 116, 201, 208) due to dilution, especially for mobile radionuclides such as C-14 and Cl-36. The activity of sorbing radionuclides (e.g. Mo-93 and Tc-99) is also affected by radioactive decay, and parameters that decrease transport rates reduce the activity from the geosphere released along the upward flow pathway. As the area-specific discharge both affects transport rates and the volumetric dilution of radionuclides in the regolith, there is no uniform relationship between this rate and the total dose.

The terrestrial biosphere object (206) that is used in the base case is a mire that has developed in a small but relatively deep lake basin, which has a relatively high specific discharge of groundwater from the bedrock. This configuration results in a relatively high annual dose that is either due to exposure from Cl-36 and Mo-93 (first 100 000 years) or due to exposure from Tc-99 (BHA after 100 000) years. The dose from C-14 in this terrestrial object is considerably lower than in discharge areas with open lakes, but total doses from lakes are still smaller than estimated total drained mire doses from object

206. Moreover, the doses in developing objects are similar to or lower than the doses from static representations (lakes or mires) of the same ecosystems (**Biosphere synthesis** and Section 7.6.6). Thus, the results indicate that using a stationary representation of the mire ecosystem in object 206 (as is done in the base case and most other evaluation cases) is a reasonable simplification of the biosphere for discharge areas in Laxemar. However, the thick layer of peat in the object prevents activity in the glacial clay from being exposed by drainage and cultivation. Thus, if the postulated release from BHA is discharged in an area with relatively thin layers of peat and post-glacial sediments overlying glacial clay (e.g. objects 121\_2 and 157\_2 in Forsmark), then the resulting dose from Tc-99 alone could be a factor of five larger than the total dose projected from object 206 (Figure 8-15).

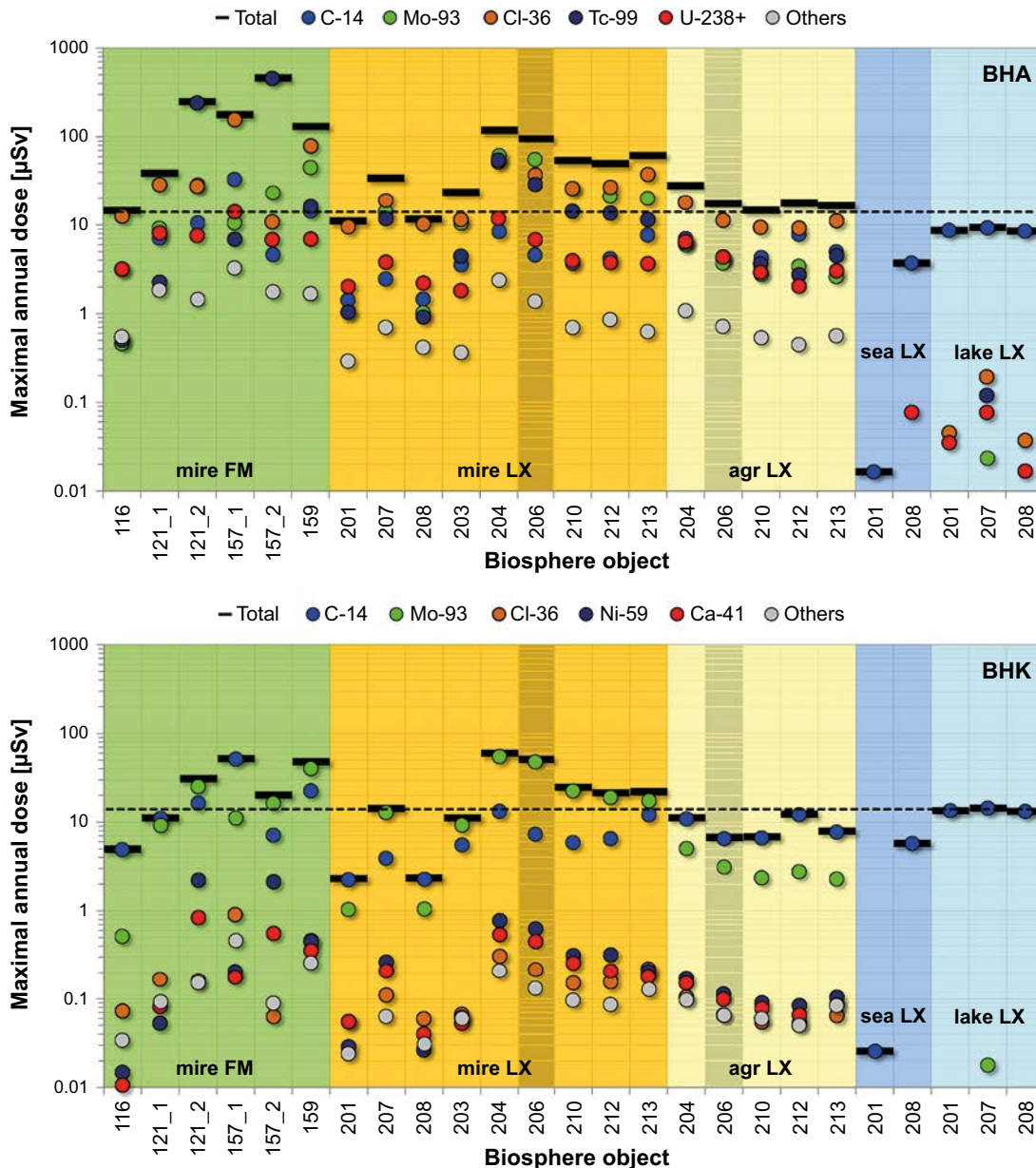


**Figure 8-15.** Maximum annual doses from the most important radionuclides in objects from Forsmark (FM, green background) and Laxemar (LX, all other background colours) from BHA (upper panel) and BHK (lower panel). The base-case object 206 is indicated in darker shade. Static mire objects in Forsmark (green background) and Laxemar (orange) are represented by drained mire doses including exposure from a dug well. Static agricultural objects (yellow) include exposure from a dug well and static sea (blue) and lake (light blue) objects are represented by doses to hunter-gatherers. The dose corresponding to the regulatory risk limit is shown with a dashed horizontal black line (14 µSv). Note that the sum of the radionuclide-specific doses can be larger than the total dose, since the doses from individual radionuclides reach their maxima at different times. Figure identical to Figure 7-16 in the *Radionuclide transport report*.

### 8.5.3 Drilled well

#### *Rationale and handling in the model*

In this evaluation case, the effect of using drinking water from a well drilled into the bedrock is analysed. Five hypothetical, 60 m deep, drilled wells are positioned in the areas north and east of the repository, where discharge from the repository occurs (Figure 8-16). In the five realisations of the stochastic fracture network, the discharge from the waste vaults primarily reaches biosphere objects 204 and 206 and, in one realisation, also biosphere object 210 (Section 4.7 in Joyce et al. 2019). Therefore, two wells are positioned close to each of objects 204 and 206, and one well is positioned close to object 210. With the postulated water withdrawal rate, only one of these five wells would receive particles from the repository at the example site. The properties from this single well are used to assess the potential dose in this evaluation case.

The exact position of the drilled well is determined accounting for three separate criteria. First, to ensure drinking water quality, a well needs to be protected from inflowing surface water and, therefore, low areas in the landscape, such as wetlands and agricultural land, are avoided. Second, to avoid an unnecessarily deep well, high points in the terrain are avoided. Third, to ensure a viable yield, the well needs to intersect at least one fracture in the flowing fracture network.

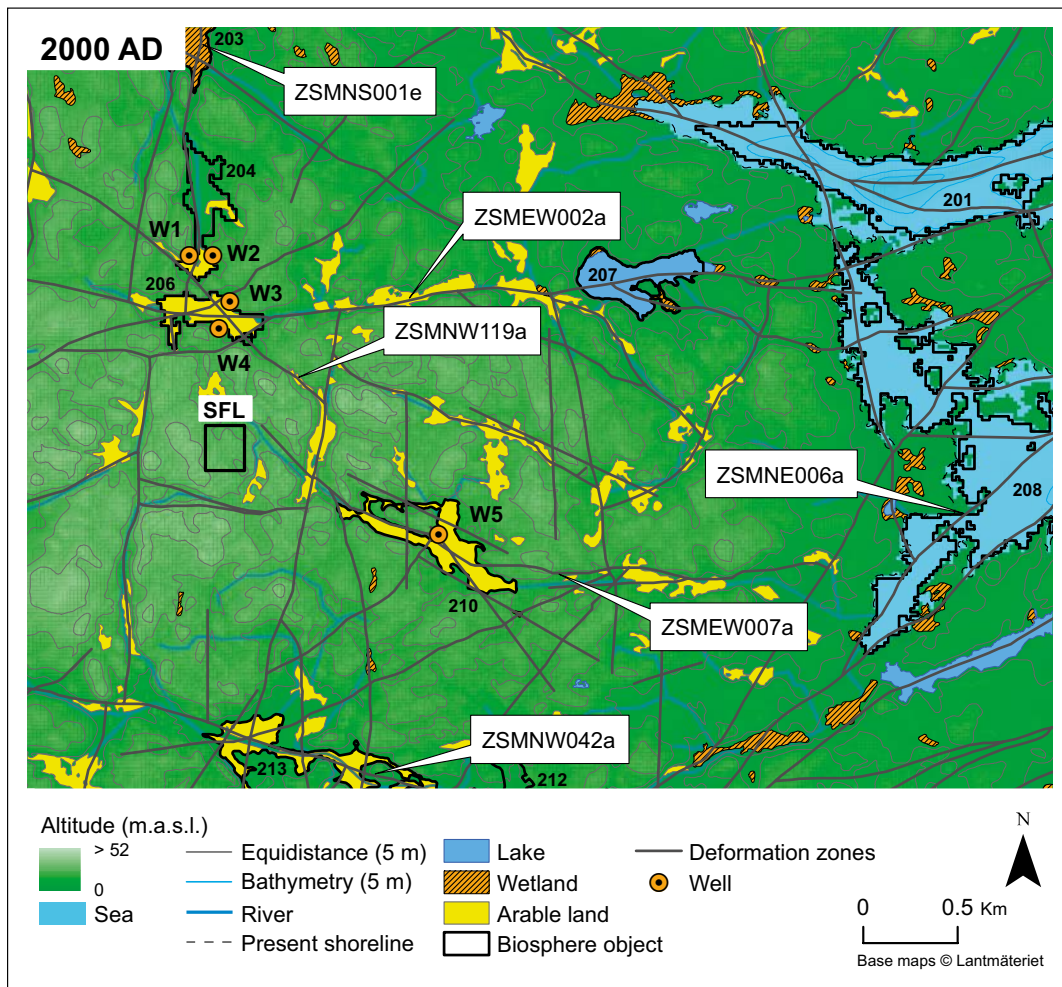


**Figure 8-16.** Well locations (orange, labelled W1 to W5) in the present Laxemar landscape. Biosphere objects are marked with numbers (e.g. 204, 206 and 210) and the names of deformation zones are given in white squares (ZSM). The spatial location and extent of deformation zones is for a depth of 20 m below sea level. The assumed location of the SFL repository (black square) is added for reference. Figure modified from Joyce et al. (2019).

The effect of the well on the hydrogeological performance measures was found to be small in the hydrogeological study (Joyce et al. 2019) and, therefore, the release from the geosphere to the well is calculated by multiplying the base case releases from the geosphere by the fraction of particle tracks that end up in well W3 (3.1 % for BHA and 2.1 % for BHK, Figure 8-16). Thus, all near-field and geosphere parameters are the same as in the base case (Section 7.8 in the **Radionuclide transport report**).

The doses from exposure to radionuclides in well water were evaluated using a garden plot household of five individuals. The members of the group are exposed through drinking water, and by ingestion of vegetables and potatoes from an irrigated kitchen garden. There are no *a priori* assumptions on the physical location of the household.

The amount of water extracted from the well is assumed to be 700 L d<sup>-1</sup> (255 m<sup>3</sup> a<sup>-1</sup>), which is higher than the water use expected from a tap in a yard, and somewhat lower than present-day levels when connected to a public water works (either of these could correspond to a garden-plot household). The water concentration is calculated by dividing the geosphere release that reaches the well by the water extraction rate.

In accordance with the guidance in the regulations (SSM 2008b), the family household utilizing a well is viewed as a small group. Consequently, the calculated annual effective dose is evaluated against an annual dose criterion of 140 µSv (which corresponds to an annual risk criterion of 10<sup>-5</sup>).

### Summary of results

The maximum annual effective dose that results from extracting water from a drilled well is above 100 µSv, is due to release from BHA, and is still rising at the end of the assessment period (Figure 8-17). Ra-226 and its decay products are the main contributors to dose, and the geosphere release of Ra-226 at times beyond 20000 AD originates from U-238 in the waste (and accumulation of uranium and thorium isotopes in the near-field and the geosphere). The primary reason for a significantly higher activity of Ra-226 in the drilled well when compared with a dug well is the reduction by radioactive decay along the transport pathway in the till (from where water from the dug well is extracted). Although the annual effective dose from the drilled well is significantly higher than that from a drained mire, the number of people exposed to water extracted from a single well is limited, and the dose from BHA is in the same order of magnitude as the annual dose corresponding to the risk criterion for a small group (140 mSv). The dose from BHK is almost two orders of magnitude below this level.

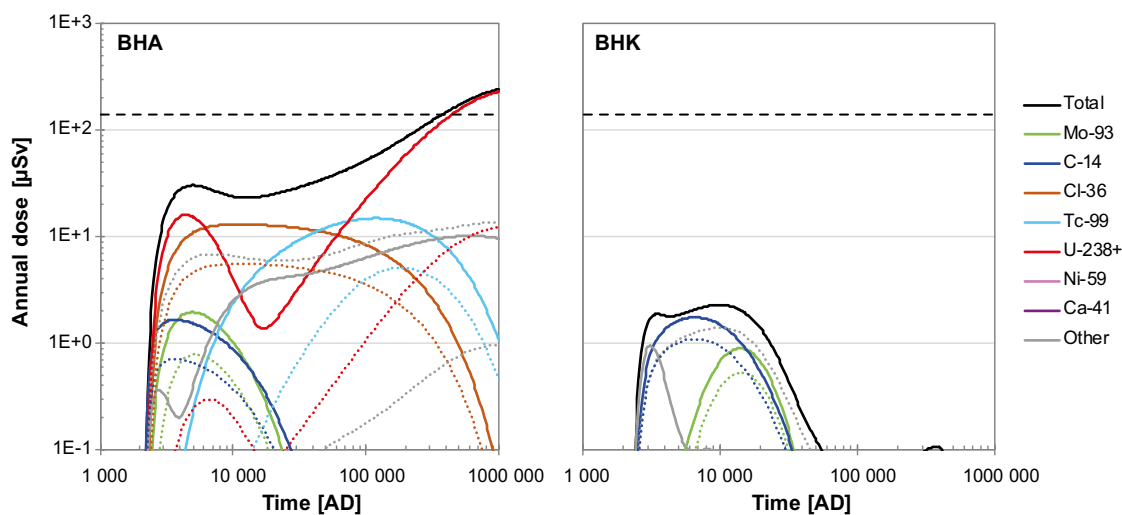


**Figure 8-17.** Annual dose from BHA and BHK to a garden plot household in the drilled well evaluation case. Colours represent doses from individual radionuclides. Dotted lines represent the dose in the base case (for a garden plot household without exposure through fertilization with ash). The dose corresponding to the regulatory risk limit for a small group (140 µSv) is shown with a dashed line.

## 8.6 Climate conditions

The future climate evolution at the example site is associated with uncertainty. To cover the most important and reasonably foreseeable sequences of future climate states that deviate from the present-day conditions in the base case, two additional climate variants are defined in the **Climate report**. Potential consequences of these climate variants are evaluated in the *increased greenhouse effect* and *simplified glacial cycle evaluation cases* (Figure 8-1). The objective is thereby to analyse if the alternative climate evolutions considered are likely to yield higher maximal annual doses than the base case climate assumptions, and to gather knowledge regarding which aspects may be important for the definition of a set of climate variants in a future safety assessment for SFL.

### 8.6.1 Increased greenhouse effect

#### ***Rationale and handling in the model***

The *increased greenhouse effect evaluation case* illustrates the effects of this specific change in external conditions on post-closure safety. The case is represented by the *increased greenhouse effect variant* of the SE-SFL reference evolution (Section 6.3). External conditions due to an increased greenhouse effect are derived from temperature and precipitation changes expected according to IPCC's intermediate emissions scenario RCP4.5 (Section 5.3 in the **Radionuclide transport report**). During the growing season, discharge and runoff may be reduced in a warmer climate (Section 6.3.5) and the water deficit for crops is expected to increase. On an annual basis, the geosphere and near-field conditions are, however, not expected to be affected by the increased greenhouse effect in a way that significantly affects repository performance. Dose consequences of a warmer climate are thus evaluated in biosphere object 206 by adjusting the atmospheric concentration of CO<sub>2</sub> and by modifying the discharge rates of ground- and surface-water. Two variants of this case are evaluated; in the first, crop water deficit is covered by an increased uptake of groundwater through capillary rise, whereas in the second variant it is covered by irrigation with surface water.

#### **Simplifications in comparison to the reference evolution**

The reference evolution of this climate variant describes a water deficit for plants (Section 6.3.2). This deficit is in the dose calculations cautiously assumed to be fully covered by increased irrigation (**Radionuclide transport report**, Section 5.3).

#### **Summary of results**

The *increased greenhouse effect evaluation case* shows that the combination of a decrease in groundwater discharge and an increase in plant water demand may increase the annual dose from some radionuclides. However, the changes in external conditions are unlikely to result in an annual dose that is substantially higher than that calculated for present-day conditions (Figure 8-18). The largest effects may be expected for weakly sorbing radionuclides; for example, the dose from Cl-36 may be increased by 50 %. However, this is not true for C-14, since dilution caused by increased atmospheric concentrations of stable CO<sub>2</sub> is likely to counteract the effect from an increased groundwater concentration. The effects of a warmer climate on radionuclides for which transport and accumulation are quantitatively affected by radioactive decay, such as Mo-93, is also expected to be less pronounced. This is because a decrease in groundwater flow will decrease the release of radionuclides discharged to upper regolith layers. The effects of a warmer climate on radionuclide accumulation may be reversed if irrigation is assumed to cover the crop water deficit since irrigation causes smaller crop activities compared with those resulting from plant root uptake, at least for the dose-contributing radionuclides examined.

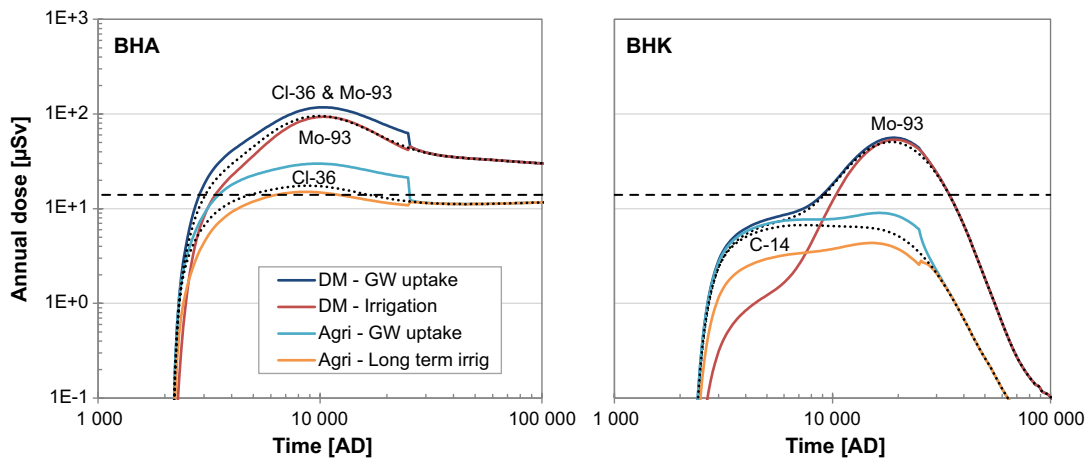


**Figure 8-18.** Annual dose for release from BHA (left) and BHK (right) in the increased greenhouse effect evaluation case. Two land-use variants are examined: draining and cultivating a mire (DM) and continuous cultivation (Agr). The crop water deficit is either covered by groundwater (GW, variant A) or by irrigation (variant B). Dose in the present-day evaluation case is shown for reference (black dotted lines). Note that external conditions return to present day characteristics at 26 000 years after repository closure, and that the time axis has been truncated at 100 000 AD. Figure identical to Figure 5-26 in the **Radionuclide transport report**.

## 8.6.2 Simplified glacial cycle

### **Rationale and handling in the model**

The *simplified glacial cycle evaluation case* is included in the analysis with the aim of covering the colder end of the range within which future climate may vary, represented by the *simplified glacial cycle variant* of the SE-SFL reference evolution (Section 6.4). Thus, it facilitates evaluation of potential impacts on releases and doses of periglacial, glacial, and submerged conditions, and the transitions between these states. This variant of the SE-SFL reference evolution describes the overall climate development in the reconstruction of the last glacial-interglacial cycle, analysed in previous safety assessments, e.g. in SR-Site (SKB 2010b, 2011a), for more details see Sections 4.1 and 4.3 of the **Climate report**. The sequence of events from 2000 AD to 102 000 AD is illustrated in Figure 6-20.

In this evaluation case, a detailed and cyclically repeated chain of events is adopted to illustrate the release of radionuclides and dose consequences due to the passage of an inland ice sheet and to shore-line displacement. Groundwater flow is changed in synchrony along the model chain and the conditions and properties of the surface system are modified according to climatic conditions and the succession of discharge areas (Section 5.4 in the **Radionuclide transport report**).

### **Handling in the near-field and geosphere models**

The properties of the engineered barriers in SFL are assumed to develop in the same way as in the *present-day evaluation case*. The changes in the external conditions in this evaluation case are assumed to influence the rate of groundwater flow in the repository and the geosphere, but to have no effect on the pattern of the flow field and thus the length of the flow pathways (Section 6.4.5). The groundwater flow rate is expressed with a scaling factor, relative to the groundwater flow rate in the *present-day evaluation case* (Figure 8-19). The derivation of the scaling factors for the different climate periods is discussed in Appendix C in the **Radionuclide transport report**. For discussion on the effects of scaling groundwater flow rates on radionuclide transport see the *lower groundwater flow evaluation case* (Section 8.4.1 in this report and Section 7.2 in the **Radionuclide transport report**).

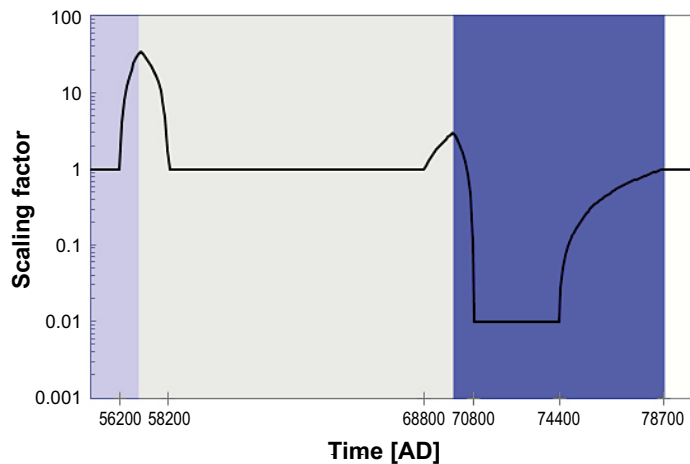


**Figure 8-19.** Scaling factor representing groundwater flow in bedrock and repository in the simplified glacial cycle evaluation case relative to present-day temperate terrestrial conditions, see further Table C-1 in the **Radionuclide transport report**. The evolution is shown for the period 52 000–82 000 AD, during which the scaling factor deviates from 1. On the x-axis are indicated the time points where the factor changes abruptly. Background colour represents climate domains, i.e. surface conditions, where lavender = periglacial, grey = glacial, blue = submerged, and white = temperate. Figure identical to Figure 5-28 in the **Radionuclide transport report**.

### Handling in the biosphere model

In periods of temperate climate, radionuclides from the repository are discharged to the same biosphere object as in the *present-day evaluation case*, namely biosphere object 206. During periods of periglacial climate, the mire in object 206 is assumed to be frozen, and consequently not connected to flowing bedrock groundwater. During this period, release is instead assumed to reach a lake via a through talik, as represented by Lake Frisksjön (object 207). Given the size of this lake (190 m radius and 4 m average water depth) it is plausible that a through talik may form under the waterbody, even when permafrost reaches a depth of 300 m (Hartikainen et al. 2010, Claesson Liljedahl et al. 2016).

When Laxemar is in the glacial climate domain, radionuclides from the geosphere are assumed to be discharged to a sea basin beyond the ice margin. The location of the ice margin is expected to vary, and it will be located at distance from the repository for much of this period. The recipient is cautiously assumed to be a semi-enclosed coastal basin with a relatively shallow water depth and low turnover, represented by the present state of object 208.

In this evaluation case, the glacial cycle is repeated ten times. When the ice sheet retreats, most unconsolidated regolith layers on top of the till are expected to be removed by glacial erosion. Moreover, the remaining regolith is assumed to be flushed out by large quantities of surface water when the ice sheet melts. Thus, the radionuclide inventory in all regolith layers is assumed to be negligible at the start of the submerged period in each interglacial-glacial cycle.

For a detailed description of the assumptions made in this evaluation case, see Section 5.4 in the **Radionuclide transport report**.

### Simplifications in comparison to the reference evolution

In the *simplified glacial cycle variant* of the reference evolution, possible mechanical, chemical, and thermal effects on the structural integrity of the waste vaults have been described (Section 6.3). Such effects are, however, neglected in the *simplified glacial cycle evaluation case*. This is a simplification, and, for instance, the ice-sheet load will have mechanical effects on the bedrock and possibly on the repository vaults. Simulations indicate that mechanical damage may occur due to increased rock stresses in the concrete backfill of BHK at the interface between the backfill and the rock (Idiart et al. 2019a). However, the effect of considering the mechanical damage in the near-field transport calculation may be limited, as the concrete is assumed to already have degraded considerably at the

onset of the glacial period in the *simplified glacial cycle evaluation case*. Nevertheless, in a full safety assessment, the combined effects of degradation (due to chemical cement leaching) and increased rock stresses would need to be evaluated. The sensitivity to glacially induced stresses of the bentonite barrier of BHA has not been evaluated but it is less likely to be affected due to its limited stiffness.

In SE-SFL, it is assumed that the repository is situated deep enough not to be frozen during permafrost conditions. In general, the effect of decreased temperature on the barrier evolution is advantageous, since chemical processes, including corrosion and material degradation, slow down. However, if the bentonite pore water freezes, a decreased barrier performance cannot be ruled out. An analysis for the Spent Fuel Repository showed that a pore-water temperature below  $-4\text{ }^{\circ}\text{C}$  is required for the buffer bentonite to freeze (SKB 2011a). The freezing temperature of concrete pore water depends on the pore size, and so will vary in time and space in the concrete barrier as chemical leaching progresses. In previous analyses from Laxemar and Forsmark (Section 9.4.3 in SKB 2006a and Section 12.3.2 in SKB 2011a) freezing to the depth evaluated in SE-SFL, 500 metres, is not expected to occur during the coming 1 million years. Nevertheless, in a future safety assessment for a selected site, the potential for freezing of pore water in SFL needs to be analysed in more detail.

When the ice-sheet advances and retreats, high groundwater flow is expected to alter the redox conditions, which in turn may affect the radionuclide speciation in the rock (and  $K_d$  values). These effects have not been accounted for in the *simplified glacial cycle evaluation case*. In SR-Site, the effect of such  $K_d$  changes was analysed with the conclusion that the releases to the biosphere increased but that this was compensated by release reaching a coastal basin with decreased human exposure (Section 13.5.6 in SKB 2011a). This conclusion is also likely to hold also for SFL.

The concrete barrier in BHK is degraded faster in periods with higher flow rates, and vice versa. However, in the reactive transport simulations for concrete degradation (Idiart and Laviña 2019), the boundary conditions have been cautiously set so that leachate concentrations in the groundwater are disregarded. This means that the use of the base-case concrete degradation development in the *simplified glacial cycle evaluation case* as well is a conservative overestimation as it is insensitive to the flow rate.

### **Summary of results**

As the chemical, thermal, and mechanical conditions associated with periglacial, glacial, and submerged conditions are assumed to have negligible additional effects on the structural integrity of the engineered barriers and the corrosion rate in the waste vaults (BHK), the annual near-field (and geosphere) releases are similar to those in the *present-day evaluation case* for large parts of the simulation period. This is especially true in periods of emerged conditions prior to the passage of the ice front, and for the first 50 000 years of the simulations, the release rates are identical to those in the present-day calculations. However, as the groundwater flow rate through the bedrock and repository is assumed to respond to inland-ice advances and retreats, and to the relative sea level, the near-field and geosphere transport is accelerated when the ice front is advancing over the repository (and to a lesser extent also during its retreat), whereas transport is retarded when the landscape above the repository is submerged.

The advection-dominated near-field release from BHK is more responsive to an increase in groundwater flow than the diffusion-dominated release from BHA, and the annual releases of dose-contributing radionuclides from BHK increase between one (C-14) and two (Ni-59) orders of magnitude when the ice front passes above the waste vault (Figure 8-20). This relatively significant response is expected, as radionuclides that have accumulated in the barriers (e.g. Ni-59) may be transiently flushed out upon changed advective conditions.

The release from BHA is also somewhat affected by groundwater flow, since the release to the bedrock will be limited by the groundwater capacity to export radionuclides at the outer backfill boundary at low flow rates. Thus, the near-field release from BHA also responds to increased rates of groundwater flow, and the releases of dose-contributing radionuclides increase by a factor of up to two (Figure 8-20).

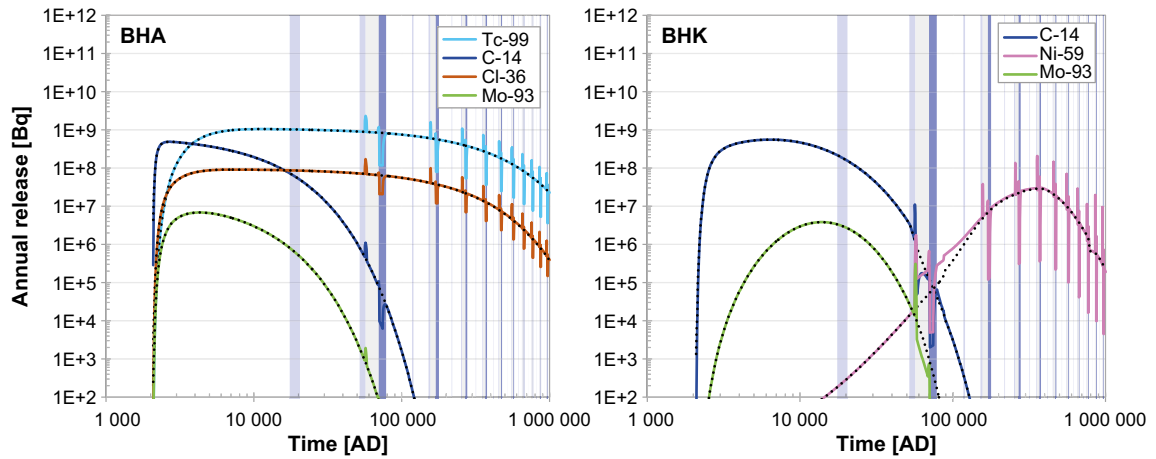


**Figure 8-20.** Annual near-field release from BHA (left) and BHK (right) in the simplified glacial cycle evaluation case. Coloured lines represent radionuclides (C-14, Cl-36, Mo-93, Tc-99 and Ni-59). The annual near-field releases in the present-day evaluation case are shown for reference (black dotted lines). Background colour represents climate domains (surface conditions); white = temperate, lavender = periglacial, light grey = glacial, and blue = submerged. Note that the simulations start at 2075 AD and that ten glacial cycles occur during the simulation time. Figure identical to Figure 5-28 in the **Radionuclide transport report**.

Although the maximum annual release of several dose-contributing radionuclides increases when the ice front passes the repository, the annual dose never exceeds the maximum levels recorded in the initial temperate period (Figure 8-21). This is because dose-contributing radionuclides like Mo-93 and C-14 have decayed significantly by the time that the ice approaches, and because the surface conditions associated with the maximum release, i.e. permafrost or submerged conditions, prevent both exposure through cultivation of mire peat with a continuous history of radionuclide accumulation, and extraction of well water.

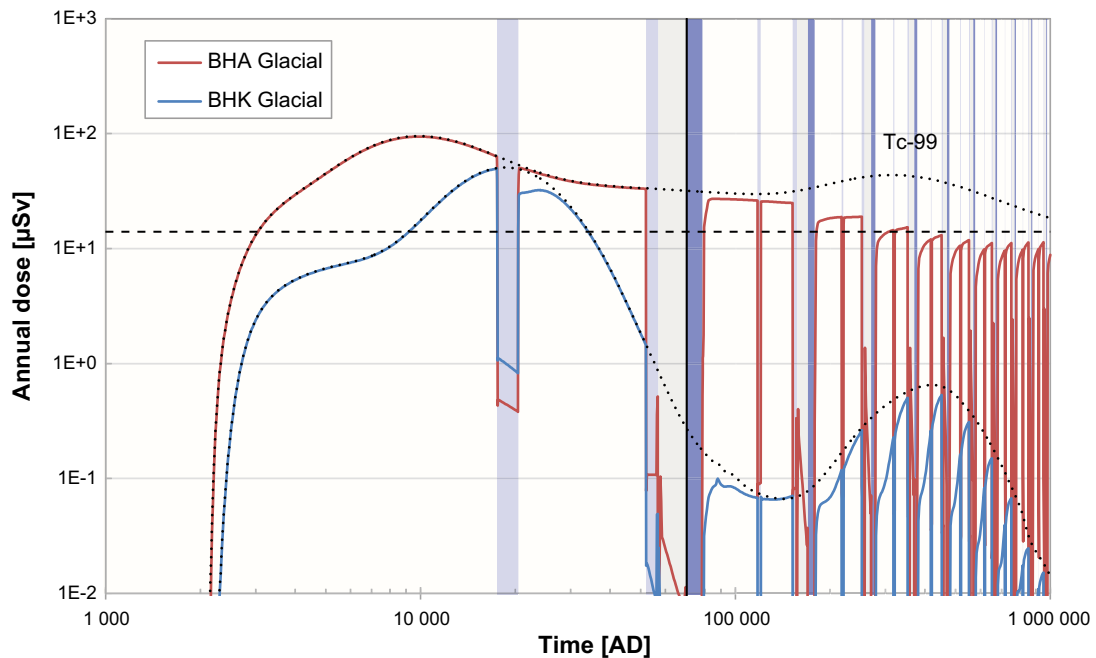


**Figure 8-21.** Annual dose for release from BHA (red line) and BHK (blue line) in the simplified glacial cycle evaluation case. Doses in the present-day evaluation case are shown for reference (black dotted lines), where exposure from Tc-99 dominates the dose from BHA during the second half of the simulation time. Background colour represents climate domains (surface conditions) as in Figure 8-17. The vertical black line indicates the start of the second interglacial–glacial cycle. Figure identical to Figure 5-30 in the **Radionuclide transport report**.

The results from the more detailed and, to some extent, more realistic, calculations in the *simplified glacial cycle evaluation case* suggest that doses estimated with the simplifying assumptions of constant external conditions (as applied in the *present-day evaluation case*) may overestimate doses in periods with a cold climate or a submerged landscape. This is also the case for the doses from radionuclides that requires several hundreds of thousands of years to reach maximum dose rates, as repeated glaciations are expected to interrupt their accumulation in the regolith layers.

## 9 Discussion

In this chapter, the results of the safety evaluation for SFL are discussed in the context of the objectives of the project. There are two main objectives for SE-SFL, as defined in step 10 of the methodology (Section 2.5). The first is to evaluate conditions in the waste, the barriers, and the repository environs under which the repository concept has the potential to fulfil the regulatory requirements for post-closure safety. The second is to provide SKB with a basis for prioritizing areas in which the level of knowledge and adequacy of methods must be improved in order to perform a full safety assessment for SFL. This is in line with the iterative safety assessment process that all SKB's repository programmes follow, in which the results from post-closure safety assessments and related activities (e.g. information from a site-characterisation process and development of safety assessment tools) are used to successively inform and improve the assessment.

### 9.1 Basic considerations for the safety evaluation

One important basis of the safety evaluation for SFL, or any safety assessment, is the inventory of radionuclides and other substances in the waste. The waste intended for BHK originates from the power plants and amounts to about 4 600 tonnes (Herschend 2014). It is mostly in the form of scrap metal and most of the activity originates from neutron irradiation of reactor components close to the core. The induced activity can be calculated with relatively good accuracy and the materials are generally known for the components of the waste. Thus, the BHK waste is well characterised. It is thought that the largest uncertainties relate to the composition of irradiated materials and, in particular, the content of trace substances that normally are not analysed when the material composition is determined. For such substances, for instance for the chlorine content in steel, cautious assumptions have been applied.

The legacy waste intended for BHA comprises about 2 700 tonnes and includes waste from several sources. For some fractions of the waste, there are relatively reliable data for actinides and some other radionuclides that are difficult to measure (such as C-14). For the largest part of the waste, however, only data from gamma spectroscopy measurements are available. The content of radionuclides that are difficult to measure is based on correlations (using a so-called radionuclide vector also denoted a radionuclide fingerprint) that has been documented by the company AB SVAFO. This vector has been established for waste clearance and acceptance purposes and therefore generally uses very conservative values for radionuclides difficult to measure, since such radionuclides are usually not limiting for clearance. When applied to the legacy waste the vector will most likely lead to an overestimation of the initial inventory for some of these radionuclides<sup>9</sup>. The inventory of chemical substances is also very uncertain. The estimation is based on the composition of a few waste packages that have been extrapolated to all waste of the same waste category, such as trash and scrap. The waste is described in more detail in Section 4.2, including radionuclide-specific activity inventories for BHA and BHK.

The proposed design is based on the SFL concept study (Elfving et al. 2013) and builds on the safety principle *retardation*. The safety principle is broken down into several safety functions for the waste domain, the bentonite and concrete barriers of BHA and BHK and the geosphere (Section 5.2). The material properties for the repository components are taken from SKB's previous safety assessments, specifically SR-PSU and SR-Site. For instance, it is assumed that the BHA backfill bentonite is similar to the buffer material described for the Spent Fuel Repository and the BHK backfill concrete is similar to the construction concrete employed in the existing SFR repository.

No site has yet been selected for SFL and therefore data from SKB's site investigation programmes for the Spent Fuel Repository and for the extension of SFR have been utilized in SE-SFL. In order to have a realistic and consistent description of a site for geological disposal of radioactive waste, data from the Laxemar site in the Oskarshamn municipality (see Figure 1-3), for which a detailed and coherent dataset exists, have been used. Based on an initial hydrogeological analysis for SE-SFL, the example

---

<sup>9</sup> Herschend B, 2015. Long-lived waste from AB SVAFO and Studsvik Nuclear AB. SKBdoc 1431282 ver 1.0, Svensk Kärnbränslehantering AB. Internal document.

location for the SFL repository was selected to be a part of what was earlier found most suitable for a potential Spent Fuel Repository within the Laxemar site at 500 m depth (SKB 2011b). The effect of different aspects related to siting is assessed in several evaluation cases in the radionuclide transport and dose modelling. The objective is to thereby give input to the future site selection and to the development of the future repository design. There is, however, no intention to evaluate uncertainties with respect to the chosen site.

The Laxemar area includes a variety of potential groundwater discharge areas that represent several different ecosystems. The radionuclide transport and dose modelling results from SE-SFL are, however, primarily linked to the conditions of one specific area (one biosphere object) where the groundwater from the repository is projected to be discharged, based on the present conditions at the site. However, there is no implication that the range of evaluation cases covers the full range of variation between sites that might be selected for the proposed facility. The biosphere area associated with the activity releases is seen as one relevant example, but the doses calculated for releases to this area need to be interpreted in the context of the uncertainties associated with the properties of the potential discharge areas once a location for the SFL repository has been selected. Such uncertainties may be related to the regolith stratigraphy and the size of the object (and its local catchment), but also to the landscape evolution and ecosystem succession during the long post-closure assessment period. Thus, to set the results derived from geosphere release to one specific discharge area in context, the importance of different site- and object-specific properties was evaluated in the *alternative discharge area* evaluation case (Section 8.5.2).

The safety analysis methodology used in SR-Site and SR-PSU was modified for the purpose of SE-SFL. The safety evaluation consists of 10 main steps (Section 2.5) and a one-million-year period was analysed. The external conditions were based on three climate developments, or variants, including the *present-day climate* base variant, an *increased greenhouse effect* variant, and a *simplified glacial cycle* variant (Section 2.5.3). The *increased greenhouse effect* variant considered climate conditions under global warming whereas the *simplified glacial cycle* variant considered shoreline displacement due to post-glacial uplift.

Based on a reference evolution of the repository and its environs for the three climate variants (Chapter 6), several evaluation cases were defined (Chapters 7-8). In SE-SFL, the term *evaluation case* is chosen instead of *scenario*, since a broader approach is applied in the selection of the cases than proposed in SSM's recommendations for scenario selection (Section 2.5.8). For these cases, radionuclide transport and dose calculations were performed.

Considerable attention has been given to uncertainty management, which is described in Section 2.6. Some simplifications have, however, been introduced and, for instance, the radionuclide transport and dose calculations have, for simplicity, only been undertaken using deterministic methods. The documentation and quality assurance of SE-SFL has been based on SKB's quality management system (Section 2.7).

Radionuclide transport and dose models used as assessment models in post-closure safety analyses represent features, events and processes (FEPs) judged to be relevant to a level of detail evaluated to be fit for the assessment purpose. Thus, these models include a multitude of simplifying assumptions. Most of the assumptions made in the radionuclide transport and dose modelling in SE-SFL are based on corresponding assumptions made in SR-PSU and/or SR-Site. The level of detail applied in the geosphere and biosphere models is similar in SE-SFL and SR-PSU and/or SR-Site.

Since this is a first evaluation of the repository concept proposed by Elfving et al. (2013) with a first estimate of the inventory of radionuclides and other materials, the near-field model is less detailed in some of its aspects than in the corresponding SR-PSU model. Some of the assumptions introduced in the evaluation are cautious (Section 7.3.2). However, as SE-SFL is the first evaluation of the repository concept, the effects of simplifying assumptions have not been fully evaluated and this will need to be addressed in future analyses.

## 9.2 Evaluation under what conditions the repository concept has potential to fulfil regulatory requirements

The conditions under which the repository concept has potential to fulfil regulatory requirements are discussed in this section based on the most important regulatory requirements, as stated in Section 2.5.9. First, the meaning of the “potential to fulfil” each requirement is discussed. Second, the conditions under which the requirements have the potential to be fulfilled are discussed (Sections 9.2.1 and 9.2.2).

It is important to note that SE-SFL, with its defined objectives, is not a full safety assessment and that the methodology adopted to address those objectives does not follow all the regulatory requirements regarding safety analysis methodology. Therefore, it has not been the intention, nor is it possible, to evaluate regulatory compliance in full. Instead, the conditions under which the requirements have the potential to be fulfilled are examined. In other words, aspects that are advantageous for the repository performance are highlighted, and these can be used to guide further work and development to support a full safety assessment. Since the calculations were performed with data that represent the example site and the design delineated in Chapter 4, the results cannot be directly interpreted in terms of the general concept implemented at a different site, but require consideration as to their implications when transposed to a different context.

The radionuclide transport and dose calculation results for the entire set of evaluation cases considered in SE-SFL are used to evaluate the conditions under which the repository concept has potential to fulfil regulatory requirements on risk. In a full safety assessment, the main scenario should result in a mean annual effective dose that is below the dose (14  $\mu$ Sv) corresponding to the risk criterion, whereas a less probable scenario with higher dose consequences can be acceptable if its contribution to risk, for example by a low probability of occurrence, is small enough that the summed risk is less than SSM’s criterion. A full scenario analysis is therefore needed to be able to link each of the calculated doses to a risk value. Such an analysis has not been carried out in SE-SFL. Instead, the annual dose criterion is used as a reference value for evaluating the protective capability of the repository vaults. Evaluation cases that result in annual doses higher than the criterion indicate that the conditions and assumptions in the calculations represent a situation for which the repository does not perform well enough to meet the risk criterion, at least if the probability of the case occurring is assumed to be one. In contrast, evaluation cases that result in annual doses considerably lower than the dose criterion indicate that the assumed conditions are favourable for meeting the risk criterion.

It should be noted that a strict quantitative comparison of the results with the regulatory risk criterion is not considered meaningful by SSM for times beyond 100 000 years after closure (general advice to SSMFS 2008:37). According to the advice, the assessment of the protective capability of the repository should instead be based on reasoning on the calculated risk together with several supplementary indicators of the protective capability of the repository. If the calculated risk exceeds the criterion of the regulations for individual risk, the underlying causes of this should be reported as well as possible measures to improve the protective capability of the repository. Thus, in the following discussion on the conditions under which the repository concept has the potential to fulfil the risk criterion, it is considered that there is a difference in the application of the criterion for the time after 100 000 years. Given the early stage of the analysis, supplementary indicators have not yet been analysed in SE-SFL, but they will be included in future steps of the SFL safety assessment process.

The requirement relating to the potential to withstand relevant FEPs is discussed based on the results from the reference evolution of the repository and the evaluation cases. A preliminary repository design was the basis for this evaluation. Moreover, it should be noted that some aspects of the evolution of the barrier system were assessed using a high level of technical detail, whereas other aspects were handled in a more generic way, utilizing information from SR-Site and SR-PSU. Additionally, certain aspects of the reference evolution that were judged to be of minor importance or high uncertainty were further simplified and sometimes omitted in the transport calculations, as described in Sections 7.4.5, 8.6.1 and 8.6.2. The set of evaluation cases representing the reference evolution will need to be further developed to reflect all aspects that must be included in a main scenario in a full safety assessment as described in the general guidance to SSM’s regulations (SSM 2008b).

Although the regulations apply to the entire facility, BHA and BHK are discussed separately. This allows the identification of the conditions under which each waste vault has the potential to perform well enough to fulfil regulatory requirements. Issues that are relevant to both waste vaults are discussed in Section 9.2.3.

The entire set of relevant evaluation cases has been used to assess the conditions under which each waste vault has the potential to fulfil the considered regulatory criteria. The base case, that is based on the present-day climate and further underlying assumptions (Section 6.2) illustrates the functioning of the repository (Section 7.5) and is used as a reference for comparison with the other evaluation cases. The other cases illustrate the effects of altering the conditions in relation to the base case (Section 8) and are thus important in the evaluation of the conditions under which the repository concept has the potential to fulfil the risk criterion and the ability of the barrier system to withstand relevant FEPs.

### 9.2.1 BHA

The intact barrier system of BHA is very efficient for retaining radionuclides in the inventory given the postulated groundwater flow rates, as the analysis of the base case shows (Section 7.5). The initial activity of C-14, Mo-93, and Ni-59 is substantially reduced within the near-field (see Figure 7-12). In addition, for the very long-lived radionuclides Tc-99 and Cl-36, a substantial part of the inventory decays in the near-field. Retention is linked to diffusion-controlled transport within and out of the bentonite, as well as sorption onto cement in the waste and onto bentonite in the backfill. The maximum annual doses are limited due to the considerable transport resistance offered by the bentonite. Nevertheless, the results indicate that the conditions assumed in the base case yield doses that are too high to comply with the risk criterion for the BHA inventory underlying SE-SFL. Thereby it can be noted that the *simplified glacial cycle* evaluation case shows that doses during cold periods do not exceed the maximum dose under present-day conditions. As resulting doses are high compared to the dose criterion further efforts are needed to improve the performance and analysis of the repository, which is discussed in Section 9.4.

#### **Potential to fulfil the risk criterion – aspects related to the waste characteristics**

The annual dose contributions are dominated by the radionuclides that dominate the initial inventory and have half-lives longer than a few thousand years, meaning the non-sorbing Mo-93, Cl-36 and C-14. Despite the generally efficient retardation, controlled by diffusion in the bentonite, the conditions underlying the base case yield results that indicate that the estimated initial inventories for Mo-93, Cl-36, and C-14 are too large for an acceptable protective performance of the repository. The analysis of the alternative climate variants *increased greenhouse effect* and *simplified glacial cycle* evaluation cases show results that are similar to those of the base case.

The calculated doses are, however, uncertain due to the large uncertainties in the BHA inventory. With one order of magnitude lower initial inventory of the dominating radionuclides, the maximum annual dose would be around the dose criterion. Thus, with an inventory that can be shown to be more than a factor of 10 lower than the estimate used in SE-SFL for the dominating radionuclides, and not substantially higher for other radionuclides, the repository concept would have the potential to meet the risk criterion, given the assumptions made in the base case.

Beyond 100 000 years after closure, Tc-99 and radionuclides from the U-238 chain contribute to calculated annual doses that exceed the dose criterion. It is noted that the initial activity inventory is dominated by Tc-99 and that it is likely to be overestimated because of the uncertainties in the inventory (Section 9.1). According to SSM's general advice, the underlying causes of a risk exceeding the criterion (illustrated by doses in the context of SE-SFL) should be reported as well as possible measures to improve the protective capability of the repository. From the *no effect of complexing agents in BHA* evaluation case (Figure 8-3, **Radionuclide transport report**, Section 6.2.2), it is demonstrated that complexing agents have a major effect on the late Tc-99 and U-238 chain doses. Thus, on the condition that complexing agents can be shown to be present at substantially lower concentrations, or that their concentrations decrease over the very long times relevant for SE-SFL, the potential for the repository to meet an acceptable level of protective performance is improved.

#### **Potential to fulfil the risk criterion – aspects related to groundwater flow rate**

A much lower geosphere groundwater flow rate than assumed in the base case would improve near-field retention and result in a significantly reduced release of Mo-93 and Tc-99 from the geosphere (see Low flow in Figure 9-1). This is primarily due to the prolonged advective travel time and corresponding increase in F-factor in the geosphere, which results in significant decay of Mo-93 and

a more efficient retention of Tc-99. If the flow is two or three orders of magnitude lower than assumed here for the example location (i.e. with a typical advective travel time of  $10^4$  to  $10^5$  years) then the performance of the repository system is expected to have the potential to meet regulatory requirements with respect to annual doses (Section 8.4.1, **Radionuclide transport report**, Section 7.2.4). However, a reduction in groundwater flow rates of only an order of magnitude (with a typical advective travel time of  $10^3$  years) is not expected to result in a substantial reduction of the near-field and geosphere releases. This is because the transfer from the bentonite backfill to the groundwater in the bedrock is controlled by diffusion and because the retention of dose-contributing radionuclides in the geosphere is only marginally affected by this magnitude of change in flow conditions. More favourable hydrogeological properties than those assumed in the base case could, according to available data, be found at other locations in Laxemar (e.g. at greater depth) and elsewhere in Sweden.

The location of the repository below the seabed could also reduce the groundwater flow in the bedrock at repository depth and associated near-field releases at early stages. The *initially submerged conditions* evaluation case therefore analyses the effect of locating SFL at a position that is currently under the seabed. In one of the variants of the evaluation case, the groundwater flow rates are assumed to be reduced by a factor 100 for 10 000 years compared with the base case (i.e. with a typical advective travel time of  $10^4$  years). The annual dose then decreases to well below the dose criterion as long as the repository is submerged, which is in line with the results of the *lower groundwater flow* evaluation case. But since the BHA inventory, as shown in the base case, potentially can sustain releases for hundreds of thousands years that yield doses comparable to that of the dose criterion, submerged conditions would have to persist for a time span of similar length to ensure conditions that have potential to fulfil the risk criterion.

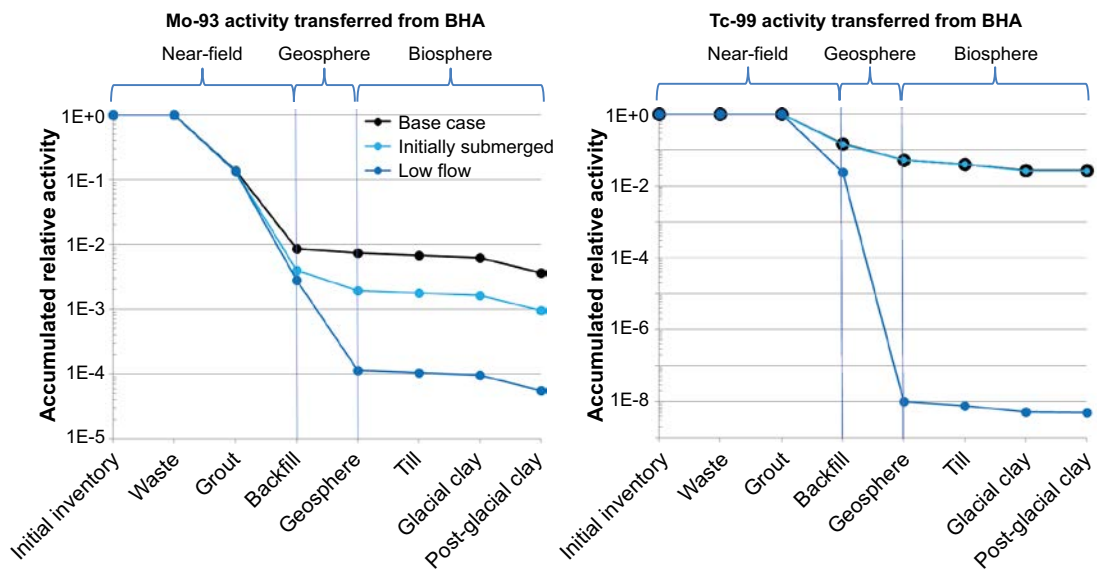


**Figure 9-1.** Activity of Mo-93 (left panel) and Tc-99 (right panel) transferred along the route from the initial inventory in BHA to the biosphere, accumulated over the entire analysis period of one million years, and normalised by the initial inventory. The relative activity transferred is shown for the base case (black), the variant with 10 000 years of initially submerged conditions (light blue) and for the variant of the lower groundwater flow evaluation case with 100 times lower groundwater flow rate than in the base case (dark blue). Note that the base case is overlain by the light blue line in the right panel. This figure is identical to Figure 8.1 in the *Radionuclide transport report*.

If groundwater flows are low enough for the repository to meet the risk criterion, then the safety function *low flow in the bedrock* (Section 5.2) would become central and would need to persist for about twenty thousand years to significantly reduce the geosphere release of Mo-93, and would need to persist for the entire analysis time to reduce the release of Tc-99. However, it is important to note that the effectiveness of a reduced groundwater flow rate for achieving an acceptable level of protection is conditional on the assumption that the safety functions of the bentonite barrier do not deteriorate significantly during the assessment period. It can, however, be noted that lower flows also imply a decreased risk for bentonite erosion and a smaller erosion rate if it should occur. Thus, the temporal evolution of the bentonite barrier discussed in the reference evolution may affect the results and thus needs to be further considered in future assessments of SFL safety (see section 6.2.9). Furthermore, there are cautious assumptions applied in the calculations, and some simplifications linked to the safety evaluation methodology that may also affect the projected release of radionuclides from BHA and the calculated doses. Some of these assumptions and the possibility to apply more realistic assumptions are discussed further in Section 9.4.

### **Potential to fulfil requirement on ability to withstand relevant FEPs**

The most relevant FEPs that influence the temporal evolution of the barrier system of BHA are processes that act on the bentonite barrier and these are discussed in the reference evolution (Section 6.2.9). The montmorillonite transformation process is being studied in an ongoing study as described in the reference evolution. There are uncertainties in the models and assumptions used in the ongoing study which will need to be further explored in a future assessment. This process will need to be considered further, for instance in relation to the design of the bentonite backfill. Furthermore, the process still needs to be assessed in terms of its influence on the safety functions of the bentonite, i.e. *low flow in the waste vault* and *good retention*. The aim should be to adequately conceptualise the process in the radionuclide transport calculations, in order to quantify the effect of the transformation process on the resulting dose in future assessments of SFL. Bentonite colloid release from the backfill in BHA due to chemical erosion, which requires groundwater with low ionic strength, is discussed in the reference evolution (Sections 6.2.9 and 6.2.7). The process has, however, not been quantified for the conditions at the example site. The results of the geochemical characterisation and modelling of the example site under the assumption of present-day climate indicate that the conditions at repository depth are expected to inhibit colloid release at least for tens of thousands of years (Section 6.2.7 and SKB 2010f, Section 6.3.1). For glacial conditions, however, the results indicate that dilute waters may penetrate to repository depth at the example site (SKB 2010f). The geochemical conditions are site specific and further study is needed in a future assessment for a selected site to assess if the process may lead to erosion and if so whether the amount of bentonite erosion from the BHA backfill is large enough to have implications for the safety functions of the bentonite barrier. It is noted that the thickness of the bentonite backfill is a design consideration that is linked to this process.

The mechanical evolution of the bentonite backfill, in particular during the process of bentonite resaturation, is discussed in the reference evolution (Section 6.2.9). The discussion indicates that effects of the resaturation process on the conditions in the waste domain and resulting near-field releases should be analysed in more detail to be able to underpin the discussion on barrier system robustness.

It is noted that the bedrock as a natural barrier is part of the barrier system to which the requirement on the ability to withstand relevant FEPs applies. Site characteristics that are favourable for upholding barrier integrity and limiting radionuclide transport will contribute to the potential to meet the regulatory requirement on the ability to withstand relevant detrimental FEPs. The evaluation is thus bound to the site characteristics and a full assessment needs to be carried out when a site has been selected for SFL.

In conclusion, a quantitative analysis of the effect of the evolution of the conditions in the waste vault and associated safety functions is needed in order to define the conditions under which the repository concept has the potential to fulfil the requirements on barrier system robustness. Moreover, it is noted that the analysis of montmorillonite transformations, colloid release and other processes in the reference evolution can inform the optimisation of the bentonite barrier properties and geometry when defining the detailed reference design for SFL.

## 9.2.2 BHK

The barrier system of BHK is efficient for retaining radionuclides in the inventory, as the analysis of the base case shows (Section 7.5). In general, the mechanisms contributing to the retention are the slow release of induced activity from the metal through corrosion, the rate of which is reduced due to the alkaline conditions in the concrete, sorption onto cement of many of the radionuclides in the inventory and slow advective transport through the concrete barrier. The maximum annual doses are limited due to the slow release relating to steel corrosion and considerable transport resistance offered by the concrete backfill. Nevertheless, the results indicate that the conditions assumed in the base case yield doses that are too high to comply with the risk criterion for the BHK inventory underlying SE-SFL. It is noted that the *simplified glacial cycle* evaluation case shows that doses during cold periods do not exceed the maximum dose under present-day conditions. As resulting doses are high compared to the dose criterion further efforts are needed to improve the performance and analysis of the repository, which is discussed in Section 9.4.

### **Potential to fulfil the risk criterion – aspects related to corrosion of metallic waste**

An important mechanism that controls the slow release of radionuclides is the corrosion of the metallic waste in the BHK waste domain. If significantly lower corrosion rates can be substantiated for the situation in the waste domain, the repository concept has the potential to meet the regulatory criterion, given the assumptions underlying the evaluation case and example site data. The corrosion rate used in the base case (10 nm/a) is higher than recently reported long-term corrosion rates. These correspond to the lower end of the range for stainless steel corrosion under alkaline anoxic conditions recommended for use in PSAR for SR-PSU (which is ten times lower than the corrosion rate used in the base case: Section 8.3.2, **Radionuclide transport report**, Section 8.5.2). Reducing the corrosion rate to this lower end of the range reduces the maximum annual activity release from the near-field (Figure 8-4, **Radionuclide transport report**, Section 6.3.2) and maximum annual doses by a factor of four. This reduction is entirely due to Mo-93, which dominates the dose in the base case. With such a reduction, annual dose levels are achieved that are lower than the dose corresponding to the risk criterion.

Further, the simplified handling of the release of radionuclides by corrosion in the model influences the calculated near-field activity releases and doses. The effects of the corrosion rate on near-field releases and resulting doses vary depending on the inventory in the instant release fraction and in the thicker metal fractions that are influenced by corrosion. Consequently, in future assessments the potential for reduced releases and doses from BHK associated with the uncertainty in corrosion rate needs to be evaluated in relation to the assumptions about, and uncertainty in, the initial distribution of the radionuclide inventory between the instant release and thicker metal fractions. Studying the steel corrosion process under the conditions prevailing in BHK in a more mechanistic way could also be considered.

### **Potential to fulfil the risk criterion – aspects related to the concrete backfill**

The quality of the concrete used as backfill material in BHK is a design consideration. With concrete properties that are more favourable than the ones assumed in the base case, and that should be achievable in practice, conditions are given under which the BHK repository concept has the potential to fulfil the risk criterion given the data from the example site and other assumptions. The *alternative concrete backfill in BHK* evaluation case uses parameter values that are comparable with the properties of a concrete containing limestone and dolomite additions that has been developed by Lagerblad et al. (2017) and used in the construction of large components representative of the caissons in 2BMA in large-scale experiments in the Äspö Hard Rock Laboratory (Mårtensson and Vogt 2019) and analysed by Idiart et al. (2019b). The results (Section 8.3.3, **Radionuclide transport report**, Section 6.4.2) show that the assumed more favourable concrete lowers the accumulated near-field releases of the dose dominating Mo-93 by more than two orders of magnitude. The effect on C-14 is not as strong but is still significant. The results assume that the effect of the alternative concrete backfill on gas transport can be neglected, which would need to be shown by an appropriate analysis. The maximum annual dose associated with the alternative concrete evaluation case is well below the dose criterion and more than an order of magnitude smaller than the maximum dose for the base case.

### Potential to fulfil the risk criterion – aspects related to groundwater flow rates

The *lower groundwater flow evaluation case* shows that a reduction of the flow rate by a factor of 10 compared with the base case (i.e. with a total flow through BHK of  $10^{-1} \text{ m}^3/\text{a}$ ) reduces the resulting annual dose to less than a tenth of the base case value and to a level well below the dose criterion (Section 8.4.1, **Radionuclide transport report**, Section 7.2). The decrease is mainly explained by the transport within and from the near-field, which becomes limited by diffusion instead of advection as in the base case. The increased travel times through the geosphere and associated changes in F-factors, however, only have a moderate effect on the doses (Figure 9-2), unless the groundwater flow rate decreases even further. Hence, conditions with reduced groundwater flow rates create the potential to meet the regulatory risk criterion given the estimated inventory for BHK and the other assumptions applied.

The results for BHK from the *lower groundwater flow* and in the *alternative concrete backfill in BHK* evaluation cases yield similar near-field releases and doses. This is due to the reduction of the near-field flow by a factor 10 and associated releases in both evaluation cases. Differences between the two evaluation cases arise because of lower groundwater flow in the geosphere in the *lower groundwater flow* evaluation case and the effects of lower porosity and diffusivity in the *alternative concrete* evaluation case.

The *initially submerged* evaluation case is also associated with decreased groundwater flow rates and associated decreases in near-field releases during the time the repository is located under the Baltic Sea. Given the factor of 100 lower groundwater flow rates and the discharge to the Baltic Sea, the resulting doses are several orders of magnitude lower than in the base case while the repository is submerged. However, when the shoreline retreats the doses become similar to those in the base case. It would require a submerged period of about 50 000 years for the dose-contributing radionuclides to decay sufficiently to result in doses that do not reach the dose criterion given the estimated BHK inventory and other underlying assumptions. Thus, conditions with a long enough initial period of submerged conditions create a potential to meet the regulatory risk criterion for the estimated inventory and other assumptions underlying the calculations.

There are a few FEPs that are included in the SE-SFL FEP catalogue that may affect the results of the evaluation, but that have not been represented in the radionuclide transport and dose calculations (see *Conditions to fulfil requirement on ability to withstand relevant FEPs*).

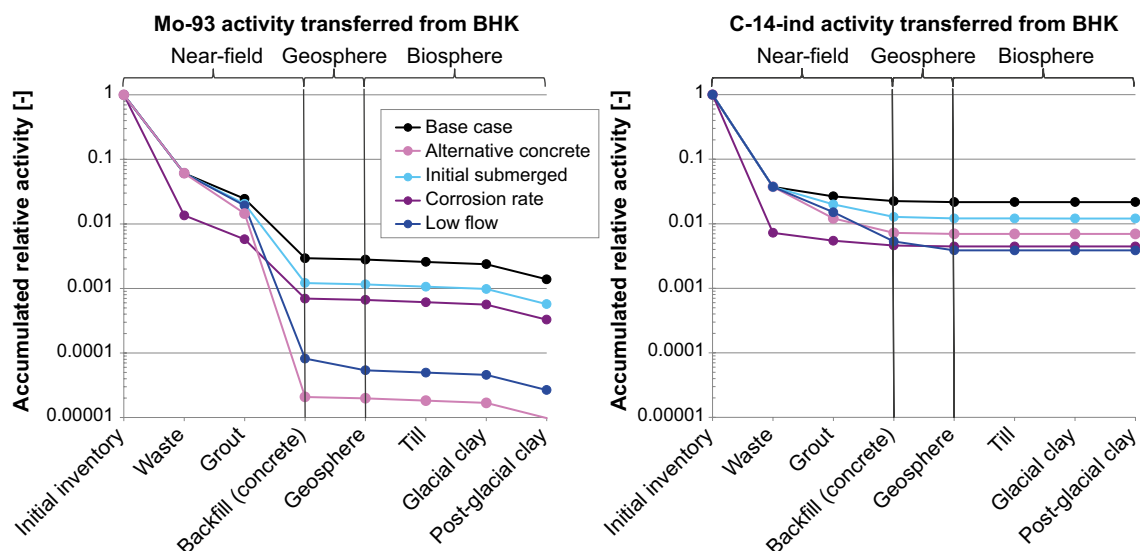


**Figure 9-2.** Activity of Mo-93 (left panel) and C-14 (right panel) transferred along the route from the initial inventory in BHK to the biosphere, accumulated over the entire analysis period of one million years, and normalised by the initial inventory. The relative activity transferred is shown for the base case (black), the variant with 10 000 years of initially submerged conditions (light blue), for ten times lower corrosion rate (yellow), for the variant of the lower groundwater flow evaluation case with 10 times lower groundwater flow rate than in the base case (dark blue) and for the case with alternative concrete (magenta). Figure is identical to Figure 8.2 in the **Radionuclide transport report**.

### **Potential to fulfil requirement on ability to withstand relevant FEPs**

The roles that the components of BHK have for post-closure safety are given by the safety functions *good retention* for the waste domain, and *low flow in the waste vault* and *good retention* for the concrete barrier (Section 5.2). In the waste domain, high pH (reducing the steel corrosion rate and thus gas production rate) and high available sorption area, provided by the cement in the grout, contribute to *good retention*. In the concrete barrier, high available sorption area and low diffusivity contribute to *good retention*. In addition, the resulting high pH influences the sorption capacity. Low hydraulic conductivity in the concrete barrier further contributes to *low flow in the waste vault*. The most relevant FEPs that influence the evolution of these conditions over time are processes that act on the concrete barrier. Concrete degradation in BHK leads to alteration of the pH, porosity, hydraulic conductivity and effective diffusivity, and is mainly driven by groundwater interactions. To capture this, a set of reactive transport models (Idiart and Shafei 2019, Idiart and Laviña 2019) of the BHK concrete backfill, considering the coupling between fluid flow, solute transport and chemical reactions, has been developed and implemented in SE-SFL. These efforts were complemented with a study of alternative concrete compositions (Idiart et al. 2019b; see further Section 9.3.1). The main conclusions were that the main process that is expected to drive the degradation of the concrete barriers is calcium leaching, which leads to a gradual loss of portlandite and CSH-gel. The degradation rate is very low, primarily due to the low water flow rate in the concrete backfill. The initial porosity and transport properties of the concrete have a stronger impact on the degradation than the concrete composition.

The low degradation rate in relation to the half-lives of the radionuclides that dominate the initial inventory leads to the conclusion that the barrier is able to withstand these FEPs, granted a sufficiently low initial porosity and favourable transport properties of the concrete (see the *alternative concrete backfill in BHK evaluation case*; Section 8.3.3) or favourable transport properties due to low flow in the repository surroundings (see the *lower groundwater flow evaluation case*; Section 8.4.1).

Chemically induced changes in the performance of the concrete barrier could potentially degrade the mechanical performance of the barrier, both in terms of stiffness and strength. Further, the concrete backfill of BHK may also be affected by mechanical stress from the rock adjacent to the repository (Sections 6.2.10, 6.4.10). To study these processes, a hydro-chemo-mechanical model was developed starting from the hydro-chemical reactive transport models (Idiart et al. 2019a). At 500 m depth, with the repository orientated in the direction of the major horizontal stress, simulations indicate that limited mechanical damage may occur internally in the concrete backfill, at the corners of the waste domain. The effect of this degradation is not explicitly considered in the radionuclide transport calculations. However, the calculations account for the damage due to leaching, which is likely to have a similar effect on radionuclide releases and doses.

An exception is the case that considers glaciation-induced stresses. In that case, mechanical damage can be substantial, extending over large regions of the concrete backfill (Idiart et al. 2019a). However, since glaciation is likely to occur only well after tens of thousands of years (Section 6.4.1), when Mo-93 and C-14 have substantially decayed, it is likely that any mechanical effects on the concrete barrier will not have substantial adverse impacts on radionuclide releases and doses.

The effects of potential earthquakes have not been taken into account in SE-SFL. These need to be analysed in a future assessment to evaluate their effect on the potential of the BHK repository concept to fulfil the requirement on its ability to withstand relevant FEPs.

### **9.2.3 Repository environs**

The analysis of radionuclide transport and accumulation in the biosphere assumes that the releases will occur in a given biosphere object at the example site. The conditions simulated will therefore not be likely to represent the actual discharges at a future selected site. However, the calculations are judged to capture the main features of transport, accumulation and exposure for a suite of possible future conditions. In the calculations, cautious assumptions have been adopted regarding selected exposure pathways, land use and diets adopted for assessment purposes (**Biosphere synthesis**). In the *alternative discharge area* evaluation case (Section 8.5.2, **Radionuclide transport report**), discussed in Section 7.6, it is demonstrated that the doses associated with biosphere object 206 that the base case considers, are reasonable robust estimates appropriate to a potential discharge area at the example site. The results also show that the doses can vary by several orders of magnitude depending

on the object properties and that the dose response to object properties may differ between radionuclides. For instance, the doses from Mo-93 and Ni-59 increase with a high rate of bedrock discharge, whereas the opposite is true for the doses from C-14 for the areas analysed (Section 8.5.2). There is also a systematic difference in the calculated doses from biosphere objects in Laxemar and Forsmark sites which is found to be related to the less pronounced topographical relief (and reduced bedrock discharge) in Forsmark. In consequence, the conditions under which the repository concept has the potential to meet the risk criterion are linked to the properties of the biosphere objects at the selected site and potential uncertainties regarding the objects into which releases occur. However, it can be noted that there is no large difference between the biosphere responses to releases in different locations along the coast of Sweden that represent alternative regional climates (Section 8.4.4).

## 9.3 Development in SE-SFL

Progress has been made with respect to several areas in SE-SFL. These areas include: formulation of evaluation cases, supporting modelling, transport modelling, and presentation and interpretation of results. The development has primarily been motivated by reviews undertaken by SSM (and their external experts) of previous safety assessments. Developments to increase the consistency in analyses and to facilitate the understanding of the results have been introduced. The most important developments are summarized below.

### 9.3.1 Repository near-field

Two near-field materials of the design analysed in SE-SFL, concrete and bentonite, are central to the long-term performance of the repository. These materials are also used in SFR and are foreseen for the Spent Fuel Repository and consequently there is a large body of work relating to their long-term evolution. Further developments have been carried out within SE-SFL regarding concrete and bentonite, because there are differences between these repositories and SFL. The temporal evolution of the barrier materials is strongly dependent on the near-field hydrogeological and hydrogeochemical conditions, which have been subject to further evaluation within SE-SFL. Moreover, there have been developments in the modelling approaches of radionuclide transport in the near-field, both in the aqueous and gas phase. These developments are summarised in the two paragraphs below.

Two studies of the near-field hydrogeology have been carried out within SE-SFL. First, the modelling of the SFL near-field hydrogeology explored the influence of host rock characteristics and barrier properties on the near-field groundwater flow at the example site (Abarca et al. 2016). Based on the results, a location for the repository vaults within the example site was chosen. Second, near-field simulations were performed for different assumptions to calculate and compile results for flows in the vaults and wastes, to serve as input to radionuclide transport calculations (Abarca et al. 2019). In the model, the concrete is considered to degrade at different rates in different parts of the concrete backfill, affecting the flow. In addition, the time needed to reach full water saturation of the SFL vaults after repository closure, has been calculated.

For SE-SFL, a model for radionuclide transport in the near-field was developed (Wessely and Shahkarami 2019). The model uses a compartment conceptualization of the near-field backfill materials and waste domain and incorporates the important transport-related processes, including diffusion, advection, sorption and chain decay. The model is implemented in the Ecolego software and is used to calculate the release of radionuclides from the BHA and BHK vaults. This model differs from those used in SR-PSU (SKB 2015c) in that a fracture representation of the bedrock is used. The fracture properties, including the equivalent flow rate,  $Q_{eq}$ , are given by the discrete fracture network used in the hydrogeological model. Three different degradation states that are reached at different points in time in different parts of the BHK concrete buffer are defined based on the concrete degradation studies described below.

#### **BHK**

The following model developments have been carried out in the context of concrete degradation and gas release in SE-SFL.

To quantify the concrete degradation, reactive transport modelling has been performed, linking Comsol Multiphysics (version 5) with Phreeqc (version 3) using a software interface named iCP (Idiart and Shafei 2019). Both 2D and 3D models were run. In contrast to the models used in SR-PSU (Höglund 2014), the model includes coupling of the chemical degradation and the water flow rate. These models simulated up to 100 000 years after repository closure and for the 2D model a range of sensitivity cases were run. In a benchmark exercise, the model results were compared with results from a PHAST model (Höglund 2014). To simulate concrete degradation for the full one-million-year analysis period, a 1D model was run in the same linked Comsol Phreeqc (iCP) model (Idiart and Laviña 2019). The focus was on evaluating the pH, porosity, effective diffusivity and hydraulic conductivity. Based on the outcomes of the 1D modelling, different concrete degradation states were defined for different times and parts of the concrete backfill, which were then used for the radionuclide transport calculations.

To evaluate the effect of alternative concrete compositions (cementitious systems) reactive transport simulations of concrete degradation in the BHK vault were performed using iCP (Idiart et al. 2019b). Simulations were carried out in 2D and 1D over 100 000 and 1 million years, respectively. Consideration of alternative compositions of the concrete mix design implies the ability to predict the phase assemblage of the hydrated mix. Cement hydration models were used to estimate the mineralogical and pore water composition of the different mixes. The hydration simulations were based on thermodynamic modelling coupled to kinetically controlled dissolution of the cement clinker and mineral additions, when present. The outputs of the hydration models after full hydration were used as inputs for the reactive transport simulations, defining the initial composition of the intact concrete. The study included a literature review of how these different mix compositions are expected to alter the chemical and physical properties. Based on the literature review, the transport properties of the intact composition of each mix were proposed. The case which considered the addition of limestone filler is the concrete mix that was found to have the best performance. According to the model results, this improvement is more related to the initially lower porosity, compared with the rest of cases, than to the chemical composition of the cementitious system.

A further development within SE-SFL has been to establish a hydro-chemo-mechanical (HCM) model implemented in iCP (Idiart et al. 2019a). The model was used to study the effect of the coupling of hydro-chemo-mechanical processes on chemically induced mechanical damage. A range of sensitivity cases was used to evaluate the influence of mechanical boundary conditions and material parameters on the results. In addition, the effect of a sulphate-rich groundwater potentially reaching the repository on the mechanical stability of the system was assessed. To this end, the model for calcium leaching was extended to account for an external sulphate attack, where expansion may occur due to precipitation of sulphate-bearing minerals in the cement matrix.

A further development within SE-SFL has been a quantification of gas release from the BHK vault (Silva et al. 2019a). The main gas-generating process involves hydrogen formation by the anoxic corrosion of steel. A 2D multiphase flow model was set up, including a cross section of the vault for metallic waste (BHK) and its surroundings. The host rock was represented using homogeneous hydraulic properties, including a deformation zone intersecting the BHK for some simulation cases. Different groundwater flow cases have been simulated, including hydrostatic, horizontal and vertical downward flow conditions. It was found that the gas generation did not significantly affect groundwater flow or saturation conditions in the near-field, nor did it influence the hydraulic behaviour of the BHK concrete barriers as parameterised in the base case.

## **BHA**

Bentonite in the BHA near-field is credited with the safety functions *low flow in the waste vault* and *good retention*. Bentonite is also used for this purpose in the silo of SFR and in the deposition holes in the Spent Fuel Repository. There are, however, clear differences between the design of the bentonite components in the three repositories, with SFL having the thickest bentonite barrier surrounding the waste. In the Spent Fuel Repository, the bentonite will not be affected by cement leachates as no concrete will be present in the vicinity of the waste deposition holes, whereas the SFR silo and the BHA vault include concrete structures that may chemically interact with the bentonite.

For analysing the interactions of the bentonite with concrete in the BHA vault, two sets of 1D reactive transport models were developed and implemented using iCP in a study that is ongoing during the preparation of present report. The first set considers only the bentonite system, treating concrete

as a boundary condition. The second set explicitly considers the interaction between the concrete and bentonite barriers. The goal of the work is to assess the mass of montmorillonite dissolution in the bentonite barrier as a result of the interaction with the cementitious fluids from the waste domain over a time span of 100 000 years. In addition, several sensitivity analyses are used to assess the impact of uncertain parameters on the results. Finally, analytical models, based on the shrinking core model, that predict the dissolution depth, will also be discussed and compared with reactive transport results.

Diffusion is the dominant transport process in the bentonite of BHA. To assess conceptual aspects of the quantification of the radionuclide transport through the bentonite backfill, several conceptual models of diffusion through compacted bentonite were tested (Idiart and Coene 2019). Two empirical models, a semi-empirical model and two mechanistic models were used. One of the latter ones is based on the multi-porosity model and the other on the single porosity Donnan equilibrium model. Several sensitivity analyses assessed the impact of chemical composition of the background electrolyte, the effective diffusion coefficient of the bentonite and the magnitude of the equivalent flow through the fractures intersecting the vault. In general, the comparison of the different modelling approaches yielded comparable results.

### **9.3.2 Bedrock system**

#### ***Hydrogeological and groundwater composition modelling of the bedrock system***

The modelling of the hydrogeology and groundwater composition has been developed further in SE-SFL in comparison with the analysis in SR-Site, by merging the site-scale and repository-scale models into a single, so-called facility focussed model. This model contains the detailed representation of the backfilled repository structures as a CPM, within a surrounding facility scale DFN model, which itself is embedded within a catchment-scale ECPM model. This approach has allowed much greater integration in the model and there is no longer any need for transfer of data between scales. Moreover, the effect of the hydrochemistry on the hydrogeological performance measures (equivalent flow rate, equivalent flux, path length, travel time, and flow-related transport resistance) was studied. The result showed that the hydrochemistry only has a minor effect on the performance measures and that it should therefore not be necessary to include such a coupling in future studies.

#### ***Radionuclide transport modelling in the bedrock system***

A new compartment tool (FARFCOMP) for simulation of transport of radionuclides released from the repository into the fractured rock was developed in SE-SFL. The code solves numerically the same governing equations and reproduces the result calculated by the semi-analytic code FARF31 (Norman and Kjellbert 1990) that has been used by SKB for previous safety analyses for the Spent Fuel Repository. The numerical solution is similar to that implemented in SAR-08 and in SR-PSU (SKB 2015c). The FARFCOMP code implementation and its verification are documented in the **Radionuclide transport report** (Appendix B).

The objective with the development of FARFCOMP was to obtain a code that is straightforward to handle through an implementation in Matlab and that allows for implementation of features and processes that are not part of the FARF31 code. For instance, the code includes the possibility to vary properties of flow paths or other parameters in time, which was used in some calculation cases in SE-SFL. In future, additional capabilities can easily be included in FARFCOMP, for example colloid-facilitated transport.

Transport from the waste vault-bedrock interface to the bedrock-regolith interface is represented by a large number of particle tracks, calculated using the groundwater flow field obtained with the hydrogeological model. In the particle-tracking calculations performed for SE-SFL, ten particles were released from each of the rock fractures intersecting the BHA and BHK vaults and tracked through the fracture network to the surface (Joyce et al. 2019). The release of radionuclides from the waste vaults is distributed on the resulting ~4 500 particle tracks. This handling differs from that implemented in SR-Site and SR-PSU. In SR-Site, for each of ten realisations, three release paths were determined, starting at a fracture that intersects the deposition hole, in the EDZ and in the deposition tunnel. For each deposition hole and each of these release paths, one particle track was used in the radionuclide transport calculation. In SR-PSU, a probabilistic approach was used to assess the uncertainty represented by the multitude of particle tracks. For each probabilistic realisation, the release from the repository was assumed to follow a specific particle track.

SE-SFL includes a limited set of deterministic simulations and the complete set of particle tracks could be included in each of the evaluation cases. In support of probabilistic analyses in future full safety assessments for SFL, a methodology to account for this uncertainty was developed. To this end, a limited set of particle tracks that represent the full set was chosen to represent the release of radionuclides at the bedrock-regolith interface with this limited set defined using the full set of particle tracks (Section B6 in the **Radionuclide transport report**).

For specific purposes, and as a complement to FARFCOMP, the computer code Migration Analysis of Radionuclides in the Far Field (MARFA) has been used. MARFA uses a particle-based Monte Carlo method to simulate the transport of radionuclides in a sparsely fractured geological medium. Within SE-SFL, the new capability of MARFA to apply the concept of dynamic  $K_d$  values in transport simulations has been tested. This may give a more realistic representation of sorption, since its degree may vary in time and space with the composition of the groundwater and the bedrock mineralogy. The new capability was tested and demonstrated in a study that provided spatially and temporally variable  $K_d$ -values for Ni, which were fed into MARFA to calculate the transport of Ni-59 from the repository near-field through the bedrock system (Trincherio et al. 2018). The results showed a reduction in the cumulative mass discharge in comparison with a static  $K_d$  approach.

In addition to representation of the aqueous transport of radionuclides, there have also been developments within SE-SFL relating to the modelling of gas migration. The implemented model calculates gas migration from the near-field through the bedrock system to the regolith interface for a given rate of hydrogen gas production. In this way, the heterogeneity of the rock, including deformation zones, is considered as well as the effects of gas release and migration on groundwater flow (Silva et al. 2019b).

### 9.3.3 Surface ecosystems

Progress has been made with respect to several areas regarding modelling of the biosphere in SE-SFL. The development has primarily been initiated by reviews by SSM and their external experts of previous safety assessments. However, developments to increase the consistency in analysis and to facilitate the understanding of the results have also been made. The most important developments are summarized below, and the potential benefits from the development in future safety analyses are summarised below.

In SE-SFL, the potential consequences of the location of the discharge area, and its properties, have been examined in the regional climate and discharge area evaluation cases. In the latter, the sensitivity of dose to object properties was explicitly examined and the importance of object size and soil depth was demonstrated. Moreover, it was shown that the landscape development had limited effect on the dose at late successional stages and it was suggested that time-independent ecosystem models give robust estimates of potential exposure for the entire landscape development period. The approach and the findings should also be applicable to future safety assessments for repositories for long-lived waste, for which the projected dose is substantial also in the far future.

In the *increased greenhouse effect evaluation case*, the potential effects of a seasonal water deficit in arable land were examined. The consequences of restoring the deficit by irrigation, and the importance of translocation of radionuclides within plants (from leaf interception to root storage), were evaluated. The evaluation of long-term irrigation utilized a new (multi-compartmental) model describing continuous cultivation. The approach and conclusions from these calculations should be relevant also in future safety analyses, if potential effects of an even warmer climate are evaluated. In the simplified glaciation cycle evaluation case, the discharge area and the groundwater flow conditions were changed in response to the advance and retreat of an ice sheet. The changes in flow conditions in the biosphere were closely co-ordinated with those in the geosphere by the handling of the hydrogeological models for the geosphere and near-surface hydrology. The approach put focus on the handling of the groundwater response across the geosphere-biosphere interface and it may be worthwhile to consider similar approaches in future analyses.

The biosphere development with the widest implications for this, and possibly future, evaluation was the introduction of stylized water balance models as an interface to the output from detailed hydrological modelling using the MIKE SHE code. The stylized models were used to interpret and summarise the water balances from MIKE SHE in terms of the driving hydrological flows, vertical distribution functions and a limited number of empirically derived parameters. Thus, percolation and discharge in the biosphere object could be determined from net precipitation, bedrock discharge, the size of the object (and its local catchment) and the average regolith stratigraphy. In SE-SFL, the approach was

primarily used to extrapolate groundwater flows to climate and ecosystem stages where data from detailed modelling were not available. Moreover, the method was scaleable with respect to object size and regolith stratigraphy, it was implemented as a model sub-routine and used to examine the sensitivity of environmental activity concentrations to object properties and hydrological drivers. This type of analysis could be valuable building understanding of model results in future safety assessments.

As a result of SSM's reviews of SR-Site and SR-PSU, the biosphere model for transport, exposure and dose calculations has been somewhat modified in SE-SFL as compared with previous assessments. The most important update, in terms of potential effects on modelling results, is the increased discretization of the lower regolith layers (i.e. till and glacial clay layers, see **Biosphere synthesis** for details). In previous assessments, a single compartment representation of these layers has been used. For radionuclides that have a residence time that is similar to, or longer than, the radioactive half-life in these layers, this approach may overestimate the activity released to the surface (due to numerical dispersion). In SE-SFL, the discretization has been increased so that the numerical dispersion mimics the expected field-scale dispersion. As the update is considered to increase the realism of the modelling, for example with respect to the timing of the breakthrough at the surface, it may be worthwhile to consider such model modifications in future safety assessments.

In addition to the developments mentioned above, the transparency, consistency and realism of the biosphere models have been increased in several areas (see the **Biosphere synthesis** for details). For example, previous parameters for stable carbon (such as peat growth rate and pore water concentrations in saturated and unsaturated soils) are calculated as functions within the SE-SFL model. These updates increase the consistency in the handling of C-12 and C-14 in the model. As the consistency is maintained in probabilistic simulations, it is also expected to reduce the uncertainty in plant-root uptake of C-14. The C-14 model development has been initiated by reviews by SSM and their requests for complementary information. However, these model updates have not substantially increased the overall biosphere assessment complexity. Thus, SKB will consider using these modifications in future safety analyses. From model comparisons, other model updates are expected to have a minor influence on model results (**Biosphere synthesis**). Nevertheless, the benefits from increased consistency and realism (as well as from model simplifications) should also be considered in future safety analyses.

Finally, the analysis and means of presentation have been refined in SE-SFL. For example, in the analysis of the base case, the accumulation and decay of radionuclides in regolith layers are visualized in holistic graphs, an overview of the influence of radionuclide properties on the dose to release relationship are presented, and the origin and fate of individual radionuclides in the U-238 decay chain are explicitly depicted. In addition, improvements have been made with respect to the analyses (and presentation) of the effects of object properties have on modelling results, both in the discharge area evaluation cases and in sensitivity analyses. Graphs that display important parameters and/or illustrate individual mechanisms that are of importance for transport and exposure have also been tailored to the individual evaluation and sensitivity cases. Taken together, the improvements in analysis and presentation of results have been significant in SE-SFL, and these developments could also be applied and developed further in future assessments of SFL to facilitate the understanding of modelling results.

#### 9.3.4 Integration and presentation of results

One of the aims in SE-SFL has been to strive for a seamless integration between the different domains of the safety evaluation. The integration has been facilitated by the development of a fully integrated radionuclide transport calculation chain from waste releases to dose calculations (Figure 7-2). The interdisciplinary work has been particularly fruitful in the identification and definition of the evaluation cases, in combination with the interpretation of results. Discussions and iterations between these two steps have resulted in stylized evaluation cases that are internally consistent and have allowed for straight forward comparisons that address the features of interest. For example, in the simplified glaciation evaluation case, temporal changes in hydrological forcing as a response to ice-sheet advance and retreat and relative sea-level changes, are consistent across the near-field, geosphere and biosphere.

A presentation of the results focusing on transport mechanisms within each model domain, that can be communicated appropriately across disciplines and potentially reach a broader target audience, has contributed to the increased integration. Furthermore, holistic analyses across model domains (see e.g. Figures 7-12, 9-1 and 9-2) have allowed for a comprehensive and insightful interpretation of results, from the waste vaults to the surface ecosystems.

## 9.4 Areas of further efforts for a forthcoming safety assessment

One central objective of SE-SFL is to provide SKB with a basis to prioritize areas in which the level of knowledge must be improved in order to perform a full safety assessment for SFL. Generally, several areas can be distinguished for which efforts have been identified that can contribute to establishing a full safety analysis that can serve as part of a license application:

- The safety analysis methodology and its implementation, given that the methodology in SE-SFL has been adopted to the purposes of the evaluation and has not strived to fulfil all the regulatory requirements related to methodology.
- Identification and definition of all requirements, and efforts to underpin compliance discussions for requirements not addressed in SE-SFL.
- The siting process and site characterisation efforts.
- Research and development linked to the cautious or simplifying assumptions underlying the radio-nuclide and dose calculations in SE-SFL.
- Technical developments that are related to the components of the repository and its interactions with its environs, to waste characterisation, and to effective methods to assess post-closure safety for SFL.

These points are discussed in the following sections.

### 9.4.1 Safety analysis methodology and its implementation

In Chapter 2, the methodology applied in SE-SFL is outlined. It is adapted to the objectives of SE-SFL and is therefore only loosely coupled to the regulatory requirements regarding the methodology. Several aspects of the methodology and its implementation will thus need to be further developed.

#### ***External conditions and description of internal processes***

In SE-SFL, the external conditions are derived from an analysis of the range within which future climate conditions and climate-related processes may vary at a Swedish Baltic coastal site (Section 2.5.3, **Climate report**, Section 4.1). Based on this, the three climate variants were derived, constituting the *base variant*, the *simplified glacial cycle variant*, and the *increased greenhouse effect variant*. According to SSM's general advice, the risk analysis should be simplified to include a few potential climate evolutions so, in a future safety assessment, it will be reconsidered if the variants defined for SE-SFL are an adequate simplification of the future climate evolution, and if the number of climate variants in SE-SFL is sufficient to cover relevant potential future developments. It can further be noted that SSM's advice states that the different climate evolutions should be selected so that they together illustrate the most important and reasonably foreseeable sequences of future climate states and their impact on the protective capability of the repository and their environmental consequences. This should imply that the climate sequences do not necessarily need to be more detailed, but that the aim should be to identify and cover reasonably foreseeable climate states that affect the protective capability and environmental consequences of the repository.

One of the steps of the safety assessment methodology is the description of internal processes (Section 2.5.4). In SE-SFL there is no specific documentation of all processes that are described in the FEP analysis. However, there is a large body of knowledge related to all the internal processes included in the FEP catalogue that is documented in SKB's safety assessment work for the Spent Fuel Repository and SFR. This work has been used to underpin the reference evolution in SE-SFL. In a future safety assessment, it may be worthwhile to reconsider in what way the complete set of processes identified in the FEP analysis should be documented in any future safety assessment for SFL. The FEPs that have not been considered in SE-SFL also need to be addressed.

#### ***Safety functions, scenario analysis, and risk calculation***

In SE-SFL, preliminary safety functions and associated indicators have been defined. In a future safety assessment, these should be further developed given a reference design and site for the facility. In SE-SFL, the safety functions have not been used to define scenarios. This is an important role for the safety functions and for the final definitions of the safety functions this role needs to be further considered. Furthermore, the temporal evolution of the safety functions should be analysed, for instance, linked to the description of the reference evolution. The implications of the safety functions that are defined on the site selection are important to consider in the site-selection process.

An important step in SKB's safety analysis methodology is the selection of scenarios. So, for a future safety assessment, a comprehensive set of scenarios is needed. According to SSM's general advice, three types of scenarios should be included: These comprise a main scenario, less probable scenarios and residual scenarios. The main scenario should be based on the probable evolution of external conditions and generally realistic assumptions with respect to the internal conditions. Less probable scenarios should be analysed for the evaluation of scenario uncertainty. Finally, residual scenarios should include sequences of events and conditions that are selected and studied independent of probabilities in order to, among other things, illustrate the significance of individual barriers and barrier functions. One important example of internal conditions that have not been treated fully realistically in SE-SFL is processes related to the evolution of the bentonite barrier and their effect on the releases and resulting doses. Potential buffer erosion and mineral transformations have not been quantified in the radionuclide transport calculations. Such calculations will be needed in future assessments to underpin a main or less probable scenario for a vault with bentonite backfill.

For the main scenario and the less probable scenarios, probabilities need to be defined. Probabilities may be based on statistics underlying important aspects of the scenarios. The general advice to SSM's regulations suggests the use of several methods including expert elicitation to deduce probabilities. In SE-SFL no probabilities have been considered, since the methodology used applies evaluation cases instead of scenarios. The probabilities of the different scenarios are needed to be able to calculate risk, based on the doses resulting from the scenarios. Such risk summations have been carried out in SR-Site and SR-PSU and the methodology can be applied also for a future safety assessment for SFL. It should be noted that the calculations within the scenarios can also use a probabilistic approach and that the risk associated with a scenario can be based on such calculations and the assumption of a probability of one for the scenario. To obtain the total risk from the combination of such scenarios the mean dose that gives the largest risk is selected for each point in time, if the scenarios are mutually exclusive and otherwise the risk contributions are summed. Such a methodology was applied for some scenarios in SR-Site (SKB 2011a). The risk summation needs to account for the way the probabilities are handled. In a future safety assessment for SFL, the methodology of handling probabilities and the risk summation needs to be defined considering the scenarios that are defined.

For the calculations that underlie the risk calculations, uncertainties need to be considered and documented. In SE-SFL, considerable efforts have been invested in the management of uncertainties and their documentation. For SR-Site and SR-PSU, however, very high standards were applied, and a similarly high level will have to be implemented in the safety assessment work for a license application for SFL. One example of importance are the uncertainties in the inventory of radionuclides and other materials in the waste that are larger than for the Spent Fuel Repository and SFR due to the legacy nature of the main part of the waste planned for BHA. These will need to be addressed adequately in a future safety assessment.

#### **9.4.2 Handling of regulatory requirements**

SE-SFL focuses on the conditions under which the repository concept has the potential to fulfil the regulatory requirements of the risk criterion and barrier system robustness. These two requirements are judged to be most important to consider in this step in the SFL repository programme. However, in a future full safety assessment that is to be part of a license application, all relevant regulatory requirements need to be addressed. In Section 2.2 the handling of the regulatory requirements in SE-SFL is discussed including the requirements that are not addressed. It is likely that in order to show compliance with the requirements that are not addressed in SE-SFL additional analyses will be needed. This may also have implications for SKB's requirements on the repository components and their further development. Some such requirements that are considered most important in the future process are discussed below.

SSM requires that the barrier system comprises several barriers so that, as far as possible, the necessary safety is maintained despite a single deficiency in a barrier. The concept underlying SE-SFL includes several barriers, as required. However, it has not been analysed in SE-SFL how different types of single deficiencies in a barrier affect the safety, and whether, if necessary, safety can be maintained despite such deficiencies. This requirement needs to be interpreted in view of what is meant by a single deficiency for the case of the barriers associated with BHA or BHK. In addition, the implications of the

wording that necessary safety shall be maintained as far as possible, need to be interpreted. Based on the interpretations, different kinds of single deficiencies need to be defined and analysed with respect to the requirement in a future safety assessment.

The requirement for the application of best available technique according to SSM implies that the siting, design, construction and operation of the repository should be carried out in a way to prevent, limit and delay releases from both the engineered and geological barriers as far as is reasonably possible. In SE-SFL, some aspects of the engineered barriers are analysed, such as the significance for safety of the characteristics of the concrete backfill in BHK or the effect of the siting. However, a comprehensive analysis is not meaningful in this step of the repository programme and has therefore not been attempted. Thus, analyses need to be carried out to substantiate compliance with the requirement to adopt best available techniques. It can, however, already be noted that the iterative safety analysis methodology and associated RD&D work supports the development of the best available technique. This effort overlaps and interacts with the optimisation process that strives to lower dose consequences and thereby risk in line with SSM requirements.

In SE-SFL, the annual mean dose corresponding to the risk criterion (14  $\mu\text{Sv/a}$ ) is the basis for evaluating the potential for the repository concept to meet regulatory criteria. According to SSM's general advice on the regulations, however, a ten times higher dose can be used for comparison if the exposed group only consists of a few individuals. This criterion may, for instance, be relevant for a well scenario in which consumption of drinking water from a well is the dominant exposure pathway. The *drilled well* evaluation case can be considered as an example of this. As the exposed group is linked to consumption of food from sources within the biosphere object that the releases occur into, the number of exposed individuals is likely to be limited. In future analyses, it may be worthwhile to consider under which other circumstances the higher criterion may be applicable, even if the main objective for the development of SFL and future analysis steps is to show that resulting doses are lower than the  $10^{-6}$  risk criterion.

SE-SFL focuses on doses to humans, because it has been found in SKB's previous safety analyses that doses to humans require higher repository protective capabilities than the protection of the environment. According to SSM's regulations, however, the final management of spent nuclear fuel and nuclear waste shall be implemented so that it is also shown that biodiversity and the sustainable use of biological resources are protected against the harmful effects of ionising radiation. Moreover, biological effects of ionising radiation in the habitats and ecosystems concerned shall be described. Hence, these aspects of the post-closure protective capability need to be addressed.

There are also several requirements that are related to the methodology and reporting that need to be met (SSMFS 2008:21, Section 11, Appendix 1), which have not been comprehensively discussed in SE-SFL. These requirements will have to be dealt with in a safety assessment for a license application.

In addition to the requirements on post-closure safety there are also requirements relating to the operation of a nuclear waste repository. Some of these are coupled to post-closure safety, as for instance the need for waste acceptance criteria that include aspects that follow from the assessment of post-closure safety. In a future assessment it is important to identify and keep track of such links.

### 9.4.3 Siting process and site characterisation

A necessary step in pursuing the SFL repository programme and finally filing the necessary applications is the identification and selection of an adequate site in a municipality that is willing to host the facility. Thus, a siting process needs to be carefully planned and implemented. Siting factors should be defined, and the results from SE-SFL, and specifically the evaluation cases related to siting (Chapter 8, **Radionuclide transport report**, Chapter 7), can be used as supporting material.

It can be noted that SKB has in depth experience from the siting processes of the Spent Fuel Repository and of SFR including its extension. When one or several potential sites have been identified, a site characterisation programme is needed to obtain the data needed for the future site-specific safety assessment. This will be a task that requires considerable efforts.

#### 9.4.4 Research and development

SE-SFL builds on a thorough understanding of the FEPs affecting the repository near-field and its environs. As SE-SFL is a first evaluation of the repository concept, simplifications have, however, been introduced. Some of the assumptions introduced in the evaluation are cautious, as described in Section 7.3.2 (see further Section 8.4 in the **Radionuclide transport report**). Additionally, certain aspects of the reference evolution that are judged to be of minor importance are further simplified and sometimes omitted in the transport calculations, and some uncertainties are handled by simplifying cautious assumptions as described in Sections 7.4.5, 8.6.1 and 8.6.2 (see further Section 8.3 in the **Radionuclide transport report**). These simplifications are recapitulated below. Further research and development, relating to some of these assumptions, may contribute to a more realistic representation of the future evolution of the repository and its environs in the scenarios and thus provide a stronger basis for the assessment of post-closure safety for SFL.

##### **Cautious simplifications used in the calculations**

Several the cautious assumptions made in the near-field increase the amount of radioactivity available for transport (Section 7.3.2). These assumptions include:

- That all radionuclides are unaffected by solubility limitations.
- That no radionuclide is affected by the presence of others (except ingrowth from parent radionuclides).
- That waste containers provide no transport resistance.
- That radionuclides released by corrosion do not re-precipitate in the corrosion products.
- That no account is taken of the potential delayed release of radionuclides from the materials in BHA, although part of the activity in BHA is likely contained in solid materials such as metals (Shahkarami 2019, Section 2.3.1).

Furthermore, better characterization of the physical form of the uranium inventory will likely lead to higher retention in the near-field, even though the ingrowth and subsequent release of progeny needs to be accounted for.

Further, the complexing agent ISA is assumed to be at the solubility limit for a cementitious environment throughout the entire analysis period in BHA, resulting in significantly reduced sorption capacity for e.g. Tc-99 and nuclides in the uranium decay chain. This is cautious, since it neglects possible degradation and out-transport of ISA, even if this is judged to be limited as long as a high pH in the alkaline environment suppresses microbial activity, and sorption onto cement leads to retention in the vault. Overall, improved knowledge of amounts and longevity of complexing agents in BHA will not change the dose from non-sorbing radionuclides. However, less conservative assumptions may reduce the dose from Tc-99 and nuclides in the U-238 decay chain, which may reduce the total dose after about 100 000 AD.

In the geosphere transport calculations, the  $K_d$  values have been cautiously chosen (Section 3.3.1 in Shahkarami 2019). For instance, the  $K_d$  value of the dose-dominating radionuclide Mo-93 is set to zero. Site-specific data from Olikiluoto suggest that Mo-93 sorption does occur (see *alternative geosphere retention* evaluation case, Section 8.4.3). Moreover, pathways through the geosphere that do not reach the geosphere-biosphere interface are neglected. One reason for particles not reaching the surface is that the flows are so low that numerical artefacts occur. Thus, neglecting such pathways disregards transport with high potential for retention.

In the *discharge area* evaluation case, it was found that the radionuclide-specific responses to biosphere object properties may differ. Specifically, aquatic releases may increase the importance of C-14 contributions in comparison with terrestrial releases. This relates to the dilution of the releases which is wholly compensated for C-14 by greater bioaccumulation. If C-14 in future analyses should turn out to be the dose dominating radionuclide, then site-specific considerations of aquatic parameters could have a substantial influence on calculated doses.

### **Simplifications in comparison with the reference evolution**

In general, important aspects of the variants of the reference evolution (Chapter 6) are extracted to the reference evolution cases, and aspects that are judged to have minor importance are simplified in the calculations. There are other aspects of the variants of the reference evolution that have been handled by cautious assumptions in order to account for uncertainties (Sections 7.4.5, 8.6.1 and 8.6.2).

Potential effects of external conditions on the barrier performance that have been neglected in the base case include: changes of salinity at repository depth and changes in the redox conditions in the rock. As detailed in the description of the reference evolution for BHA, intrusion of dilute waters and glacial meltwaters might possibly lead to physical bentonite erosion (Section 6.4.9). If bentonite erosion is sustained over sufficiently long times, it could impair the performance of the barrier functions. In contrast, the concrete barrier in BHK is unlikely to be affected by dilute waters reaching repository depth and thus the performance of the BHK should not be influenced significantly.

In addition, the chemical interactions of the concrete in the waste domain with the bentonite backfill leading to clay mineral transformations could potentially influence bentonite barrier performance (Section 6.2.9). The effects of clay mineral transformations on the near-field transport processes would need to be quantified to evaluate potential implications for repository performance. It needs, for instance, to be considered that the plug resistance at the interface between the bentonite and rock fractures is an important part of the total transport resistance, whereas the mineral transformations in the bentonite are developing from the inner concrete structure outwards and may not reach the interface between the bentonite and rock fractures within the relevant timescale. The effect of the selected bentonite thickness may also be an important factor to consider.

In the glacial variant of the reference evolution, mechanical, chemical, or thermal effects on the structural integrity of the waste vaults have been described (Section 6.3). Such effects are, however, neglected in the *simplified glacial cycle evaluation case*. This is a simplification, and, for instance, the ice-sheet load will have mechanical effects on the bedrock and possibly also on the repository vaults. Simulations indicate that mechanical damage may occur due to increased rock stresses in the concrete backfill of BHK at the interface between the backfill and the rock (Idiart et al. 2019a). However, the effect of considering the mechanical damage in the near-field transport calculation may be limited, as the concrete is assumed to already have degraded considerably at the onset of the glacial period in the *simplified glacial cycle evaluation case*. Nevertheless, in a full safety assessment, the combined effects of degradation (due to chemical cement leaching) and increased rock stresses would need to be evaluated with respect to the potential timing of future glacial conditions. The effect of changes in rock stress on the bentonite barrier of BHA has not been evaluated, but it is less likely to be affected by changes in the rock stresses due to its limited stiffness.

During periglacial conditions, the temperature has decreased around the repository but, in SE-SFL it is assumed that the repository is situated deep enough not to be frozen during permafrost. It can be noted that in previous analyses of Laxemar and Forsmark (Section 9.4.3 in SKB 2006a and Section 12.3.2 in SKB 2011a), freezing of repository barriers at the depth evaluated in SE-SFL, 500 m, is not expected to occur during the coming 1 million years. Nevertheless, in a future safety assessment for a selected site, the potential for freezing of pore water in the repository needs to be analysed.

When an ice-sheet advances and retreats over the repository site, high groundwater flows are expected to alter the redox conditions, which in turn may affect the radionuclide speciation in the rock (and  $K_d$  values). These effects have not been accounted for in the *simplified glacial cycle evaluation case*. In SR-Site, the effect of such  $K_d$  changes was analysed with the conclusion that the releases to the biosphere increased but that this was compensated by the release reaching a coastal basin with decreased human exposure (Section 13.5.6 in SKB 2011a). As the inventory of C-14 is expected to have decayed to insignificant levels at the time of the ice-sheet advance, and as the dose from sorbing radionuclides like Ni-63 and Tc-99 is reduced by three orders of magnitude in aquatic ecosystems, this conclusion is likely to hold also for SFL.

### 9.4.5 Technical developments

The design assumed in SE-SFL is based on the concept study of Elfving et al. (2013). In a future full safety assessment for SFL, the design of the facility will need to be refined to establish a reference design that, in principle, could be implemented for a future facility at a selected site. Technical developments might be advantageous to optimize the reference design, for example, regarding geometry and material properties in order to improve the repository robustness and to further reduce releases and doses. Attempts were made in SE-SFL to represent variants of the repository design, for example, varying the thickness of the bentonite backfill in BHA, to provide input to optimisation of the design. However, the results were found to be difficult to interpret given the conceptualisation of the cases. Increased functionality in the groundwater flow and radionuclide transport modelling chain would be advantageous to guide choices on BAT and optimization. A more flexible representation of the interface between the waste vaults and the bedrock is of specific interest in this context.

As discussed above, the inventory for BHA is uncertain and the resulting doses are proportional to the inventory. A better characterisation of the waste would therefore be an improvement that potentially could have a large impact on the results of the safety assessment. It is likely that the uncertainties in the inventory of radionuclides and other materials, associated with the legacy nature of the main part of the waste planned for BHA, will be larger than for the waste planned for the Spent Fuel Repository and SFR. Therefore, the uncertainty management may need further consideration for future safety assessments for SFL.

As has been shown in the *no effect of complexing agents in BHA* evaluation case, complexing agents have a large impact on the doses at very late times. Tc-99 and the U-238 decay chain that together dominate late doses in the base case do not show any significant dose contributions in the absence of complexing agents.

The potential degradation of the bentonite barrier in BHA and its mechanical influence on the waste domain has not been considered in the evaluation of doses in SE-SFL. Further analysis is needed to support realistic assumptions regarding the temporal evolution of the waste domain and the bentonite barrier. Such an analysis might be helpful in optimising the design of the bentonite barrier, its geometry and the material properties, for example, in order to improve the repository robustness and to further reduce releases and doses.

The mechanical evolution of BHK has been analysed as part of the reference evolution, however, such considerations have not been implemented in the radionuclide transport and dose calculations. One aspect of the mechanical development is the influence of the altered stress conditions at repository depth due to glaciation, another is the effect of earthquakes on the repository. Further analysis might be required to show that the barrier system is robust with respect to these FEPs.

The corrosion rate applied for the metal waste components in BHK influence the near-field releases and resulting doses together with the distribution of the inventory between metal fractions of different thicknesses and the assumptions regarding the instant release fractions. Consequently, in future assessments the potential for reduced releases and doses from BHK associated with the uncertainty in corrosion rate could be evaluated in relation to the assumptions about, and uncertainty in, the initial distribution of the radionuclide inventory between the instant release and thicker metal fractions. Furthermore, it could be considered if it is worthwhile to study the effect of including the formation of corrosion products and their impact on radionuclide releases, for instance co-precipitation of Mo and Fe.

In SE-SFL, the radionuclide inventory originating from ESS has been treated separately and was not included in the base case, due to large uncertainties in the radionuclide inventory. Therefore, the ESS activity and chemical inventory needs to be added to the total inventory of BHA and BHK in a future safety assessment.

## 10 Conclusions

A safety evaluation for the repository concept proposed for SFL has been carried out with the purpose to provide input to the subsequent, consecutive steps in the development of SFL. The evaluation has been performed by analysing several evaluation cases that together indicate under what conditions the repository concept has the potential to fulfil regulatory requirements (Chapter 9). The suitability of the proposed repository vaults for the ESS waste has also been analysed. SE-SFL is based on extensive analysis and the main references include the **Biosphere synthesis**, the **Climate report**, the **FEP report**, the **Initial state report**, and the **Radionuclide transport report**. Furthermore, the results have been used to identify areas for further RD&D, including safety analysis methodology and its implementation, efforts needed to address the full set of post-closure regulatory requirements, the siting process, assessment model development, and technical design improvements (Chapter 9).

The evaluation has been carried out for the example site of Laxemar for which a realistic and consistent description of a site for geological disposal of radioactive waste is available. The evaluation has to a large degree made use of available data and existing modelling codes, but several new codes have also been developed. These codes have been implemented successfully and can with adequate documentation be used in a future full safety assessment. All in all, efforts have been undertaken in SE-SFL to demonstrate an understanding of the repository evolution and to ensure the applicability of models, parameter values and other assumptions used for the description and quantification of repository performance.

SE-SFL is further developed in comparison to the previous assessments and associated repository concepts (SKB 1993, 1999a, Wiborg 1995). Important improvements in SE-SFL are the development of the repository concept, an updated inventory, and a more detailed account of internal and external processes. Moreover, the biosphere was in the previous assessment handled in a simplified manner, whereas it is handled in a more comprehensive way in SE-SFL. The availability of data from the Spent Fuel Repository site investigations has allowed for more detailed representations of the geosphere. In general, SKB's experiences with safety analysis work have led to many developments since the late 1990s.

The evaluation shows that the repository concept for SFL has the potential to fulfil regulatory requirements under suitable conditions, given that further efforts will need to be undertaken in a future full safety assessment to underpin a compliance discussion. In total the results of the radionuclide transport and dose calculations indicate that the conditions assumed in the base case yield doses that are too high to comply with the risk criterion for the BHA and BHK inventories underlying SE-SFL. However, the full set of evaluation cases indicate conditions and further efforts that could improve the performance and analysis of the repository, as briefly described in the following and discussed in more detail in Chapters 9. This is in line with the iterative safety analysis process that the SFL repository programme follows, in which the results from post-closure safety analyses and related activities are used to successively inform and improve the analysis. In accordance with the Nuclear Activities Act (SFS 1984:3), important research needs for the SFL programme that emerge as a result of SE-SFL will be reported in the research development and demonstration (RD&D) programme. An important aspect of the RD&D programme is to ensure that the industry has well founded information to support long-term planning, to which the results of SE-SFL have contributed.

### 10.1 Conditions under which the repository concept has potential to meet regulatory criteria

The conclusions regarding the conditions under which the repository concept has the potential to fulfil regulatory requirements on limited risk of harmful effects to humans and repository robustness are presented in this section. Although the regulations apply to the entire facility, conclusions regarding BHA and BHK are presented separately, since the conditions under which each waste vault has the potential to perform well enough to fulfil regulatory requirements relate to different aspects (Sections 10.1.1 and 10.1.2). Issues that are related to the repository environs and thus are relevant for both waste vaults are discussed in Section 10.1.3. The different possibilities to improve the repository performance and its analysis will need to be carefully evaluated in the future steps of the SFL repository programme.

### 10.1.1 BHA

The barrier system of BHA is effective in retaining and retarding radionuclides in the inventory, as the analysis of the base case shows (Section 7.5). The initial activity of C-14, Mo-93, and Ni-59 is substantially reduced within the near-field. For the very long-lived Tc-99 and Cl-36, a large part of the inventory also decays in the near-field. Retention is linked to diffusion-controlled transport within and out of the bentonite. The maximum annual doses are limited due to the considerable transport resistance offered by the bentonite. Nevertheless, the results indicate that the conditions assumed in the base case yield doses that are too high to comply with the risk criterion for the BHA inventory underlying SE-SFL. Also, it is noted that the simplified glacial evaluation case shows that doses during cold periods do not exceed the maximum dose under present-day conditions. As the resulting doses are high compared with the dose criterion, further efforts are needed in comparison with SE-SFL to be able to underpin a compliance discussion.

One important aspect that has been the objective of SE-SFL is to analyse under what conditions the repository concept has the potential to fulfil the regulatory criteria. Based on the set of evaluation cases that have been analysed in SE-SFL, the following can be concluded regarding the conditions under which the analysed repository concept for BHA has the potential to fulfil the regulatory criterion on risk.

- With an inventory for the dominating radionuclides Mo-93, Cl-36, C-14 that can be shown to be more than a factor 10 lower than the estimate used in SE-SFL, and not substantially higher for other radionuclides, the repository concept would have the potential to meet the risk criterion given the assumptions made in the base case.
- At times after 100 000 years after repository closure, Tc-99 becomes dominating. As for the other dose-dominating radionuclides, a 10 times lower inventory would imply that the dose corresponding to the regulatory risk limit would not be exceeded. An even more pronounced effect can be achieved if the cautious assumption of high concentrations of complexing agents in the waste domain persisting for the entire analysis period can be relaxed. A further consideration is that according to SSM's general advice, a strict comparison of the risk limit is not meaningful after 100 000 years after closure. Besides using supplementary indicators of the protective capability of the repository, the underlying causes of a risk exceeding the criterion (illustrated by doses in the context of SE-SFL) after 100 000 years after closure should be reported together with possible measures to improve the protective capability of the repository.
- With 100 times lower groundwater flow rates than assumed in the base case (i.e. with a typical advective travel time of  $10^4$  years) the resulting doses become significantly lower than the dose corresponding to the risk criterion given the other assumptions in the base case. In contrast, a factor 10 lower groundwater flow rate (i.e. with a typical advective travel time of  $10^3$  years) implies dose results exceeding the dose corresponding to the risk criterion. Lower flows can be achieved by selecting a site with lower flows than at the example site or possibly by increasing the depth of the repository.
- Initially submerged conditions, with initially 100 times lower groundwater flow rates than assumed in the base case that limit the near-field releases, are advantageous for the protective capability of the repository for as long as they persist. But since the BHA inventory, as shown in the base case, potentially can sustain releases for hundreds of thousands of years that yield doses comparable to the dose criterion, submerged conditions would have to persist for a time span of similar length to ensure conditions that have the potential to fulfil the risk criterion.
- The expected evolution of the bentonite barrier needs to be analysed in a full assessment to demonstrate that it will uphold its safety functions for relevant time scales. Moreover, the detailed design of the waste domain and bentonite barrier should be optimised in order to improve repository performance.

### 10.1.2 BHK

The barrier system of BHK is efficient for retarding and retaining radionuclides in the inventory, as the analysis of the base case shows (Section 7.5). In general, the mechanisms contributing to the retention are the slow release of induced activity from the metal through corrosion, sorption onto cement of many of the radionuclides in the inventory and the slow advective transport through the concrete

barrier. The maximum annual doses are limited due to the slow release relating to steel corrosion and considerable transport resistance offered by the concrete backfill. Nevertheless, the results indicate that the conditions assumed in the base case yield doses that are too high to comply with the risk criterion for the BHK inventory underlying SE-SFL. Again, it is noted that the simplified glacial evaluation case shows that doses during cold periods do not exceed the maximum dose under present-day conditions. As the resulting doses are high compared to the dose criterion, further efforts are needed in comparison with SE-SFL to be able to underpin a compliance discussion.

One important aspect that has been the objective of SE-SFL is to analyse under what conditions the repository concept has the potential to fulfil the regulatory criteria. Based on the set of evaluation cases that have been analysed in SE-SFL, the following can be concluded regarding the conditions under which the repository concept for BHK has potential to fulfil the regulatory criteria on risk.

- Less pessimistic assumptions regarding the steel corrosion rate than in the base case improves the potential for the repository to meet regulatory requirements. The potential for reduced releases and doses from BHK associated with the uncertainty in corrosion rate needs to be evaluated in relation to the assumptions about, and uncertainty in, the initial distribution of the radionuclide inventory between the instant release and thicker metal fractions. If smaller instant release fractions can be substantiated, the effect of less pessimistic corrosion rates increases. Studying the steel corrosion process under the conditions prevailing in BHK in a more mechanistic way could also be considered.
- An optimized concrete backfill material that has low hydraulic conductivity, porosity, and diffusivity improves the potential for the repository to meet regulatory requirements. The properties of the concrete developed for the extension of SFR potentially yields a sufficiently good near-field performance. Improved concrete properties should also improve the ability of the concrete to withstand degradation due to cement leaching. The effect of using a concrete with improved properties on gas transport needs to be considered.
- With 10 times lower groundwater flow rates than assumed in the base case (i.e. with a total flow through BHK of  $10^{-1} \text{ m}^3/\text{a}$ ), the doses resulting from BHK become significantly lower than the dose corresponding to the risk criterion, given the other assumptions in the base case.
- Initially submerged conditions, with initially 100 times lower groundwater flow rates than assumed in the base case and thus with a total flow through BHK of  $10^{-2} \text{ m}^3/\text{a}$ , are advantageous and yield low doses for as long as they persist. It would require a submerged period of about 50 000 years, with low releases associated with the low groundwater flows, for the dose-contributing radionuclides to decay sufficiently to result in doses that do not exceed the dose criterion given the estimated BHK inventory and other underlying assumptions.
- The detailed design of the waste domain and concrete barrier, for example its geometry and material parameters, should be optimised in order to improve repository performance.

### 10.1.3 Repository environs

The repository environs affect the repository performance in several ways. As discussed in previous sections, lower groundwater flow conditions are favourable and sufficiently low flow creates conditions under which the repository concept has the potential to fulfil the regulatory criteria.

The external conditions related to different climate sequences as analysed in the *increased greenhouse effect* and *simplified glacial cycle evaluation cases* result in doses that are similar to, or lower than, the base case. The *alternative regional climate* evaluation case furthermore shows that there is no large difference between the biosphere responses to releases in different locations along the coast of Sweden that represent alternative regional climates.

The analysis of biosphere transport in the base case assumes that the releases will occur in a given biosphere object at the example site. The conditions simulated will therefore not necessarily represent the actual discharges at a future selected site. However, the calculations are judged to capture the main features of transport, accumulation and exposure for a suite of possible future conditions. The results of the *alternative discharge area* evaluation show that the resulting doses can vary over several orders of magnitude depending on the biosphere object properties, and that the base case yields among the highest doses. Moreover, the radionuclide-specific dose response to object properties may differ between

radionuclides. In consequence, the conditions under which the repository concept has the potential to meet the risk criterion are linked to the properties of the biosphere objects at the selected site. Potential uncertainties regarding into which biosphere objects releases occur are therefore important to consider in future site-specific analyses.

## 10.2 Suggested future efforts

One central objective of SE-SFL is to provide SKB with a basis to prioritize areas in which the level of knowledge must be improved in order to perform a full safety assessment for SFL. In Section 9.4 four areas were distinguished in order to discuss potential future efforts. In this section this discussion is summarised.

The safety analysis methodology applied in SE-SFL is adapted from the methodology used by SKB in SR-Site and SR-PSU to the purposes of evaluating conditions under which the concept has potential to fulfil regulatory criteria and areas for further efforts. A future assessment needs to address all regulatory requirements related to methodology. SKB's safety assessment methodology as applied in SR-Site and SR-PSU fulfils all requirements and can therefore also be implemented for SFL. Given the reference design and potential site chosen for a full safety assessment, it should be reconsidered if the different climate evolutions together adequately illustrate the most important and reasonably foreseeable sequences of future climate states. If not, modified or additional climate evolutions will need to be defined. The climate sequences do not necessarily need to be more detailed, but the aim should be to identify and cover the climate states that affect the protective capability and environmental consequences of the repository. Furthermore, the safety functions should be adjusted to the chosen reference design and potential site. The role of the safety functions in the scenario selection in a future safety assessment may also have implications for their definition. A comprehensive set of scenarios needs to be defined and assessed with respect to resulting risk. In a future safety assessment for SFL that is to underpin a license application, all relevant regulatory requirements need to be addressed. Among other things, this implies that not only the effects on humans need to be assessed, but also that the effects on non-human biota need to be considered. A further requirement that needs to be addressed in future analyses is the effects of single deficiencies in a barrier. Furthermore, regulatory compliance needs to be shown for the requirements on the application of best available technique and optimisation, which may imply a need for supporting assessments.

A result of the safety evaluation that may not be very surprising is that the siting of the SFL facility, and, in particular, the groundwater flow conditions, are important for the repository performance. Therefore, a siting process needs to be carefully planned and implemented in order to find a suitable location for the repository. A site characterisation will be needed to substantiate a site-specific safety analysis for the proposed site.

SE-SFL builds on a thorough understanding of the FEPs affecting the repository near-field and its environs. As SE-SFL is a first evaluation of the repository concept suggested by Elfving et al. (2013), simplifications have, however, been introduced. As discussed in Section 9.4.4, some of the simplifications introduced in the evaluation are cautious, including the availability of radionuclides from the source term, handling of complexing agents, and geosphere retention properties. In general, important aspects of the variants of the reference evolution (Chapter 6) are extracted to the reference evolution cases and aspects that are judged to have minor importance are simplified in the calculations. As discussed in Section 9.4.4, there are other aspects of the variants of the reference evolution, relating to the effects of altered conditions in the environment on barrier performance, which have been handled by cautious assumptions in order to account for uncertainties. Further research and development, relating to some of these assumptions, may contribute to a more realistic representation of the future evolution of the repository and its environs in the scenarios and thus a stronger basis for the assessment of post-closure safety for SFL.

In a future full safety assessment for SE-SFL, the design of the facility will need to be refined to establish a reference design that, in principle, could be implemented for a future facility at a selected site. Technical developments might be advantageous to optimize the reference design, e.g. regarding

geometry and material properties in order to improve the repository robustness and to further reduce releases and doses. To this end, increased functionality in the groundwater flow and radionuclide transport modelling chain would be advantageous to guide choices on BAT and optimization, as discussed in Section 9.4.5.

A fundamental aspect is the characterisation of the waste inventory and its chemical properties. Reduced uncertainties could potentially have a large impact on the results of the safety assessment.



## References

SKB's (Svensk Kärnbränslehantering AB) publications can be found at [www.skb.com/publications](http://www.skb.com/publications). SKBdoc documents will be submitted upon request to [document@skb.se](mailto:document@skb.se).

### **References with abbreviated names**

**Main report, 2019.** Post-closure safety for a proposed repository concept for SFL. Main report for the safety evaluation SE-SFL. SKB TR-19-01, Svensk Kärnbränslehantering AB.

**Biosphere synthesis, 2019.** Biosphere synthesis for the safety evaluation SE-SFL. SKB TR-19-05, Svensk Kärnbränslehantering AB.

**Climate report, 2019.** Climate and climate-related issues for the safety evaluation SE-SFL. SKB TR-19-04, Svensk Kärnbränslehantering AB.

**FEP report, 2019.** Features, events and processes for the safety evaluation SE-SFL. SKB TR-19-02, Svensk Kärnbränslehantering AB.

**Initial state report, 2019.** Initial state for the repository for the safety evaluation SE-SFL. SKB TR-19-03, Svensk Kärnbränslehantering AB.

**Radionuclide transport report, 2019.** Radionuclide transport and dose calculations for the safety evaluation SE-SFL. SKB TR-19-06, Svensk Kärnbränslehantering AB.

### **Other references**

**Abarca E, Sampietro D, Miret M, von Schenck H, 2016.** Initial modelling of the near-field hydrogeology. Exploring the influence of host rock characteristics and barrier properties. Report for the safety evaluation SE-SFL. SKB R-16-02, Svensk Kärnbränslehantering AB.

**Abarca E, Sampietro D, Molinero J, 2019.** Modelling of the near-field hydrogeology – temperate climate conditions. Report for the safety evaluation SE-SFL. SKB R-19-03, Svensk Kärnbränslehantering AB.

**Andersson E, 2010.** The limnic ecosystems at Forsmark and Laxemar-Simpevarp. SKB TR-10-02, Svensk Kärnbränslehantering AB.

**Andersson J, Riggare P, Skagius K, 1998.** Project SAFE. Update of the SFR-1 safety assessment – Phase 1. SKB R-98-43, Svensk Kärnbränslehantering AB.

**Andra, 2005.** Dossier 2005 Argile. Safety evaluation of a geological repository. Châtenay-Malabry: Agence nationale pour la gestion des déchets radioactifs (Andra).

**Anunti Å, Larsson H, Edelborg M, 2013.** Decommissioning study of Forsmark NPP. SKB R-13-03, Svensk Kärnbränslehantering AB.

**Aquilonius K (ed), 2010.** The marine ecosystems at Forsmark and Laxemar-Simpevarp. SR-Site Biosphere. SKB TR-10-03, Svensk Kärnbränslehantering AB.

**Bassil N M, Bryan N, Lloyd J R, 2015.** Microbial degradation of isosaccharinic acid at high pH. The ISME Journal 9, 310–320.

**Bengtsson A, Blom A, Johansson L, Taborowski T, Eriksson L, Pedersen K, 2017.** Bacterial sulphide-producing activity in water saturated iron-rich Rokle and iron-poor Gaomiaozi bentonite at wet densities from 1 750 to 1 950 kg m<sup>-3</sup>. SKB TR-17-05, Svensk Kärnbränslehantering AB.

**Berger A, Loutre M F, 2002.** An exceptionally long interglacial ahead? Science 297, 1287–1288.

**Birgersson M, Karnland O, Nilsson U, 2010.** Freezing of bentonite. Experimental studies and theoretical considerations. SKB TR-10-40, Svensk Kärnbränslehantering AB.

**Bosson E, Sassner M, Sabel U, Gustafsson L-G, 2010.** Modelling of present and future hydrology and solute transport at Forsmark. SR-Site Biosphere. SKB R-10-02, Svensk Kärnbränslehantering AB.

- Boulton G S, Kautsky U, Morén L, Wallroth T, 2001.** Impact of long-term climate change on a deep geological repository for spent nuclear fuel. SKB TR-99-05, Svensk Kärnbränslehantering AB.
- Brenner D J, Doll R, Goodhead D T, Hall E J, Land C E, Little J B, Lubin J H, Preston D L, Preston R J, Puskin J S, Ron E, Sach R K, Samet J M, Setlow R B, Zaider M, 2003.** Cancer risks attributable to low doses of ionizing radiation: assessing what we really know. *Proceedings of the National Academy of Sciences* 100, 13761–13766.
- Brown P W, Taylor H F, 1999.** The role of ettringite in external sulfate attack. *Materials Science of Concrete* 5, 73–98.
- Brunberg A-K, Carlsson T, Brydsten L, Strömgren M, 2004.** Oskarshamn site investigation. Identification of catchments, lake-related drainage parameters and lake habitats. SKB P-04-242, Svensk Kärnbränslehantering AB.
- Bruno J, González-Siso M R, Duro L, Gaona X, Altmaier M, 2018.** Key master variables affecting the mobility of Ni, Pu, Tc and U in the near field of the SFR repository. Main experimental findings and PA implications of the PhD thesis. SKB TR-18-01, Svensk Kärnbränslehantering AB.
- Brydsten L, 2004.** A mathematical model for lake ontogeny in terms of filling with sediments and macrophyte vegetation. SKB TR-04-09, Svensk Kärnbränslehantering AB.
- Brydsten L, 2009.** Sediment dynamics in the coastal areas of Forsmark and Laxemar during an interglacial. SKB TR-09-07, Svensk Kärnbränslehantering AB.
- Brydsten L, Strömgren M, 2010.** A coupled regolith-lake development model applied to the Forsmark site. SKB TR-10-56, Svensk Kärnbränslehantering AB.
- Claesson Liljedahl L, Kontula A, Harper J, Näslund J-O, Selroos J-O, Pitkänen P, Puigdomenech I, Hobbs M, Follin S, Hirschorn S, Jansson P, Kennell L, Marcos N, Ruskeeniemi T, Tullborg E-L, Vidstrand P, 2016.** The Greenland Analogue Project: Final report. SKB TR-14-13, Svensk Kärnbränslehantering AB.
- Crawford J, 2018.** Screening of radionuclides for radionuclide and dose calculations. Report for the safety evaluation SE-SFL. SKB P-16-09, Svensk Kärnbränslehantering AB.
- Cronstrand P, 2016.** Long-term performance of the bentonite barrier in the SFR silo. SKB TR-15-08, Svensk Kärnbränslehantering AB.
- Duro L, Grivé M, Domènech C, Roman-Ross G, Bruno J, 2012.** Assessment of the evolution of the redox conditions in SFR 1. SKB TR-12-12, Svensk Kärnbränslehantering AB.
- Elfving M, Evins L Z, Gontier M, Graham P, Mårtensson P, Tunbrant S, 2013.** SFL concept study. Main report. SKB TR-13-14, Svensk Kärnbränslehantering AB.
- Engkvist I, Albinsson Y, Johansson Engkvist W, 1996.** The long-term stability of cement – Leaching tests. SKB TR 96-09, Svensk Kärnbränslehantering AB.
- Evins L Z, 2013.** Progress report on evaluation of long-term safety of proposed SFL concepts. SKB R-13-41, Svensk Kärnbränslehantering AB.
- Fetter C W, 1999.** Contaminant hydrogeology. 2nd ed. Upper Saddle River, NJ: Prentice Hall.
- Follin S, 2008.** Bedrock hydrogeology Forsmark. Site descriptive modelling, SDM-Site Forsmark. SKB R-08-95, Svensk Kärnbränslehantering AB.
- French H M, 2007.** The periglacial environment. 3rd ed. Chichester, UK: Wiley.
- Ganopolski A, Winkelmann R, Schellnhuber H J, 2016.** Critical insolation–CO<sub>2</sub> relation for diagnosing past and future glacial inception. *Nature* 529, 200–203.
- Gierszewski P, Avis J, Calder N, D’Andrea A, Garisto F, Kitson C, Melnyk T, Wei K, Wojciechowski L, 2004.** Third case study – postclosure safety assessment. Report 06819-REP-01200-10109-R00, Ontario Power Generation, Nuclear Waste Management Division, Canada.
- Gimeno M J, Auqué L F, Gómez J B, Salas J, Molinero J, 2010.** Hydrogeochemical evolution of the Laxemar Site. SKB R-10-60, Svensk Kärnbränslehantering AB.

- Gimeno M J, Auqué L F, Gómez J B, 2019.** Hydrogeochemical conditions during periods with glacial and periglacial climate conditions. Report for the safety evaluation SE-SFL. SKB R-19-08, Svensk Kärnbränslehantering AB.
- Giroud N, Tomonaga Y, Wersin P, Briggs S, King F, Vogt T, Diomidis N, 2018.** On the fate of oxygen in a spent fuel emplacement drift in Opalinus Clay. *Applied Geochemistry* 97, 270–278.
- Glaus M, Van Loon L, 2008.** Degradation of cellulose under alkaline conditions: new insights from a 12 years degradation study. *Environmental Science & Technology* 42, 2906–2911.
- Graham P, Luterkort D, Mårtensson P, Nilsson F, Nyblad B, Oxfall M, Stojanovic B, 2013.** SFL Concept study. Technical design and evaluation of potential repository concepts for long-lived low and intermediate level waste. SKB R-13-24, Svensk Kärnbränslehantering AB.
- Griffiths G M, Garrett T J, Cloutier W A, Adler J J, 2008.** Decommissioning cost analysis for Barsebäck nuclear station. Document S33-1567-002 rev 0, TLG Services, Inc.
- Grolander S, 2013.** Biosphere parameters used in radionuclide transport modelling and dose calculations in SR-PSU. SKB R-13-18, Svensk Kärnbränslehantering AB.
- Grolander S, Jaeschke B, 2019.** Biosphere parameters used in radionuclide transport modelling and dose calculations in SE-SFL. SKB R-19-18, Svensk Kärnbränslehantering AB.
- Gustafsson B G, 2004.** Millennial changes of the Baltic Sea salinity. Studies of the sensitivity of the salinity to climate change. SKB TR-04-12, Svensk Kärnbränslehantering AB.
- Hakami E, Fredriksson A, Lanaro F, Wrafter J, 2008.** Rock mechanics Laxemar. Site descriptive modelling, SDM-Site Laxemar. SKB R-08-57, Svensk Kärnbränslehantering AB.
- Hakanen M, Ervanne H, Puukko E, 2014.** Safety case for the disposal of spent nuclear fuel at Olkiluoto – radionuclide migration parameters for the geosphere. Posiva 2012-41, Posiva Oy, Finland.
- Hansson T, Norberg T, Knutsson A, Fors P, Sandebert C, 2013.** Ringhals Site Study 2013 – An assessment of the decommissioning cost for the Ringhals site. SKB R-13-05, Svensk Kärnbränslehantering AB.
- Hartikainen J, Kouhia R, Wallroth T, 2010.** Permafrost simulations at Forsmark using a numerical 2D thermo-hydro-chemical model. SKB TR-09-17, Svensk Kärnbränslehantering AB.
- Herschend B, 2014.** Long-lived intermediate level waste from Swedish nuclear power plants. Reference inventory. SKB R-13-17, Svensk Kärnbränslehantering AB.
- Höglund L O, 2014.** The impact of concrete degradation on the BMA barrier functions. SKB R-13-40, Svensk Kärnbränslehantering AB.
- Hökmark H, Lönnqvist M, Kristensson O, Sundberg J, Hellström G, 2009.** Strategy for thermal dimensioning of the final repository for spent nuclear fuel. SKB R-09-04, Svensk Kärnbränslehantering AB.
- Hökmark H, Lönnqvist M, Fälth B, 2010.** THM-issues in repository rock. Thermal, mechanical, thermo-mechanical and hydro-mechanical evolution of the rock at the Forsmark and Laxemar sites. SKB TR-10-23, Svensk Kärnbränslehantering AB.
- IAEA, 2009.** Determination and use of scaling factors for waste characterization in nuclear power plants. Vienna: International Atomic Energy Agency. (IAEA Nuclear Energy Series NW-T-1.18)
- IAEA, 2018.** IAEA safety glossary: terminology used in nuclear safety and radiation protection. Vienna: International Atomic Energy Agency.
- ICRP, 2000.** Radiation protection recommendations as applied to the disposal of long-lived solid radioactive waste. Oxford: Pergamon Press. (ICRP Publication 81; Annals of the ICRP 28)
- ICRP, 2006.** Assessing dose of the representative person for the purpose of radiation protection of the public and the optimisation of radiological protection: broadening the process. Oxford: Pergamon. (ICRP Publication 101; Annals of the ICRP 36)
- Idiart A, Coene E, 2019.** Modelling diffusion through compacted bentonite in the BHA vault. Report for the safety evaluation SE-SFL. SKB R-19-10, Svensk Kärnbränslehantering AB.

- Idiart A, Laviña M, 2019.** Modelling of concrete degradation in a one-million-year perspective – Hydro-chemical processes. Report for the safety evaluation SE-SFL. SKB R-19-13, Svensk Kärnbränslehantering AB.
- Idiart A, Shafei B, 2019.** Modelling of concrete degradation – Hydro-chemical processes. Report for the safety evaluation SE-SFL. SKB R-19-11, Svensk Kärnbränslehantering AB.
- Idiart A E, López C M, Carol I, 2011.** Chemo-mechanical analysis of concrete cracking and degradation due to external sulfate attack: a meso-scale model. *Cement and Concrete Composites* 33, 411–423.
- Idiart A, Laviña M, Coene E, 2019a.** Modelling of concrete degradation – Hydro-chemo-mechanical processes. Report for the safety evaluation SE-SFL. SKB R-19-12, Svensk Kärnbränslehantering AB.
- Idiart A, Olmeda J, Laviña M, 2019b.** Modelling of concrete degradation – influence of concrete mix design. Report for the safety evaluation SE-SFL. SKB R-19-14, Svensk Kärnbränslehantering AB.
- JNC, 2000.** H12 – Project to establish the scientific and technical basis for HLW disposal in Japan main report and four supplementary reports. JNC Technical Report TN1410 2000-001, JNC TN1410 2000-002 – 005, Japan Nuclear Fuel Cycle Development Institute.
- Johansson E, Sassner M, 2019.** Development of methodology for flow path analysis in the surface system – Numerical modelling in MIKE SHE for Laxemar. A report for the safety evaluation SE-SFL. SKB R-19-04, Svensk Kärnbränslehantering AB.
- Johansson P-O, 2008.** Description of surface hydrology and near-surface hydrogeology at Forsmark. Site descriptive modelling, SDM-Site Forsmark. SKB R-08-08, Svensk Kärnbränslehantering AB.
- Joyce S, Simpson T, Hartley L, Applegate D, Hoek J, Jackson P, Roberts D, Swan D, Gylling B, Marsic N, Rhén I, 2010.** Groundwater flow modelling of periods with temperate climate conditions Laxemar. SKB R-09-24, Svensk Kärnbränslehantering AB.
- Joyce S, Appleyard P, Hartley L, Tsitsopoulos V, Woollard H, Marsic N, Sidborn M, Crawford J, 2019.** Groundwater flow and reactive transport modelling of temperate conditions. Report for the safety evaluation SE-SFL. SKB R-19-02, Svensk Kärnbränslehantering AB.
- Kalinowski B (ed), 2009.** Background complementary hydrogeochemical studies. Site descriptive modelling SDM-Site Laxemar. SKB R-08-111, Svensk Kärnbränslehantering AB.
- Keith-Roach M, Lindgren M, Källström K, 2014.** Assessment of complexing agent concentrations in SFR. SKB R-14-03, Svensk Kärnbränslehantering AB.
- King F, 2008.** Corrosion of carbon steel under anaerobic conditions in a repository for SF and HLW in Opalinus Clay. Nagra Technical Report 08-12, Nagra, Switzerland.
- Kjellström E, Strandberg G, Brandefelt J, Näslund J-O, Smith B, Wohlfart B, 2009.** Climate conditions in Sweden in a 100 000-year time perspective. SKB TR-09-04, Svensk Kärnbränslehantering AB.
- Koistinen T, Stephens M B, Bogatchev V, Nordgulen O, Wennerström M, Korhonen J, 2001.** Geological map of the Fennoscandian Shield, scale 1:2 000 000. Geological Surveys of Finland, Norway and Sweden and the North-West Department of Natural Resources of Russia.
- Laaksoharju M, Smellie J, Tullborg E-L, Wallin B, Drake H, Gascoyne M, Gimeno M, Gurbam I, Hallbeck L, Molinero J, Nilsson A-C, Waber N, 2009.** Bedrock hydrogeo-chemistry Laxemar. Site descriptive modelling, SDM-Site Laxemar. SKB R-08-93, Svensk Kärnbränslehantering AB.
- Lagerblad B, Rogers P, Vogt C, Mårtensson P, 2017.** Utveckling av konstruktionsbetong till kassunerna i 2BMA. SKB R-17-21, Svensk Kärnbränslehantering AB. (In Swedish.)
- Lagerblad B, Trägårdh J, 1994.** Conceptual model for concrete long time degradation in a deep nuclear waste repository. SKB TR 95-21, Svensk Kärnbränslehantering AB.

- La Pointe P, Fox A, Hermanson J, Öhman J, 2008.** Geological discrete fracture network model for the Laxemar site. Site descriptive modelling, SDM-Site Laxemar. SKB R-08-55, Svensk Kärnbränslehantering AB.
- Larsson H, Anunti Å, Edelborg M, 2013.** Decommissioning study of Oskarshamn NPP. SKB R-13-04, Svensk Kärnbränslehantering AB.
- Lindborg T (ed), 2010.** Landscape Forsmark – data, methodology and results for SR-Site. Updated 2013-08. SKB TR-10-05, Svensk Kärnbränslehantering AB.
- Lindgren M, Gylling B, Elert M, 2002.** FARF31 Version 1.2 – User’s guide. SKB TS-02-03, Svensk Kärnbränslehantering AB.
- Lindgren M, Pettersson M, Wiborgh M, 2007.** Correlation factors for C-14, Cl-36, Ni-59, Ni-63, Mo-93, Tc-99, I-129 and Cs-135 in operational waste for SFR 1. SKB R-07-05, Svensk Kärnbränslehantering AB.
- Lindow V, 2012.** Ågesta rivningsstudie – Samlad bedömning och uppskattning av rivningskostnaden för Ågesta kraftvärmeverk. Dok.ID AE-NPR 2012-027 (PN-S 12-072), Vattenfall AB. (In Swedish.)
- Losjö K, Johansson B, Bringefelt B, Oleskog I, Bergström S, 1999.** Groundwater recharge – climatic and vegetation induced variations. Simulations in the Emån and Äspö areas in southern Sweden. SKB TR-99-01, Svensk Kärnbränslehantering AB.
- Lothenbach B, Kunther W, Idiart A, 2012.** Thermodynamic modeling of sulfate interaction. In Alexander M G, Beushausen H-D, Dehn F, Moyo P (eds). Proceedings of the 3rd International Conference on Concrete Repair, Rehabilitation and Retrofitting, ICCRRR-3, Cape Town, South Africa, 3–5 September 2012. Leiden: CRC Press, 1444–1449.
- Lund B, Schmidt P, Hieronymus C, 2009.** Stress evolution and fault stability during the Weichselian glacial cycle. SKB TR-09-15, Svensk Kärnbränslehantering AB.
- Lundin L, Lode E, Stendahl J, Björkvald L, Hansson J, 2005.** Oskarshamn site investigation. Soils and site types in the Oskarshamn area. SKB R-05-15, Svensk Kärnbränslehantering AB.
- Luterkort D, Gylling B, Johansson R, 2012.** Closure of the Spent Fuel Repository in Forsmark. Studies of alternative concepts for sealing of ramp, shafts and investigation boreholes. SKB TR-12-08, Svensk Kärnbränslehantering AB.
- Luterkort D, Nyblad B, Wimelius H, Pettersson A, Aghili B, 2014.** SFR förslutningsplan. SKBdoc 1358612 ver 1.0, Svensk Kärnbränslehantering AB.
- Löfgren A (ed), 2010.** The terrestrial ecosystems at Forsmark and Laxemar-Simpevarp. SR-Site Biosphere. SKB TR-10-01, Svensk Kärnbränslehantering AB.
- McNeish J, 2002.** Total system performance assessment – license application methods and approach. TDR-WIS-PA-000006 REV 00, Bechtel SAIC Company, Las Vegas, Nevada.
- Mårtensson P, Vogt C, 2019.** Concrete caissons for 2BMA. Large scale test of design and material. SKB TR-18-12, Svensk Kärnbränslehantering AB.
- Nagra, 2002.** Project Opalinus Clay. Safety report. Demonstration of disposal feasibility of spent fuel, vitrified high-level waste and long-lived intermediate-level waste (Entsorgungsnachweis). Nagra Technical Report 02-05, Nagra, Switzerland.
- Nardi A, Idiart A, Trincherro P, de Vries L M, Molinero J, 2014.** Interface COMSOL-PHREEQC (iCP), an efficient numerical framework for the solution of coupled multiphysics and geochemistry. Computers & Geosciences 69, 10–21.
- NEA, 1997a.** Lessons learnt from ten performance assessment studies. Paris: Nuclear Energy Agency, Organisation for Economic Co-operation and Development.
- NEA, 1999a.** Confidence in the long-term safety of deep geological repositories: its development and communication. Paris: Nuclear Energy Agency, Organisation for Economic Co-operation and Development.

- NEA, 2001.** Scenario development methods and practices: an evaluation based on the NEA Workshop on Scenario Development, Madrid, Spain, May 1999. Paris: Nuclear Energy Agency, Organisation for Economic Co-operation and Development.
- NEA, 2004a.** The handling of timescales in assessing post-closure safety: lessons learnt from the April 2002 Workshop in Paris, France. Paris: Nuclear Energy Agency, Organisation for Economic Co-operation and Development.
- NEA, 2004b.** Post-closure safety case for geological repositories: nature and purpose. Paris: Nuclear Energy Agency, Organisation for Economic Co-operation and Development.
- NEA, 2006.** Electronic version 2.1 of the NEA FEP database developed on behalf of the Nuclear Energy Agency by Safety Assessment Management Ltd.
- NEA, 2009.** International Experiences in Safety Cases for Geological Repositories (INTESC): Outcomes of the INTESC Project. Paris: Nuclear Energy Agency, Organisation for Economic Co-operation and Development.
- NEA, 2012.** Methods for safety assessment of geological disposal facilities for radioactive waste outcomes of the NEA MeSA Initiative. NEA Report 6923, Nuclear Energy Agency, Organisation for Economic Co-operation and Development.
- Norman S, Kjellbert N, 1990.** FARF31 – A far field radionuclide migration code for use with the PROPER package. SKB TR 90-01, Svensk Kärnbränslehantering AB.
- Nyman H, Sohlenius G, Strömngren M, 2008.** Depth and stratigraphy of regolith. Site descriptive modelling SDM-Site Laxemar. SKB R-08-06, Svensk Kärnbränslehantering AB.
- Näslund J-O, Brandefelt J, Claesson Liljedahl L, 2013.** Climate considerations in long-term safety assessments for nuclear waste repositories. *Ambio* 42, 393–401.
- Ochs M, Talerico C, 2004.** SR-Can. Data and uncertainty assessment. Migration parameters for the bentonite buffer in the KBS-3 concept. SKB TR-04-18, Svensk Kärnbränslehantering AB.
- Odén M, Follin S, Öhman J, Vidstrand P, 2014.** SR-PSU Bedrock hydrogeology. Groundwater flow modelling methodology, setup and results. SKB R-13-25, Svensk Kärnbränslehantering AB.
- ONDRAF/NIRAS, 2001.** SAFIR:2 Safety Assessment and Feasibility Interim Report 2. NIROND 2001-06E, ONDRAF/NIRAS.
- Pedersen K, Nilsson E, Arlinger J, Hallbeck L, O'Neill A. 2004.** Distribution, diversity and activity of microorganisms in the hyper-alkaline spring waters of Maqarin in Jordan. *Extremophiles* 8, 151–164.
- Peçkala M, Olmeda J, Grivé M, Bruno J, 2015.** Assessment of redox state and its impact on the solubility and speciation of selected radionuclides in the SFL repository. Final report. Amphos 21. SKBdoc 1533627 ver 1.0, Svensk Kärnbränslehantering AB.
- Persson G, Asp M, Berggreen-Clausen S, Berglöv G, Björck E, Axén Mårtensson J, Nylén L, Ohlsson A, Persson H, Sjökvist E, 2015.** Framtidsklimat i Kalmar län – enligt RCP-scenarier. Norrköping: SMHI. (Klimatologi 26)
- Persson J, Lydmark S, Edlund J, Pääjärvi A, Pedersen K, 2011.** Microbial incidence on copper and titanium embedded in compacted bentonite clay. SKB R-11-22, Svensk Kärnbränslehantering AB.
- Persson P, 2015.** Characteristics of radioactive waste from ESS to be disposed in SKB facilities. Technical Report, Document number ESS 0036701, Revision 2(3). European Spallation Source. SKBdoc 1701742 ver 1.0, Svensk Kärnbränslehantering AB.
- Posiva, 2013.** Safety case for the disposal of spent nuclear fuel at Olkiluoto – models and data for the repository system 2012. Posiva 2013-01, Posiva Oy, Finland.
- Posiva SKB, 2017.** Safety functions, performance targets and technical design requirements for a KBS-3V repository, conclusions and recommendations from a joint SKB and Posiva working group. Posiva SKB Report 01, Posiva Oy, Svensk Kärnbränslehantering AB.
- Pässe T, 2001.** An empirical model of glacio-isostatic movements and shore-level displacement in Fennoscandia. SKB R-01-41, Svensk Kärnbränslehantering AB.

- Rhén I, Hartley L, 2009.** Bedrock hydrogeology Laxemar. Site descriptive modelling, SDM-Site Laxemar. SKB R-08-92, Svensk Kärnbränslehantering AB.
- Rhén I, Follin S, Hermanson J, 2003.** Hydrogeological Site Descriptive Model – a strategy for its development during Site Investigations. SKB R-03-08, Svensk Kärnbränslehantering AB.
- Rhén I, Forsmark T, Hartley L, Jackson C P, Roberts D, Swan D, Gylling B, 2008.** Hydrogeological conceptualisation and parameterisation. Site descriptive modelling, SDM-Site Laxemar. SKB R-08-78, Svensk Kärnbränslehantering AB.
- Rhén I, Forsmark T, Hartley L, Joyce S, Roberts D, Gylling B, Marsic N, 2009.** Bedrock hydrogeology. Model testing and synthesis. Site descriptive modelling, SDM-Site Laxemar. SKB R-08-91, Svensk Kärnbränslehantering AB.
- Saetre P, Nordén S, Keesmann S, Ekström P-A, 2013.** The biosphere model for radionuclide transport and dose assessment in SR-PSU. SKB R-13-46, Svensk Kärnbränslehantering AB.
- Sakuragi T, Yoshida S, Kato O, Tateishi T, 2016.** Study of stainless steel corrosion by hydrogen measurement under deoxygenated, low-temperature and basic repository conditions. Progress in Nuclear Energy 87, 26–31.
- Sandén T, Börgesson L, 2010.** Early effects of water inflow into a deposition hole. Laboratory test results. SKB R-10-70, Svensk Kärnbränslehantering AB.
- Sassner M, Sabel U, Bosson E, Berglund S, 2011.** Numerical modelling of present and future hydrology at Laxemar-Simpevarp. SKB R-11-05, Svensk Kärnbränslehantering AB.
- SFS 1984:3.** The Act on Nuclear Activities (1984:3).
- Shahkarami P, 2019.** Input data report for near-field and geosphere radionuclide transport modelling in the safety evaluation SE-SFL. SKB R-19-09, Svensk Kärnbränslehantering AB.
- Silva O, Coene E, Moliner J, Laviña M, Idiart A, 2019a.** Gas release from the BHK vault – Multiphase flow modelling of the near-field. Report for the safety evaluation SE-SFL. SKB R-19-06, Svensk Kärnbränslehantering AB.
- Silva O, Sáinz-García Á, Molinero J, 2019b.** Gas release from the SFL repository and migration through the geosphere. Report for the safety evaluation SE-SFL. SKB R-19-07, Svensk Kärnbränslehantering AB.
- SKB, 1993.** Plan 93. Costs for management of the radioactive waste from nuclear power production. SKB TR 93-28, Svensk Kärnbränslehantering AB.
- SKB, 1999a.** Deep repository for long-lived low- and intermediate-level waste. Preliminary safety assessment. SKB TR-99-28, Svensk Kärnbränslehantering AB.
- SKB, 1999b.** Deep repository for spent nuclear fuel. SR 97 – Post-closure safety. Main report – Vol. I, Vol. II and Summary. SKB TR-99-06, Svensk Kärnbränslehantering AB.
- SKB, 2001.** Project SAFE. Compilation of data for radionuclide transport analysis. SKB R-01-14, Svensk Kärnbränslehantering AB.
- SKB, 2006a.** Long-term safety for KBS-3 repositories at Forsmark and Laxemar – a first evaluation. Main report of the SR-Can project. SKB TR-06-09, Svensk Kärnbränslehantering AB.
- SKB, 2006b.** FEP report for the safety assessment SR-Can. SKB TR-06-20, Svensk Kärnbränslehantering AB.
- SKB, 2006c.** Climate and climate-related issues for the safety assessment SR-Can. SKB TR-06-23, Svensk Kärnbränslehantering AB.
- SKB, 2008a.** Säkerhetsredovisning SFR 1. Allmän del 2 – långsiktig säkerhet. Svensk Kärnbränslehantering AB. (In Swedish.)
- SKB, 2008b.** Site description of Forsmark at completion of the site investigation phase. SDM-Site Forsmark. SKB TR-08-05, Svensk Kärnbränslehantering AB.
- SKB, 2009.** Site description of Laxemar at completion of the site investigation phase. SDM-Site Laxemar. SKB TR-09-01, Svensk Kärnbränslehantering AB.

**SKB, 2010a.** Geosphere process report for the safety assessment SR-Site. SKB TR-10-48, Svensk Kärnbränslehantering AB.

**SKB, 2010b.** Climate and climate-related issues for the safety assessment SR-Site. SKB TR-10-49, Svensk Kärnbränslehantering AB.

**SKB, 2010c.** FEP report for the safety assessment SR-Site. SKB TR-10-45, Svensk Kärnbränslehantering AB.

**SKB, 2010d.** Components, processes and interactions in the biosphere. SKB R-10-37, Svensk Kärnbränslehantering AB.

**SKB, 2010e.** Buffer, backfill and closure process report for the safety assessment SR-Site. SKB TR-10-47, Svensk Kärnbränslehantering AB.

**SKB, 2010f.** Comparative analysis of safety related site characteristics. SKB TR-10-54, Svensk Kärnbränslehantering AB.

**SKB, 2010g.** Radionuclide transport report for the safety assessment SR-Site. SKB TR-10-50, Svensk Kärnbränslehantering AB.

**SKB, 2010h.** Biosphere analyses for the safety assessment SR-Site – synthesis and summary of results. SKB TR-10-09, Svensk Kärnbränslehantering AB.

**SKB, 2010i.** Data report for the safety assessment SR-Site. SKB TR-10-52, Svensk Kärnbränslehantering AB.

**SKB, 2010j.** Design, production and initial state of the backfill and plug in deposition tunnels. SKB TR-10-16, Svensk Kärnbränslehantering AB.

**SKB, 2011a.** Long-term safety for the final repository for spent nuclear fuel at Forsmark. Main report of the SR-Site project. Updated 2015-05. SKB TR-11-01, Svensk Kärnbränslehantering AB.

**SKB, 2011b.** Site selection – siting of the final repository for spent nuclear fuel. SKB R-11-07, Svensk Kärnbränslehantering AB.

**SKB, 2013a.** Components, features, processes and interactions in the biosphere. SKB R-13-43, Svensk Kärnbränslehantering AB.

**SKB, 2013b.** Site description of the SFR area at Forsmark at completion of the site investigation phase. SDM-PSU Forsmark. SKB TR-11-04, Svensk Kärnbränslehantering AB.

**SKB, 2014a.** Waste form and packaging process report for the safety assessment SR-PSU. SKB TR-14-03, Svensk Kärnbränslehantering AB.

**SKB, 2014b.** Engineered barrier process report for the safety assessment SR-PSU. SKB TR-14-04, Svensk Kärnbränslehantering AB.

**SKB, 2014c.** Geosphere process report for the safety assessment SR-PSU. SKB TR-14-05, Svensk Kärnbränslehantering AB.

**SKB, 2014d.** Climate and climate-related issues for the safety assessment SR-PSU. SKB TR-13-05, Svensk Kärnbränslehantering AB.

**SKB, 2014e.** FEP report for the safety assessment SR-PSU. SKB TR-14-07, Svensk Kärnbränslehantering AB.

**SKB, 2014f.** Biosphere synthesis for the safety assessment SR-PSU. SKB TR-14-06, Svensk Kärnbränslehantering AB.

**SKB, 2014g.** Handling of future human actions in the safety assessment SR-PSU. SKB TR-14-08, Svensk Kärnbränslehantering AB.

**SKB, 2014h.** Data report for the safety assessment SR-PSU. SKB TR-14-10, Svensk Kärnbränslehantering AB.

**SKB, 2015a.** Safety analysis for SFR. Long-term safety. Main report for the safety assessment SR-PSU. Revised edition. SKB TR-14-01, Svensk Kärnbränslehantering AB.

- SKB, 2015b.** Low and intermediate level waste in SFR. Reference inventory for waste 2013. SKB R-15-15, Svensk Kärnbränslehantering AB.
- SKB, 2015c.** Radionuclide transport and dose calculations for the safety assessment SR-PSU. Revised edition. SKB TR-14-09, Svensk Kärnbränslehantering AB.
- SKB, 2015d.** Handling of biosphere FEPs and recommendations for model development in SR-PSU. SKB R-14-02, Svensk Kärnbränslehantering AB.
- SKB, 2019.** Fud-program 2019. Program för forskning, utveckling och demonstration av metoder för hantering och slutförvaring av kärnavfall. Svensk Kärnbränslehantering AB. (In Swedish.)
- SKI/SSI, 2001.** SKI:s och SSI:s gemensamma granskning av SKB:s preliminära säkerhetsanalys för slutförvar för långlivat låg- och medelaktivt avfall. Granskningsrapport. SKI rapport 01:14, Statens kärnkraftinspektion, SSI-rapport 2001:10, Statens strålskyddsinstitut. (In Swedish.)
- Smart N R, Blackwood D J, Werme L, 2001.** The anaerobic corrosion of carbon steel and cast iron in artificial groundwaters. SKB TR-01-22, Svensk Kärnbränslehantering AB.
- Sohlenius G, Hedenström A, 2008.** Description of regolith at Laxemar-Simpevarp. Site descriptive modelling SDM-Site Laxemar. SKB R-08-05, Svensk Kärnbränslehantering AB.
- SSM, 2008a.** The Swedish Radiation Safety Authority's regulations concerning safety in connection with the disposal of nuclear material and nuclear waste. Stockholm: Swedish Radiation Safety Authority. (SSMFS 2008:21)
- SSM, 2008b.** The Swedish Radiation Safety Authority's regulations and general advice concerning the protection of human health and the environment in connection with the final management of spent nuclear fuel and nuclear waste. Stockholm: Swedish Radiation Safety Authority. (SSMFS 2008:37)
- Sundberg J, Wrafter J, Back P-E, Rosén L, 2008.** Thermal properties Laxemar. Site descriptive modelling SDM-Site Laxemar. SKB R-08-61, Svensk Kärnbränslehantering AB.
- Swanton S, Alexander W, Berry J, 2010.** Review of the behaviour of colloids in the near field of a cementitious repository. Report to NDA RWMD. Serco/TAS/000475/01, Serco, UK.
- Söderbäck B (ed), 2008.** Geological evolution, palaeoclimate and historic development of the Forsmark and Laxemar-Simpevarp areas. Site descriptive modelling, SDM-Site. SKB R-08-19, Svensk Kärnbränslehantering AB.
- Trincherio P, Ebrahimi H, Colas E, Fernández-García D, 2018.** Assessing nickel and molybdenum transport in the bedrock at SFL using a dynamic  $K_d$  approach. Report for the safety evaluation SE-SFL. SKB R-17-03, Svensk Kärnbränslehantering AB.
- Tröjbom M, Söderbäck B, 2006.** Chemical characteristics of surface systems in the Simpevarp area. Visualisation and statistical evaluation of data from surface water, precipitation, shallow groundwater, and regolith. SKB R-06-18, Svensk Kärnbränslehantering AB.
- Tröjbom M, Söderbäck B, Kalinowski B, 2008.** Hydrochemistry of surface water and shallow groundwater. Site descriptive modelling, SDM-Site Laxemar. SKB R-08-46, Svensk Kärnbränslehantering AB.
- Van Loon L R, Glaus M A, 1998.** Experimental and theoretical studies on alkaline degradation of cellulose and its impact on the sorption of radionuclides. PSI-Bericht 98-07, Paul Scherrer Institute, Villigen, Switzerland. Also published as Nagra TR 97-04, Nagra, Switzerland.
- Vidstrand P, Svensson U, Follin S, 2006.** Simulation of hydrodynamic effects of salt rejection due to permafrost. Hydrogeological numerical model of density-driven mixing, at a regional scale, due to a high salinity pulse. SKB R-06-101, Svensk Kärnbränslehantering AB.
- Vidstrand P, Rhén I, Zugec N, 2010a.** Groundwater flow modelling of periods with periglacial and glacial climate conditions – Laxemar. SKB R-09-25, Svensk Kärnbränslehantering AB.
- Vidstrand P, Follin S, Zugec N, 2010b.** Groundwater flow modelling of periods with periglacial and glacial climate conditions – Forsmark. SKB R-09-21, Svensk Kärnbränslehantering AB.

- Vidstrand P, Follin S, Selroos J-O, Näslund J-O, Rhén I, 2013.** Modeling of groundwater flow at depth in crystalline rock beneath a moving ice-sheet margin, exemplified by the Fennoscandian Shield, Sweden. *Hydrogeology Journal* 21, 239–255.
- Vidstrand P, Follin S, Selroos J-O, Näslund J-O, 2014a.** Groundwater flow modeling of periods with periglacial and glacial climate conditions for the safety assessment of the proposed high level nuclear waste repository site at Forsmark, Sweden. *Hydrogeology Journal* 22, 1251–1267.
- Vidstrand P, Follin S, Öhman J, 2014b.** SR-PSU Hydrogeological modelling. TD13 – Periglacial climate conditions. SKB P-14-06, Svensk Kärnbränslehantering AB.
- Vieno T, Nordman H, 1999.** Safety assessment of spent fuel disposal in Hästholmen, Kivetty, Olkiluoto and Romuvaara. TILA-99. Posiva 99-07, Posiva Oy, Finland.
- von Schenck H, 2018.** Thermal evolution of the repository – the effect of heat generating waste. Report for the safety evaluation SE-SFL. SKB R-18-04, Svensk Kärnbränslehantering AB.
- von Schenck H, Källström K, 2014.** Reactive transport modelling of organic complexing agents in cement stabilized low and intermediate level waste. *Physics and Chemistry of the Earth, Parts A/B/C* 70–71, 114–126.
- Wahlgren C-H, Curtis P, Hermanson J, Forssberg O, Öhman J, Fox A, La Pointe P, Drake H, Triumf C-A, Mattsson H, Thunehed H, Juhlin C, 2008.** Geology Laxemar. Site descriptive modelling, SDM-Site Laxemar. SKB R-08-54, Svensk Kärnbränslehantering AB.
- Werner K, Bosson E, Berglund S, 2006.** Description of climate, surface hydrology, and near-surface hydrogeology. Preliminary site description Laxemar subarea – version 1.2. SKB R-05-61, Svensk Kärnbränslehantering AB.
- Wessely O, Shahkarami P, 2019.** Development of radionuclide transport models for the near-field. Report for the safety evaluation SE-SFL. SKB R-19-05, Svensk Kärnbränslehantering AB.
- Wiborgh M (ed), 1995.** Prestudy of final disposal of long-lived low and intermediate level waste. SKB TR-95-03, Svensk Kärnbränslehantering AB.
- Winberg A, 2010.** Säkerhetsrelaterade platsegenskaper – en relativ jämförelse av Forsmark med referensområden. SKB R-10-63, Svensk Kärnbränslehantering AB. (In Swedish.)
- Yumoto I, 2007.** Environmental and taxonomic biodiversities of Gram-positive alkaliphiles. In Gerday C, Glansdorff N (eds). *Physiology and biochemistry of extremophiles*. Washington, DC: ASM Press, 295–310.
- Åkesson M, Kristensson O, Börgesson L, Dueck A, Hernelind J, 2010.** THM modelling of buffer, backfill and other system components. Critical processes and scenarios. SKB TR-10-11, Svensk Kärnbränslehantering AB.
- Öhman J, Bockgård N, Follin S, 2012.** Site investigation SFR. Bedrock hydrogeology. SKB R-11-03, Svensk Kärnbränslehantering AB.

## Piping and erosion calculations

Piping and erosion are described in Section 6.2.9. The mass loss/redistribution from piping and subsequent erosion has not been studied specifically in SE-SFL. However, a simple estimate can be made using the available volumes together with the rate expression from SR-Site (Sandén and Börgesson 2010). According to the expression provided, the accumulated mass of eroded bentonite is related to the accumulated mass of eroding water. Based on experimental tests, an exponential erosion model described by the equation below has been suggested:

$$m_s = \beta \times (m_w)^\alpha \quad \text{A-1}$$

where

$m_s$  = accumulated mass of eroded bentonite [g],

$m_w$  = accumulated mass of eroding water [g],

$\beta$  = 0.02–2.0 (general), 0.02–0.2 (vertical piping) = parameter defined by the level of erosion at unit accumulated water flow,

$\alpha$  = 0.65 = parameter representing the deviation from linearity of the  $m_s$  dependence on  $m_w$ .

$m_w$  can be calculated based on the initial void in the BHA vault. The dimensions are presented in Table A-1, based on data given in Chapter 4. The parameters and results are then discussed.

**Table A-1. Void volumes used for the calculation of the extent of piping/erosion. The porosities in the table represent the value available for inflow during the operational phase, not the total porosity.**

Component	Dimensions L × W × H (m × m × m)	Volume (m <sup>3</sup> )	Assumed porosity (%) available for inflowing water	Void (m <sup>3</sup> )
Waste	140 × 16 × 8.4	18 816	9.3 <sup>a</sup>	1750
Pellets ceiling	170 × 20.6 × 3.7	12 957	48 <sup>b</sup>	6220
Block part	170 × 20.6 × 14.8	33 014	2 <sup>b</sup>	660
Side filling × 2	170 × 0.5 × 18.5	3 145	48 <sup>b</sup>	1 510
Bottom filling	170 × 20.6 × 0.5	1 751	48 <sup>b</sup>	840
Front/rear filling × 2	0.5 × 20.6 × 18.5	381.1	48 <sup>b</sup>	183

<sup>a</sup> Shahkarami (2019) and Höglund 2014.

<sup>b</sup> Åkesson et al. 2010.

The void for the waste is calculated based on the assumption of a porosity of 31 % (Shahkarami 2019), and a degree of saturation of 70 % (Höglund 2014).

The pellets in the ceiling are assumed to have the same initial properties as the pellets in the backfill in the Spent Fuel Repository (SKB 2010j). Experience from work with pellets filling shows that the dry density of the filling will be about 1 000 kg/m<sup>3</sup>, which yields

$$\rho_d = 1000 \text{ (kg/m}^3\text{)}$$

$$e = 1.78 \text{ (void ratio)}$$

$$n = 0.64 \text{ (porosity)}$$

The initial water content in the pellets in the backfill is planned to be  $w = 0.17$ . The porosity is thus 64 % but about 25 % of the pore space in the backfill pellets is already filled with water due to the initial water content. This means that the air-filled porosity is about 48 % in the backfill pellet filling and is available for inflowing water. In addition to these empty volumes there are of course the unfilled pores in the bentonite blocks and in the slots between the blocks. The slow wetting means that only the slots between the blocks can be expected to be filled. According to SKB (2010j), the total volume of these slots is expected to be about 2 % of the total block volume.

The rock/backfill interface volume in the front, rear, sides and bottom of BHA is not described in the **Initial state report**. In this assessment, it is assumed that these volumes are filled with the same type of pellets as the pellet ceiling. No additional volume has been assigned to the ceiling. The assumption a rectangular instead of an arc shaped-volume already compensates for this.

The total volume available for inflow is 11 163 m<sup>3</sup> (Table A-1). In addition, it should be expected that there would be some leakage through the plug, depending on the tightness of the plug. It is presently not known how tight these plugs can be made, so we assume for now that additionally 10 % of the total volume in the tunnel will leak out through the plug. This yields a total possible water flow into the tunnel of 12 280 m<sup>3</sup>.

Thus, a total volume of about 12 280 m<sup>3</sup> = 1.23 × 10<sup>10</sup> g water is expected to flow into the cavern before it is filled with water and sealed, including possible leakage through the plug. If all water comes from one single fracture the eroding mass of bentonite will, according to Equation A-1 with β = 0.02–2, be:

$$m_s = \beta(1.23 \times 10^{10})^{0.65}, \quad m_s(\beta = 0.02) = 72 \text{ kg}, \quad m_s(\beta = 2) = 7230 \text{ kg} \quad \text{A-2}$$

The maximum lost mass, 7230 kg, corresponds to a volume of 4.6 m<sup>3</sup> given a dry density of 1 570 kg/m<sup>3</sup> (Section 4.3.2), which is less than 0.01 % of the total backfill volume. At the Laxemar site, it is rather likely that the inflow will come from several fractures into the cavern. If the total flow entered equally from 10 fractures instead of one the maximum global erosion would be 16 180 kg and the local erosion would be 1 618 kg. In general, high local erosion is considered to be worse than high global, since the local effects sets the requirements on the swelling and homogenisation ability of the bentonite backfill.

A weakness of the current model is that it is purely empirical; it is difficult to theoretically derive a model. However, this is the case for many geotechnical models (e.g. strength and friction angle relations) that still see wide and successful use within the field. The range 0.02 < β < 2 has an upper erosion limit that is about 10 times larger than that measured during vertical flow (Åkesson et al. 2010), and the resulting piping estimates are thus conservatively high. The equations were derived for canister deposition holes for SR-Site, and their applicability to the much larger BHA waste vault should be verified in future safety assessments.





